IEEE P802.15
Wireless Personal Area Networks

Project	IEEE P802.15 Working Group for Wireless Personal Area Networks (WPANs)	
Title	**Narrowband On-Body to Off-Body Channel Characterization for Body Area Networks**	
Date Submitted	Friday 1st August, 2008	
Source	Dino Miniutti, Leif Hanlen, David Smith, Andrew Zhang, Daniel Lewis, David Rodda, Ben Gilbert NICTA 7 London Circuit, Canberra ACT 2600, Australia	Voice: +61-2-6267-6256 Fax: +61-2-6267-6220 Email: dino.miniutti@nicta.com.au
Re:	15-08-0033-02-0006-draft-of-channel-model-for-body-area-network	
Abstract	This document presents the results of narrowband on-body to off-body wireless channel measurements around the 900 and 2400 MHz ISM bands.	
Purpose	This document is intended to aid in the formation of a channel model for the IEEE 802.15.6 BAN standard.	
Notice	This document has been prepared to assist the IEEE P802.15. It is offered as a basis for discussion and is not binding on the contributing individual(s) or organization(s). The material in this document is subject to change in form and content after further study. The contributor(s) reserve(s) the right to add, amend or withdraw material contained herein.	
Release	The contributor acknowledges and accepts that this contribution becomes the property of IEEE and may be made publicly available by P802.15.	

Contents

1 Introduction

The authors of this paper previously submitted a contribution to The Institute of Electrical and Electronic Engineers (IEEE) 802.15.6 task group which presented the results of narrowband on-body wireless channel measurements around the 900 and 2400 MHz ISM bands [1]. This report is an extension to that previous report; the main difference being that it considers on-body to off-body narrowband wireless channels (at the same frequencies). It is hoped that this paper will provide assistance in the design of a channel model for the IEEE 802.15.6 Body Area Network (BAN) standard [2].

This paper presents a number of channel measurements conducted with a transmitting antenna located on the body of a test subject and another receiving antenna located off the body some distance away. The transmitting antenna is worn on either the chest or the right wrist with measurements taken while the the test subject: 1) performs two different actions (standing still or walking on the spot); 2) faces in four different directions; and 3) stands either 1, 2, 3 or 4 meters from the receive antenna.

A more detailed description of the experimental method follows in the next section. Section 3 describes the analytical results found from measurements taken, including: - description of the channel's power spectral density; a characterization of path loss in all measurement positions; a statistical description of received power; and channel coherence time analysis. The final section provides some concluding remarks. There is an appendix (after references) which gives a comprehensive catalog of analytical results described in Section 3.

2 Experimental Method

The channel measurements conducted in this report are an extension to the previously reported measurements in [1]; the main difference here is that the receiving antenna is located off the body instead of on the body.

The experimental method and equipment used for these measurements was identical to those used for the previous measurements in [1], except for a few minor changes. For brevity, we do not repeat the entire experimental method, instead we list the differences between the two experiments below. Hence we refer the reader to [1] for a detailed description of the experiment and equipment.

2.1 Experimental method: differences

The measurements were conducted in the same environment with the same test subject as the previous on-body to on-body measurements in [1]. The differences between the experiments are listed below:

- The transmit antenna was placed at two locations on the test subject: front of chest and right wrist. The transmit antenna locations are illustrated in Figure 1.
- The receive antenna was placed on an aluminum tripod (Inca AT330A) that was fit with a perspex stand to hold the receive antenna. A diagram of the tripod is shown in Figure 2.
- Measurements were taken with the test subject standing in four different locations in the room. The distance between the test subject and receive antenna was either 1, 2, 3 or 4 m at these locations. See Figure 3 for an illustration.
- At each location in the room, measurements were taken with the test subject facing in four different directions: 0°, 90°, 180° and 270°, with 0° representing the subject facing the receive antenna and 90° representing the subject facing 90° to the right of the receive antenna.
- For each orientation and location in the room, measurements were taken with the subject standing still and walking on the spot.
- The total duration of each measurement was 5 s (instead of 10 s as in the previous experiment).

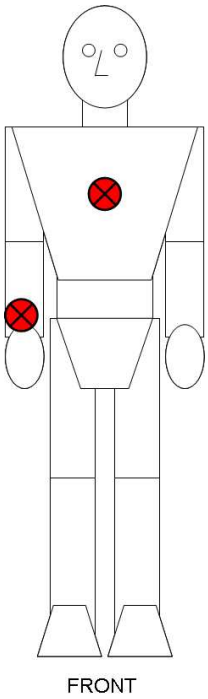

Figure 1: Transmit antenna locations: front of chest and right wrist.

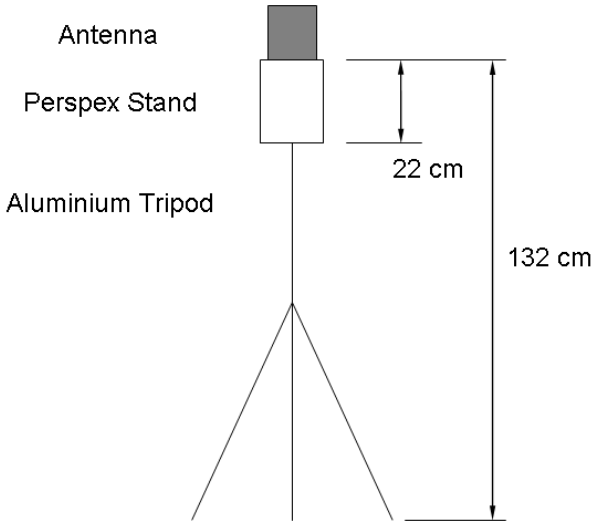

Figure 2: A schematic of the tripod used to support the receive antenna.

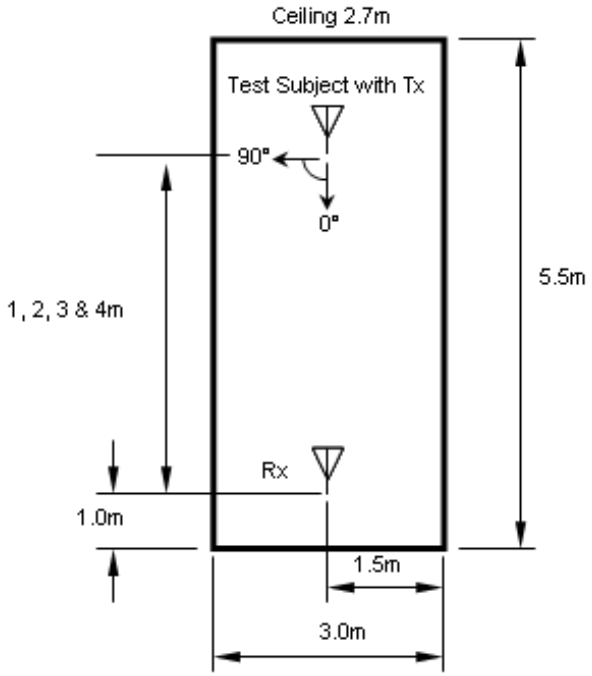

Figure 3: Experimental environment. Measurements were performed with the test subject 1, 2, 3 and 4 meters from the receiver. An angle of 0 ° corresponds to the test subject facing the receive antenna.

3 Results of Channel Measurement Analysis

This section presents the results of analysis performed on the channel measurements detailed in the previous section. A comprehensive catalog of the results has been placed in the Appendix at the end of this document for the convenience of those who do not want to print out the large number of figures contained therein.

We note that all measures of distance for which results of analysis are recorded in this section are the horizontal distance from the spot on which the subject is standing or walking to the receiver (Rx) located off the body.

3.1 Channel Power Spectral Density

This section presents a qualitative discussion of the channel response through the examination of the channel's power spectral density (PSD). This analysis was performed with the intent of providing the reader with a high-level understanding of the on-body to off-body wireless channel through illustration, rather than analysis.

3.1.1 PSD Calculation

The following technique was used to produce surface plots of the channel gain:

The samples within a single 40 μs capture were separated into eight vectors $\{v_1, v_2, \ldots, v_8\}$, each representing the duration of a single PN sequence. These vectors were then averaged to reduce the effects of noise in subsequent operations. The average received PN sequence vector $\bar{v}$ was calculated by

$$\bar{v}[n] = \frac{1}{8} \sum_{i=1}^{8} v_i[n]. \tag{1}$$

Given the relatively short duration of a single capture, it is assumed that the channel is static during the period of each capture. Therefore, performing an averaging operation over the eight sets of PN sequences would not destroy information.

The power spectral density for each capture was obtained by correlating $\bar{v}$ for each capture with a replica of the transmitted PN sequence and then applying a fast Fourier transform. The resultant PSD represents the power spectral density of a system that includes the channel and two root-raised-cosine filters. The root-raised-cosine filters have a relatively flat passband within 5 MHz of DC, with a 1 dB roll-off near the edge. Hence, their effect on the power spectral density is small within $\pm$5 MHz of the carrier frequency, allowing us to disregard their effect (for this section's qualitative analysis) within that region and consider the PSD to be that of the channel alone.

3.1.2 Observations

Frequency selective fading can be observed in many of the PSD plots while the subject is stationary; however this can not be observed in the walking scenario, as the magnitude of this frequency selective fading is much less than the magnitude of the time-selective fading caused by movement.

The PSD varies most while the subject is walking, with antenna attached to the wrist. In this scenario the antenna has the largest range of movement.

3.2 Path Loss Characterization

This section presents results for channel path loss performance analysis found by measuring the received signal power for each respective combination of transmit and receive antenna position, antenna separation, test subject orientation and action (standing still or walking).

3.2.1 Path Loss Calculation

Each channel measurement is of approximately 5 s in duration and consists of multiple 40 μs blocks that are separated in time by 2.5 ms. The RMS power of the received baseband signal (i.e., after down-conversion and sampling, no pulse-shaping) was calculated for each 40 μs block. Path loss is then calculated as the difference between transmitted power and received power. As the received signal amplitude is measured after the amplifiers, these effects must be removed from the path loss. The channel path loss $PL(t)$ at a given time t is given by

$$PL(t) = P_{tx} - P_{rx}(t) + G_{amplifiers} - L_{cable}, \tag{2}$$

where P_{tx} is transmitted power, $P_{rx}(t)$ is the RMS received power at time t, $G_{amplifiers}$ is amplifier gain, and L_{cable} is cable loss. The amplifier gains and cable losses were measured at 820 MHz and 2.36 GHz, with the appropriate result removed from the path loss.

Note that, due to finite receiver sensitivity, the path loss must be less than 78 dB at 820 MHz and 76 dB at 2.36 GHz to distinguish the transmitted signal from noise. The noise floor of the receiver is calculated by taking a measurement with the transmitting antenna replaced by a 50 Ω load. The measurement then taken at the receiver represented thermal noise and cross-talk between transmitter and receiver which, for the purpose of this study, are consolidated into a single noise figure. The maximum observable path loss then follows from (2).

3.2.2 Observations

It can be observed from Table 1 that the orientation of the subject has a large effect on path loss. There is on average 7 dB and up to 19 dB greater path loss for orientation 180° compared to orientation 0°. This is due to the shadowing effect of the body. In orientation 180° the on-body transmitting antenna is on the opposite side of the body to the off-body receiving antenna and there exists no line of sight path, whereas in orientation 0° the on-body antenna is on the same side of the body and there exists a line of sight path between them.

The path loss variation is at most 4 dB while stationary, and is on average 1.2–1.3 dB for both chest and wrist antenna positions. When walking, the path loss varies up to 24 dB with transmit antenna on the chest, and up to 27 dB with transmit antenna on the wrist. The average variation is higher for the wrist position than the chest position, as would be expected since the wrist has a greater range of movement than the chest while walking.

In general, path loss increases as distance increases. However due to the rich scattering nature of the office environment used, the path loss may decrease with increased distance in some measurements.

In several of the standing scenarios, the measured path loss is significantly larger when the antenna is connected to the wrist than when it is connected to the chest. Although the antenna was placed on the wrist and the subject was stationary, the antenna was effectively sandwiched between the subject's wrist and hip. This caused a noticeable increase in path loss due to increased shadowing from the human body.

Table 1: Average Path Loss (dB)

(a) 820 MHz

Rx Distance (m)	Orientation (°)	Transmitter Location / Action:			
		Chest		Right Wirst	
		Standing	Walking	Standing	Walking
1	0	43.51	42.05	47.84	48.12
	90	50.22	50.90	56.95	53.72
	180	60.13	45.93	60.27	51.85
	270	50.56	51.08	56.61	55.92
2	0	52.73	48.80	65.29	57.42
	90	46.23	49.03	64.11	57.31
	180	56.34	61.44	65.60	57.51
	270	50.06	49.92	69.07	62.44
3	0	54.60	51.56	65.72	59.02
	90	56.21	57.11	67.96	62.99
	180	64.67	62.07	70.94	63.19
	270	52.16	57.65	65.64	63.80
4	0	49.78	52.07	70.72	58.65
	90	51.41	50.78	68.43	63.19
	180	58.67	63.62	74.43	62.51
	270	61.74	62.11	70.55	64.72

(b) 2.36 GHz

Rx Distance (m)	Orientation (°)	Transmitter Location / Action:			
		Chest		Right Wirst	
		Standing	Walking	Standing	Walking
1	0	53.81	44.46	59.78	55.68
	90	66.56	64.94	69.51	54.19
	180	61.81	59.48	69.30	58.26
	270	62.84	60.66	61.37	62.34
2	0	53.12	51.59	73.04	58.90
	90	63.79	60.98	71.56	59.90
	180	68.64	70.30	72.62	60.89
	270	63.13	62.19	66.12	64.53
3	0	56.04	52.14	67.20	61.92
	90	66.60	64.07	71.33	63.14
	180	60.12	63.98	73.72	61.92
	270	66.14	63.71	69.96	65.11
4	0	64.72	60.81	63.61	65.18
	90	63.30	63.78	73.91	62.60
	180	63.10	62.56	74.40	63.15
	270	62.24	66.62	72.96	68.37

Table 2: Path Loss Variation(dB)

(a) 820 MHz

Rx Distance (m)	Orientation (°)	Transmitter Location / Action:			
		Chest		Right Wirst	
		Standing	Walking	Standing	Walking
1	0	0.23	5.88	0.49	20.59
	90	0.36	23.77	0.62	22.98
	180	2.02	19.67	0.34	17.78
	270	1.20	11.73	0.78	18.21
2	0	1.31	12.82	0.77	9.28
	90	0.44	7.16	0.78	23.24
	180	1.21	15.17	0.81	16.73
	270	1.10	8.31	0.79	12.02
3	0	1.84	6.02	1.09	21.18
	90	0.70	12.05	1.26	14.66
	180	1.38	11.91	1.42	16.63
	270	0.87	15.46	1.51	9.77
4	0	0.57	5.23	1.13	14.48
	90	0.48	6.31	1.14	17.85
	180	1.19	12.60	1.25	12.75
	270	1.31	12.87	1.72	13.14

(b) 2.36 GHz

Rx Distance (m)	Orientation (°)	Transmitter Location / Action:			
		Chest		Right Wirst	
		Standing	Walking	Standing	Walking
1	0	0.37	2.55	1.38	24.71
	90	3.32	8.57	1.75	26.71
	180	3.66	6.68	2.11	24.62
	270	1.77	19.66	1.32	15.80
2	0	0.38	3.40	1.36	24.23
	90	0.69	8.93	0.95	22.31
	180	2.48	8.63	0.84	21.83
	270	2.17	13.04	0.98	15.46
3	0	0.88	4.50	3.95	20.21
	90	0.99	12.02	1.82	19.11
	180	1.21	10.09	0.92	20.05
	270	1.90	7.49	0.79	17.50
4	0	0.87	6.41	0.81	15.52
	90	2.41	11.06	0.98	18.84
	180	1.22	10.85	1.36	16.54
	270	1.06	11.30	1.11	11.46

3.3 Statistical Description of Received Power

This section presents a statistical analysis of the received signal power received away from the subject's body, when transmitting from the subject's body, used to describe path loss in the previous section 3.2. Statistical distributions were fit to each set of a data for any given scenario, the Gamma distribution, the Lognormal distribution and the Normal distribution as in the previous report for on-body measurements [1]. In this report we also attempted to fit the Nakagami-m, Weibull and Rayleigh distributions.

The probability density functions of these distributions are defined as follows:-

- Gamma probability density function (PDF)

$$y = f(x|a,b) = \frac{1}{b^a \Gamma(a)} x^{a-1} e^{\frac{x}{b}} \tag{3}$$

  where $\Gamma(\cdot)$ is the Gamma function.

- Normal PDF

$$y = f(x|\mu,\sigma) = \frac{1}{\sigma\sqrt{2\pi}} e^{\frac{-(x-\mu)^2}{2\sigma^2}} \tag{4}$$

- Lognormal PDF

$$y = f(x|\mu,\sigma) = \frac{1}{x\sigma\sqrt{2\pi}} e^{\frac{-(\ln(x)-\mu)^2}{2\sigma^2}} \tag{5}$$

  where $\ln(\cdot)$ represents the natural logarithm.

- Nakagami-m

$$f(x|m,\omega) = \frac{2m^m}{\Gamma(m)} \frac{x^{2m-1}}{\omega^m} \exp\left\{-\frac{m}{w}x^2\right\} \tag{6}$$

- Weibull

$$f(x|a,b) = \begin{cases} ba^{-b}x^{b-1} \exp\left\{-x/a^b\right\} & x \geq 0 \\ 0 & \text{else} \end{cases} \tag{7}$$

- Rayleigh

$$f(x|b) = \frac{x}{b^2} \exp\left\{\frac{-x}{2b^2}\right\} \tag{8}$$

The measured received power across one set of measurements for a given scenario was normalized according to the maximum received power for that set of measures. Thus, due to normalization, distributions are fitted to data that can only take values between 0 and 1, and we effectively ignore those parts of fitted distribution that takes on values outside this range.

Thus, for each scenario we match a best fit from the six distributions, using maximum-likelihood parameter estimates, and choose the best of these "best fits" as the distribution that best matches the measured data set for normalized receive power. These best distributions, for each scenario at the two operating frequencies of 820 MHz and 2.36 GHz, are listed in Table 3 when transmitting from the chest to off the body and Table 4 when transmitting from the right wrist to off the body.

A comprehensive set of figures showing the probability density function (PDF) for each scenario is given in the appendix.In each figure, the three PDFs for the "best-fits" of three distributions are overlayed over the empirical PDF. The bin size for the histogram used to describe the PDF from

the measured data is chosen according to the "Freedman-Diaconis" rule [3](defined in previous report [1]) . Each PDF shows the Lognormal and Normal distributions overlayed, with the better of "best-fits" between the Weibull, Gamma, Nakagami-m distributions.

3.3.1 Observations

It is clear from Table 3 and Table 4 that there is no distribution that is consistently the best match to normalized receive power for all scenarios. It is clear however, that generally the best match, with the subject walking or standing, with the transmitter on the chest or the wrist, is the Lognormal distribution. We also note that by comparison of log-likelihood, which we can be seen graphically, in most cases where the Lognormal distribution is not the best fit, it is still a reasonable fit. (This is evident from investigation of the figures in the appendix).

We also note that the cases for which the Normal distribution is the best fit, are only for the subject standing. From Tables 3, 4 we can also see the Nakagami-m, Gamma and Weibull distributions provide the best fitting model for approximately equivalent number of scenarios. We also note that in no cases, using negative log-likelihood measure, is the Rayleigh distribution the best fit.

In contrast to the previous report for on-body measurements [1]. We note that for the distribution fits compiled in Table 4, the best fits are more accurate in the cases where the subject is standing still transmitting off-the body from the right wrist, than for the case of transmitting from the body to the receiver on the body documented in [1]. In general the best fits are slightly more accurate for the distribution fits compiled in Table 3 transmitting off the body from the chest when standing still than those documented in [1]. This is illustrated in the majority of the probability density function figures placed in the appendix for the case of the subject standing.

Table 3: Scenarios and the distribution (with parameters) that gives the best of the "best fits" to those scenarios transmitting from Chest to receiver off the body at 820 MHz and 2.36 GHz (Angle is orientation of the subject with respect to the receiver, D. is horizontal distance from subject to receiver)

Action	D.	Angle	Distribution	
			820 MHz	2.36 GHz
Stand	1 m	0^o	Lognormal ($\mu = -0.025, \sigma = 0.012$)	Weibull ($a = 0.97, b = 60.7$)
Stand	1 m	90^o	Weibull ($a = 0.98, b = 70.0$)	Lognormal ($\mu = -0.39, \sigma = 0.23$)
Stand	1 m	180^o	Lognormal ($\mu = -0.27, \sigma = 0.12$)	Nakagami-m ($m = 4.13, \omega = 0.51$)
Stand	1 m	270^o	Weibull ($a = 0.92, b = 14.7$)	Normal ($\mu = 0.829, \sigma = 0.071$)
Walk	1 m	0^o	Nakagami-m ($\mu = 3.54, \omega = 0.39$)	Lognormal ($\mu = -0.31, \sigma = 0.12$)
Walk	1 m	90^o	Gamma ($a = 1.26, b = 0.13$)	Gamma ($a = 5.7, b = 0.084$)
Walk	1 m	180^o	Normal ($\mu = 0.47, \sigma = 0.17$)	Weibull ($a = 0.65, b = 3.98$)
Walk	1 m	270^o	Lognormal ($a = -1.38, b = 0.58$)	Gamma ($a = 2.04, b = 0.090$)
Stand	2 m	0^o	Lognormal ($\mu = -0.14, \sigma = 0.090$)	Lognormal ($\mu = -0.051, \sigma = 0.018$)
Stand	2 m	90^o	Normal ($\mu = 0.95, \sigma = 0.022$)	Lognormal ($\mu = -0.098, \sigma = 0.023$)
Stand	2 m	180^o	Lognormal ($\mu = -0.14, \sigma = 0.086$)	Weibull ($a = 0.85, b = 8.98$)
Stand	2 m	270^o	Lognormal ($\mu = -0.13, \sigma = 0.068$)	Lognormal ($\mu = -0.34, \sigma = 0.14$)
Walk	2 m	0^o	Lognormal ($\mu = -1.54, \sigma = 0.50$)	Lognormal ($\mu = -0.41, \sigma = 0.19$)
Walk	2 m	90^o	Lognormal ($\mu = -0.78, \sigma = 0.28$)	Weibull ($a = 0.61, b = 2.43$)
Walk	2 m	180^o	Lognormal ($\mu = -1.81, \sigma = 0.72$)	Gamma ($a = 5.47, b = 0.073$)
Walk	2 m	270^o	Weibull ($a = 0.59, b = 2.48$)	Gamma ($a = 2.94, b = 0.11$)
Stand	3 m	0^o	Lognormal ($\mu = -0.31, \sigma = 0.11$)	Lognormal ($\mu = -0.13, \sigma = 0.031$)
Stand	3 m	90^o	Normal ($\mu = 0.93, \sigma = 0.032$)	Weibull ($a = 0.93, b = 31.9$)
Stand	3 m	180^o	Lognormal ($\mu = -0.15, \sigma = 0.082$)	Lognormal ($\mu = -0.14, \sigma = 0.045$)
Stand	3 m	270^o	Lognormal ($\mu = -0.11, \sigma = 0.050$)	Lognormal ($\mu = -0.28, \sigma = 0.075$)
Walk	3 m	0^o	Weibull ($a = 0.67, b = 3.93$)	Nakagami-m ($m = 7.17, \omega = 0.43$)
Walk	3 m	90^o	Lognormal ($\mu = -1.31, \sigma = 0.67$)	Nakagami-m ($m = 1.23, \omega = 0.27$)
Walk	3 m	180^o	Gamma ($a = 2.80, b = 0.13$)	Lognormal ($\mu = -0.99, \sigma = 0.39$)
Walk	3 m	270^o	Lognormal ($\mu = -1.43, \sigma = 0.76$)	Weibull ($a = 0.74, b = 5.02$)
Stand	4 m	0^o	Lognormal ($\mu = -0.072, \sigma = 0.031$)	Lognormal ($\mu = -0.10, \sigma = 0.031$)
Stand	4 m	90^o	Lognormal ($\mu = -0.057, \sigma = 0.031$)	Lognormal ($\mu = -0.30, \sigma = 0.16$)
Stand	4 m	180^o	Lognormal ($\mu = -0.15, \sigma = 0.049$)	Normal ($\mu = 0.90, \sigma = 0.053$)
Stand	4 m	270^o	Weibull ($a = 0.90, b = 14.5$)	Normal ($\mu = 0.91, \sigma = 0.037$)
Walk	4 m	0^o	Nakagami-m ($m = 4.01, \omega = 0.46$)	Lognormal ($\mu = -0.77, \sigma = 0.33$)
Walk	4 m	90^o	Weibull ($a = 0.69, b = 3.43$)	Nakagami-m ($a = 1.24, b = 0.26$)
Walk	4 m	180^o	Lognormal ($\mu = -1.25, \sigma = 0.65$)	Weibull ($a = 0.54, b = 2.37$)
Walk	4 m	270^o	Lognormal ($\mu = -1.47, \sigma = 0.69$)	Gamma ($a = 2.60, b = 0.15$)

Table 4: Scenarios and the distribution (with parameters) that gives the best of the "best fits" to those scenarios transmitting from Right wrist to receiver off the body at 820 MHz and 2.36 GHz,(Angle is orientation of the subject with respect to the receiver, D. is horizontal distance from subject to receiver)

Action	D.	Angle	Distribution	
			820 MHz	2.36 GHz
Stand	1 m	0^o	Normal ($\mu = 0.94, \sigma = 0.025$)	Gamma ($a = 217.5, b = 0.0039$)
Stand	1 m	90^o	Normal ($\mu = 0.93, \sigma = 0.033$)	Lognormal ($\mu = -0.20, \sigma = 0.0.089$)
Stand	1 m	180^o	Lognormal ($\mu = -0.041, \sigma = 0.014$)	Nakagami-m ($m = 15.2, \omega = 0.65$)
Stand	1 m	270^o	Lognormal ($\mu = -0.13, \sigma = 0.033$)	Lognormal ($\mu = -0.18, \sigma = 0.066$)
Walk	1 m	0^o	Gamma ($a = 0.67, b = 0.45$)	Gamma ($a = 0.82, b = 0.26$)
Walk	1 m	90^o	Lognormal ($\mu = -2.26, \sigma = 1.33$)	Lognormal ($\mu = -2.51, \sigma = 1.70$)
Walk	1 m	180^o	Nakagami-m ($m = 0.84, \omega = 0.23$)	Lognormal ($\mu = -3.17, \sigma = 1.50$)
Walk	1 m	270^o	Nakagami-m ($m = 0.72, \omega = 0.19$)	Gamma ($a = 2.22, b = 0.12$)
Stand	2 m	0^o	Weibull ($a = 0.95, b = 37.5$)	Lognormal ($\mu = -0.21, \sigma = 0.044$)
Stand	2 m	90^o	Lognormal ($\mu = -0.099, \sigma = 0.028$)	Lognormal ($\mu = -0.12, \sigma = 0.047$)
Stand	2 m	180^o	Lognormal ($\mu = -0.094, \sigma = 0.038$)	Gamma ($a = 1164, b = 0.00079$)
Stand	2 m	270^o	Lognormal ($\mu = -0.095, \sigma = 0.032$)	Lognormal ($\mu = -0.11, \sigma = 0.046$)
Walk	2 m	0^o	Lognormal ($\mu = -1.06, \sigma = 0.46$)	Gamma ($a = 1.03, b = 0.13$)
Walk	2 m	90^o	Lognormal ($\mu = -1.95, \sigma = 1.38$)	Lognormal ($\mu = -2.63, \sigma = 1.44$)
Walk	2 m	180^o	Gamma ($a = 2.49, b = 0.13$)	Lognormal ($\mu = -2.58, \sigma = 1.28$)
Walk	2 m	270^o	Gamma ($a = 2.96, b = 0.12$)	Lognormal ($\mu = -1.65, \sigma = 0.77$)
Stand	3 m	0^o	Lognormal ($\mu = -0.15, \sigma = 0.043$)	Lognormal ($\mu = -0.51, \sigma = 0.25$)
Stand	3 m	90^o	Lognormal ($\mu = -0.16, \sigma = 0.058$)	Weibull ($a = 0.88, b = 13.8$)
Stand	3 m	180^o	Normal ($\mu = 0.87, \sigma = 0.050$)	Lognormal ($\mu = -0.10, \sigma = 0.035$)
Stand	3 m	270^o	Lognormal ($\mu = -0.19, \sigma = 0.075$)	Normal ($\mu = 0.92, \sigma = 0.024$)
Walk	3 m	0^o	Lognormal ($\mu = -2.38, \sigma = 1.40$)	Lognormal ($\mu = -2.15, \sigma = 1.10$)
Walk	3 m	90^o	Lognormal ($\mu = -1.55, \sigma = 0.93$)	Lognormal ($\mu = -2.38, \sigma = 1.21$)
Walk	3 m	180^o	Nakagami-m ($m = 0.57, \omega = 0.26$)	Lognormal ($\mu = -2.47, \sigma = 1.32$)
Walk	3 m	270^o	Gamma ($a = 5.14, b = 0.085$)	Lognormal ($\mu = -2.21, \sigma = 0.83$)
Stand	4 m	0^o	Normal ($\mu = 0.88, \sigma = 0.039$)	Lognormal ($\mu = -0.099, \sigma = 0.041$)
Stand	4 m	90^o	Normal ($\mu = 0.89, \sigma = 0.043$)	Normal ($\mu = 0.90, \sigma = 0.030$)
Stand	4 m	180^o	Lognormal ($\mu = -0.16, \sigma = 0.036$)	Lognormal ($\mu = -0.19, \sigma = 0.059$)
Stand	4 m	270^o	Lognormal ($\mu - 0.24, \sigma = 0.064$)	Normal ($\mu = 0.89, \sigma = 0.034$)
Walk	4 m	0^o	Nakagami-m ($m = 0.77, \omega = 0.18$)	Lognormal ($\mu = -1.68, \sigma = 0.79$)
Walk	4 m	90^o	Nakagami-m ($m = 0.65, \omega = 0.20$)	Lognormal ($\mu = -2.04, \sigma = 1.16$)
Walk	4 m	180^o	Lognormal ($\mu = -1.36, \sigma = 0.64$)	Lognormal ($\mu = -1.69, \sigma = 0.82$)
Walk	4 m	270^o	Nakagami-m ($m = 0.78, \omega = 0.20$)	Lognormal ($\mu = -1.32, \sigma = 0.50$)

3.4 Channel Time-Coherence

As for the on-body measurement report [1], instead of using correlation analysis [1], we use **channel variation factor**, ρ, which is the ratio between the standard deviation (square root of variance) and the root-mean-square power of a sequence $\mathbf{s} = \{s_0, s_1, \ldots, s_{M-1}\}$

$$\rho = \sqrt{\frac{\text{var}(\mathbf{s})}{\frac{1}{M}\sum_{m=0}^{M-1}|s_m|^2}}, \tag{9}$$

where var($\mathbf{s}$) denotes the variance of a vector $\mathbf{s}$.

The variance of a sequence characterizes the variation of the sequence well. By normalizing the standard deviation by the root-mean-square power, the channel variation factor becomes independent of the signal power and is consistent over the whole observation period. Furthermore, it is clear that $0 \leq \rho \leq 1$.

The mathematical application of the channel variation factor to the measured channel response is the same as for the on-body report [1], which we repeat here. We note the following about the channel variation factor ρ:

There are gaps of approximately 2.5 ms between subsets of measurements within a complete measurement set that spans 5 s. The discontinuity between measurement subsets introduces random phase shifts to every measured channel response. To account for this, only the magnitude of the channel response is considered in the following analysis. Note that the magnitude of channel response generally describe the variability of channel quite well as the channel rarely only varies in phase.

Secondly, from the measured channel response, we observe that signals from different propagation paths are mostly overlapped and unresolvable, and they cause extended symbol period and waveform distortion. Hence, the received signal is upsampled at the output of the pulse shaping filter before being correlated with a copy of the transmitted PN sequence. Thus for the mth channel response, we have a vector of L samples, denoted as $\mathbf{h}_m = \{h_m(0), h_m(1), \ldots, h_m(L-1)\}$, with $L = 11$ used in the analysis here. These samples include the peak point and five points on either side of the peak. Channel responses at different times over the complete measurement span are aligned with respect to the peak of all channel responses. For a period of $\tau = MT_f$ (from kT_f to $(k+M-1)T_f$), where T_f is the interval between two adjoint measured channel responses, the overall channel variation factor is computed as follows: 1) Compute the constituent channel variation factor for the ℓth sample $h_m(\ell)$, $\ell = 0, 1, \cdots, L-1$, in the M channel responses according to (9) to obtain $\rho(\ell)$; 2) Compute the mean over all L samples. Mathematically, this is written as

$$\rho(\ell) = \sqrt{\frac{\text{var}\big(\{|h_k(\ell)|, |h_{k+1}(\ell)|, \cdots, |h_{k+M-1}(\ell)|\}\big)}{\frac{1}{M}\sum_{m=k}^{M+k-1}|h_m(\ell)|^2}}; \tag{10}$$

and

$$\rho = \frac{1}{L}\sum_{\ell=0}^{L-1}\rho(\ell). \tag{11}$$

[1] for channel time coherence analysis, conventional correlation analysis can not characterize the variation of the channel within a time period well. This is because the correlation method detects only linear dependencies between two sequences, rather than the variability of the two sequences

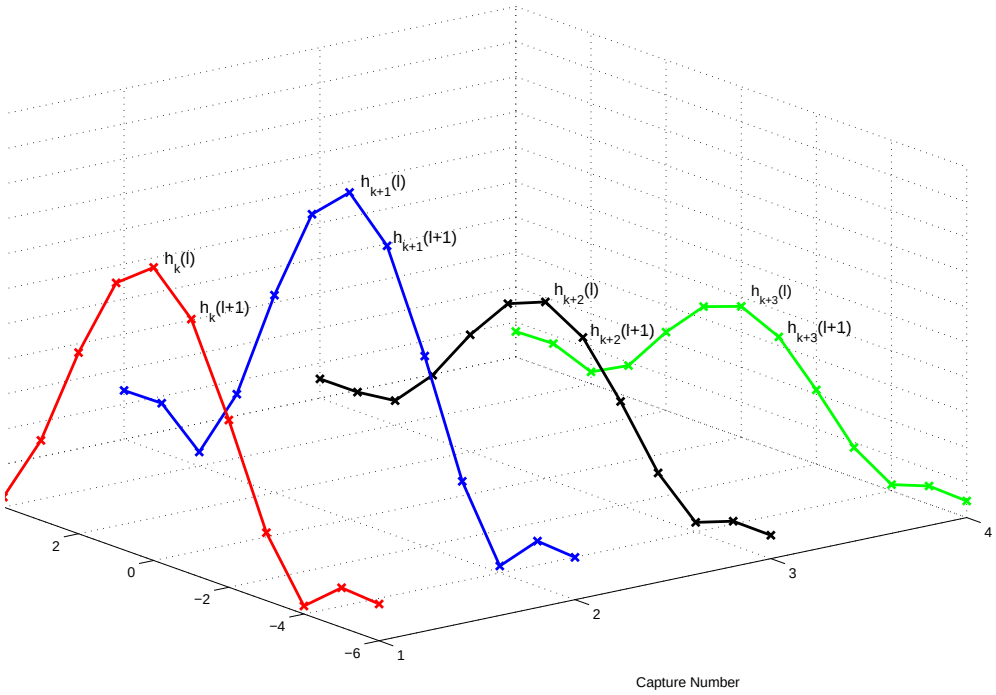

Figure 4: Illustration of some measured impulse responses over time span, $\tau = 4T_f$, (measured along the *Capture Number* axis) used in the calculation of the channel variation factor.

Illustrative example:
In Figure 4 we show four typical measured impulse responses (time span of $4T_f$) in a 3-D graph. The overall channel variation factor ρ over a time span of $\tau = MT_f$ is computed in the following steps:

1. Align the impulse responses according to the peak so that the peaks have the same index ℓ in all impulse responses;
2. Compute the constituent channel variation factor, $\rho(\ell)$, for the ℓth sample $h_m(\ell)$, $\ell = \{0, 1, \ldots, L-1\}$, in the M channel responses according to (10) to get $\rho(\ell)$;
3. Compute the mean over all L samples as in (11) to obtain ρ.

The analysis described above was conducted with channel variation spanning periods τ of 5 ms, 10 ms and 25 ms for the subject standing and walking, physical orientations with respect to the off-body receiver, and distances from the receiver.

In the appendix there are some figures showing the values of ρ over the 5 s meaurement time, for the four subject orientations of 0^o, 90^o, 180^o and 270^o shown within the one figure, with channel variation time varying period τ of 25 ms, with the subject walking on the spot at a horizontal distance of 3m from the receiver; Fig. 325 transmitting from the chest at 820 MHz; Fig. 326 transmitting from the right wrist at 820 MHz; Fig. 327 transmitting from the chest at 2360 MHz; and Fig. 328 transmitting from the right wrist at 2360 MHz. These Figures clearly suggest that

transmitting from the right wrist to the receiver off the body may be less stable than transmitting from the chest to off the body. These Figures also suggest that there is greatest stability when the subject is facing the receiver away from the subject (that is the orientation of 0^o).

To better characterize the channel stability, statistical analysis over the channel variation factors was performed on all measurements. We computed empirical cumulative distribution functions (CDFs) from the measured data for the factors for all scenarios. We combine in one figure CDF results for 820 MHz and 2.36 GHz for $\tau = 5$, $\tau = 10$ and $\tau = 25$ ms for each scenario (subject standing or walking, given distance and orientation). From these Figures we make the following observations: -

- In general there is a sharper rise in cumulative probability for channel variation factors closer to zero is evident while the subject is standing as opposed to walking, indicating greater stability.
- It is also clearly depicted in the CDFs that transmitting from the chest is more stable than transmitting from the right wrist, and there is generally greater stability at 820 MHz, than at 2.36 GHz.
- It is indicated that the slower the rise in cumulative probability is with respect to increase in channel variation for the larger the time-varying period, indicating less stability, over $\tau = 25$ ms than $\tau = 10$ ms, and less stability over $\tau = 10$ ms than $\tau = 5$ ms.

Based on these empirical CDFs as a way of describing the stability of the channel, we compute the probability, for a given scenario and time period, that the variation factor is less than 0.1, or 10% (Thus the greater the probability the more stable the channel by this measure). These probabilities for all scenarios are given in Table 5 when transmitting from the chest, and Table 6 when transmitting from right wrist to the receiver off the body. There are a few noteworthy trends: -

- For all scenarios transmitting from the chest there is very good stability in all cases, with marginally greater stability at the lower measurement frequency of 820 MHz than at 2.36 GHz.
- Transmitting from the right wrist, the channel is less stable than for transmission from the chest; with far less stability transmitting from the right wrist at 2.36 GHz than for transmitting from the chest at 2.36 GHz.
- Furthermore when transmitting from the right wrist the channel is far more stable at 820 MHz than at 2.36 GHz.
- When standing there is generally greatest stability with the orientation of the subject's body facing the receiver away from the body (at 0^o).
- The channel is in generally most stable when the subject is at a distance of 1m from the receiver, as opposed to greater distances away from the receiver.
- In general the channel is more stable when the subject is standing than when walking.

Table 5: Probabilities, based on cumulative distribution functions, that the channel variation factor, for coherence is < 0.1 (or 10%) for time varying periods of 5ms, 10ms and 25ms respectively, transmitting from the chest; S-Standing, W-Walking, Angle is orientation of the subject with respect to the receiver

Distance (m)	Action	Angle (^{o})	Probability channel variation factor < 0.1					
			Periods at 2.36 GHz			Periods at 820 MHz		
			5 ms	10 ms	25 ms	5 ms	10 ms	25 ms
1	S	0	1	1	1	1	1	1
1	S	90	0.989	0.9975	1	1	1	1
1	S	180	0.9945	1	1	1	1	1
1	S	270	0.999	1	1	1	1	1
1	W	0	0.995	0.9885	0.9719	0.9895	0.998	0.9895
1	W	90	0.9795	0.9725	0.8714	0.969	0.9029	0.969
1	W	180	0.9795	0.9755	0.9638	0.9765	0.9434	0.9765
1	W	270	0.959	0.9259	0.7996	0.9795	0.9735	0.9795
2	S	0	1	1	1	1	1	1
2	S	90	1	1	1	1	1	1
2	S	180	0.9775	0.9965	1	1	1	1
2	S	270	1	1	1	1	1	1
2	W	0	0.995	0.989	0.99	0.999	1	0.999
2	W	90	0.981	0.993	0.9879	0.9905	0.994	0.9905
2	W	180	0.9055	0.8593	0.6514	0.976	0.9499	0.976
2	W	270	0.9795	0.993	0.9824	0.981	0.9745	0.981
3	S	0	1	1	1	1	1	1
3	S	90	0.983	1	1	0.991	1	0.991
3	S	180	0.977	0.9599	0.9327	1	1	1
3	S	270	0.969	0.998	1	1	1	1
3	W	0	0.998	0.9975	0.997	1	1	1
3	W	90	0.9655	0.9639	0.9076	0.9715	0.974	0.9715
3	W	180	0.9575	0.9624	0.9588	0.9815	0.9479	0.9815
3	W	270	0.969	0.969	0.9588	0.9845	0.9745	0.9845
4	S	0	0.999	1	1	1	1	1
4	S	90	0.9775	0.9995	1	1	1	1
4	S	180	0.968	0.9865	0.998	1	1	1
4	S	270	1	1	1	1	1	1
4	W	0	0.988	0.985	0.9784	0.988	0.984	0.988
4	W	90	0.9835	0.992	0.9548	0.977	0.9725	0.977
4	W	180	0.978	0.9745	0.9643	0.963	0.9169	0.963
4	W	270	0.9785	0.97	0.897	0.983	0.9629	0.983

Table 6: Probabilities, based on cumulative distribution functions, that the channel variation factor, for coherence is < 0.1 (or 10%) for time varying periods of 5ms, 10ms and 25ms respectively, transmitting from the right wrist

Distance (m)	Action	Angle (^{o})	Probability channel variation factor < 0.1					
			Periods at 2.36 GHz			Periods at 820 MHz		
			5 ms	10 ms	25 ms	5 ms	10 ms	25 ms
1	S	0	1	1	1	1	1	1
1	S	90	0.969	0.9935	1	0.908	0.8908	0.908
1	S	180	0.968	0.987	1	1	1	1
1	S	270	1	1	1	1	1	1
1	W	0	0.8914	0.7301	0.3837	0.99	0.9815	0.99
1	W	90	0.9205	0.8443	0.5892	0.98	0.9449	0.98
1	W	180	0.8209	0.6094	0.2813	0.978	0.9619	0.978
1	W	270	0.8309	0.642	0.3516	0.9695	0.9204	0.9695
2	S	0	0.9205	0.9524	0.99	1	1	1
2	S	90	0.8419	0.8062	0.8458	0.995	1	0.995
2	S	180	0.8779	0.8863	0.9332	1	1	1
2	S	270	0.8884	0.9324	0.9794	0.999	1	0.999
2	W	0	0.8529	0.6495	0.334	0.97	0.9609	0.97
2	W	90	0.8414	0.6465	0.4144	0.964	0.9239	0.964
2	W	180	0.8289	0.6244	0.2873	0.968	0.9349	0.968
2	W	270	0.8879	0.7271	0.2833	0.9815	0.9624	0.9815
3	S	0	0.9425	0.9359	0.9638	0.9895	0.9915	0.9895
3	S	90	0.6423	0.4672	0.2823	0.9995	1	0.9995
3	S	180	0.7914	0.7366	0.6715	0.8694	0.9054	0.8694
3	S	270	0.9865	1	1	0.9955	1	0.9955
3	W	0	0.7909	0.5904	0.2642	0.9625	0.9339	0.9625
3	W	90	0.8484	0.7276	0.5394	0.968	0.9139	0.968
3	W	180	0.8064	0.6249	0.3451	0.904	0.7947	0.904
3	W	270	0.8069	0.5734	0.2009	0.978	0.9574	0.978
4	S	0	1	1	1	1	1	1
4	S	90	0.5858	0.3665	0.1557	1	1	1
4	S	180	0.7454	0.653	0.549	0.99	1	0.99
4	S	270	0.7544	0.695	0.6399	0.976	0.9895	0.976
4	W	0	0.8494	0.6795	0.2712	0.9705	0.9574	0.9705
4	W	90	0.8789	0.7882	0.5008	0.939	0.8793	0.939
4	W	180	0.9035	0.7692	0.4048	0.9575	0.9319	0.9575
4	W	270	0.8324	0.6575	0.3169	0.937	0.8693	0.937

4 Concluding Remarks

In the case of transmission on the human body to off the body in an indoor environment, the movement of the human body causing time-selective fading is the dominant fading effect. However in some cases there is clearly observable frequency-selective fading, mainly in the case of the subject standing still (because there is not time-selective fading due to movement).

The path loss transmitting from on the body to off the body is generally less than the path loss around the human body documented in [1] (particularly for smaller separation between transmitter on the body and receiver off the body). There is greater path loss at 2.36 GHz than at 820 MHz, as expected.

The Lognormal distribution is the best matching model to data sets of normalized received power for on-body to off-body communications while the subject is in motion and standing still, independent of location of antenna on the human body (chest or right wrist), independent of orientation of body and independent of off-body receiver separation. We also note that in terms of received power, in no cases does the Rayleigh distribution provide the best fit, and the Normal distribution only provides the best cases in a few cases of the subject standing still.

Generally, from time varying coherence analysis, it can be observed that the channel is generally quite stable, and more so at 820 MHz than 2.36 GHz. The motion of the subject has some impact on the stability of the channel, particularly as the period of interest increases. The generally greater stability at lower frequency can be attributed to the longer wavelength, particularly when transmitting from the wrist. When transmitting from the wrist to off-the body there is less stability at 2.36 GHz, than the chest. When transmitting from the chest the channel is only marginally more stable at the lower frequency. From coherence analysis it could be concluded that carrier frequency, and prospective placement of transmitting antenna, need to be carefully considered in on-body to off-body wireless system design. Carrier frequency and antenna placement in on-body to off-body communications appear more important than human body motion (at least in the case of limited movement).

References

[1] D. Miniutti, L. Hanlen, D. Smith, A. Zhang, D. Lewis, D. Rodda, and B. Gilbert, "Narrowband channel characterization for body area networks," 15-08-0421-00-0006-narrowband-channel-characterization-for-BAN.

[2] K. Yazdandoost and K. Sayrafian, "Channel Model for Body Area Network (BAN)," 15-08-0033-02-0006-draft-of-channel-model-for-body-area-network.

[3] D. Freedman and P. Diaconis, "On the histogram as a density estimator:L_2 theory," *Probability Theory and Related Fields*, vol. 57, no. 4, pp. 453–476, December 1981.

A Appendix

This appendix catalogs the entire set of results obtained from the measurements that were performed. It is located at the end of the document to accommodate those who wish to print this section separately, or not at all.

A.1 Channel Power Spectral Density

A.1.1 820 MHz Measurements

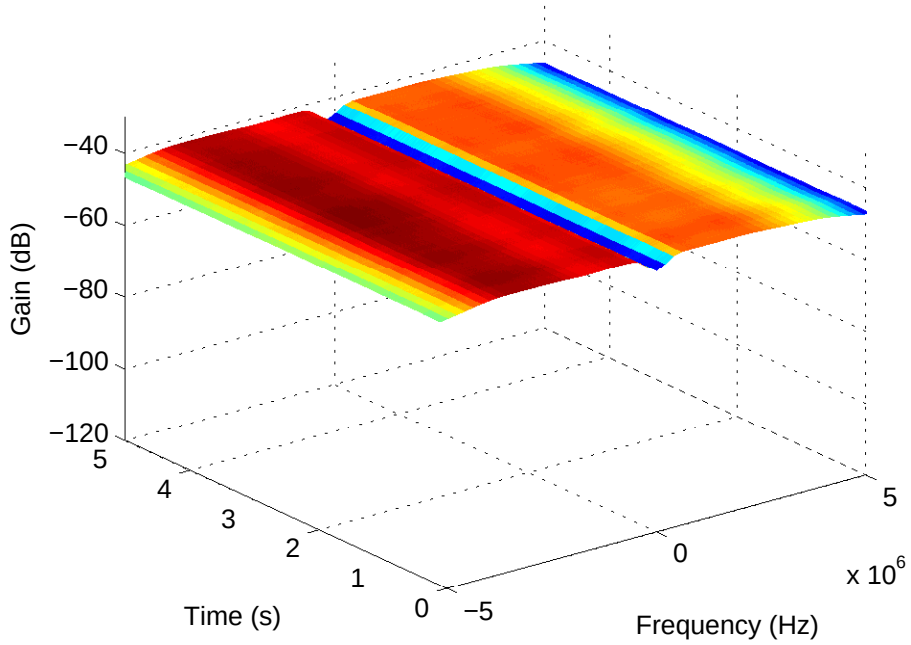

Figure 5: PSD at 820 MHz: chest to off-body; Standing; 1 m separation; 0° orientation

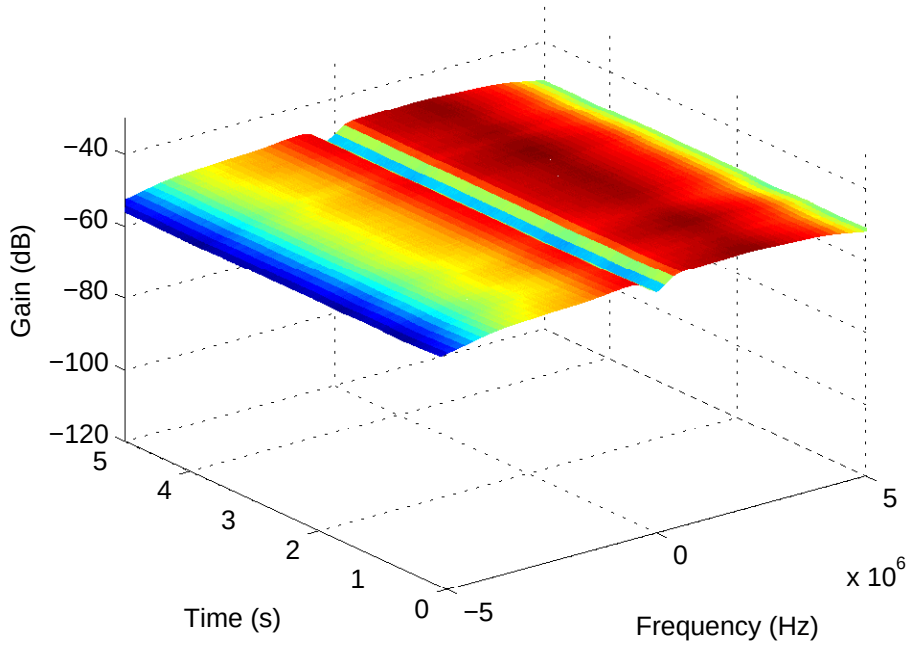

Figure 6: PSD at 820 MHz: chest to off-body; Standing; 1 m separation; 90° orientation

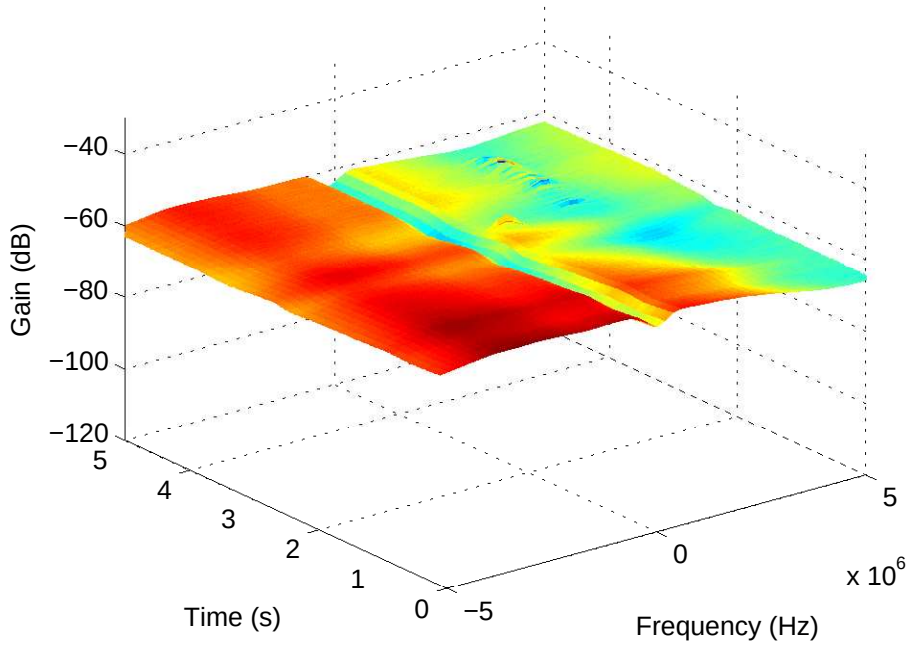

Figure 7: PSD at 820 MHz: chest to off-body; Standing; 1 m separation; 180° orientation

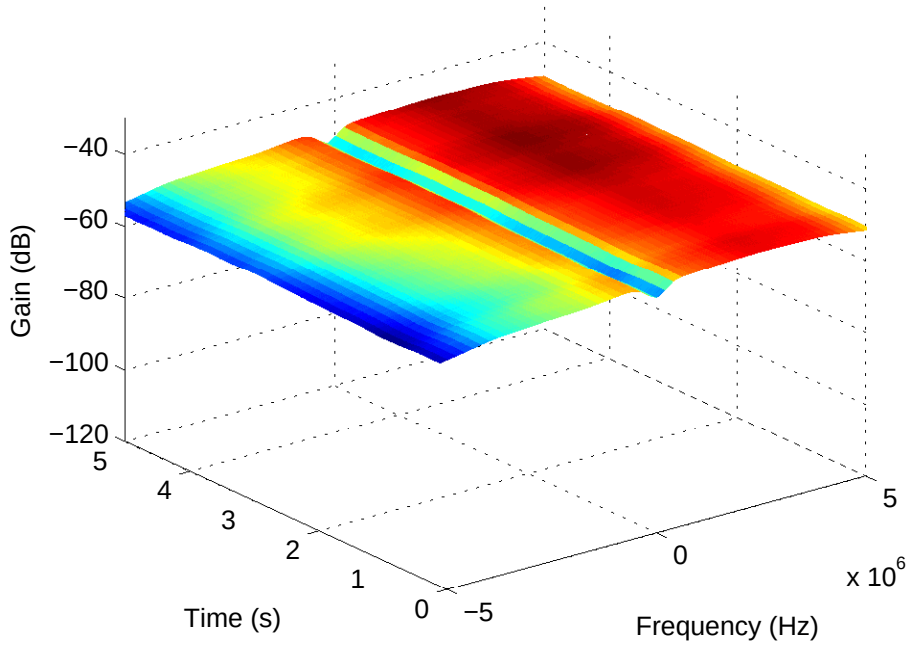

Figure 8: PSD at 820 MHz: chest to off-body; Standing; 1 m separation; 270° orientation

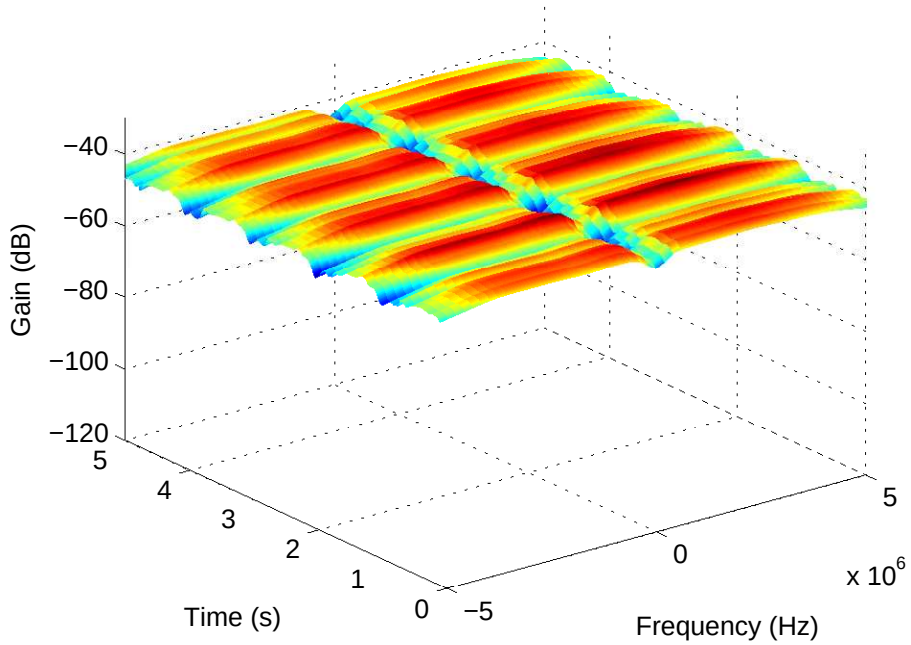

Figure 9: PSD at 820 MHz: chest to off-body; Walking; 1 m separation; 0° orientation

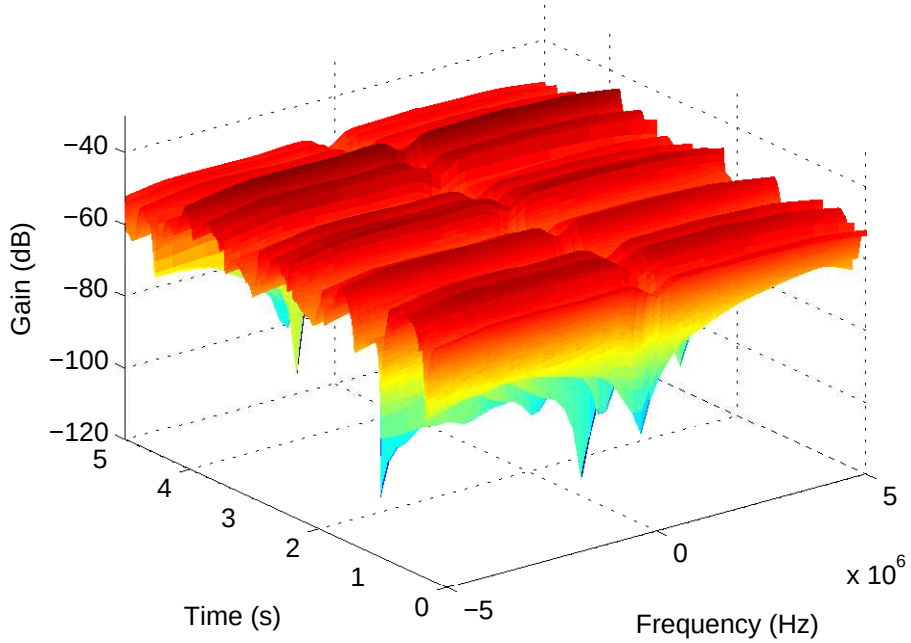

Figure 10: PSD at 820 MHz: chest to off-body; Walking; 1 m separation; 90° orientation

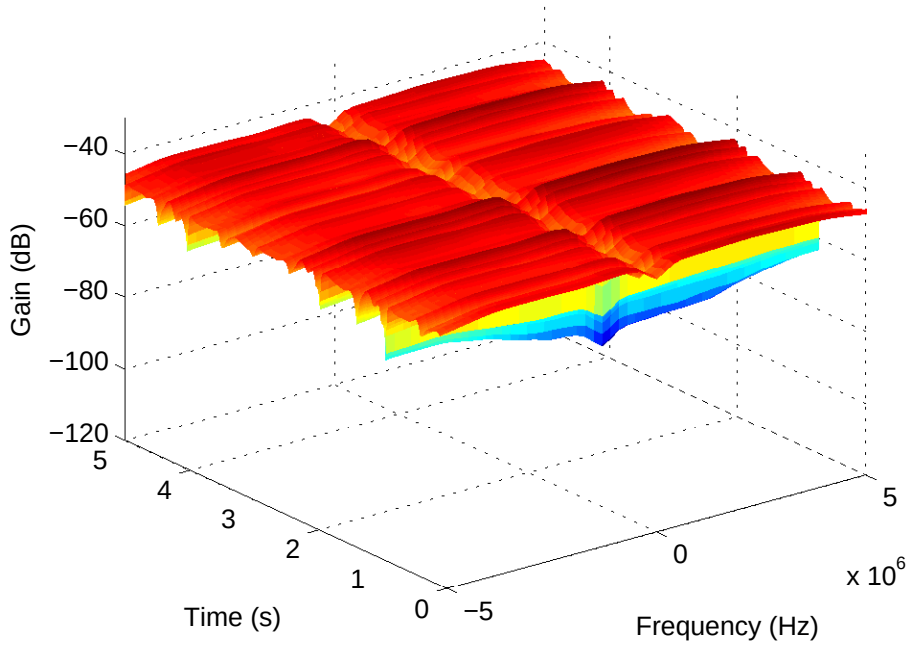

Figure 11: PSD at 820 MHz: chest to off-body; Walking; 1 m separation; 180° orientation

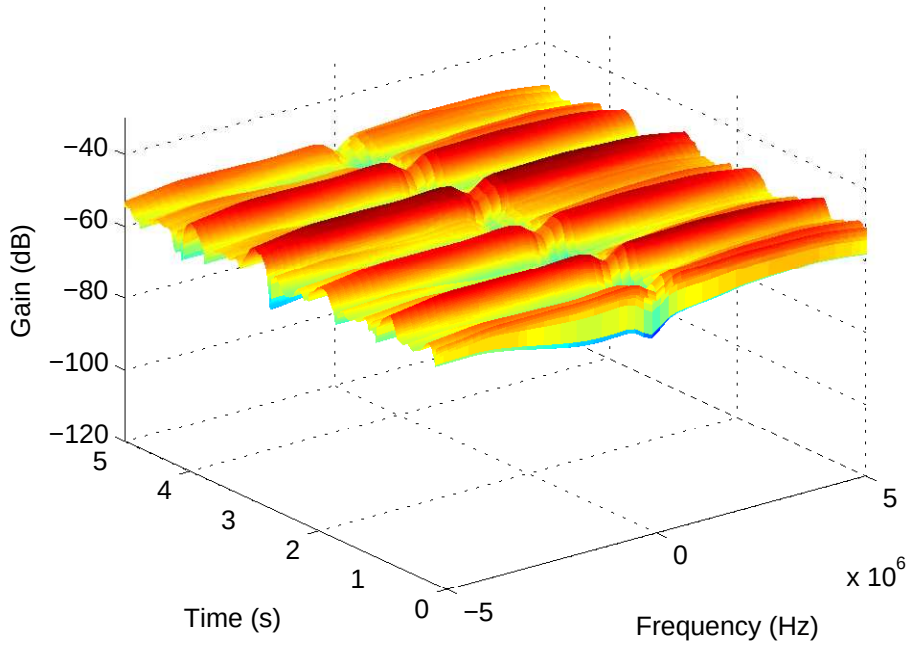

Figure 12: PSD at 820 MHz: chest to off-body; Walking; 1 m separation; 270° orientation

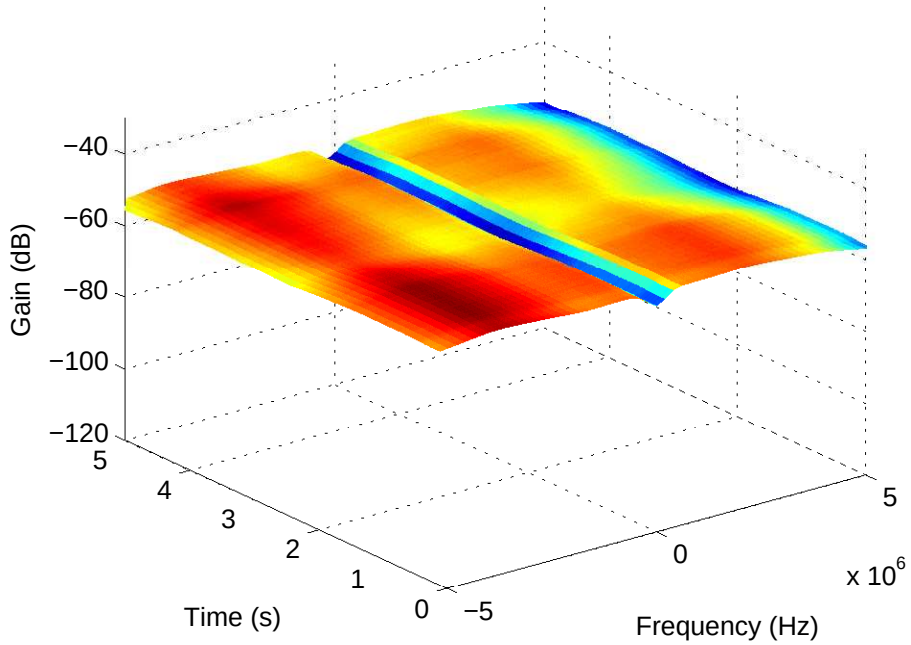

Figure 13: PSD at 820 MHz: chest to off-body; Standing; 2 m separation; 0° orientation

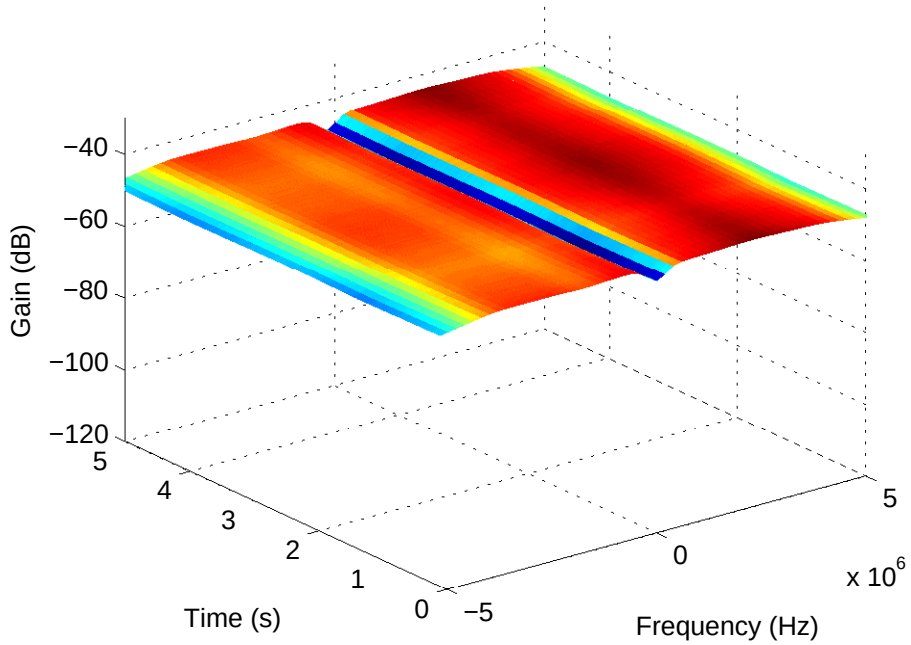

Figure 14: PSD at 820 MHz: chest to off-body; Standing; 2 m separation; 90° orientation

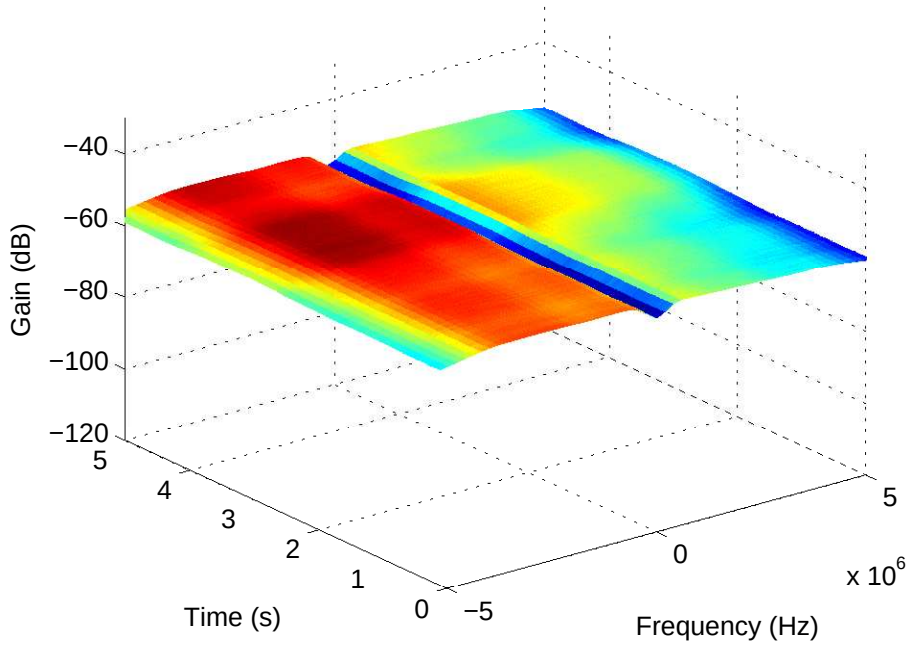

Figure 15: PSD at 820 MHz: chest to off-body; Standing; 2 m separation; 180° orientation

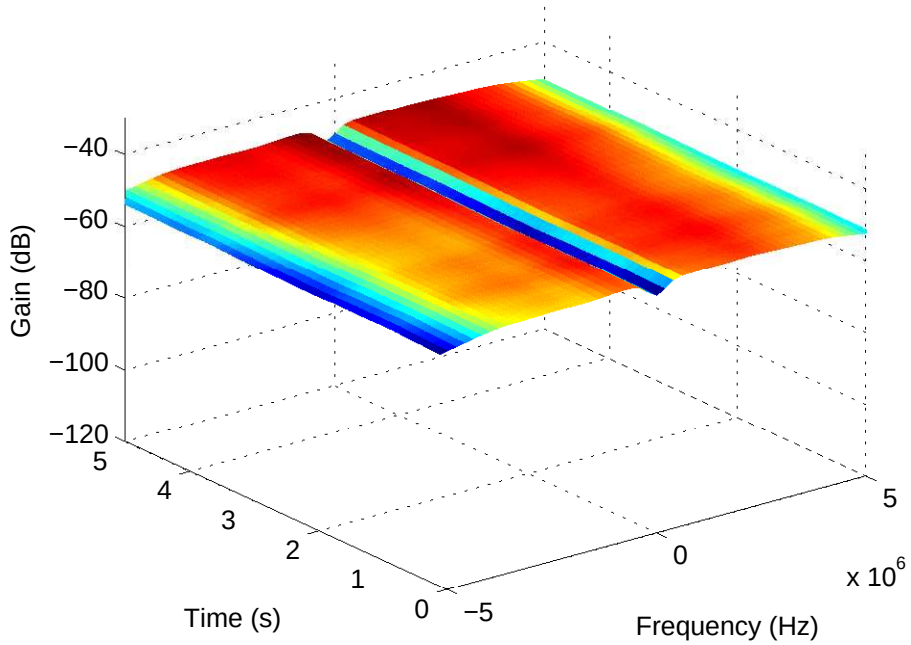

Figure 16: PSD at 820 MHz: chest to off-body; Standing; 2 m separation; 270° orientation

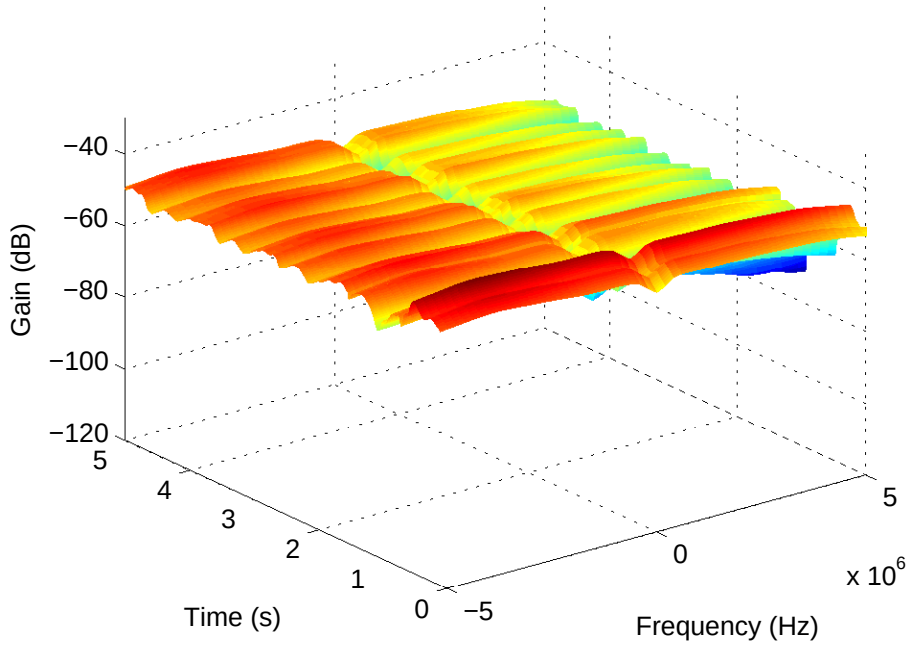

Figure 17: PSD at 820 MHz: chest to off-body; Walking; 2 m separation; 0° orientation

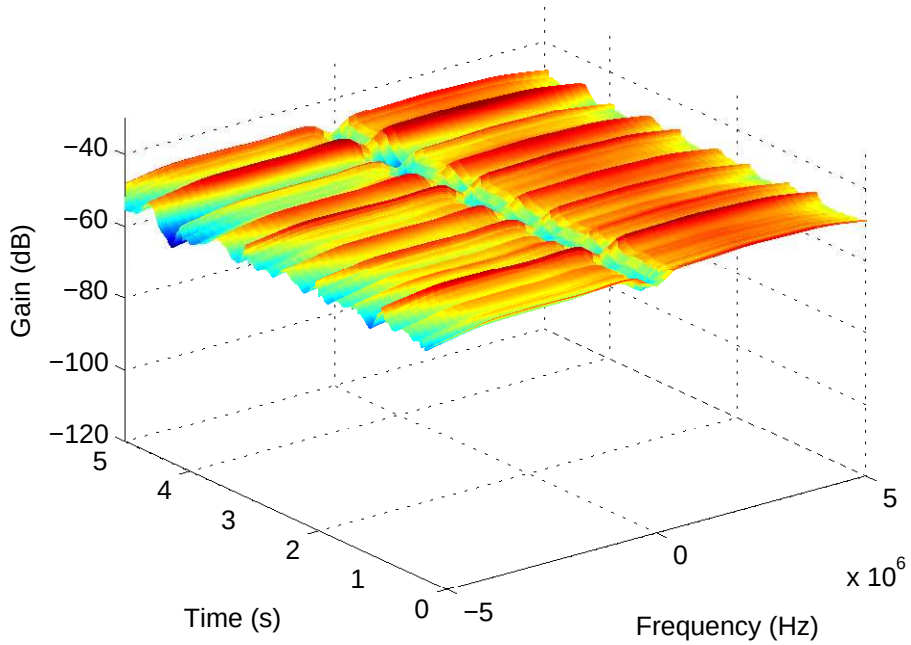

Figure 18: PSD at 820 MHz: chest to off-body; Walking; 2 m separation; 90° orientation

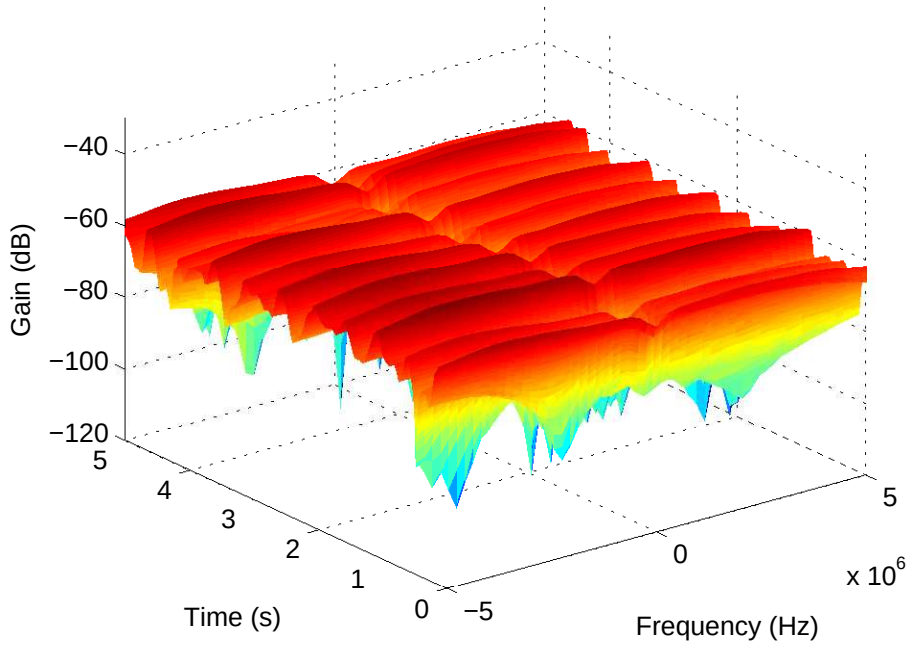

Figure 19: PSD at 820 MHz: chest to off-body; Walking; 2 m separation; 180° orientation

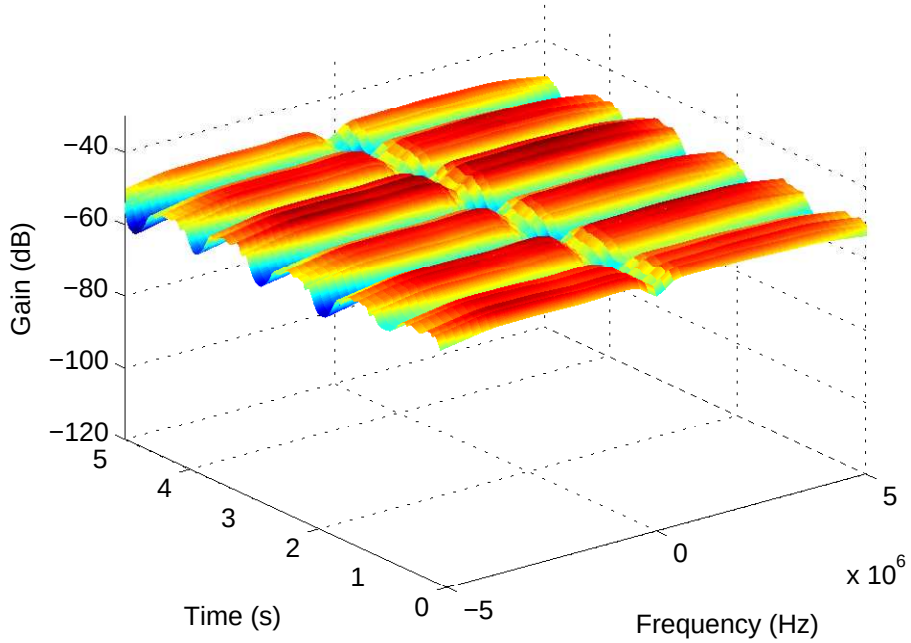

Figure 20: PSD at 820 MHz: chest to off-body; Walking; 2 m separation; 270° orientation

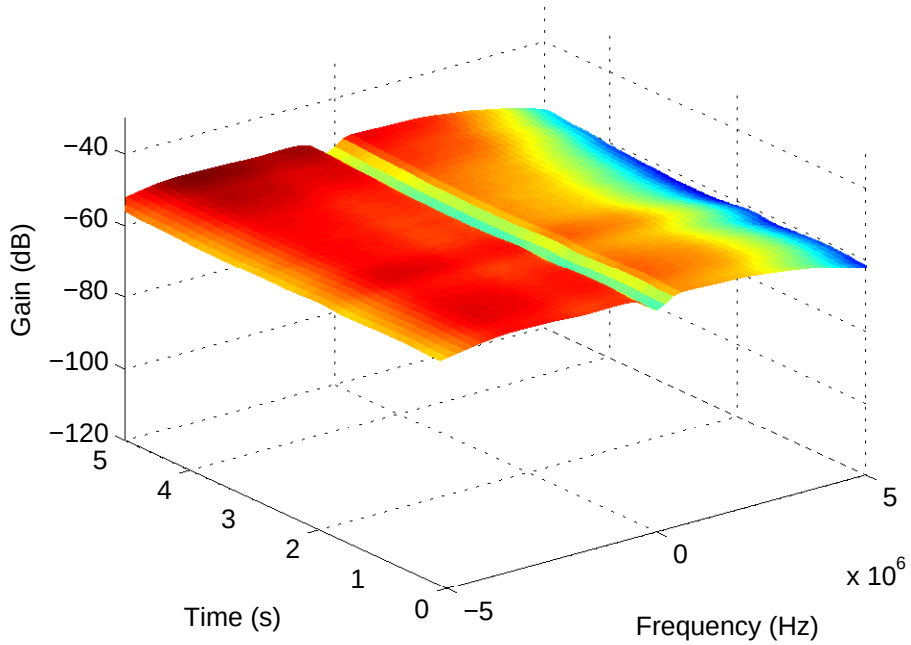

Figure 21: PSD at 820 MHz: chest to off-body; Standing; 3 m separation; 0° orientation

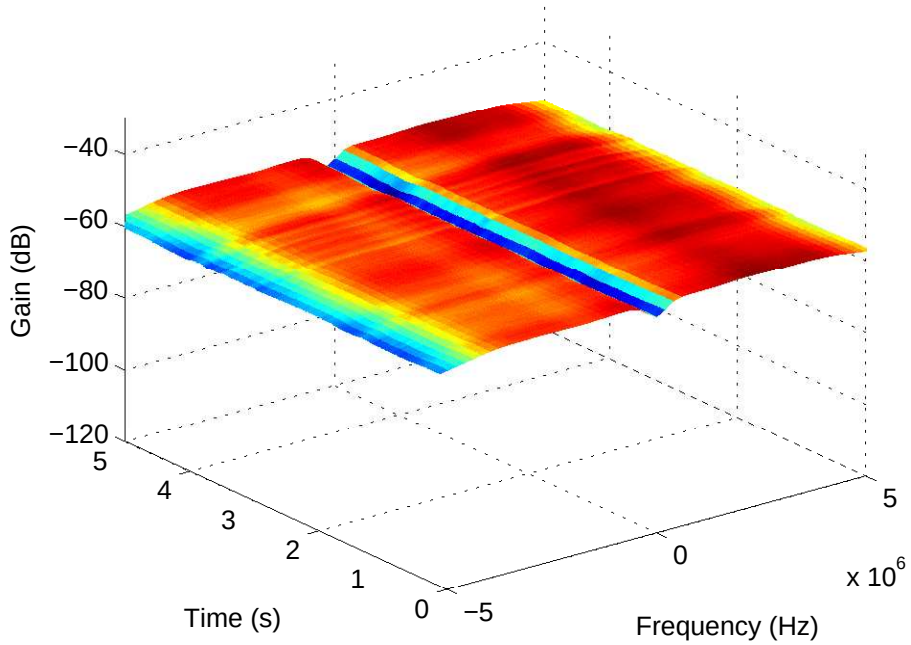

Figure 22: PSD at 820 MHz: chest to off-body; Standing; 3 m separation; 90° orientation

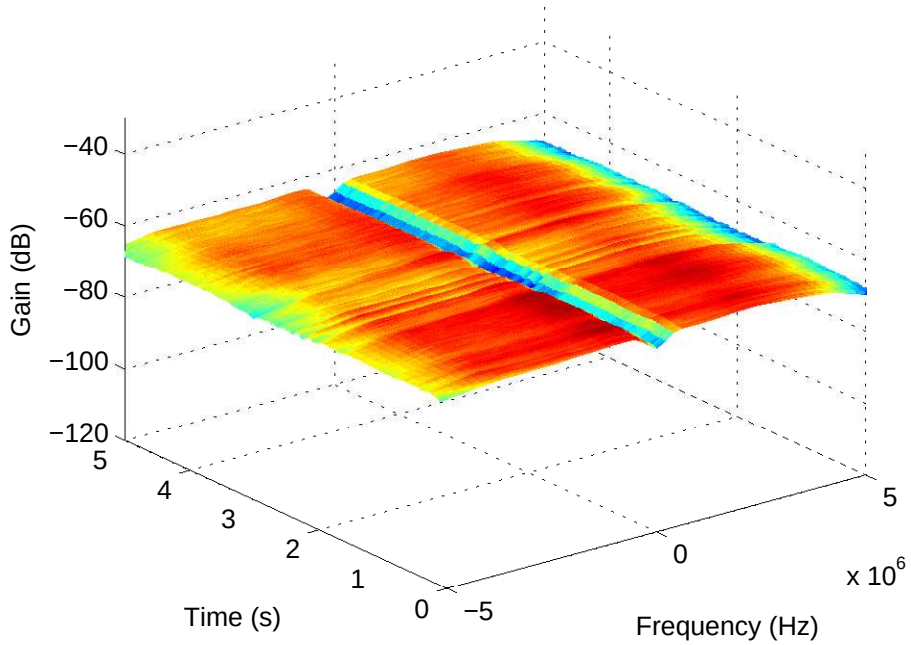

Figure 23: PSD at 820 MHz: chest to off-body; Standing; 3 m separation; 180° orientation

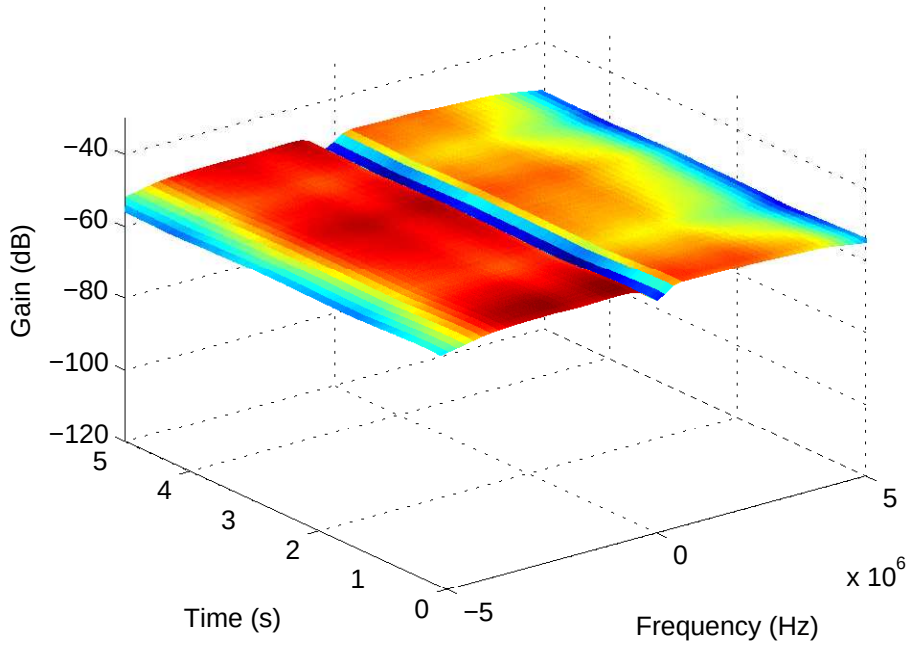

Figure 24: PSD at 820 MHz: chest to off-body; Standing; 3 m separation; 270° orientation

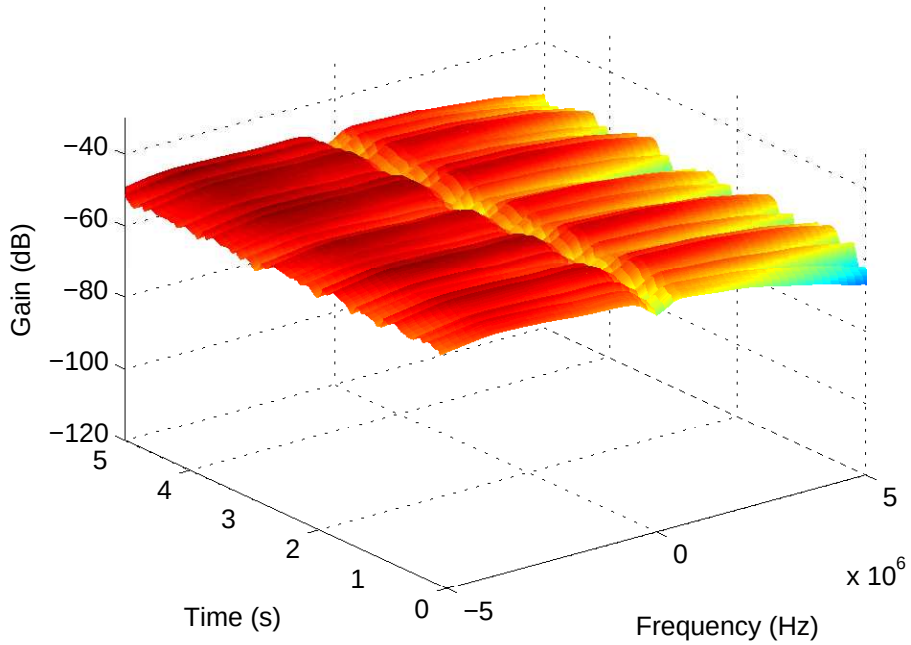

Figure 25: PSD at 820 MHz: chest to off-body; Walking; 3 m separation; 0° orientation

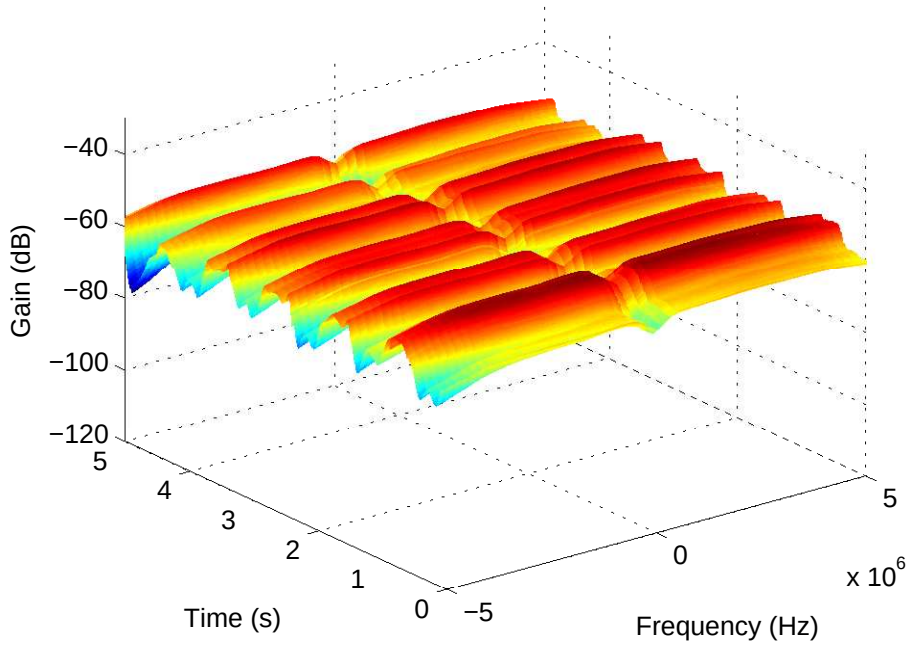

Figure 26: PSD at 820 MHz: chest to off-body; Walking; 3 m separation; 90° orientation

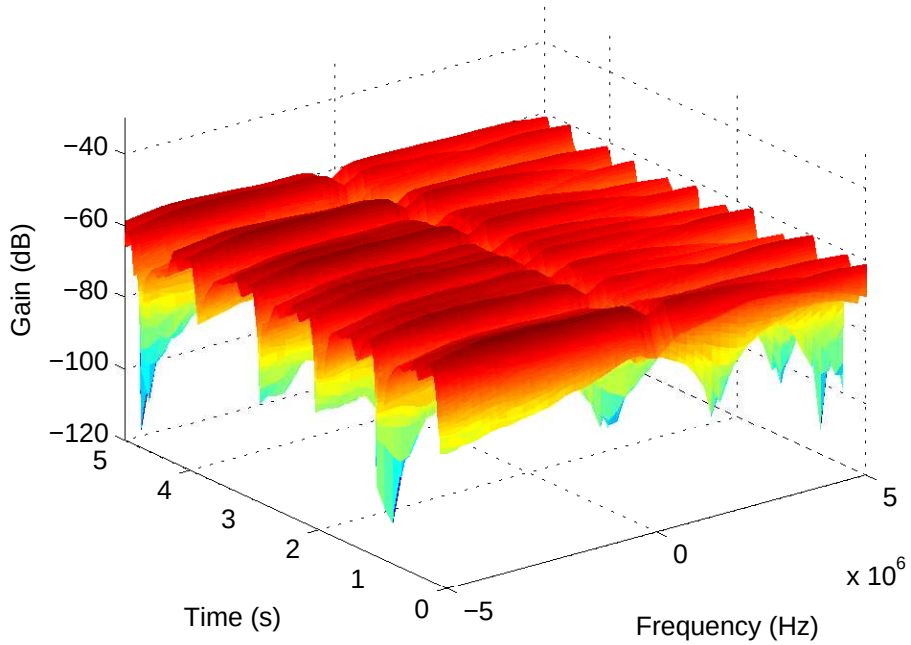

Figure 27: PSD at 820 MHz: chest to off-body; Walking; 3 m separation; 180° orientation

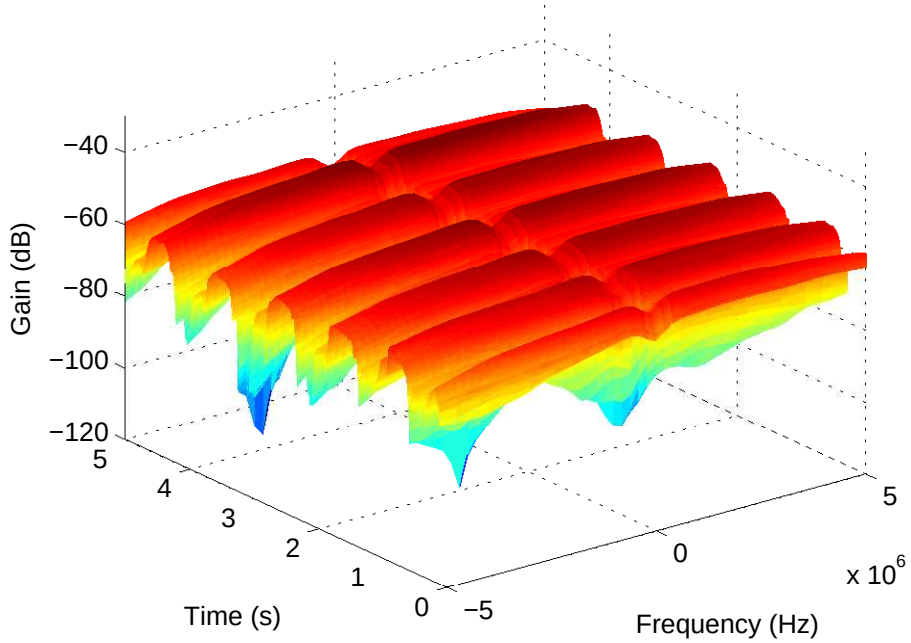

Figure 28: PSD at 820 MHz: chest to off-body; Walking; 3 m separation; 270° orientation

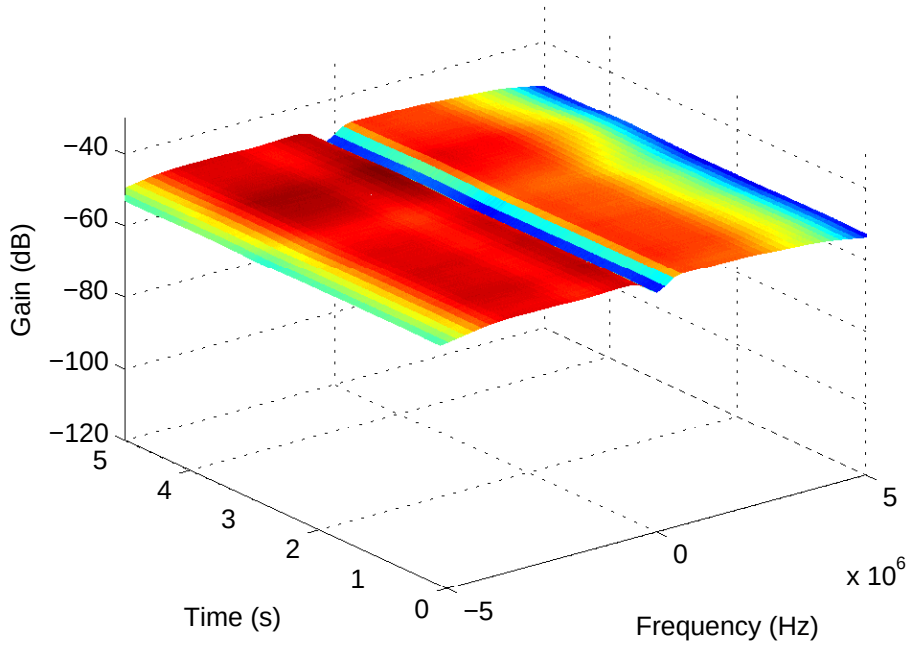

Figure 29: PSD at 820 MHz: chest to off-body; Standing; 4 m separation; 0° orientation

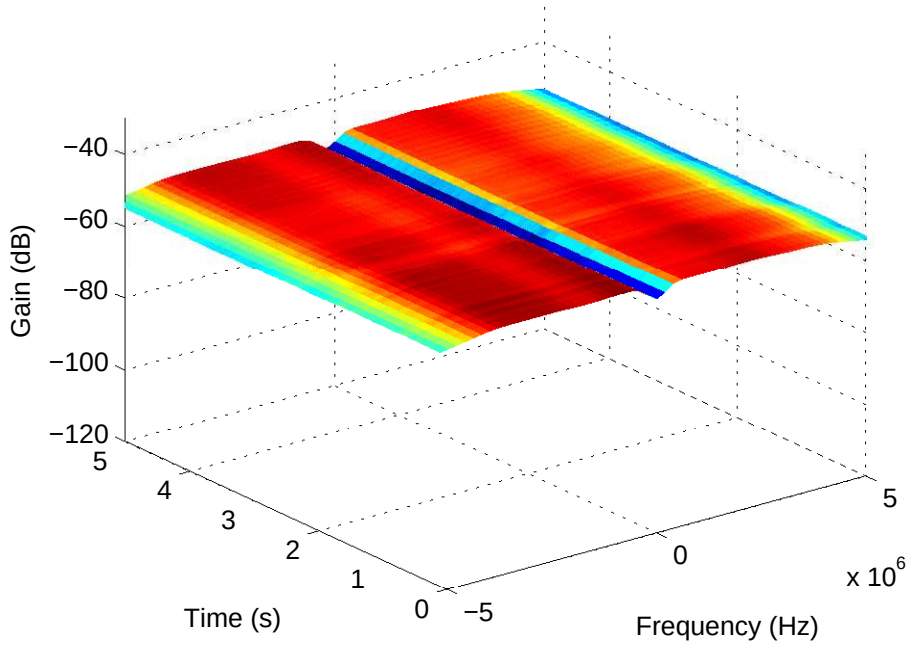

Figure 30: PSD at 820 MHz: chest to off-body; Standing; 4 m separation; 90° orientation

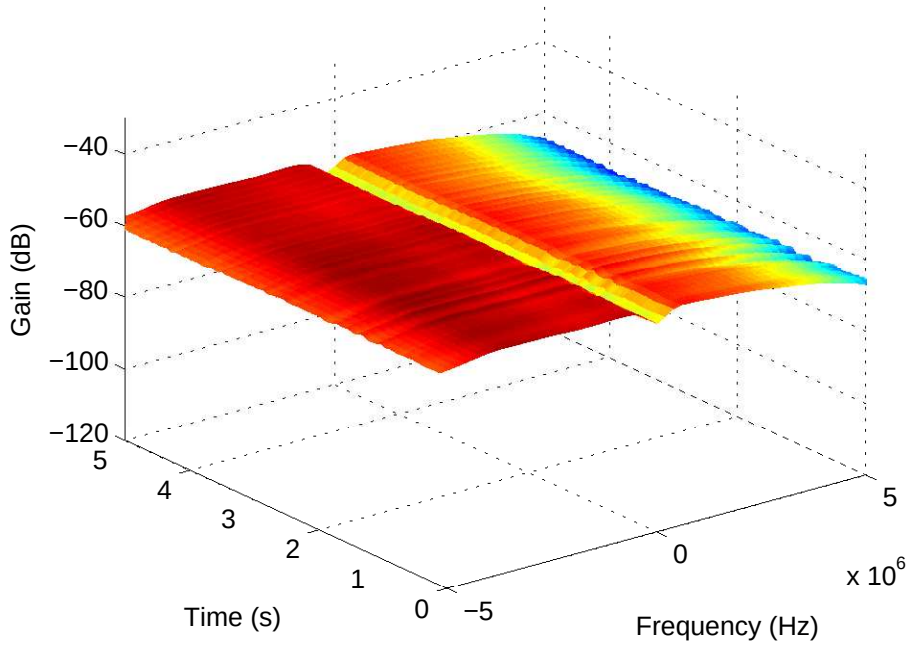

Figure 31: PSD at 820 MHz: chest to off-body; Standing; 4 m separation; 180° orientation

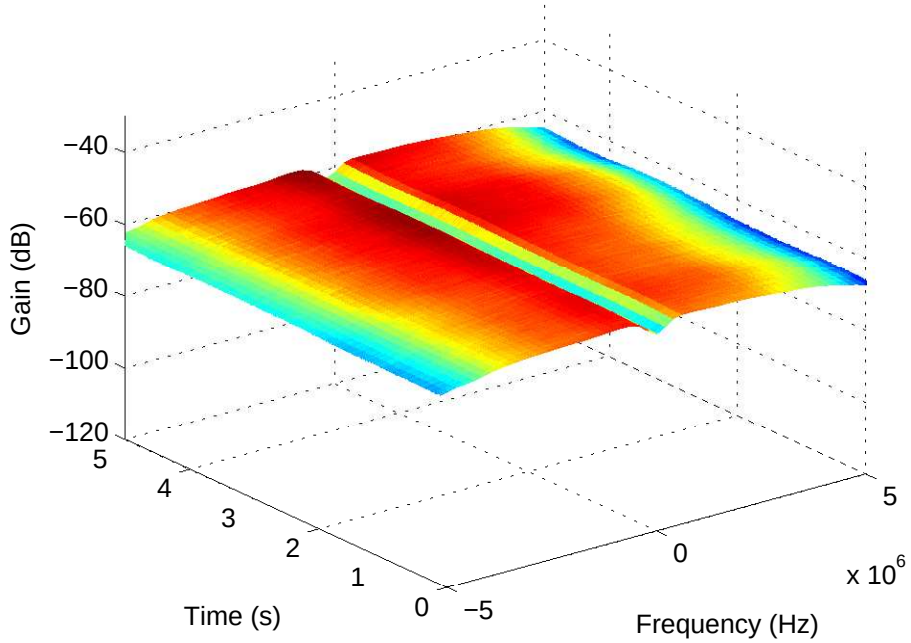

Figure 32: PSD at 820 MHz: chest to off-body; Standing; 4 m separation; 270° orientation

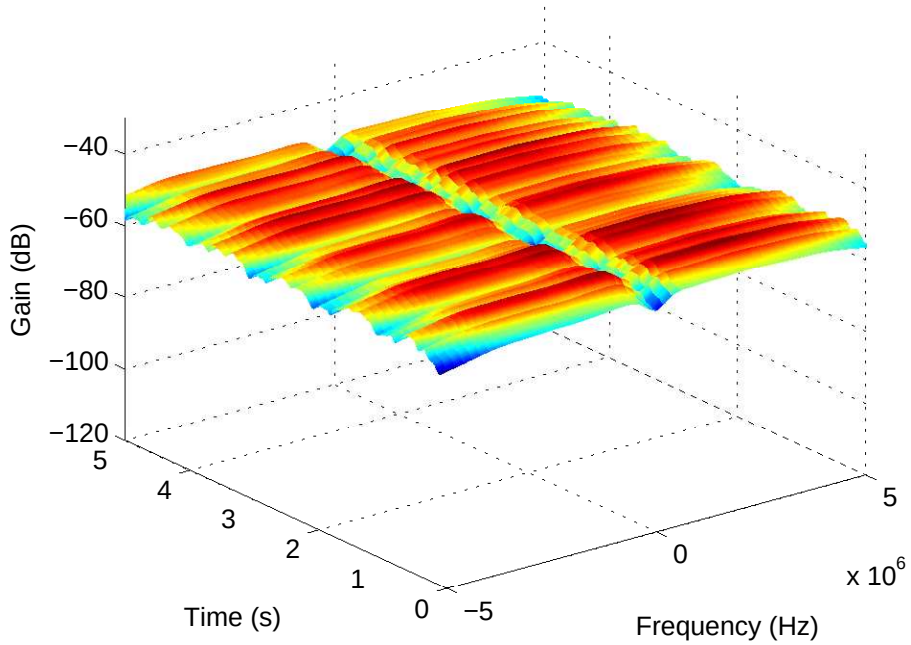

Figure 33: PSD at 820 MHz: chest to off-body; Walking; 4 m separation; 0° orientation

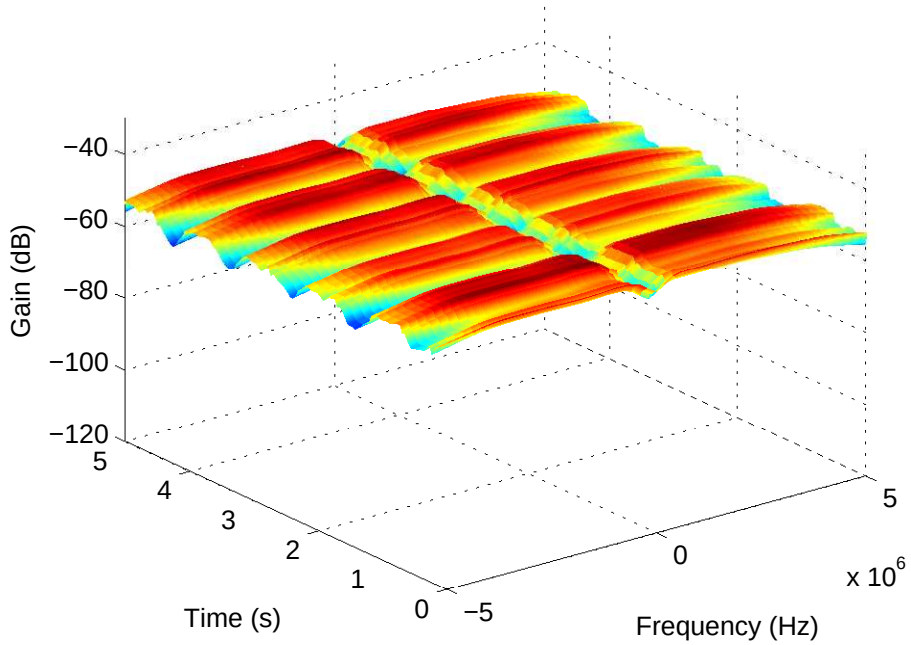

Figure 34: PSD at 820 MHz: chest to off-body; Walking; 4 m separation; 90° orientation

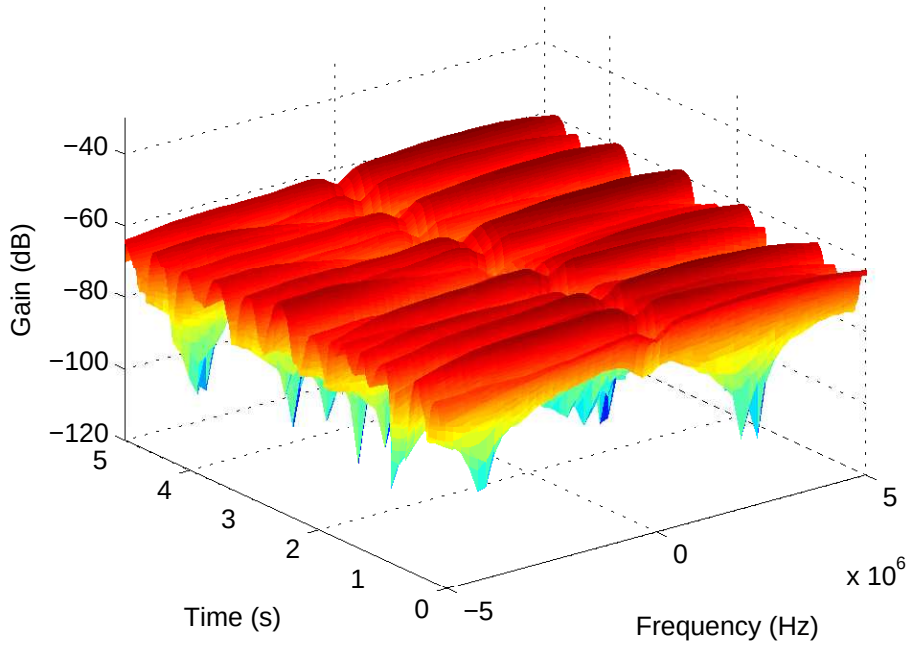

Figure 35: PSD at 820 MHz: chest to off-body; Walking; 4 m separation; 180° orientation

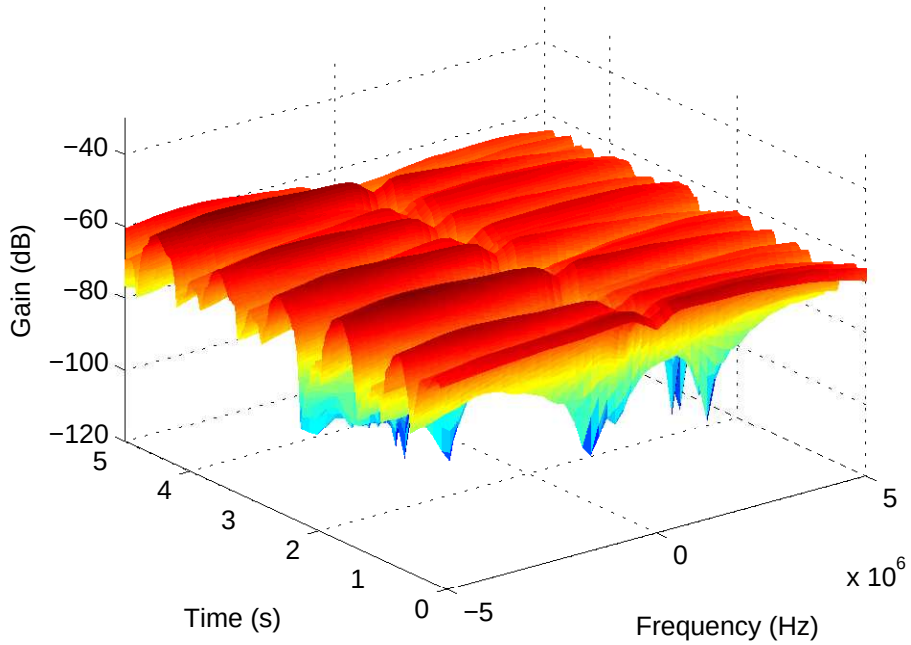

Figure 36: PSD at 820 MHz: chest to off-body; Walking; 4 m separation; 270° orientation

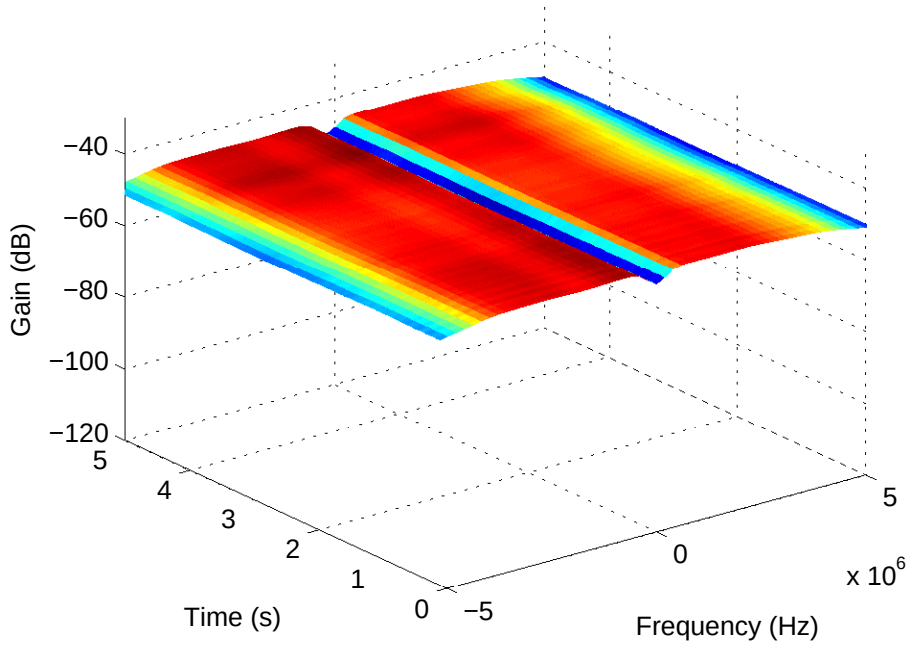

Figure 37: PSD at 820 MHz: right wrist to off-body; Standing; 1 m separation; 0° orientation

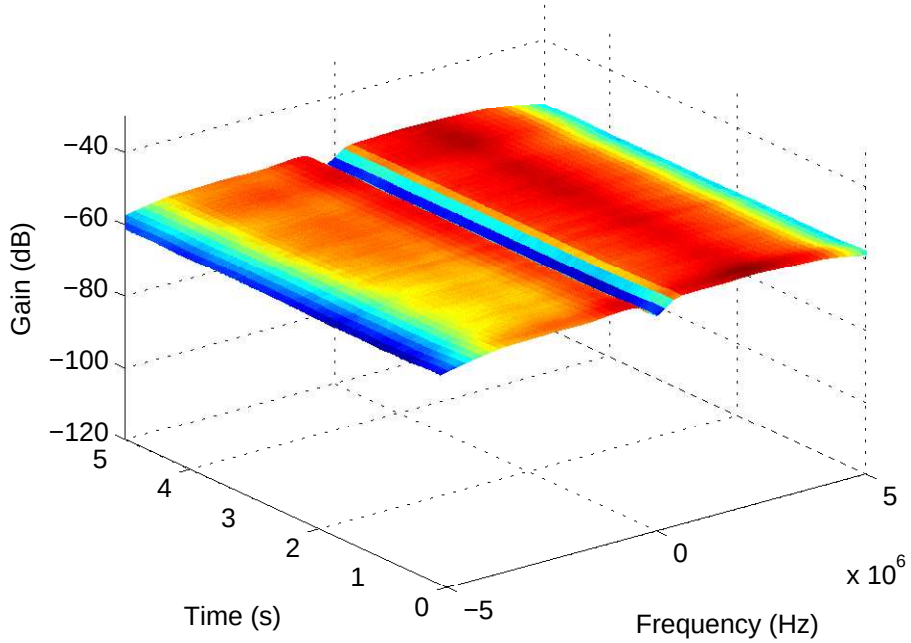

Figure 38: PSD at 820 MHz: right wrist to off-body; Standing; 1 m separation; 90° orientation

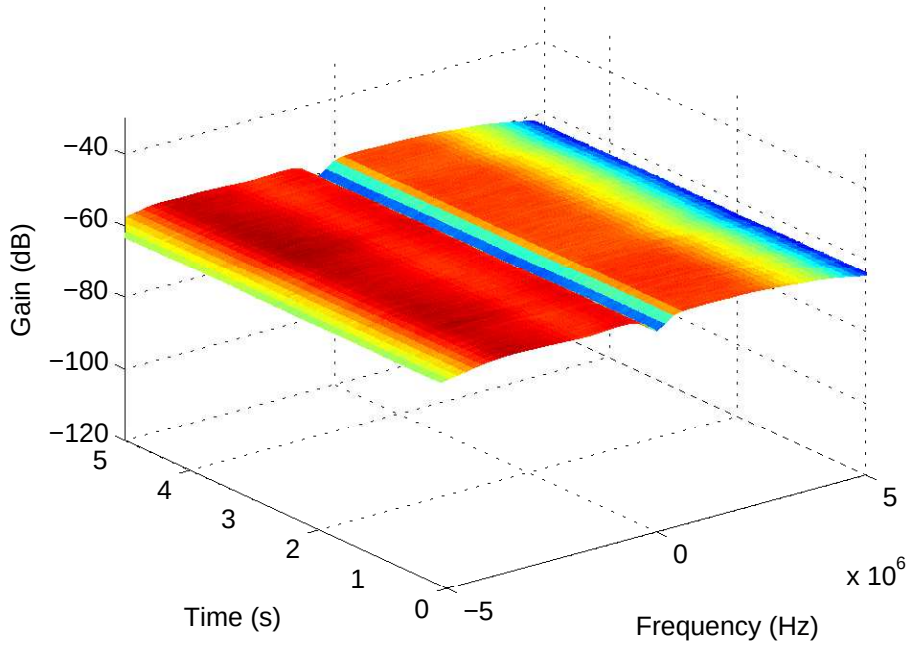

Figure 39: PSD at 820 MHz: right wrist to off-body; Standing; 1 m separation; 180° orientation

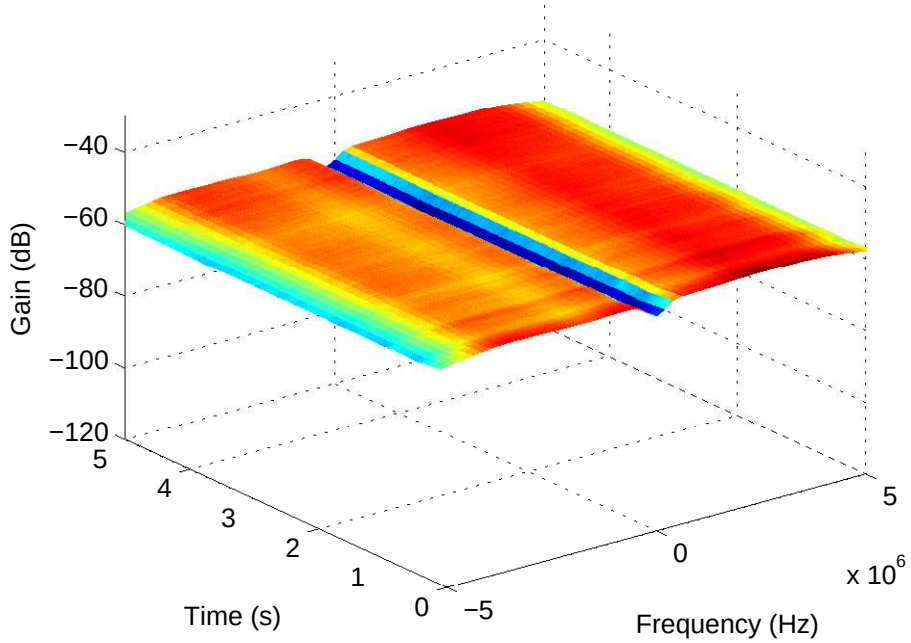

Figure 40: PSD at 820 MHz: right wrist to off-body; Standing; 1 m separation; 270° orientation

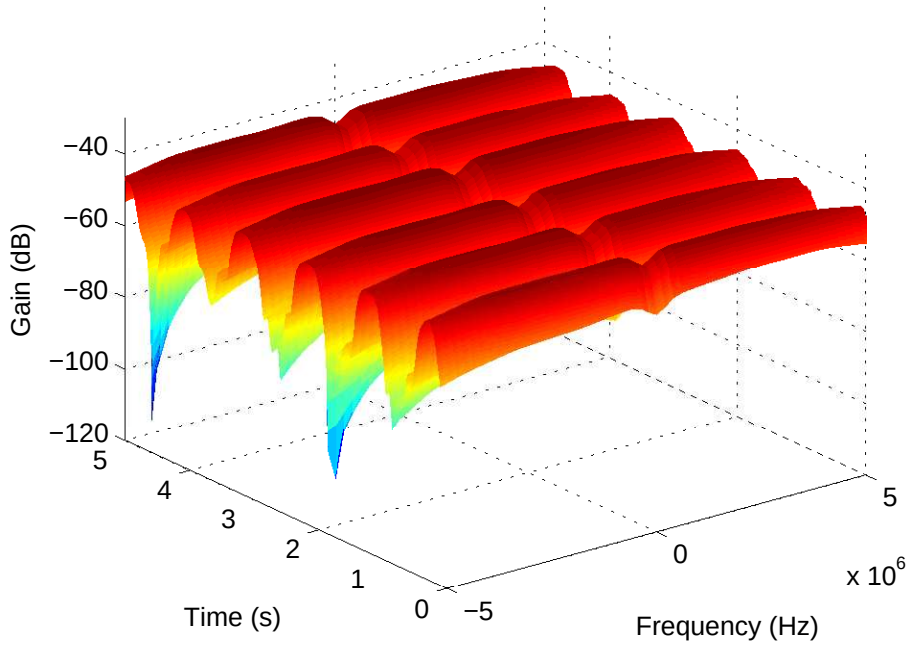

Figure 41: PSD at 820 MHz: right wrist to off-body; Walking; 1 m separation; 0° orientation

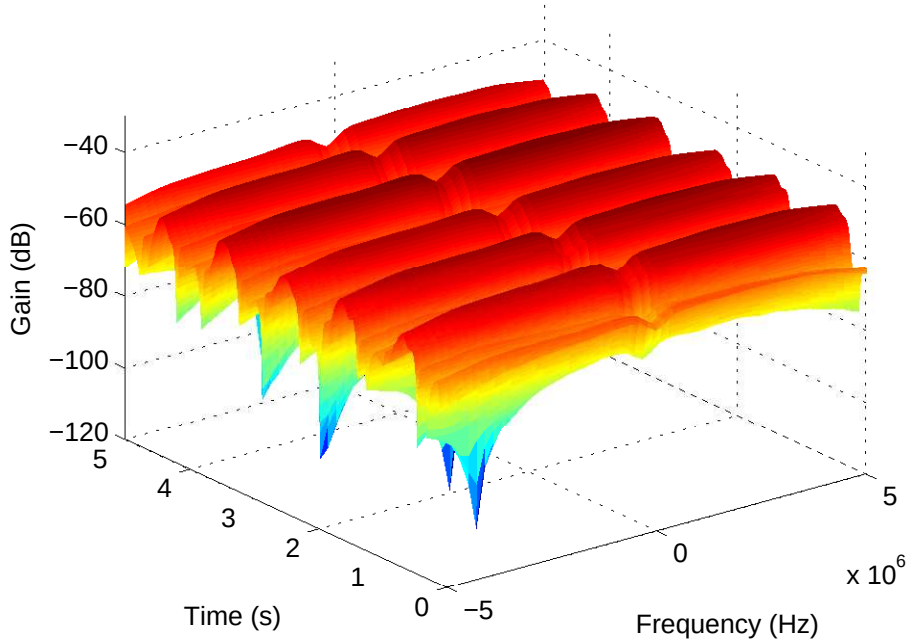

Figure 42: PSD at 820 MHz: right wrist to off-body; Walking; 1 m separation; 90° orientation

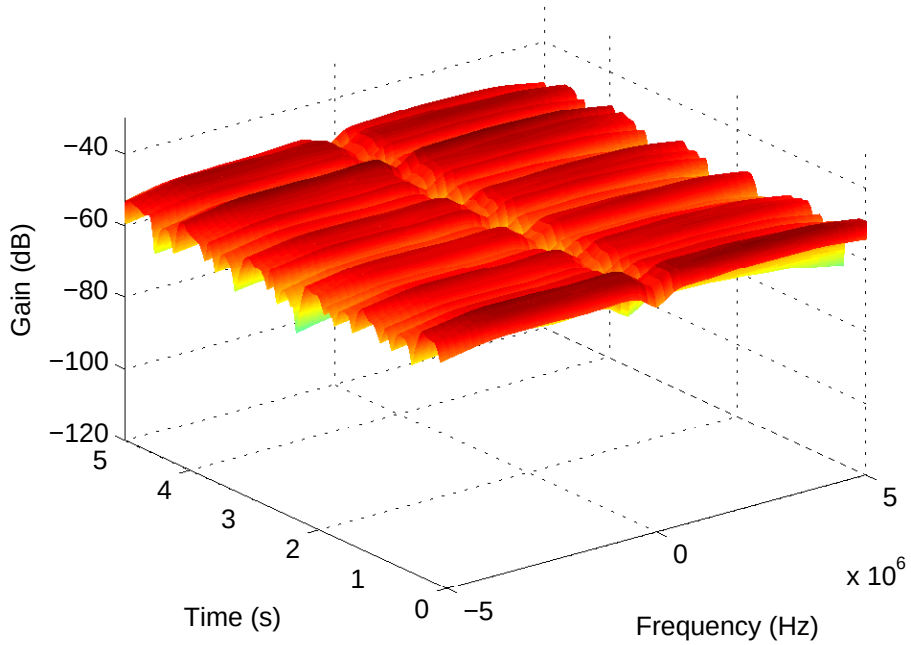

Figure 43: PSD at 820 MHz: right wrist to off-body; Walking; 1 m separation; 180° orientation

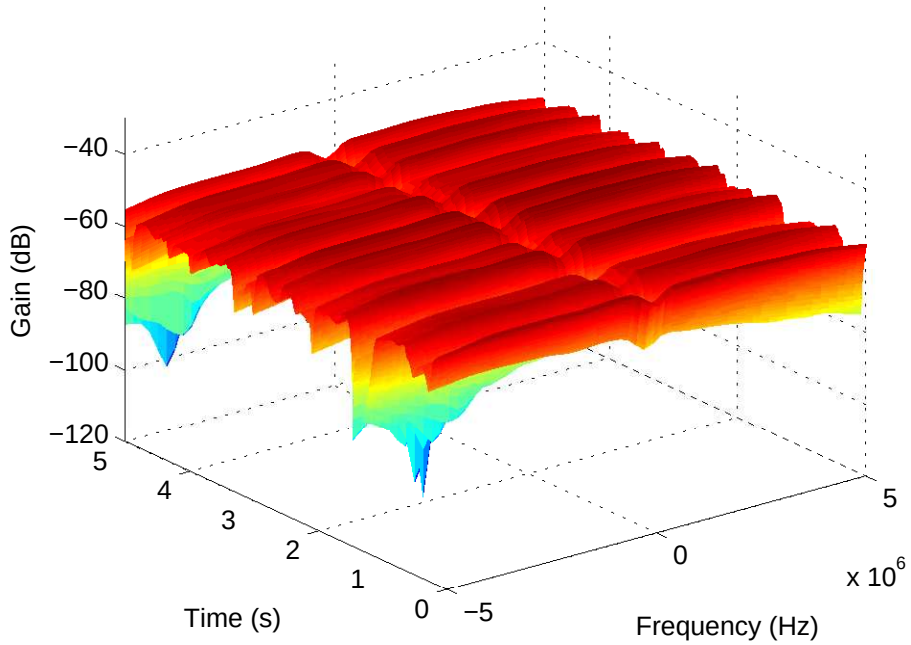

Figure 44: PSD at 820 MHz: right wrist to off-body; Walking; 1 m separation; 270° orientation

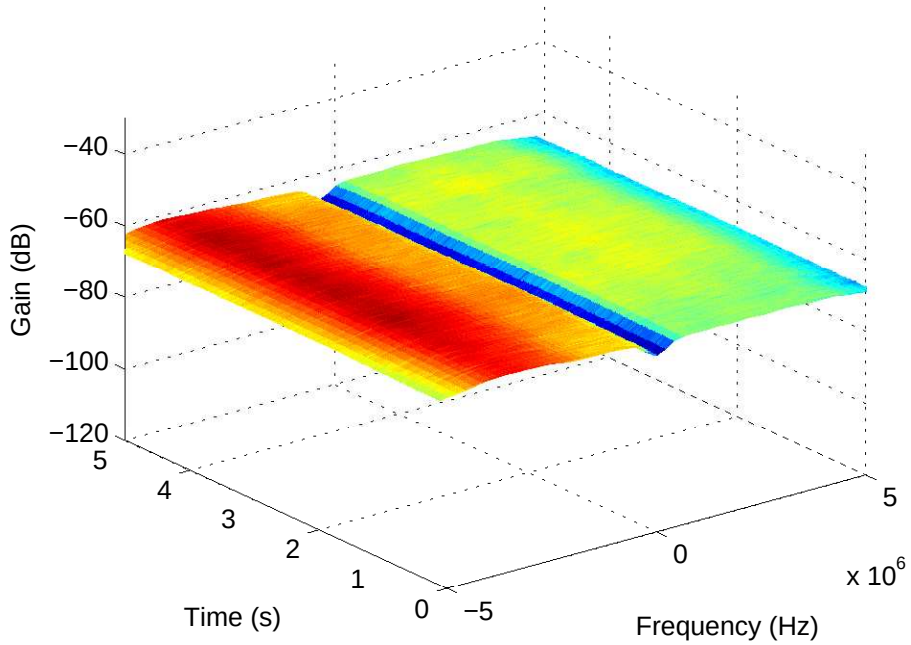

Figure 45: PSD at 820 MHz: right wrist to off-body; Standing; 2 m separation; 0° orientation

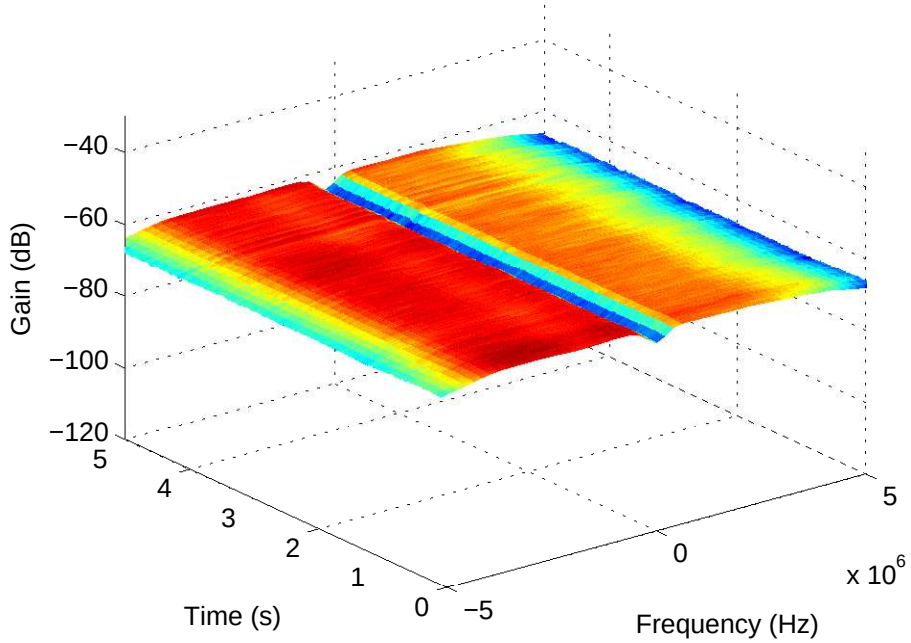

Figure 46: PSD at 820 MHz: right wrist to off-body; Standing; 2 m separation; 90° orientation

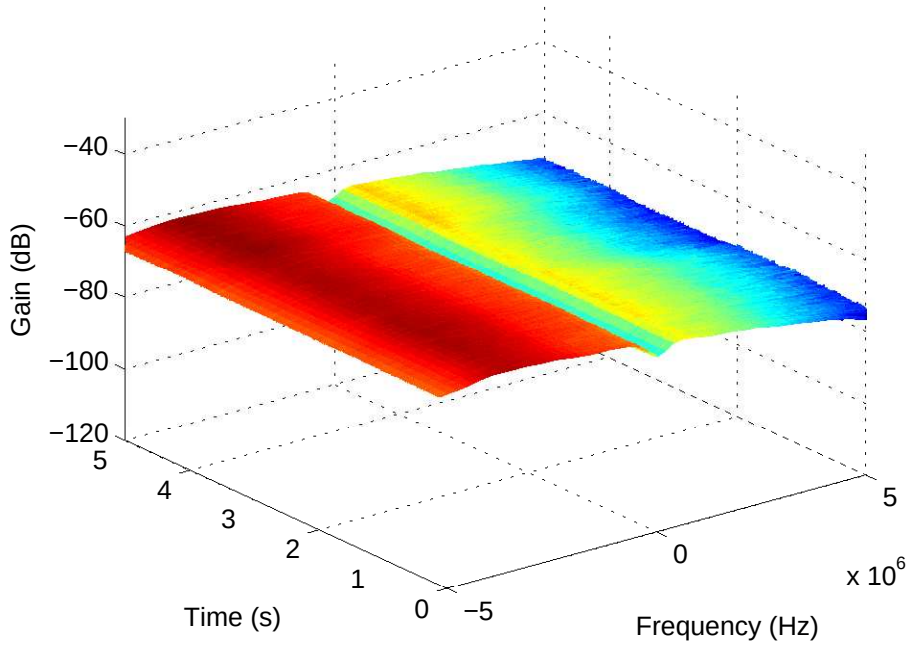

Figure 47: PSD at 820 MHz: right wrist to off-body; Standing; 2 m separation; 180° orientation

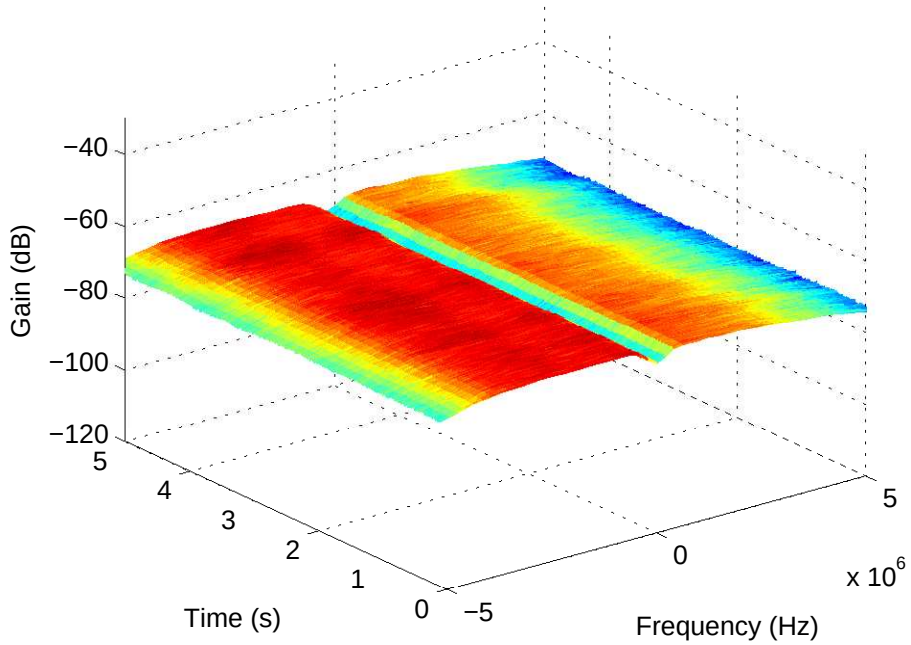

Figure 48: PSD at 820 MHz: right wrist to off-body; Standing; 2 m separation; 270° orientation

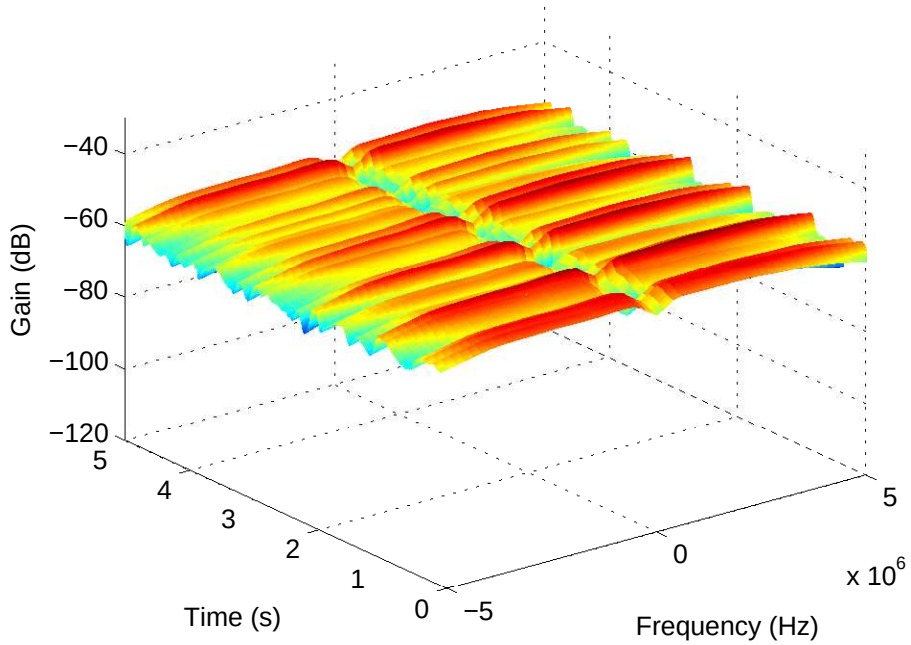

Figure 49: PSD at 820 MHz: right wrist to off-body; Walking; 2 m separation; 0° orientation

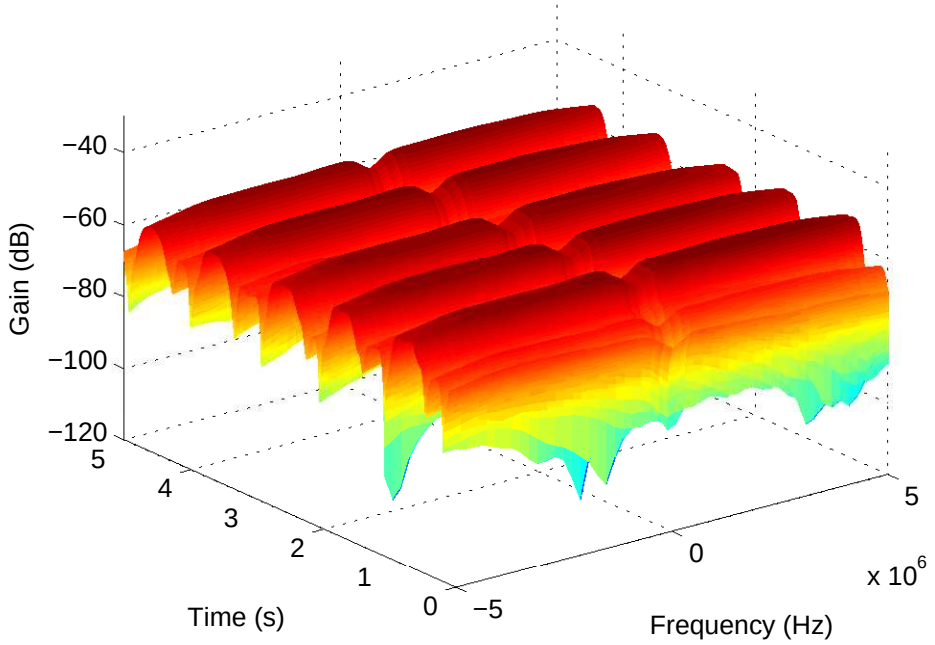

Figure 50: PSD at 820 MHz: right wrist to off-body; Walking; 2 m separation; 90° orientation

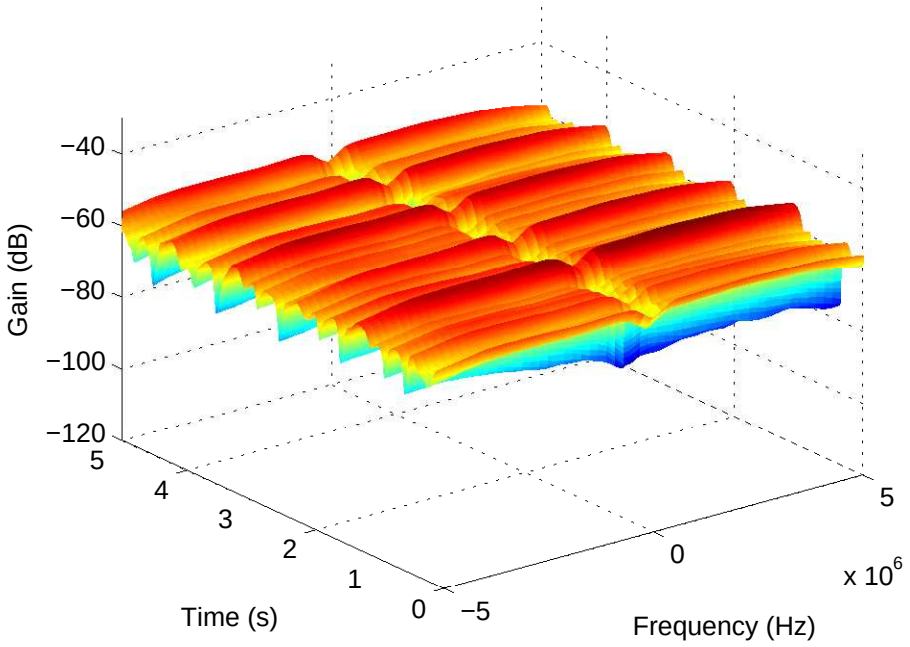

Figure 51: PSD at 820 MHz: right wrist to off-body; Walking; 2 m separation; 180° orientation

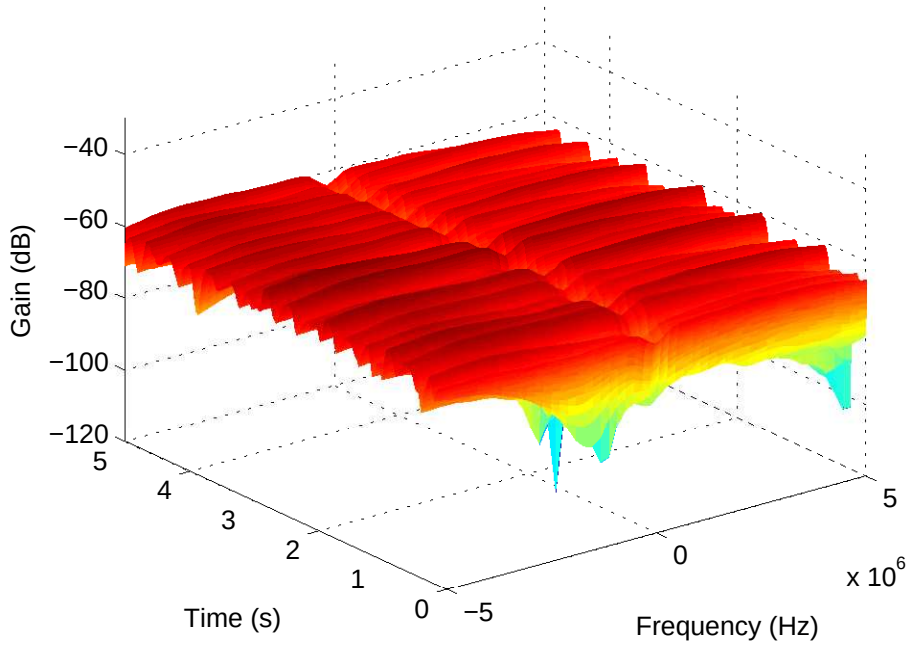

Figure 52: PSD at 820 MHz: right wrist to off-body; Walking; 2 m separation; 270° orientation

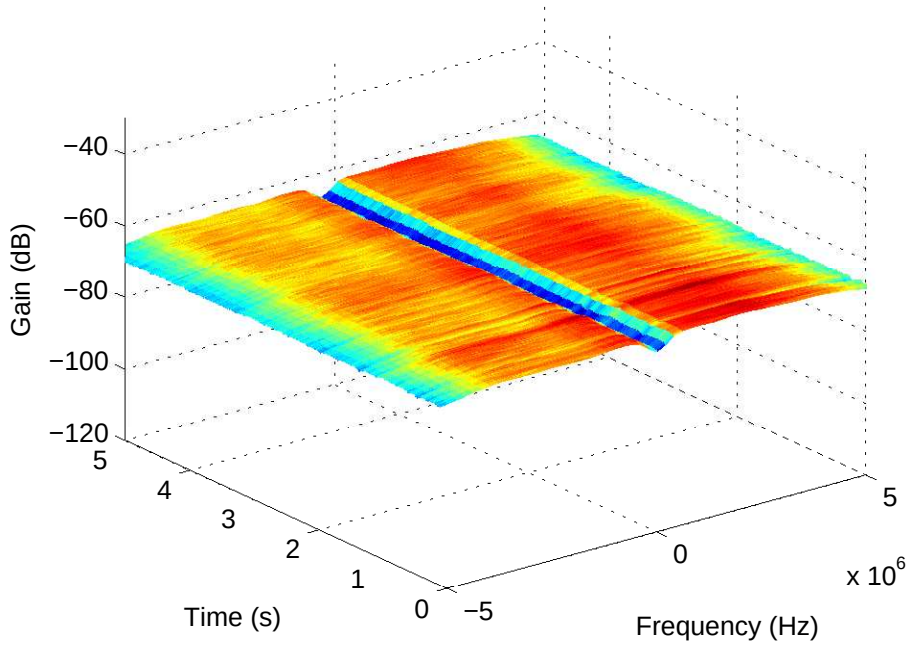

Figure 53: PSD at 820 MHz: right wrist to off-body; Standing; 3 m separation; 0° orientation

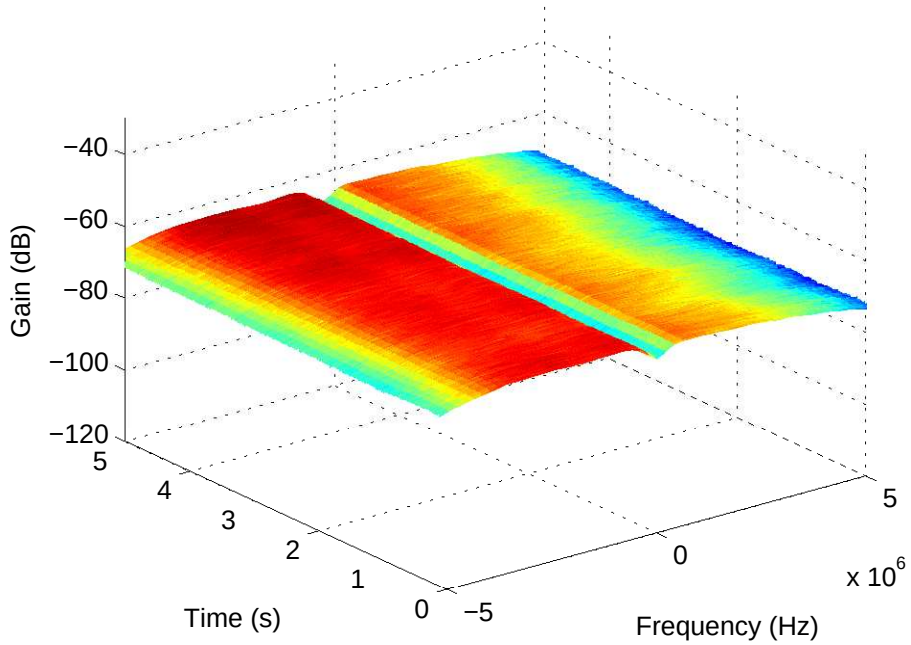

Figure 54: PSD at 820 MHz: right wrist to off-body; Standing; 3 m separation; 90° orientation

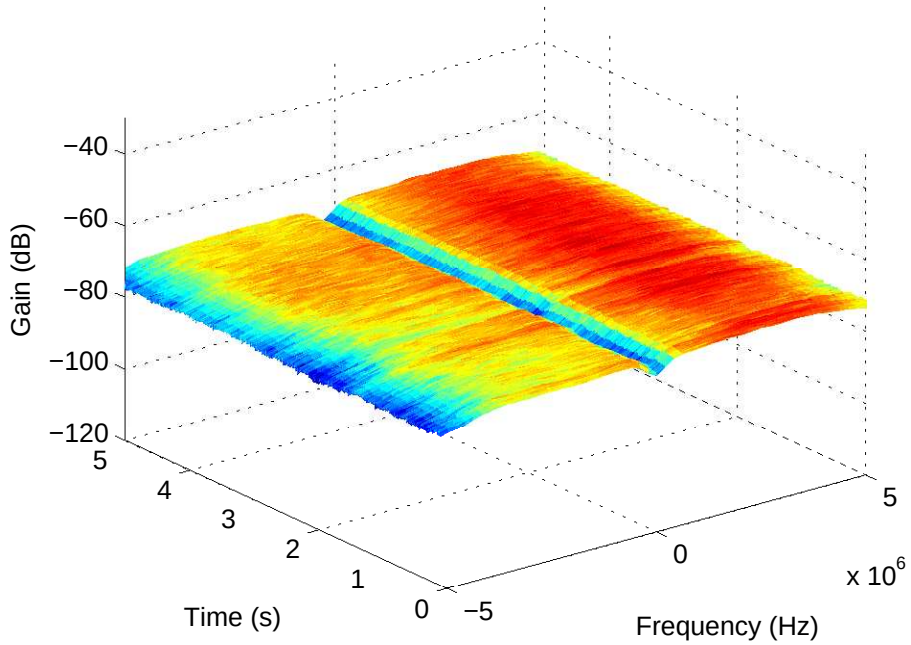

Figure 55: PSD at 820 MHz: right wrist to off-body; Standing; 3 m separation; 180° orientation

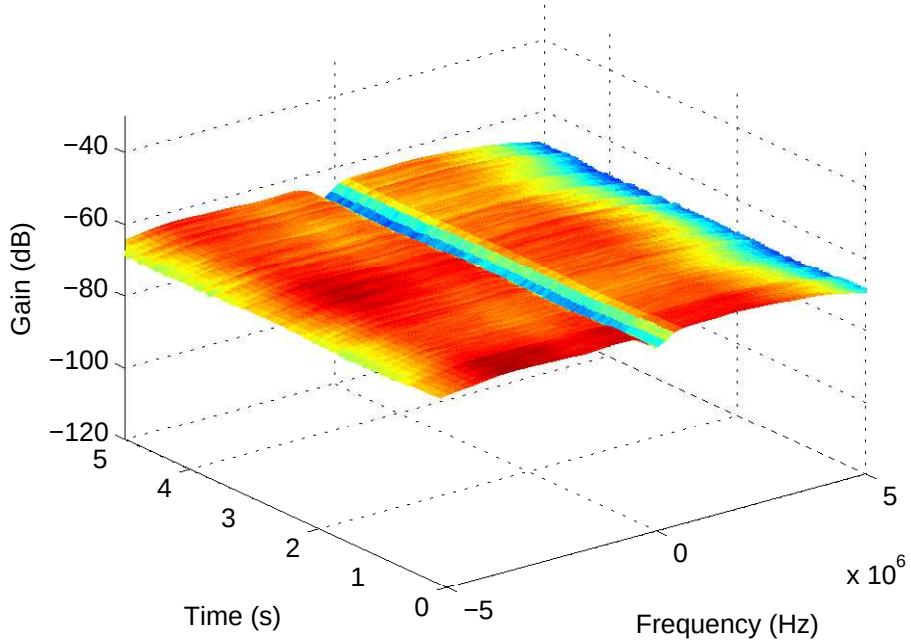

Figure 56: PSD at 820 MHz: right wrist to off-body; Standing; 3 m separation; 270° orientation

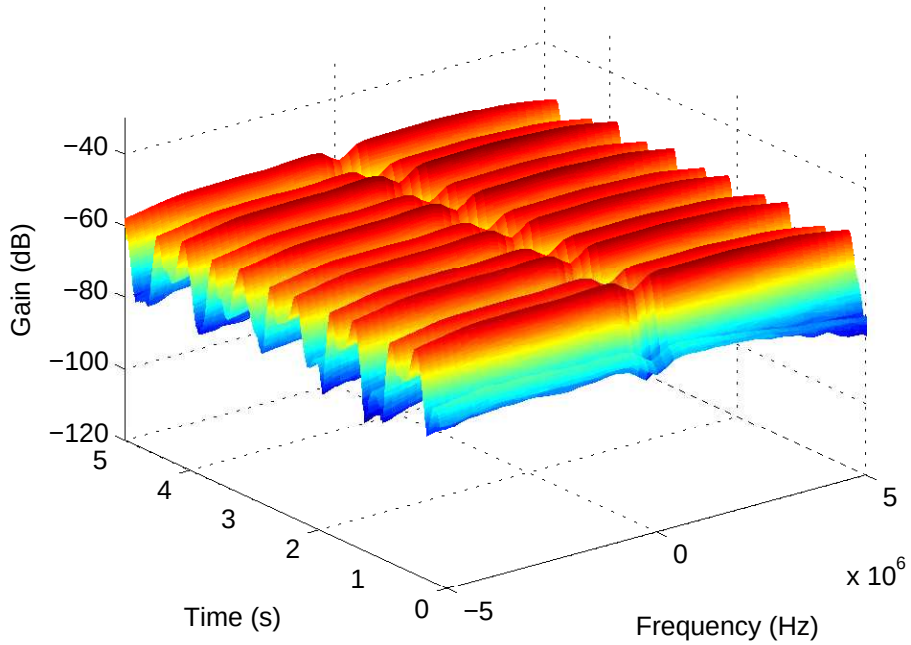

Figure 57: PSD at 820 MHz: right wrist to off-body; Walking; 3 m separation; 0° orientation

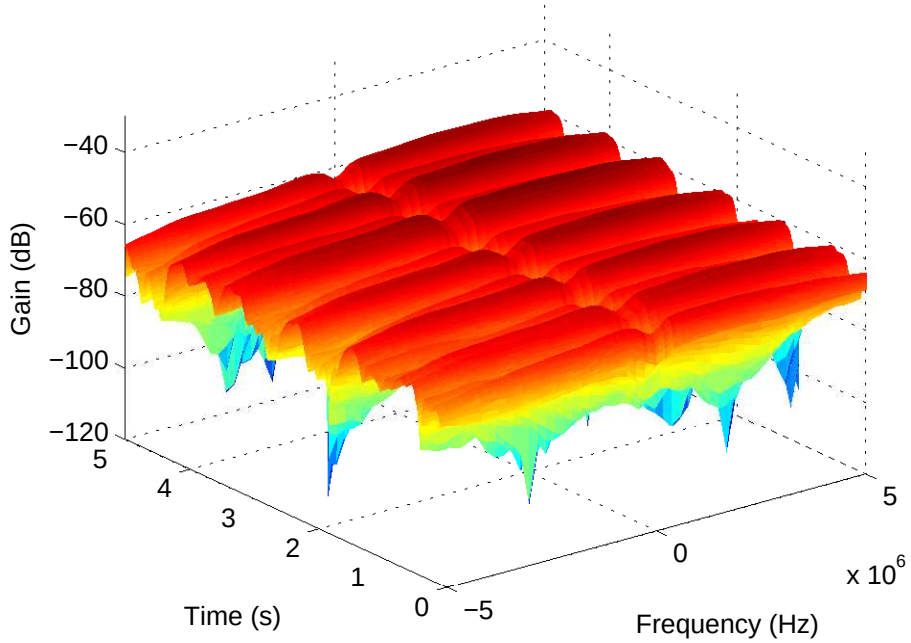

Figure 58: PSD at 820 MHz: right wrist to off-body; Walking; 3 m separation; 90° orientation

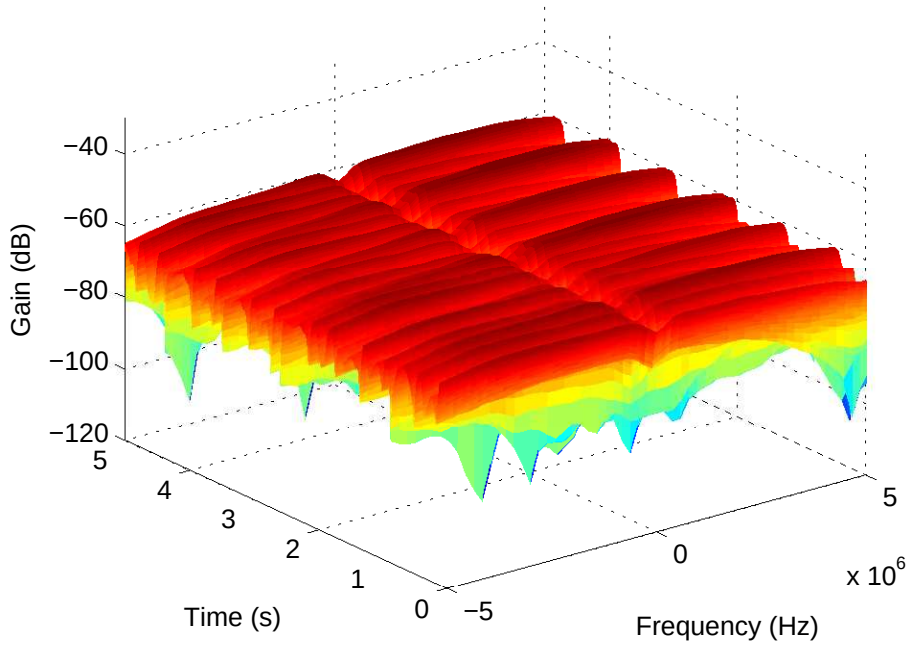

Figure 59: PSD at 820 MHz: right wrist to off-body; Walking; 3 m separation; 180° orientation

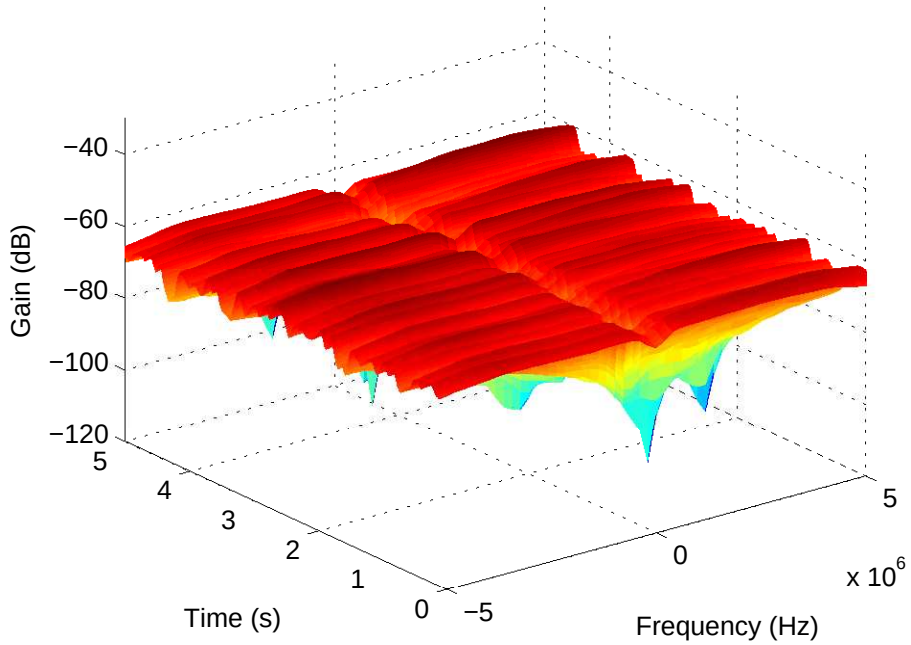

Figure 60: PSD at 820 MHz: right wrist to off-body; Walking; 3 m separation; 270° orientation

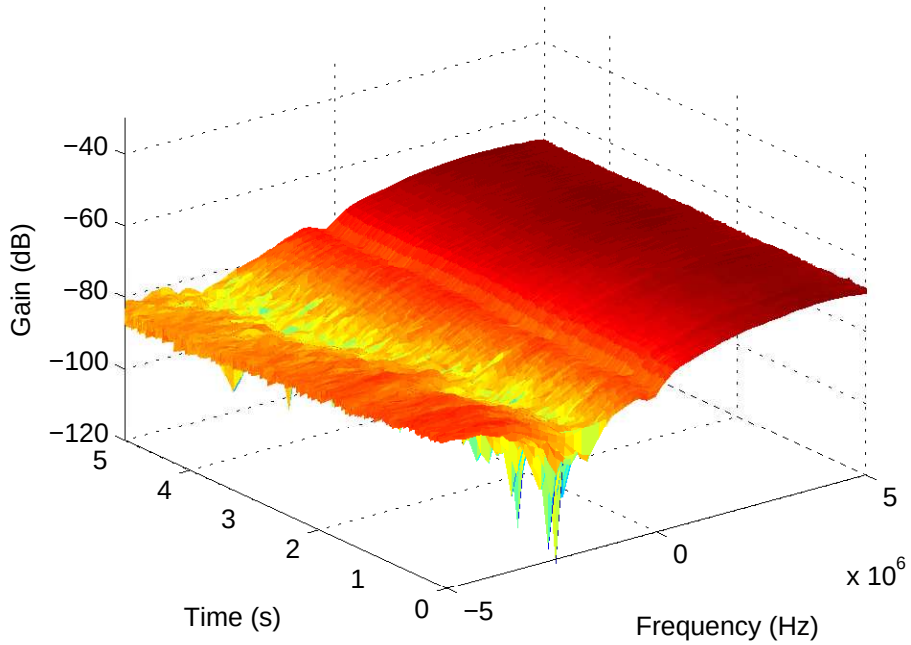

Figure 61: PSD at 820 MHz: right wrist to off-body; Standing; 4 m separation; 0° orientation

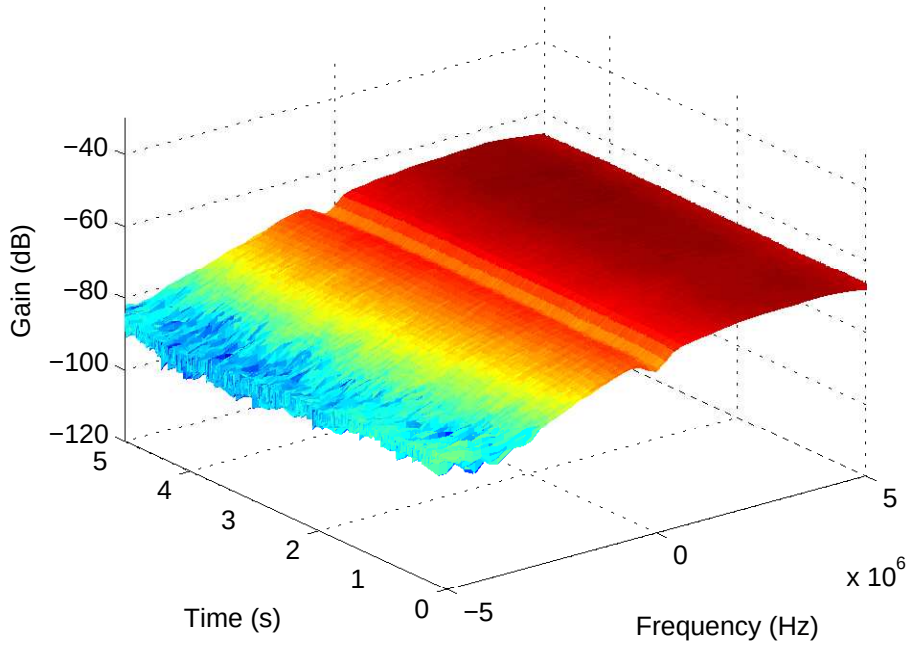

Figure 62: PSD at 820 MHz: right wrist to off-body; Standing; 4 m separation; 90° orientation

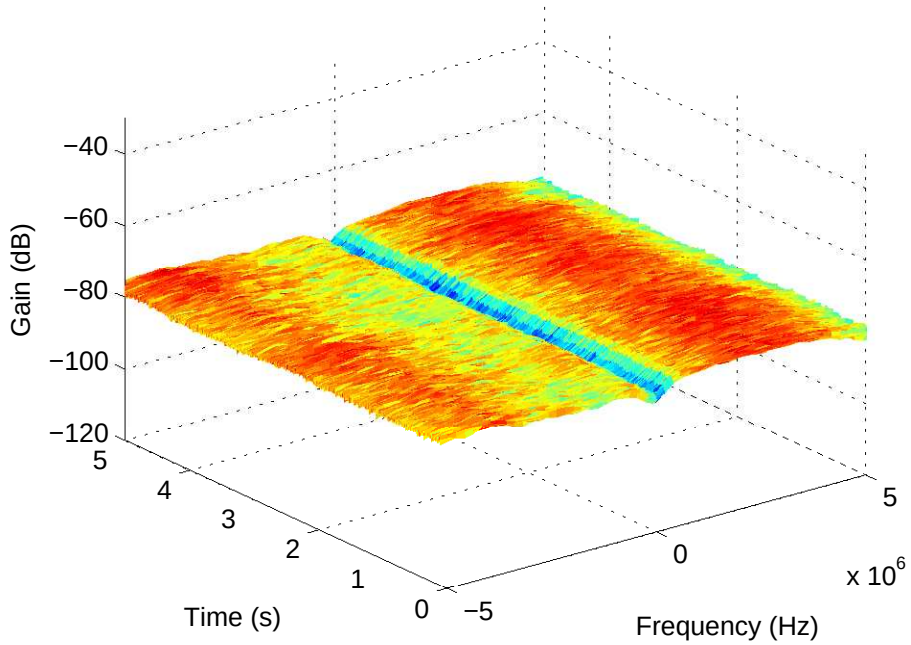

Figure 63: PSD at 820 MHz: right wrist to off-body; Standing; 4 m separation; 180° orientation

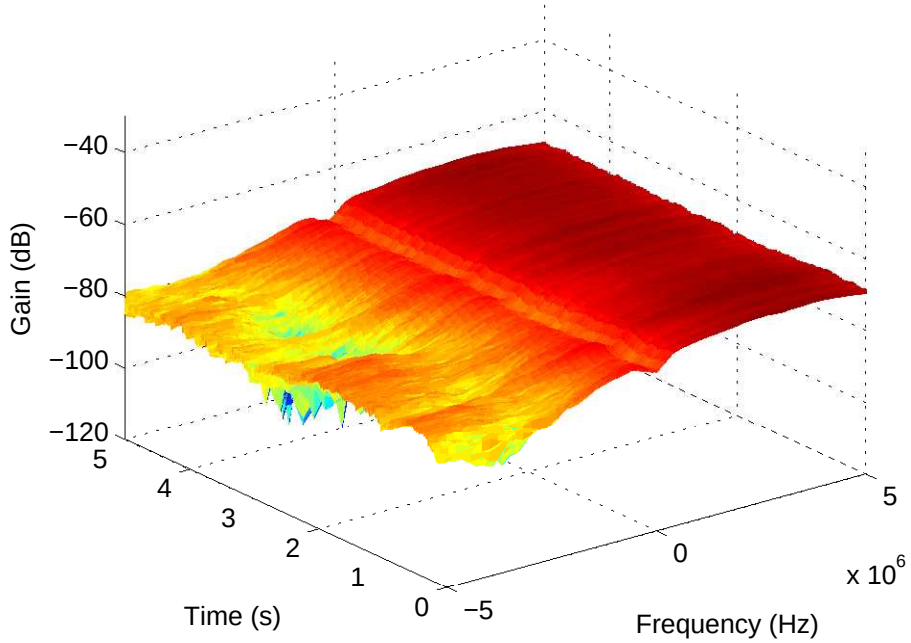

Figure 64: PSD at 820 MHz: right wrist to off-body; Standing; 4 m separation; 270° orientation

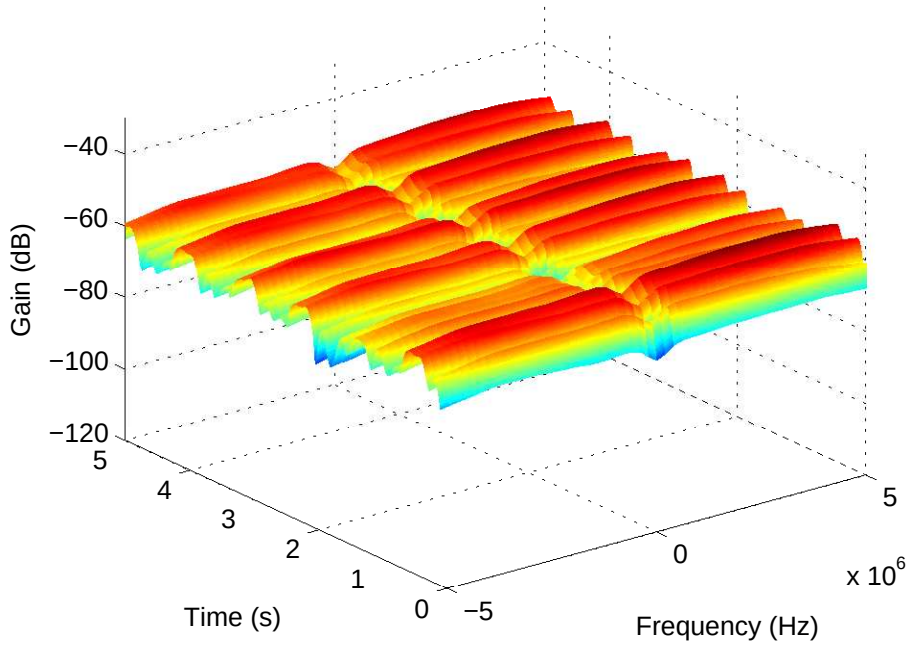

Figure 65: PSD at 820 MHz: right wrist to off-body; Walking; 4 m separation; 0° orientation

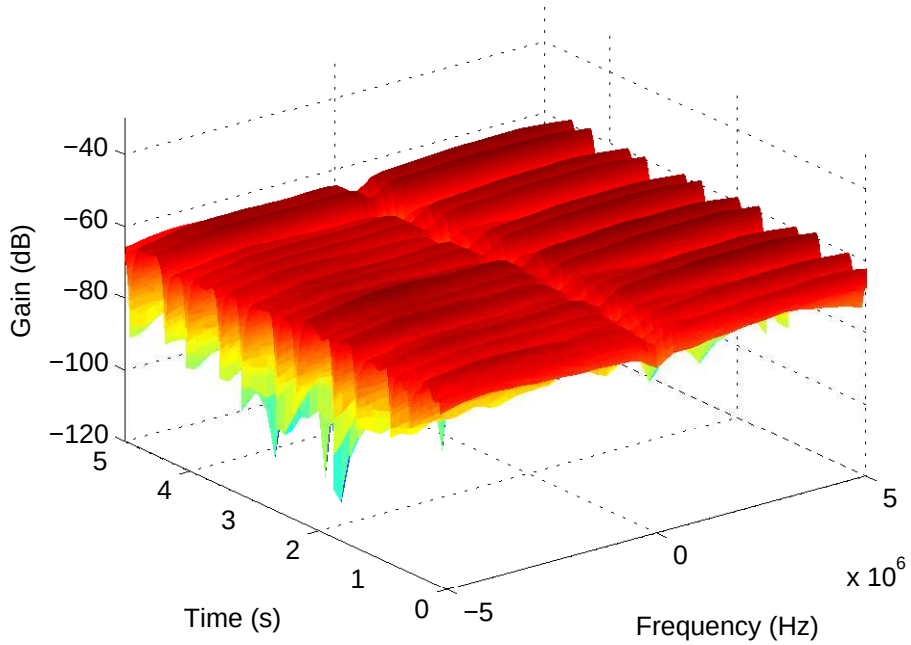

Figure 66: PSD at 820 MHz: right wrist to off-body; Walking; 4 m separation; 90° orientation

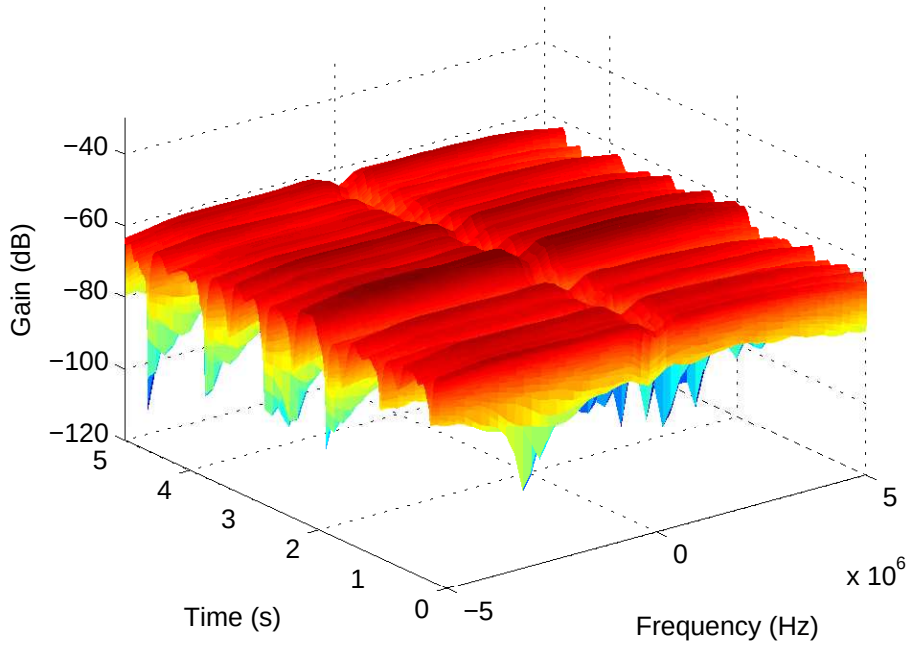

Figure 67: PSD at 820 MHz: right wrist to off-body; Walking; 4 m separation; 180° orientation

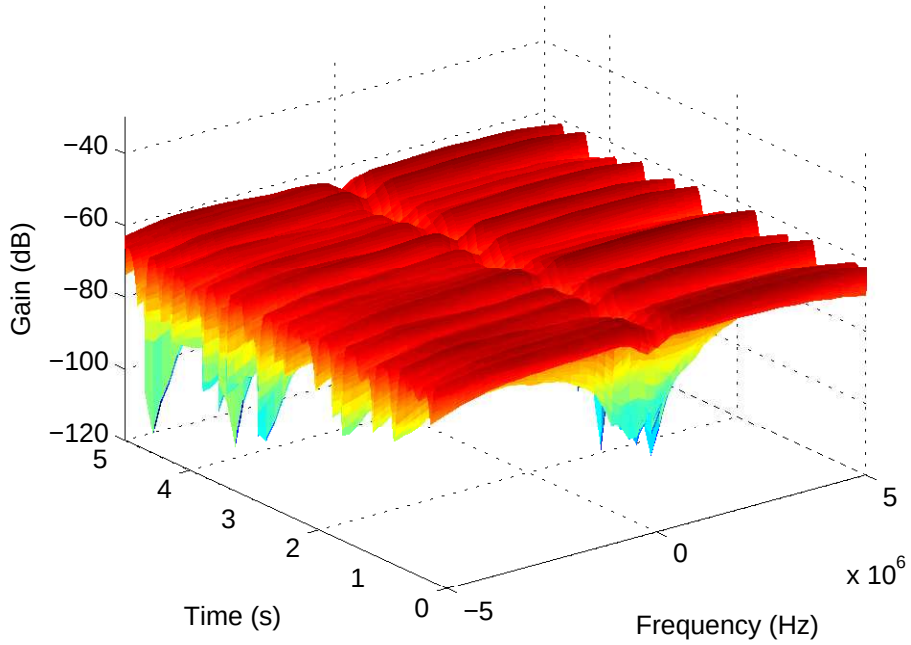

Figure 68: PSD at 820 MHz: right wrist to off-body; Walking; 4 m separation; 270° orientation

A.1.2 2.36 GHz Measurements

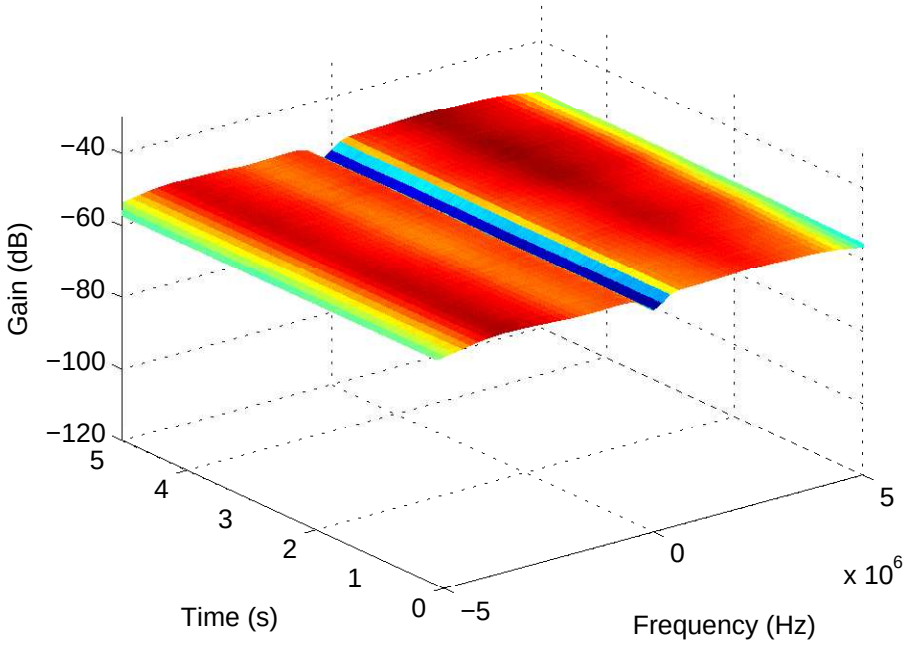

Figure 69: PSD at 2360 MHz: chest to off-body; Standing; 1 m separation; 0° orientation

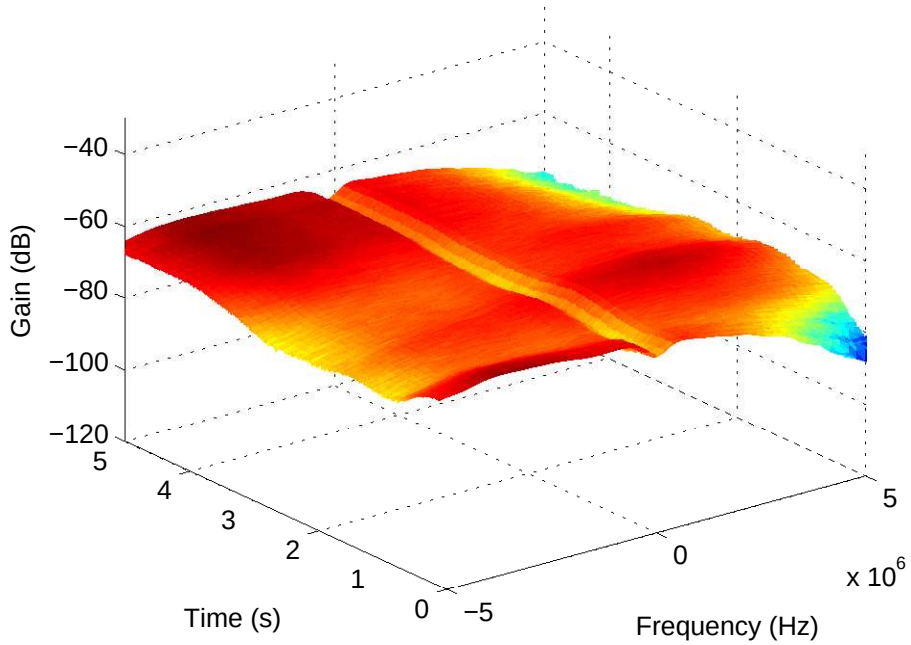

Figure 70: PSD at 2360 MHz: chest to off-body; Standing; 1 m separation; 90° orientation

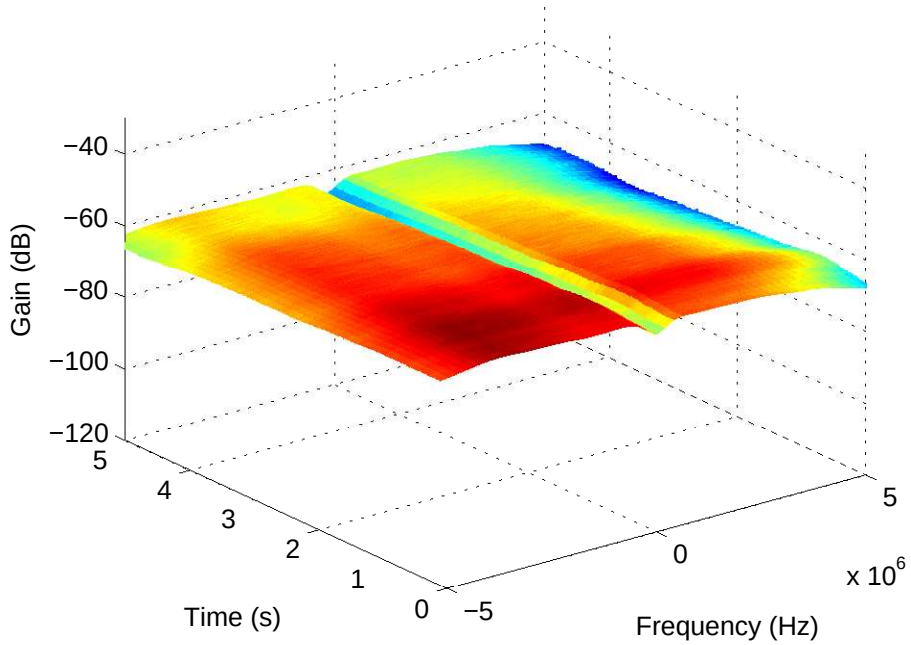

Figure 71: PSD at 2360 MHz: chest to off-body; Standing; 1 m separation; 180° orientation

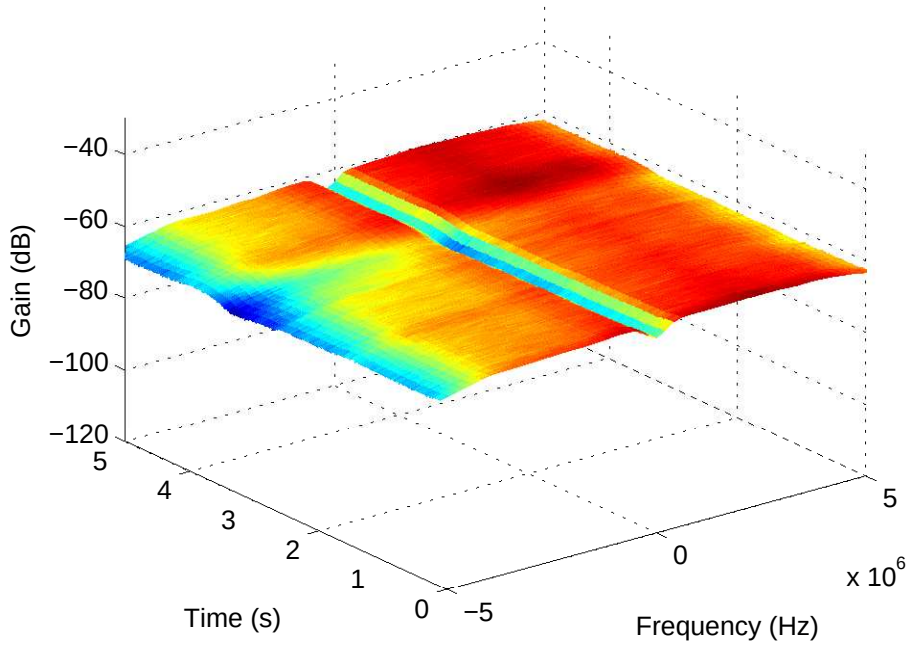

Figure 72: PSD at 2360 MHz: chest to off-body; Standing; 1 m separation; 270° orientation

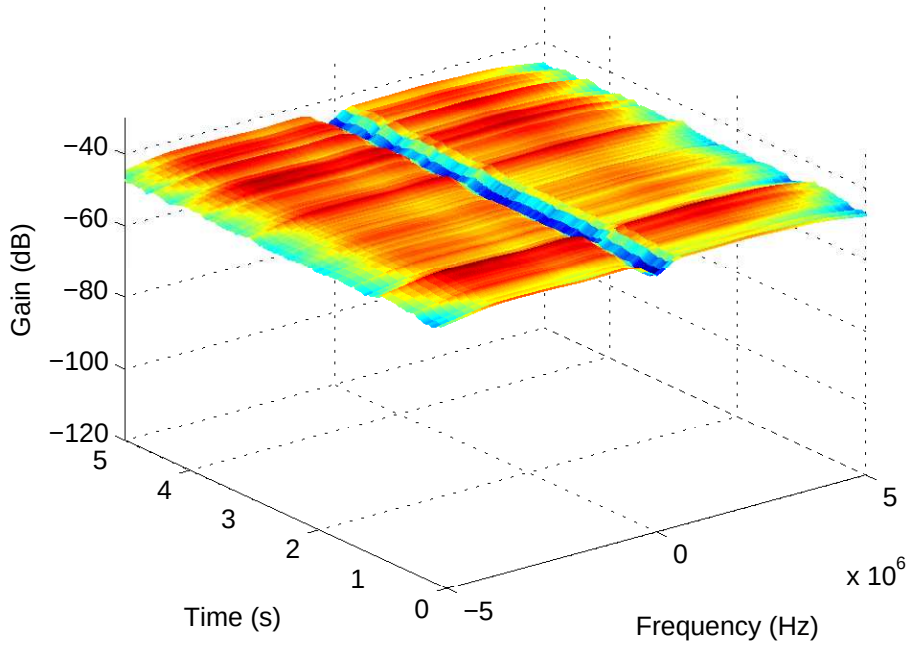

Figure 73: PSD at 2360 MHz: chest to off-body; Walking; 1 m separation; 0° orientation

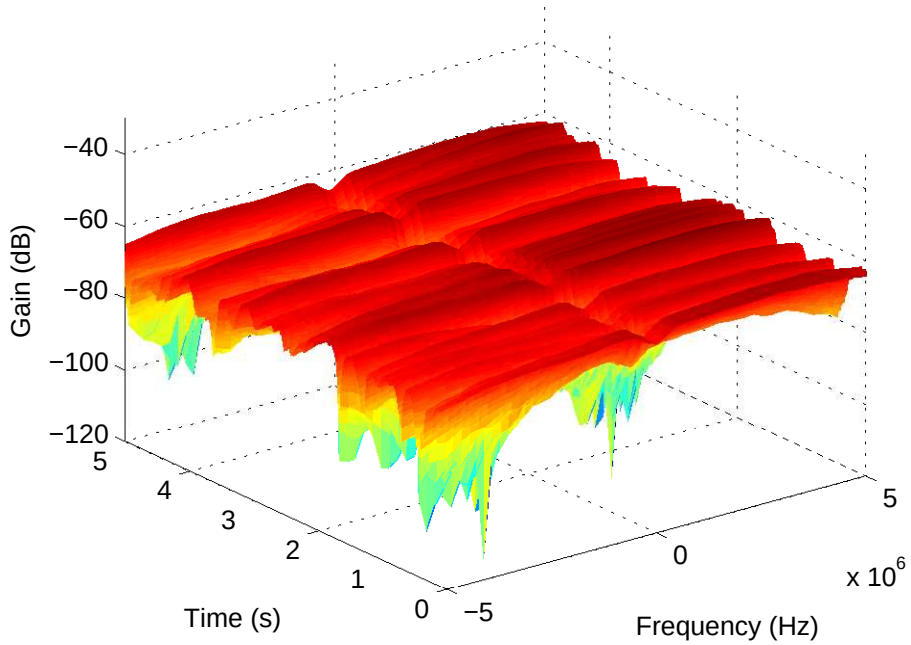

Figure 74: PSD at 2360 MHz: chest to off-body; Walking; 1 m separation; 90° orientation

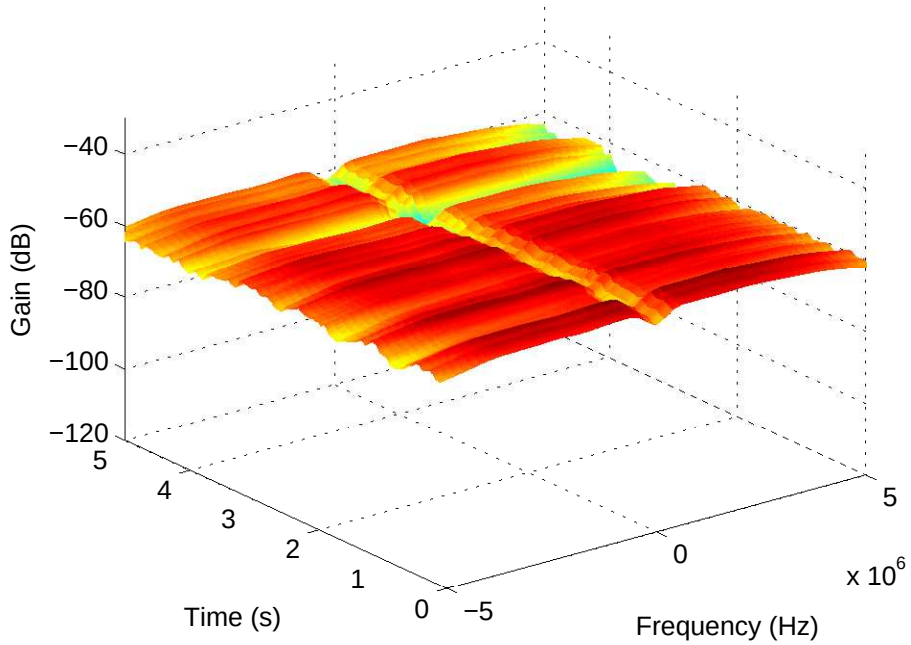

Figure 75: PSD at 2360 MHz: chest to off-body; Walking; 1 m separation; 180° orientation

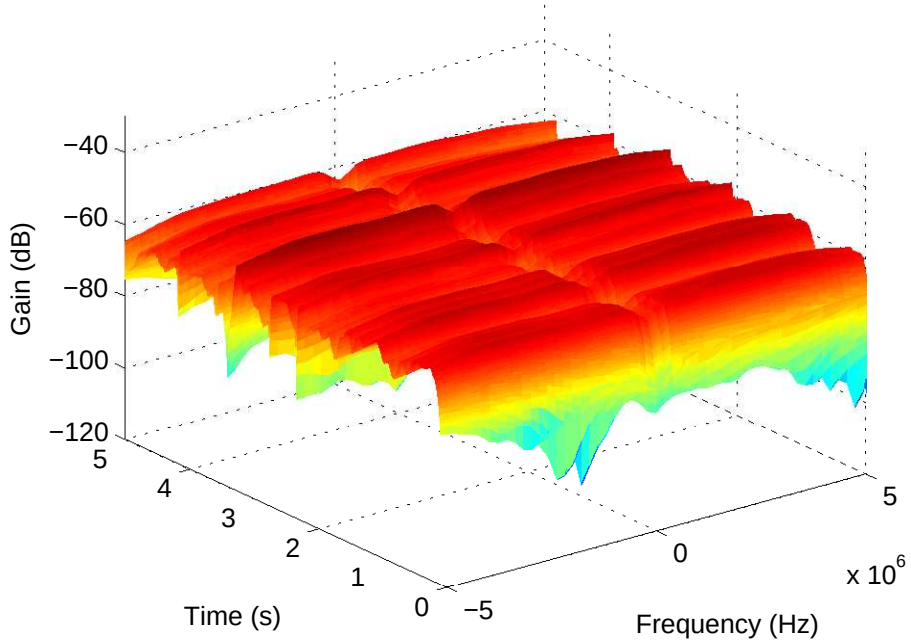

Figure 76: PSD at 2360 MHz: chest to off-body; Walking; 1 m separation; 270° orientation

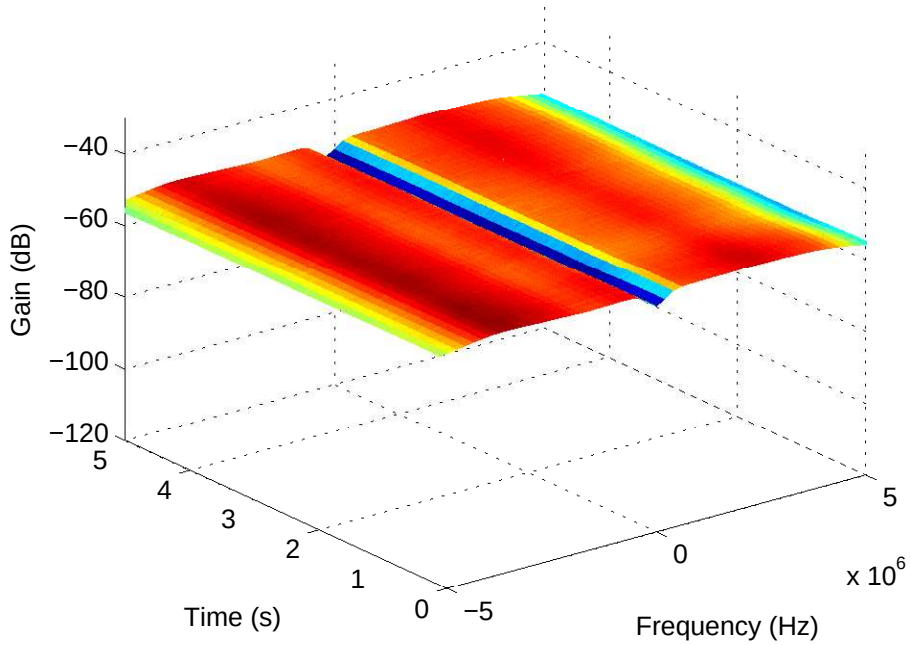

Figure 77: PSD at 2360 MHz: chest to off-body; Standing; 2 m separation; 0° orientation

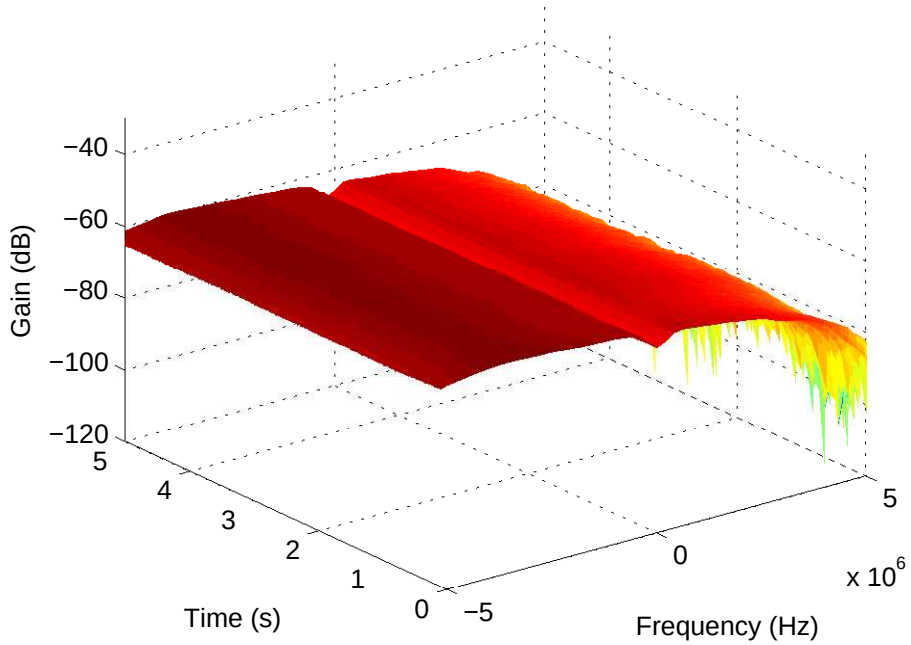

Figure 78: PSD at 2360 MHz: chest to off-body; Standing; 2 m separation; 90° orientation

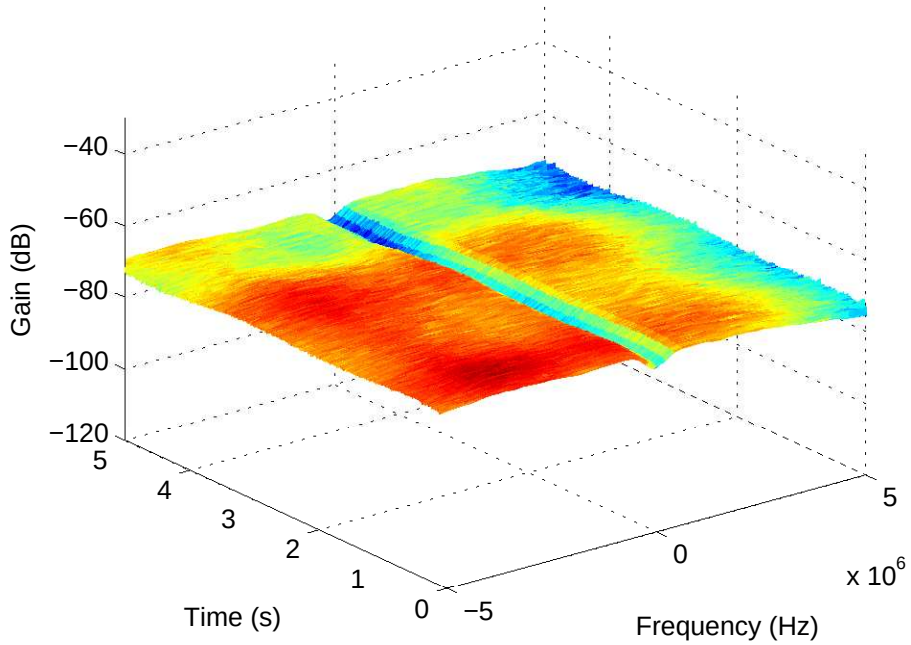

Figure 79: PSD at 2360 MHz: chest to off-body; Standing; 2 m separation; 180° orientation

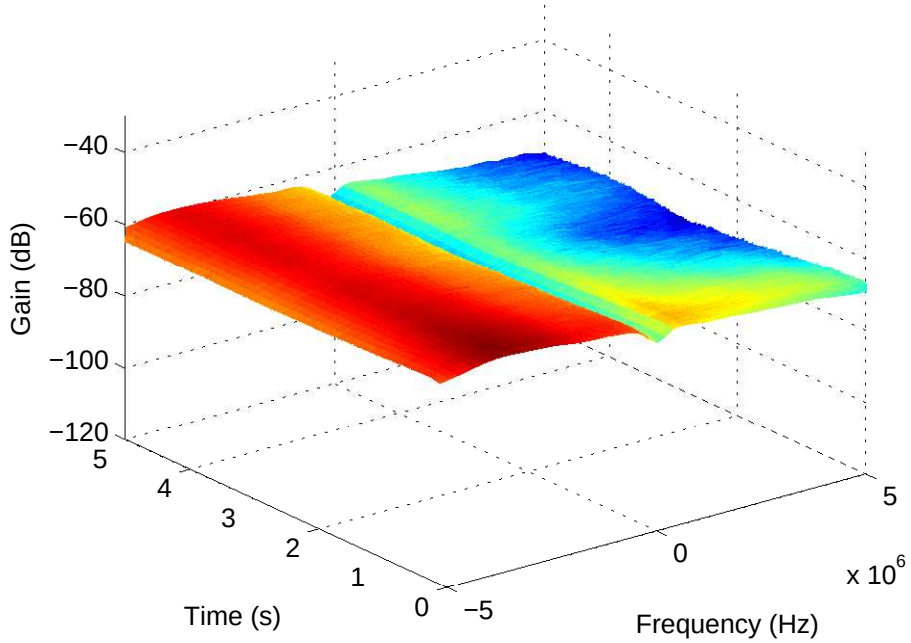

Figure 80: PSD at 2360 MHz: chest to off-body; Standing; 2 m separation; 270° orientation

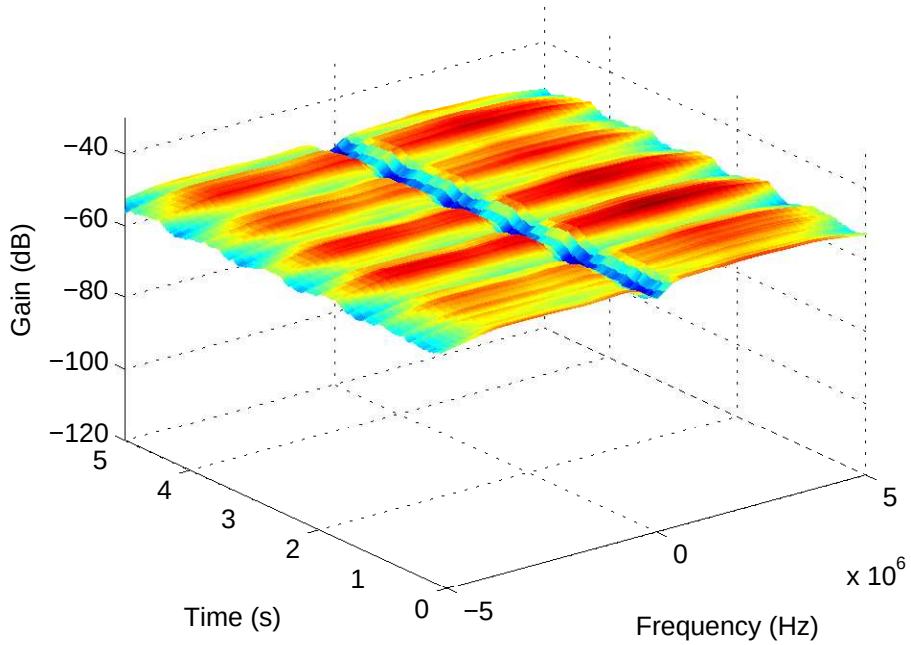

Figure 81: PSD at 2360 MHz: chest to off-body; Walking; 2 m separation; 0° orientation

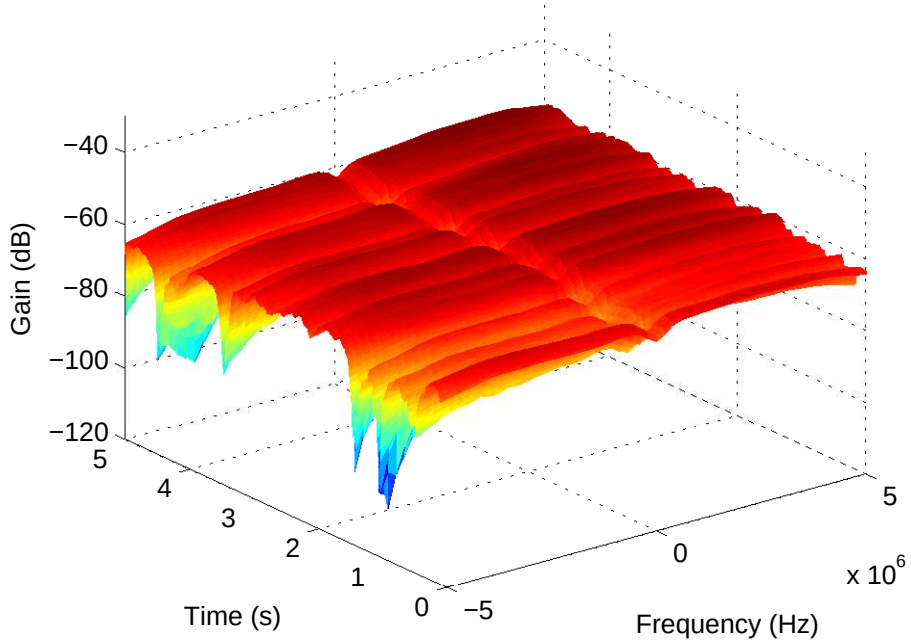

Figure 82: PSD at 2360 MHz: chest to off-body; Walking; 2 m separation; 90° orientation

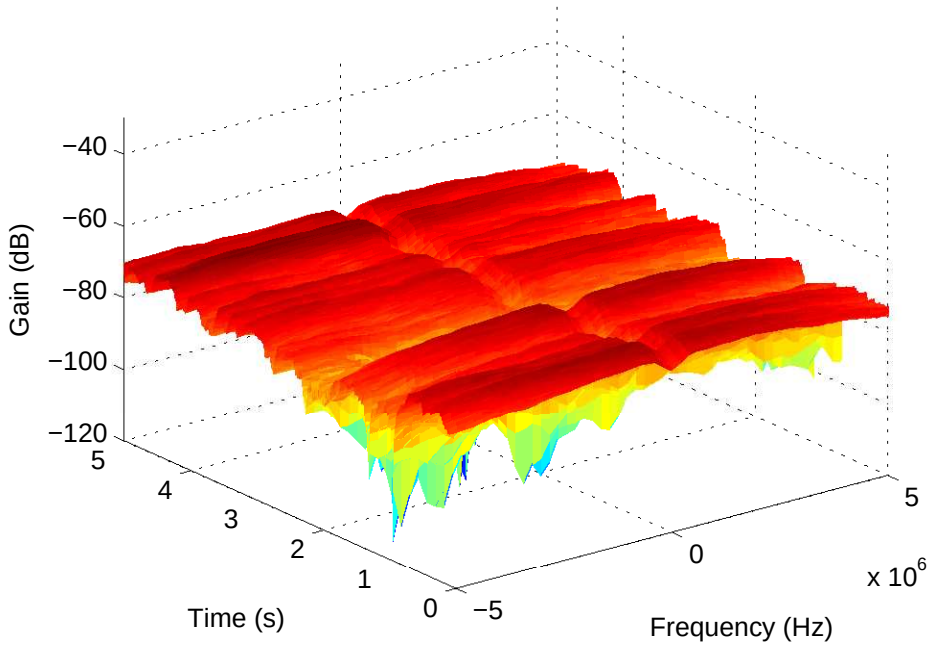

Figure 83: PSD at 2360 MHz: chest to off-body; Walking; 2 m separation; 180° orientation

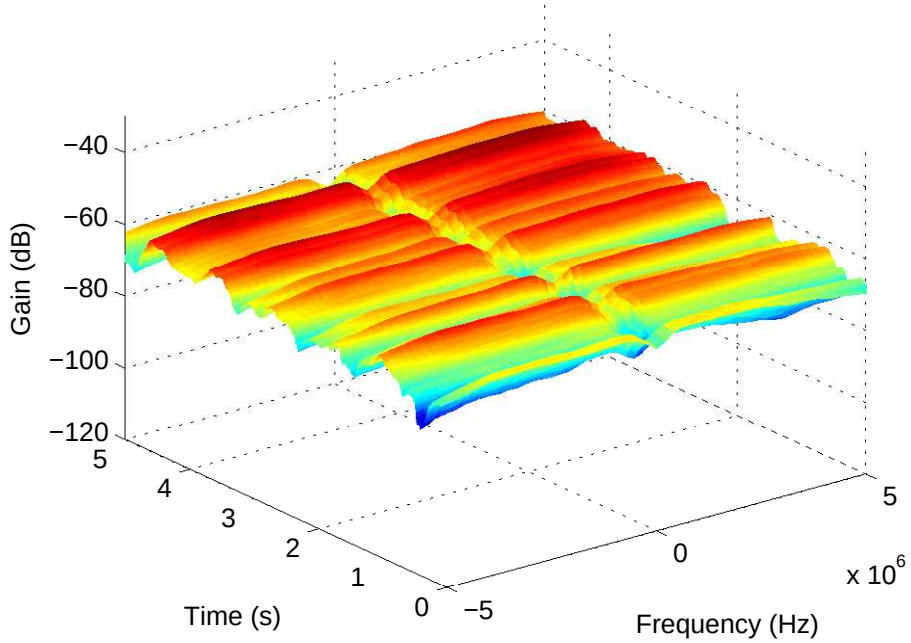

Figure 84: PSD at 2360 MHz: chest to off-body; Walking; 2 m separation; 270° orientation

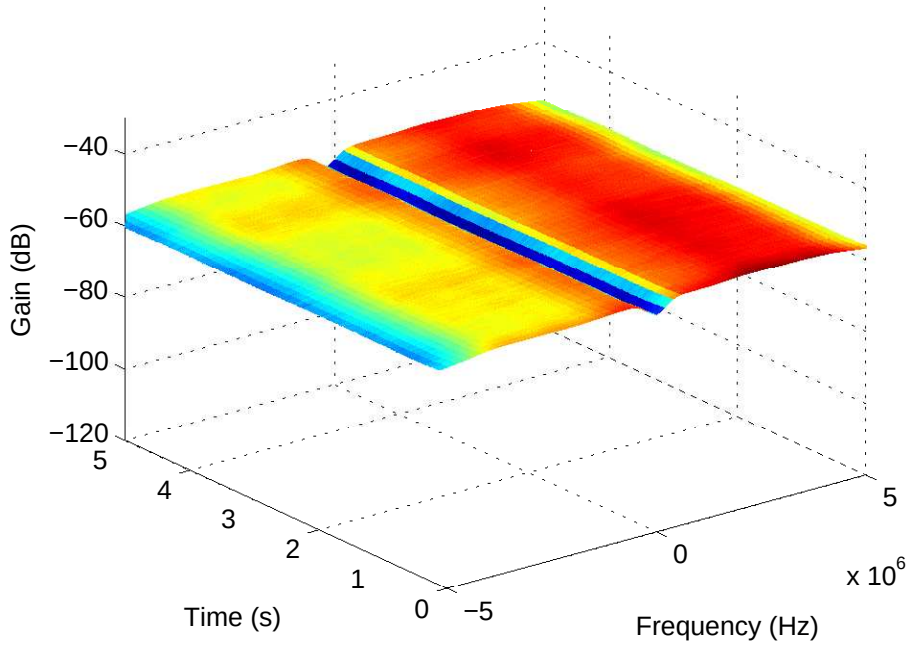

Figure 85: PSD at 2360 MHz: chest to off-body; Standing; 3 m separation; 0° orientation

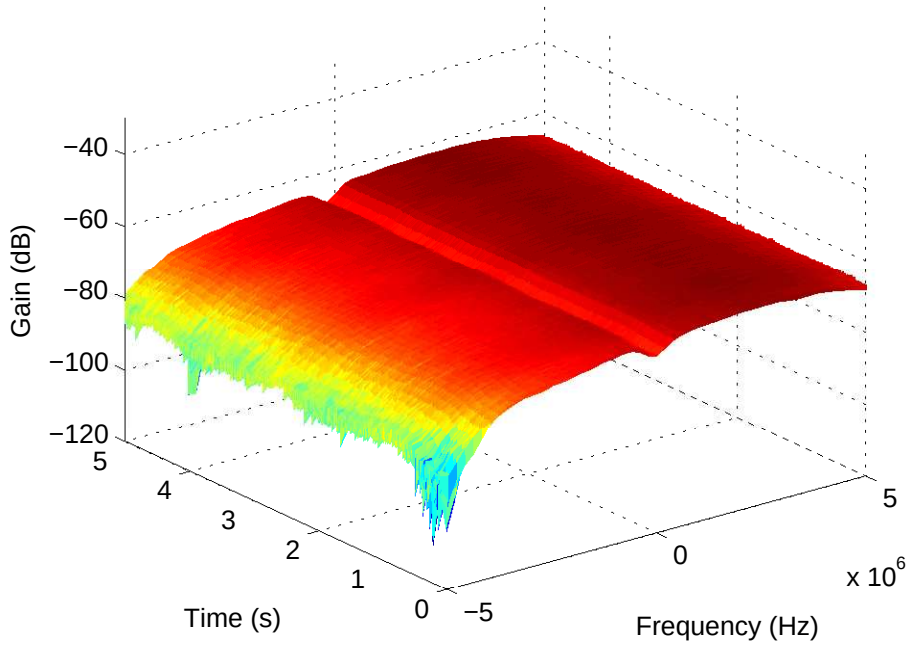

Figure 86: PSD at 2360 MHz: chest to off-body; Standing; 3 m separation; 90° orientation

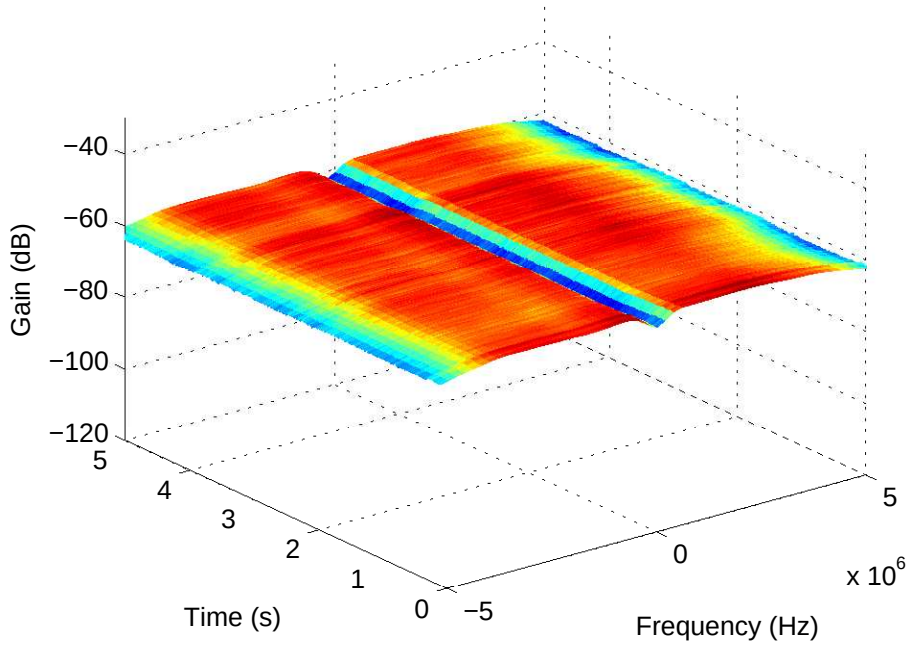

Figure 87: PSD at 2360 MHz: chest to off-body; Standing; 3 m separation; 180° orientation

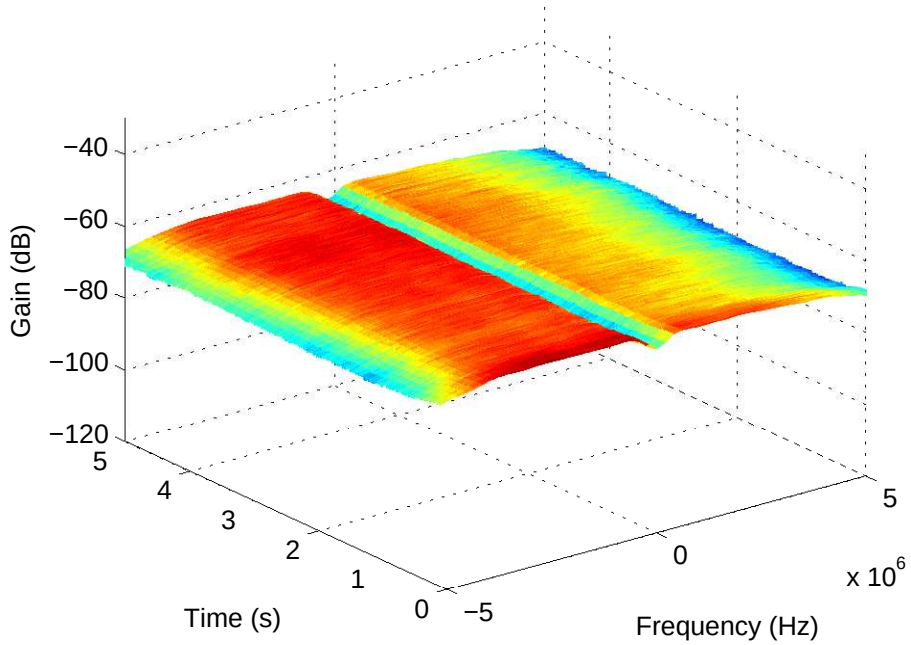

Figure 88: PSD at 2360 MHz: chest to off-body; Standing; 3 m separation; 270° orientation

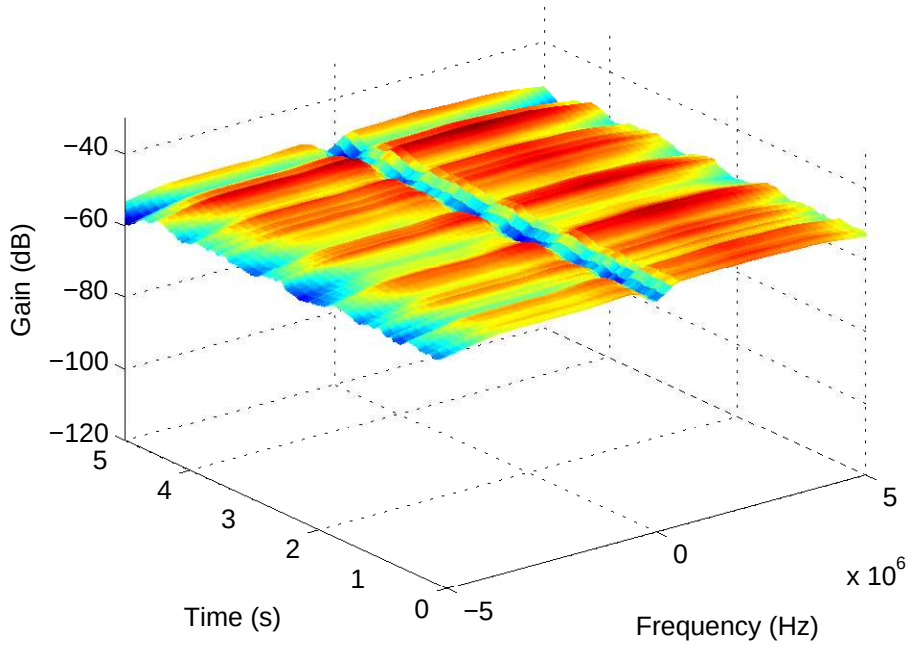

Figure 89: PSD at 2360 MHz: chest to off-body; Walking; 3 m separation; 0° orientation

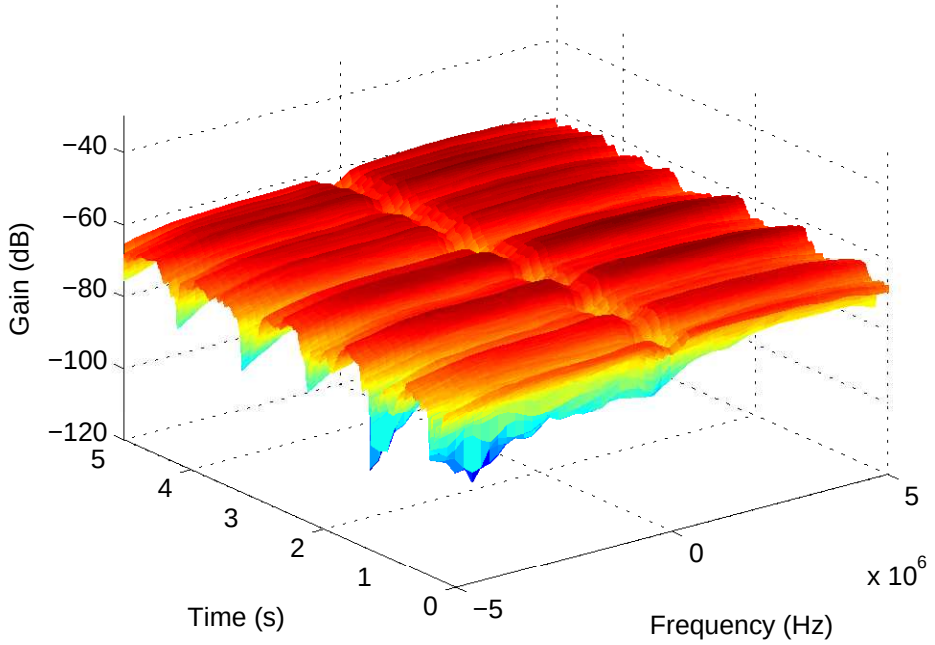

Figure 90: PSD at 2360 MHz: chest to off-body; Walking; 3 m separation; 90° orientation

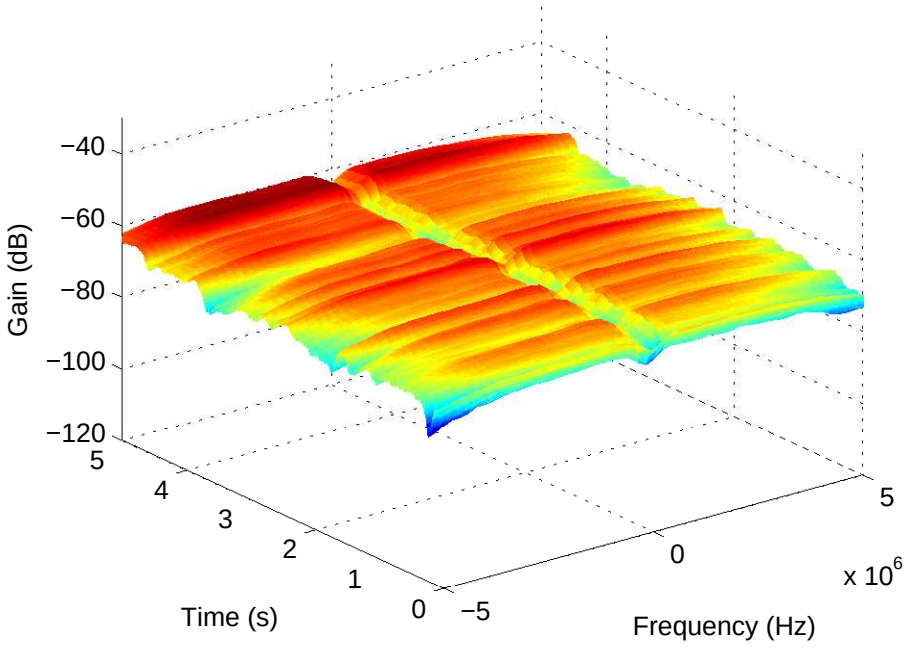

Figure 91: PSD at 2360 MHz: chest to off-body; Walking; 3 m separation; 180° orientation

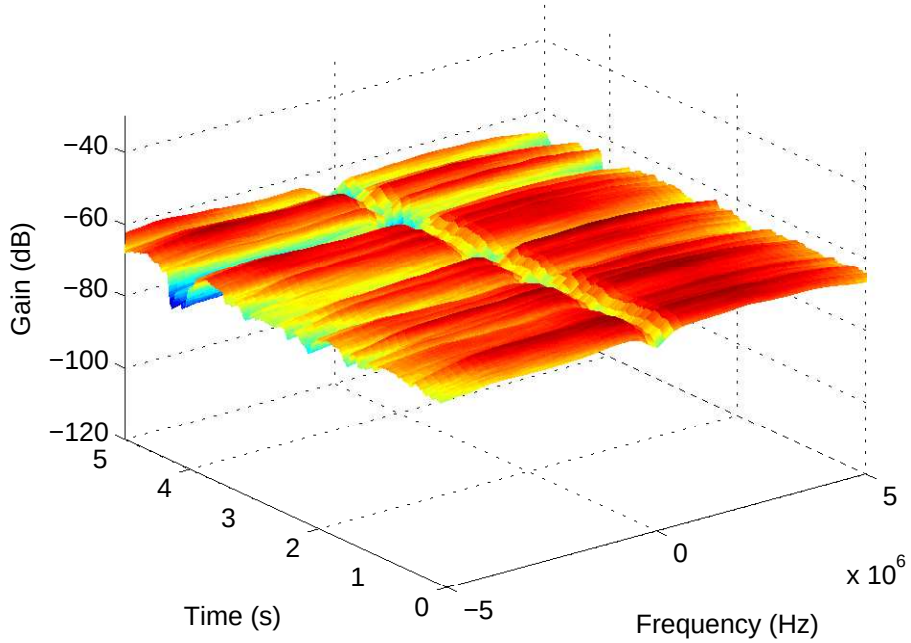

Figure 92: PSD at 2360 MHz: chest to off-body; Walking; 3 m separation; 270° orientation

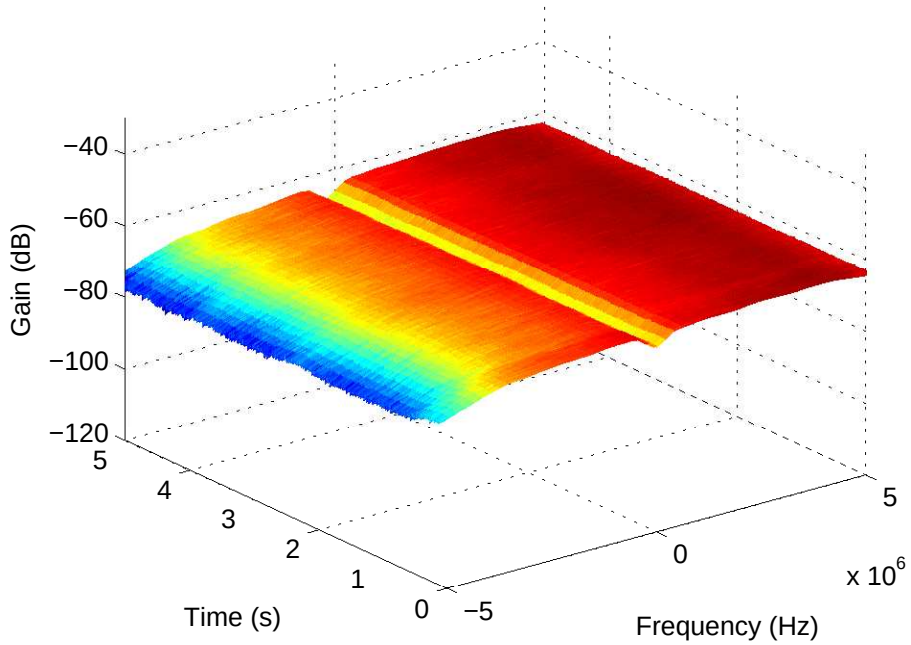

Figure 93: PSD at 2360 MHz: chest to off-body; Standing; 4 m separation; 0° orientation

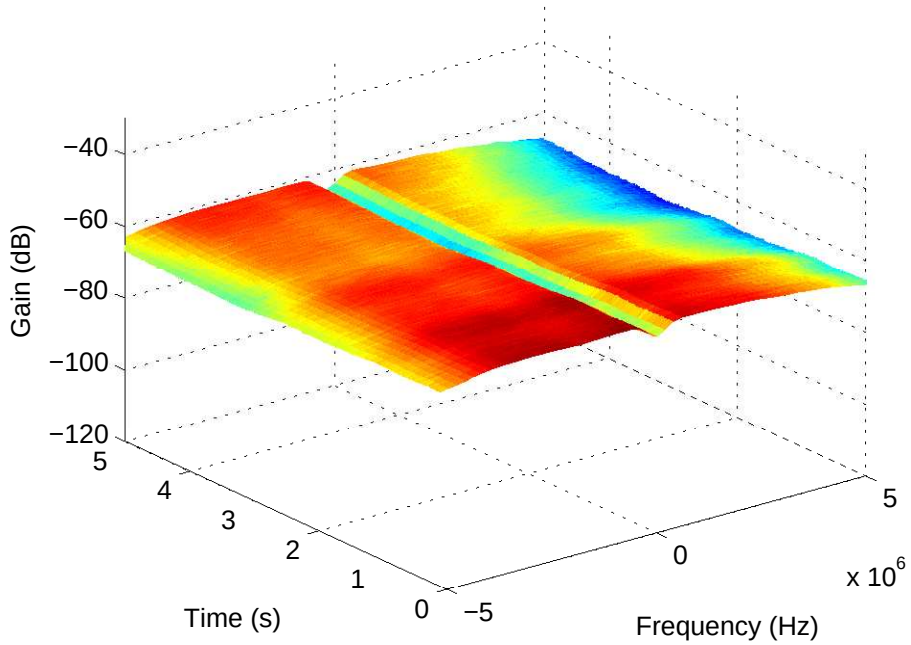

Figure 94: PSD at 2360 MHz: chest to off-body; Standing; 4 m separation; 90° orientation

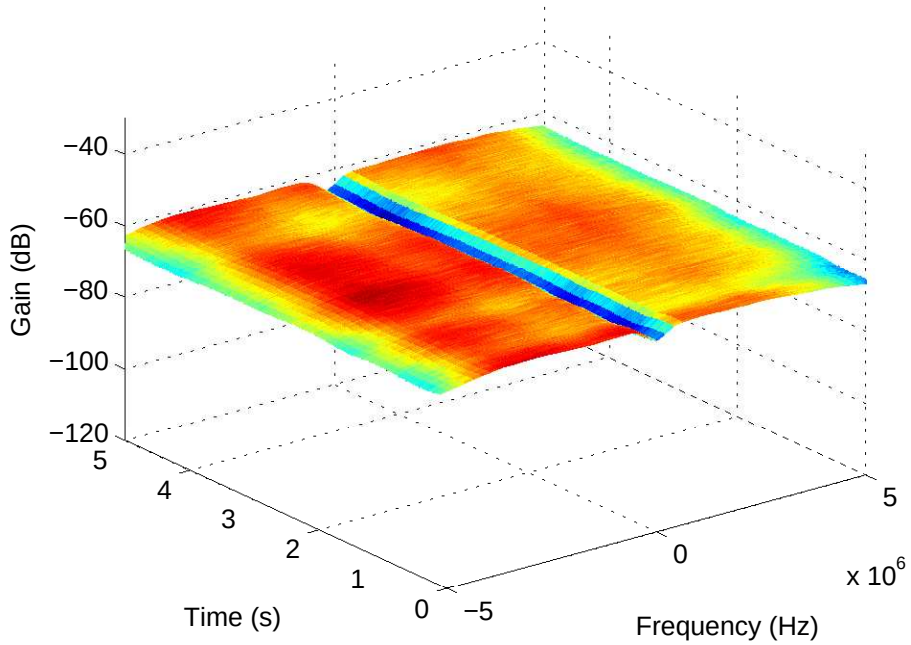

Figure 95: PSD at 2360 MHz: chest to off-body; Standing; 4 m separation; 180° orientation

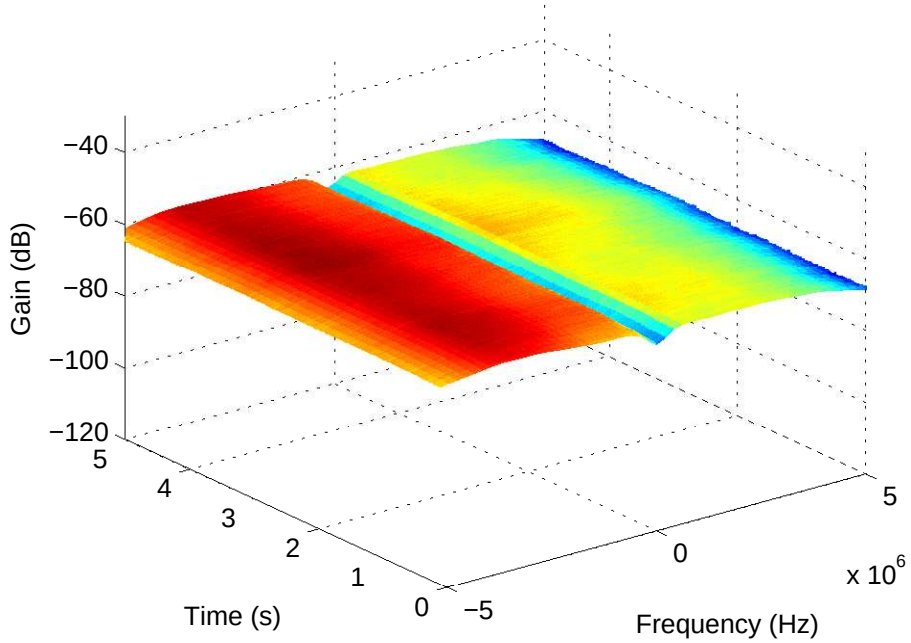

Figure 96: PSD at 2360 MHz: chest to off-body; Standing; 4 m separation; 270° orientation

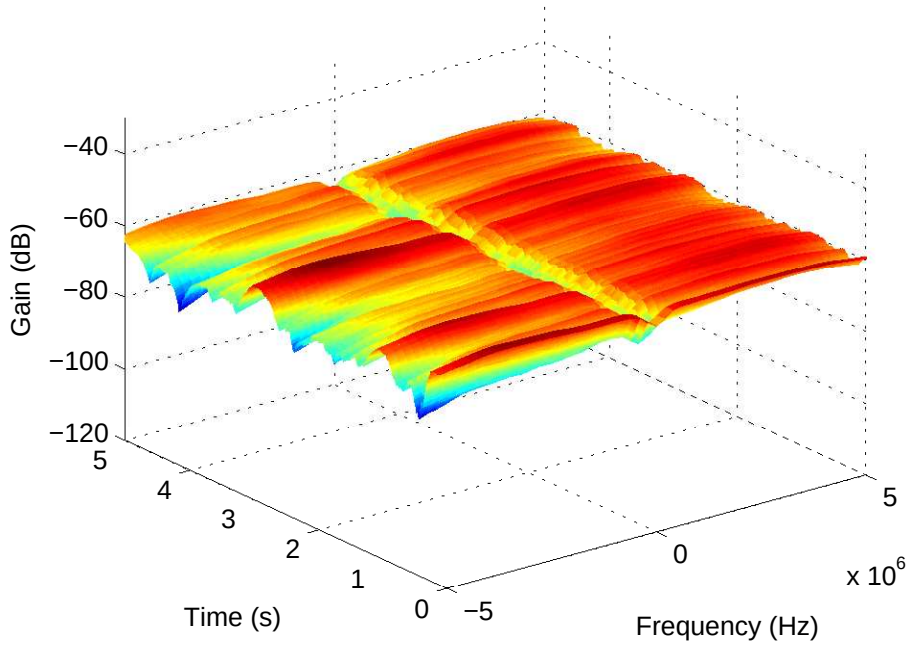

Figure 97: PSD at 2360 MHz: chest to off-body; Walking; 4 m separation; 0° orientation

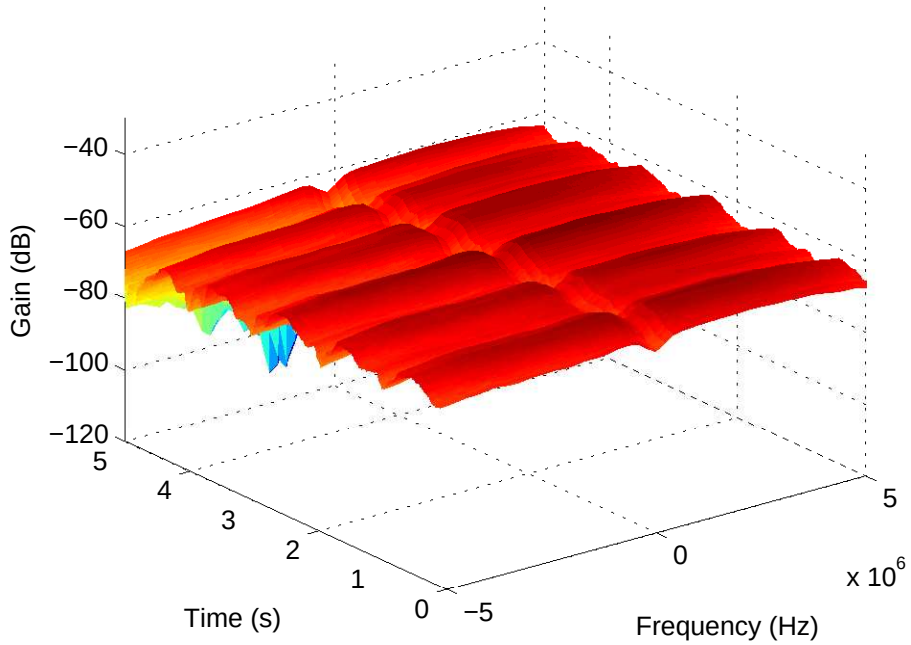

Figure 98: PSD at 2360 MHz: chest to off-body; Walking; 4 m separation; 90° orientation

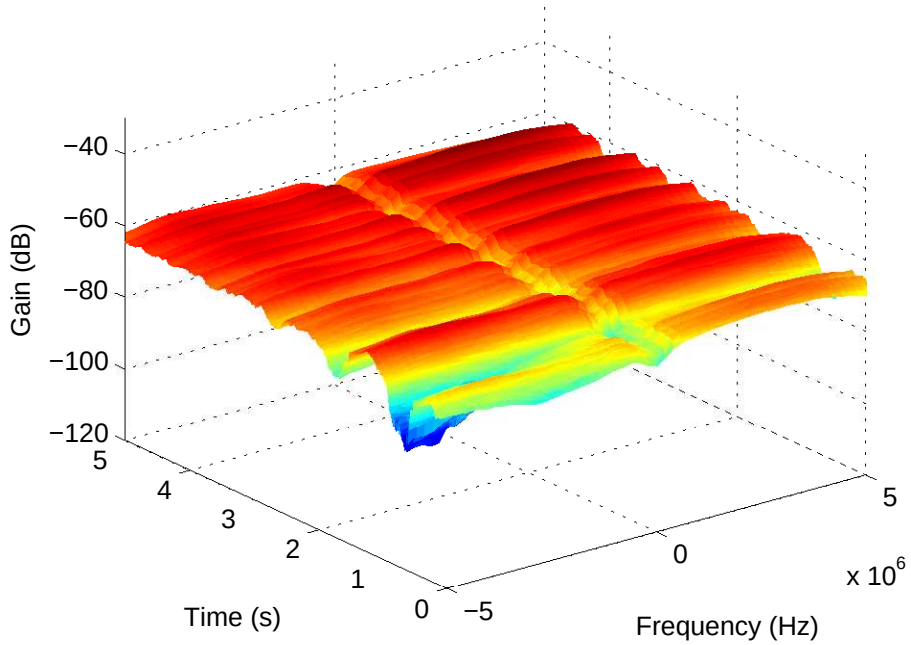

Figure 99: PSD at 2360 MHz: chest to off-body; Walking; 4 m separation; 180° orientation

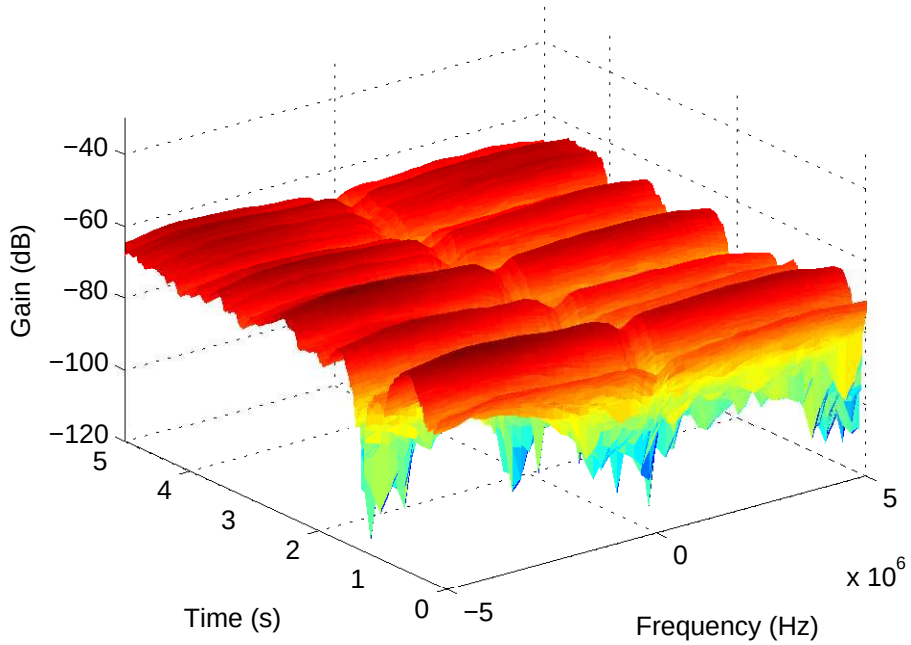

Figure 100: PSD at 2360 MHz: chest to off-body; Walking; 4 m separation; 270° orientation

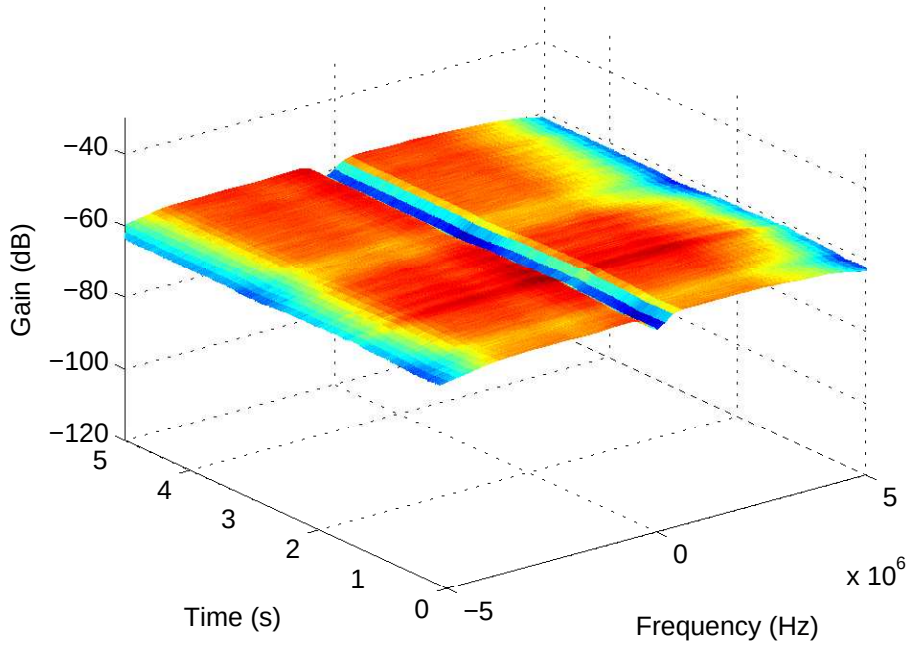

Figure 101: PSD at 2360 MHz: right wrist to off-body; Standing; 1 m separation; 0° orientation

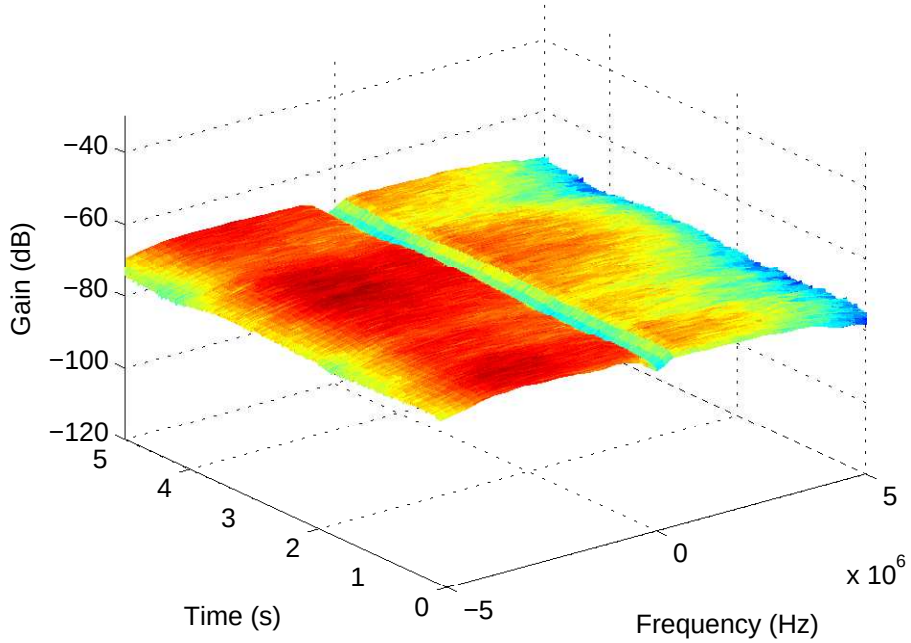

Figure 102: PSD at 2360 MHz: right wrist to off-body; Standing; 1 m separation; 90° orientation

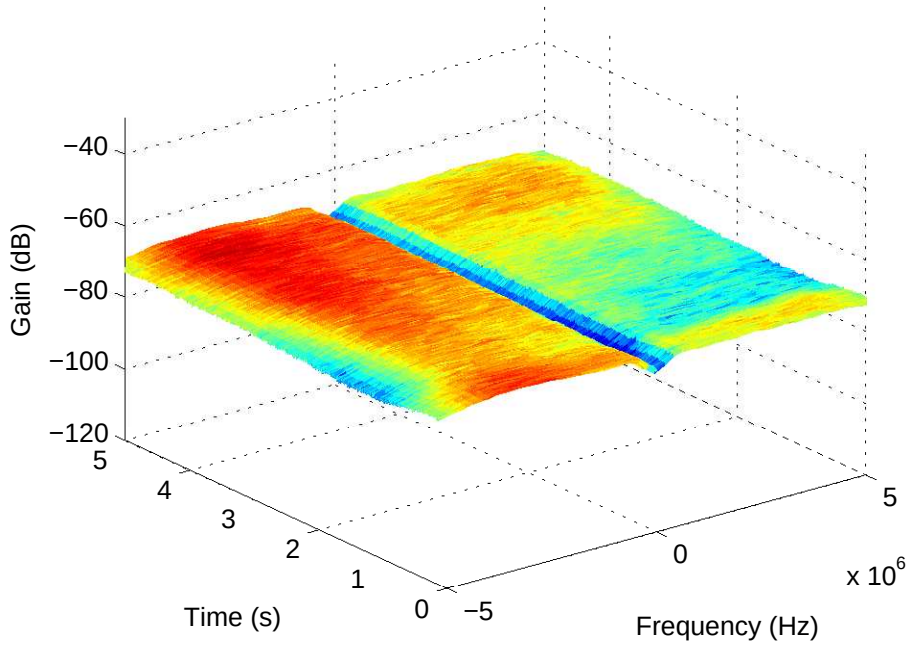

Figure 103: PSD at 2360 MHz: right wrist to off-body; Standing; 1 m separation; 180° orientation

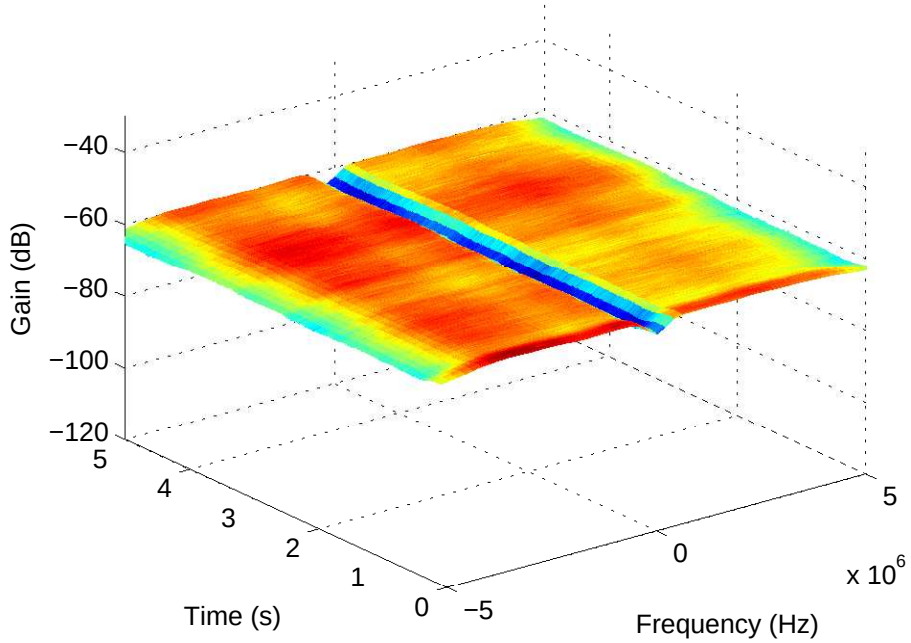

Figure 104: PSD at 2360 MHz: right wrist to off-body; Standing; 1 m separation; 270° orientation

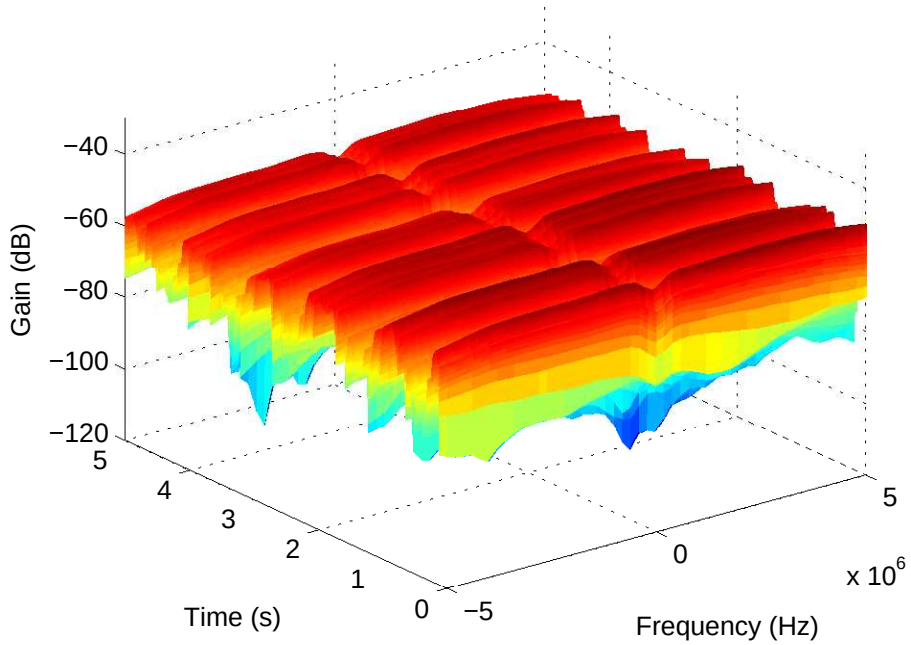

Figure 105: PSD at 2360 MHz: right wrist to off-body; Walking; 1 m separation; 0° orientation

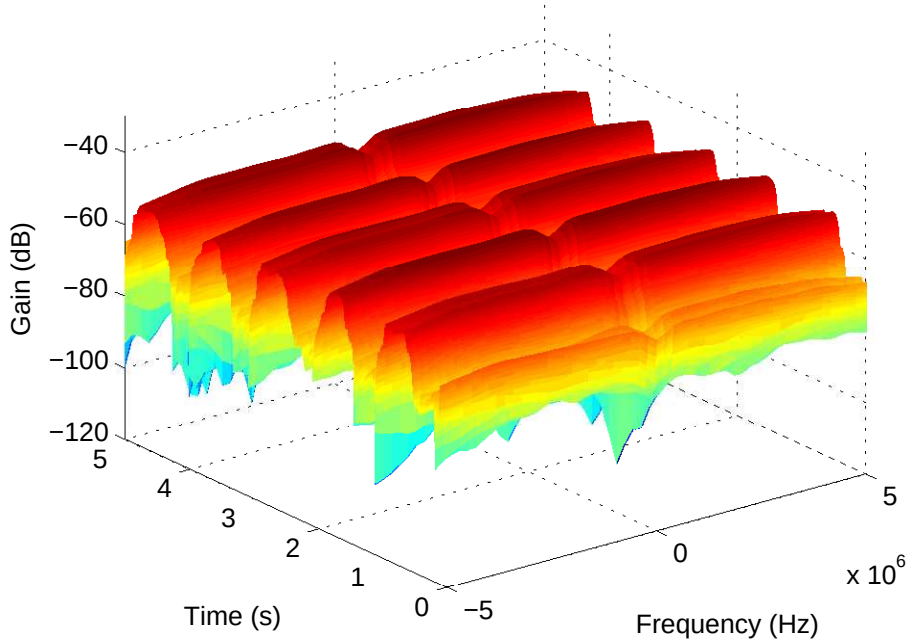

Figure 106: PSD at 2360 MHz: right wrist to off-body; Walking; 1 m separation; 90° orientation

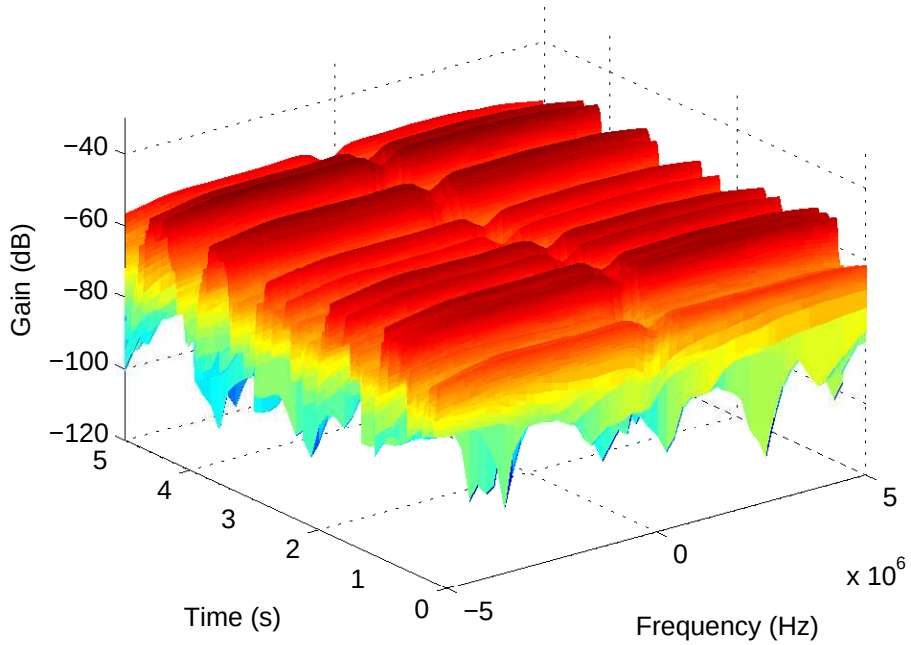

Figure 107: PSD at 2360 MHz: right wrist to off-body; Walking; 1 m separation; 180° orientation

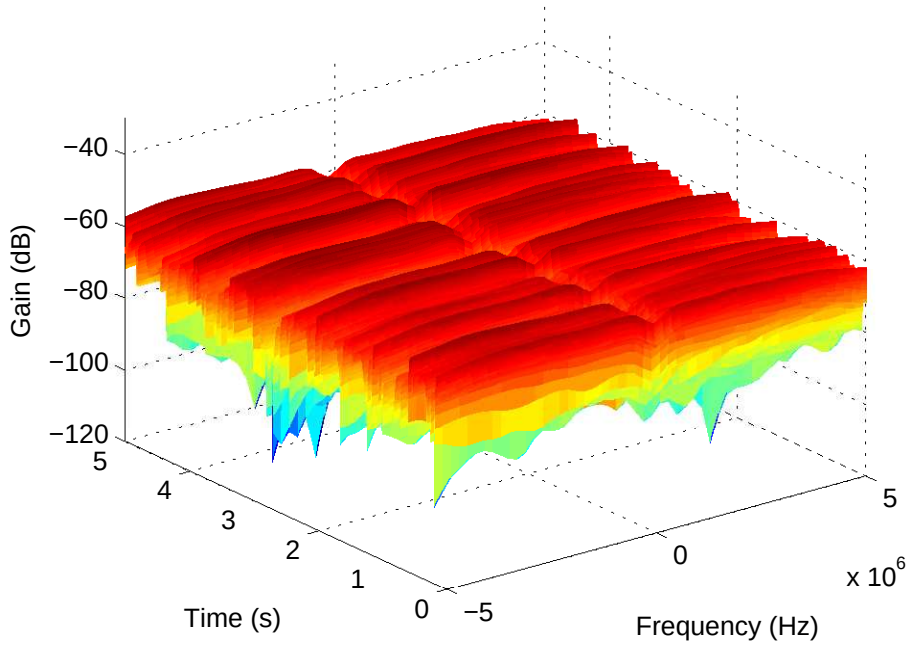

Figure 108: PSD at 2360 MHz: right wrist to off-body; Walking; 1 m separation; 270° orientation

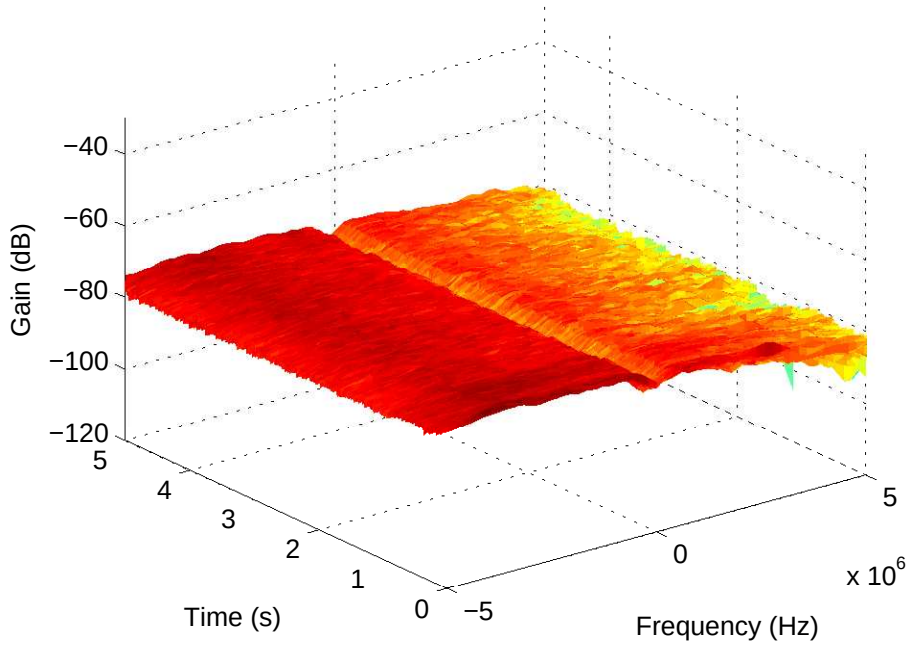

Figure 109: PSD at 2360 MHz: right wrist to off-body; Standing; 2 m separation; 0° orientation

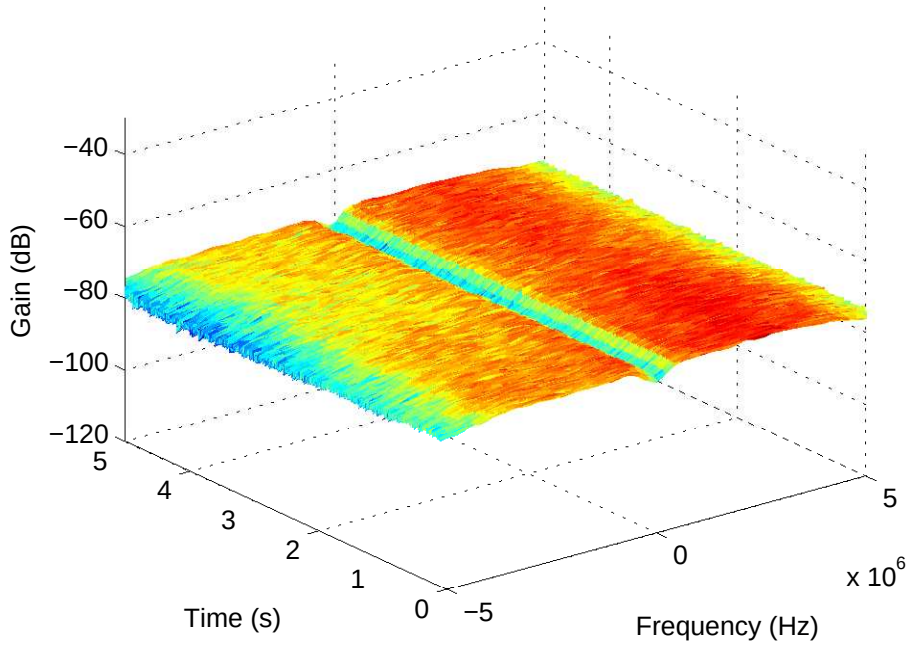

Figure 110: PSD at 2360 MHz: right wrist to off-body; Standing; 2 m separation; 90° orientation

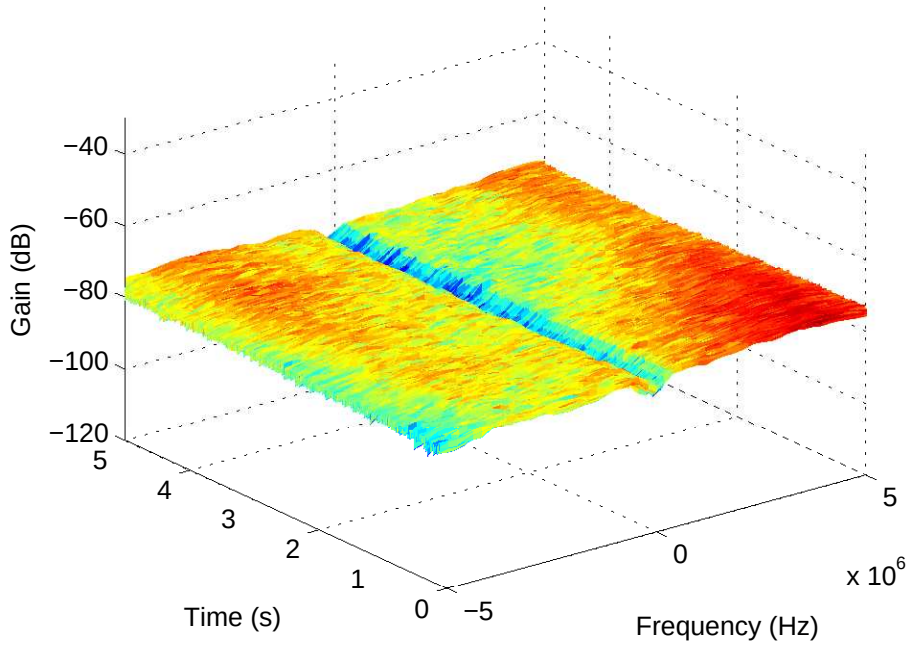

Figure 111: PSD at 2360 MHz: right wrist to off-body; Standing; 2 m separation; 180° orientation

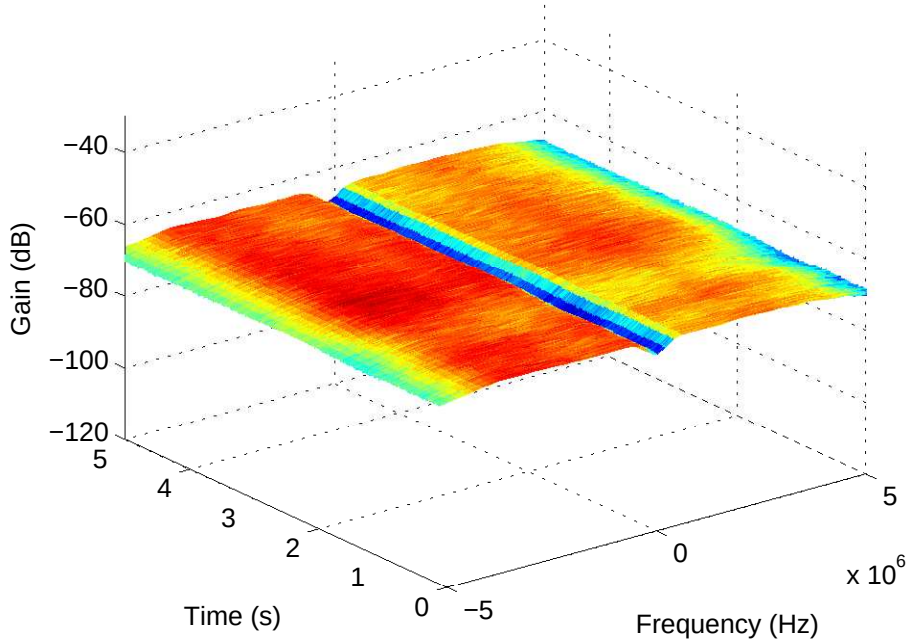

Figure 112: PSD at 2360 MHz: right wrist to off-body; Standing; 2 m separation; 270° orientation

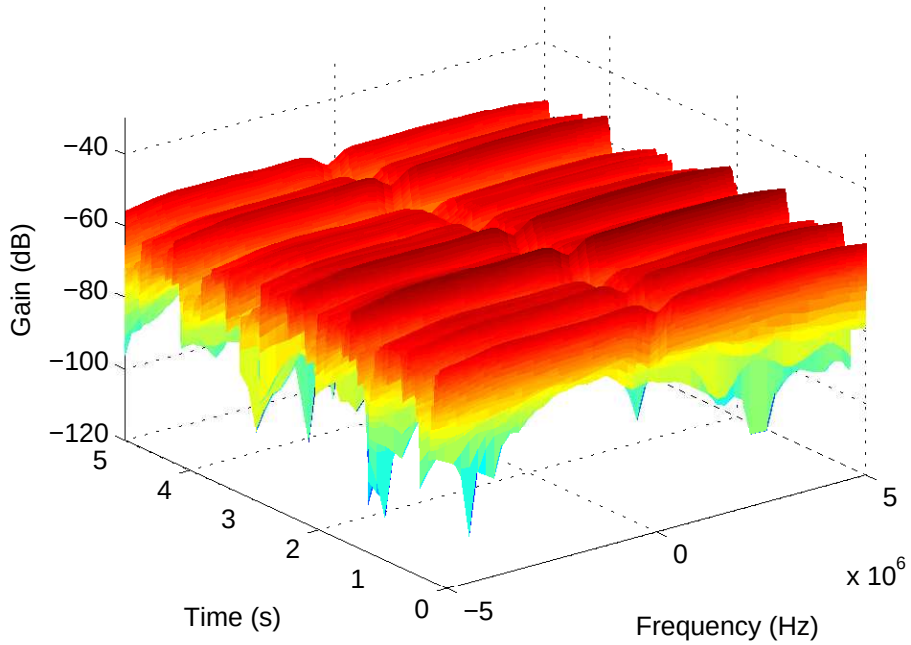

Figure 113: PSD at 2360 MHz: right wrist to off-body; Walking; 2 m separation; 0° orientation

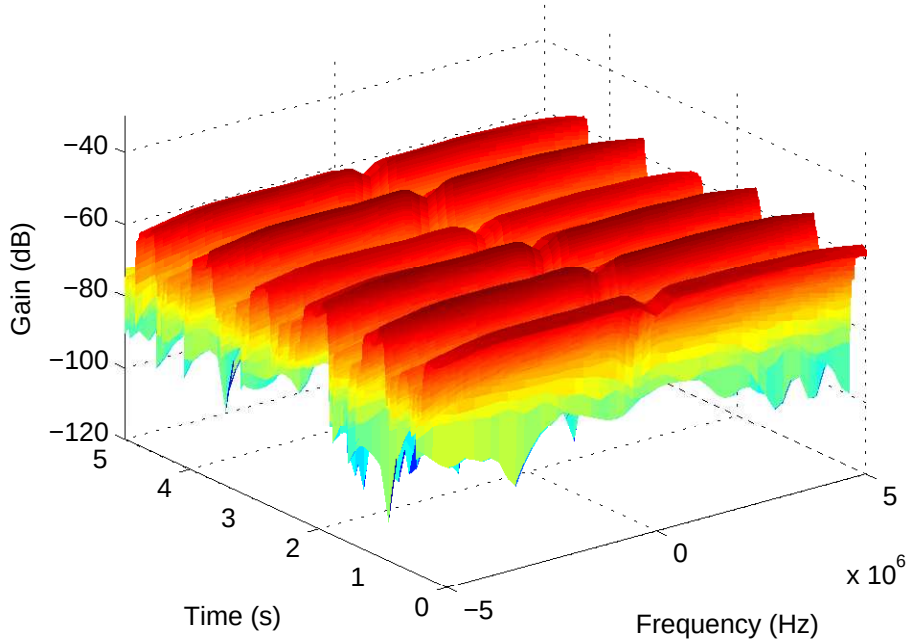

Figure 114: PSD at 2360 MHz: right wrist to off-body; Walking; 2 m separation; 90° orientation

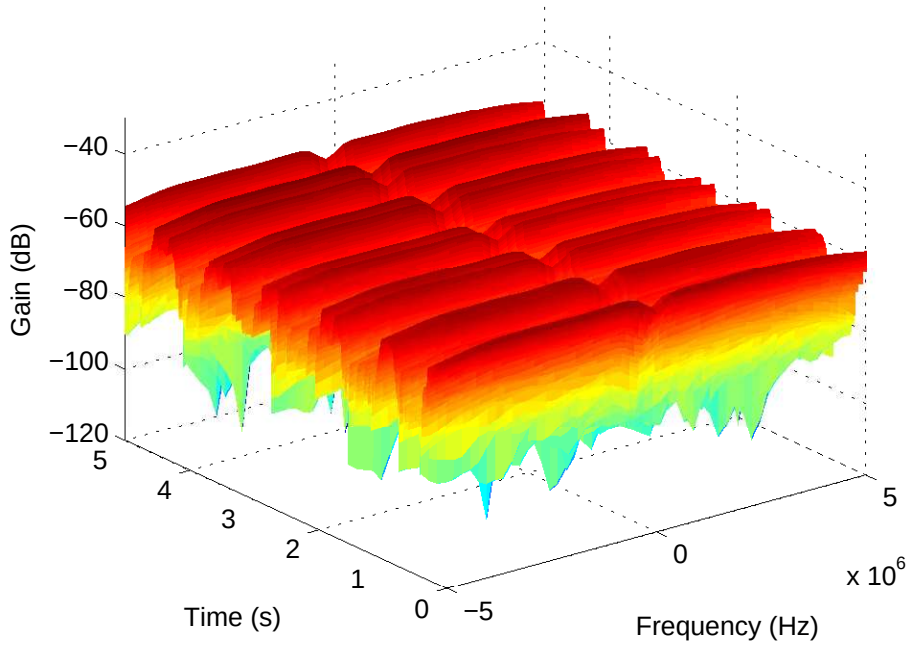

Figure 115: PSD at 2360 MHz: right wrist to off-body; Walking; 2 m separation; 180° orientation

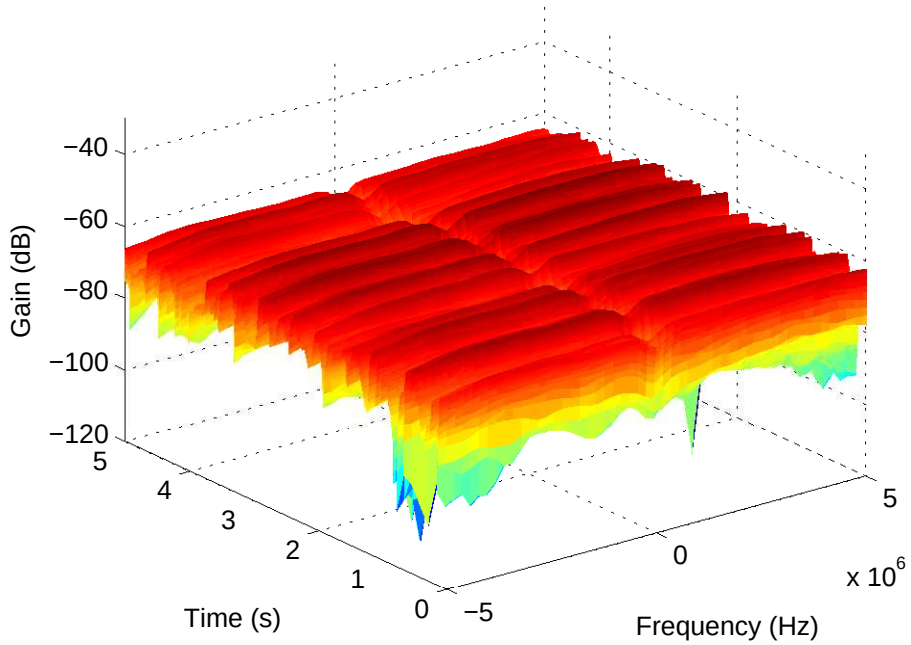

Figure 116: PSD at 2360 MHz: right wrist to off-body; Walking; 2 m separation; 270° orientation

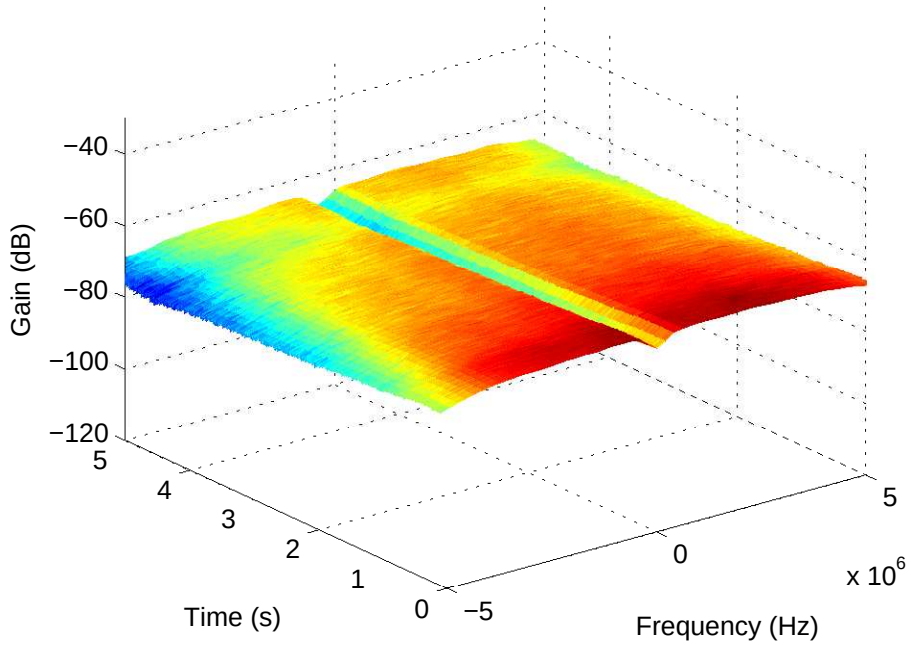

Figure 117: PSD at 2360 MHz: right wrist to off-body; Standing; 3 m separation; 0° orientation

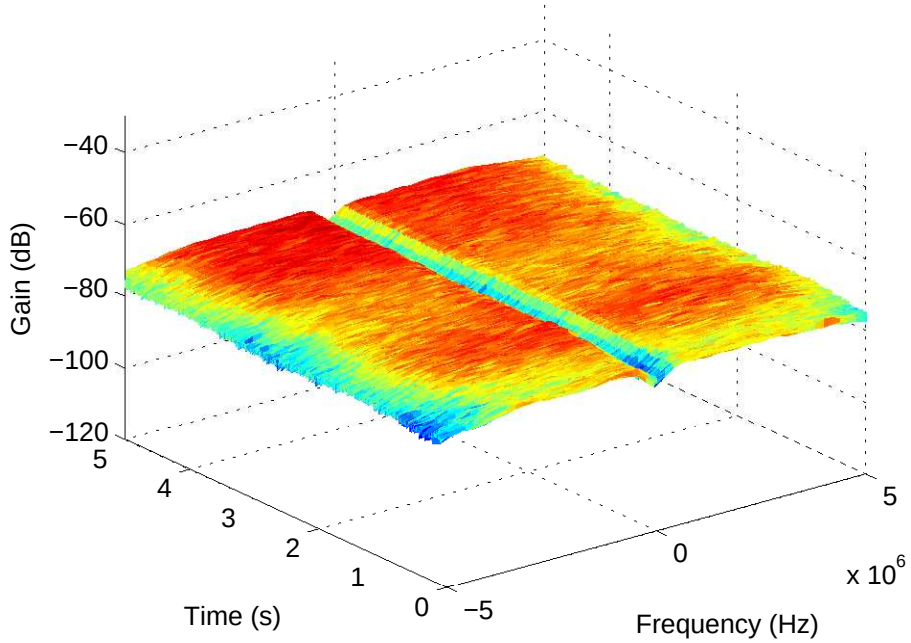

Figure 118: PSD at 2360 MHz: right wrist to off-body; Standing; 3 m separation; 90° orientation

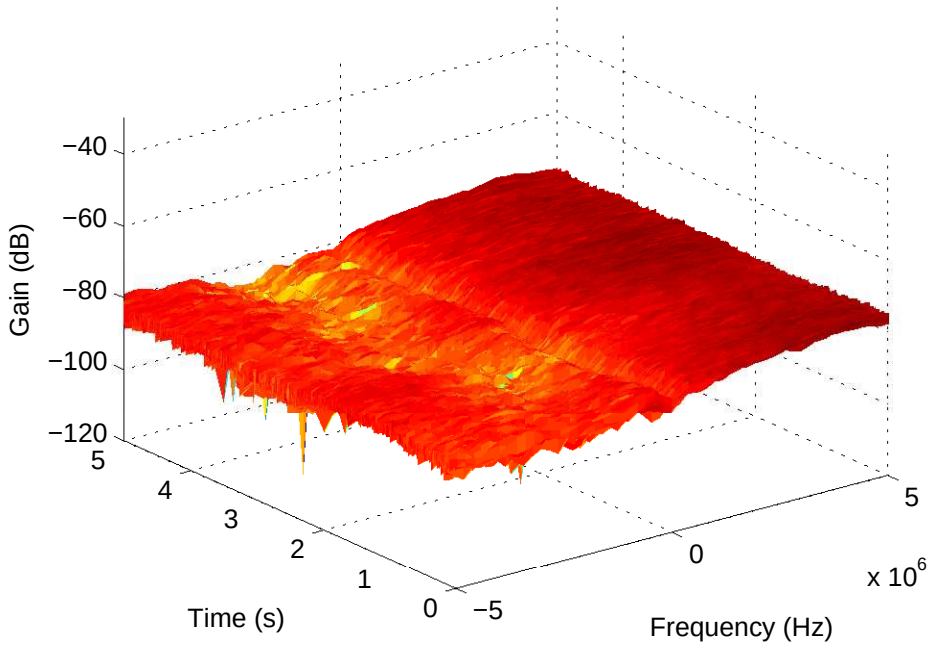

Figure 119: PSD at 2360 MHz: right wrist to off-body; Standing; 3 m separation; 180° orientation

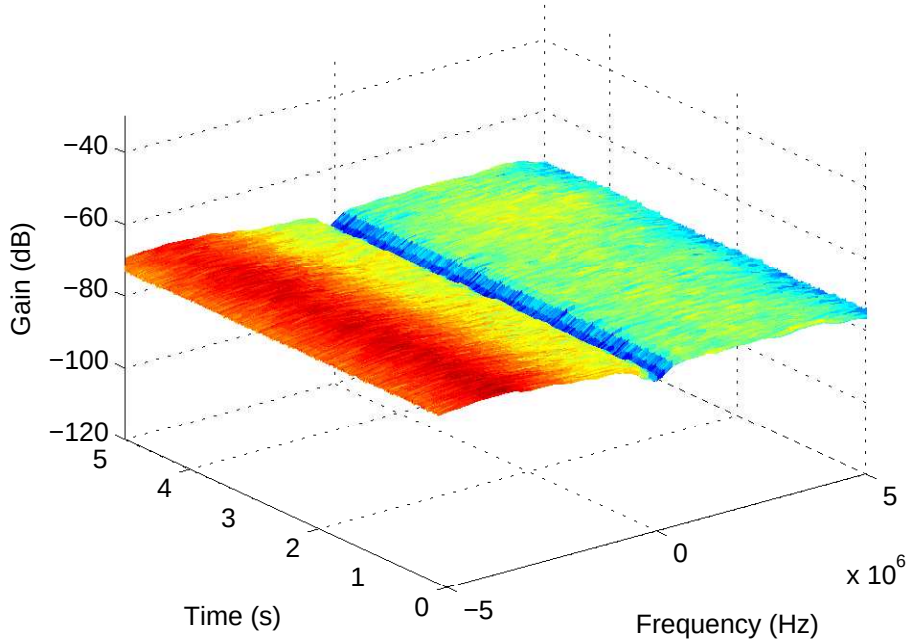

Figure 120: PSD at 2360 MHz: right wrist to off-body; Standing; 3 m separation; 270° orientation

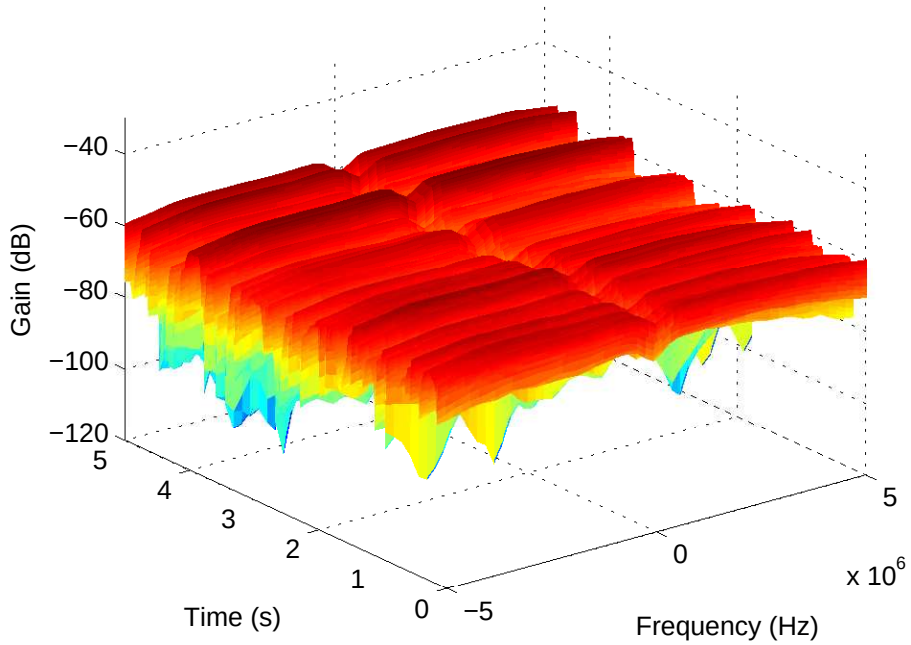

Figure 121: PSD at 2360 MHz: right wrist to off-body; Walking; 3 m separation; 0° orientation

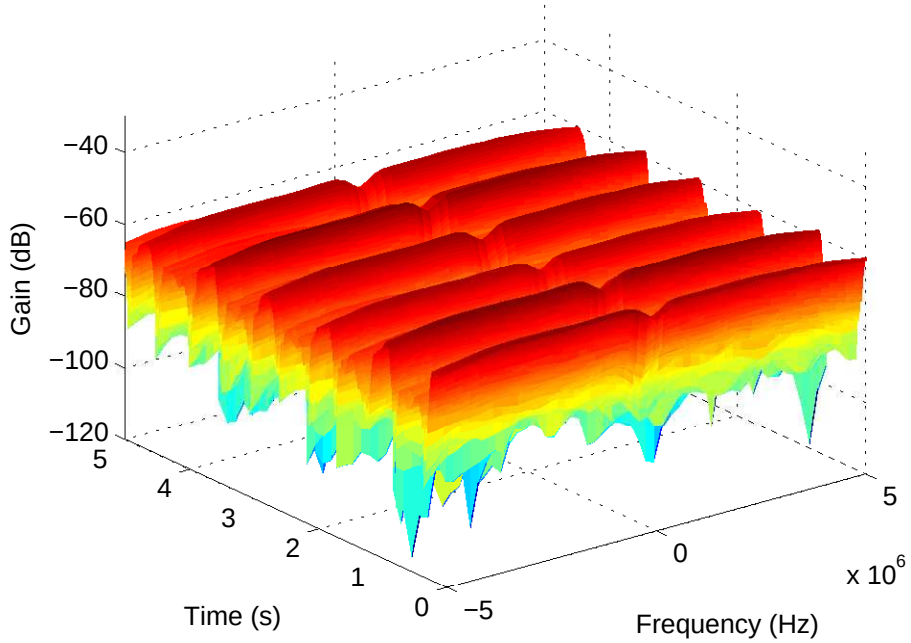

Figure 122: PSD at 2360 MHz: right wrist to off-body; Walking; 3 m separation; 90° orientation

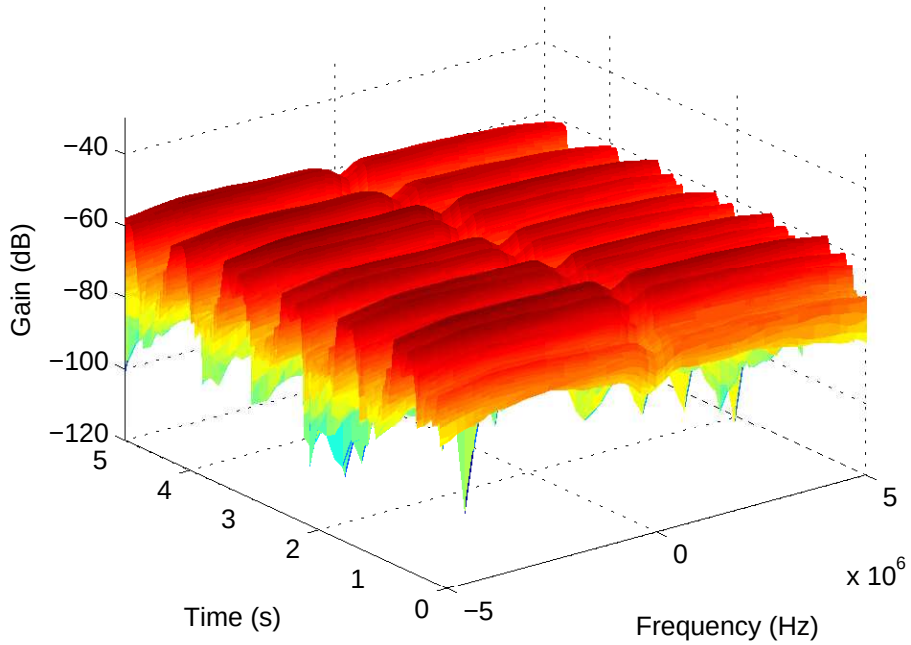

Figure 123: PSD at 2360 MHz: right wrist to off-body; Walking; 3 m separation; 180° orientation

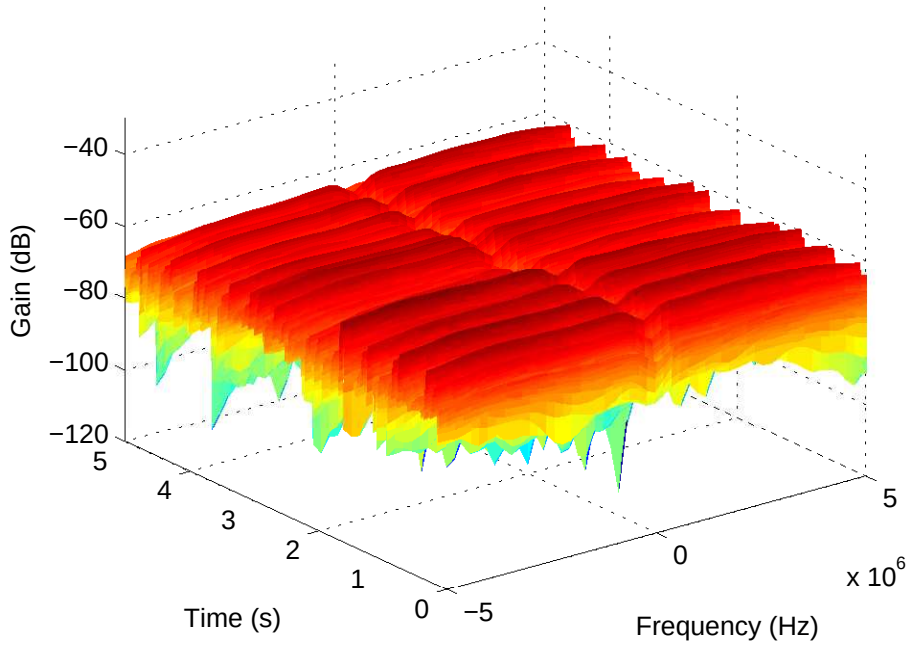

Figure 124: PSD at 2360 MHz: right wrist to off-body; Walking; 3 m separation; 270° orientation

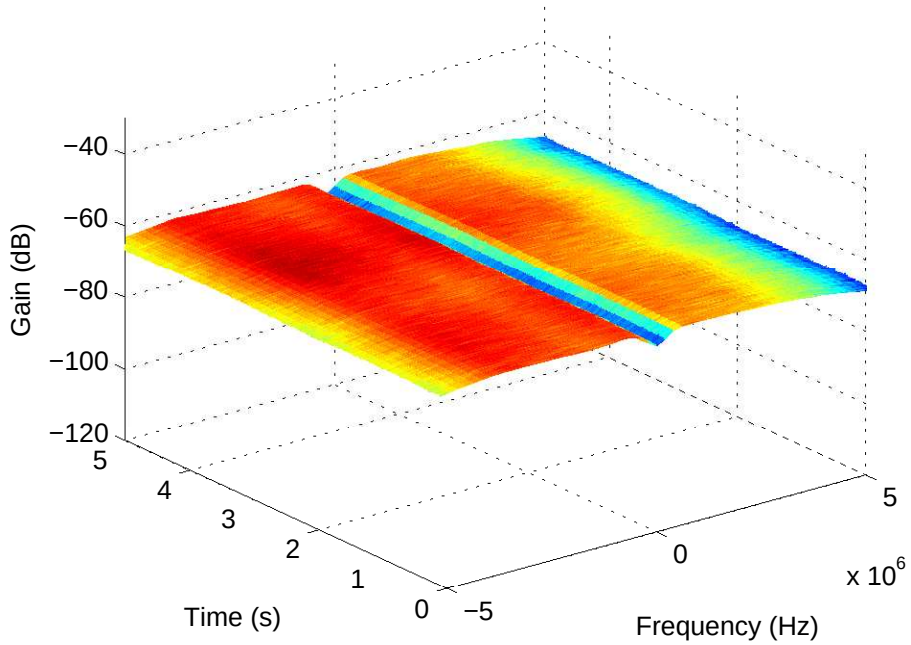

Figure 125: PSD at 2360 MHz: right wrist to off-body; Standing; 4 m separation; 0° orientation

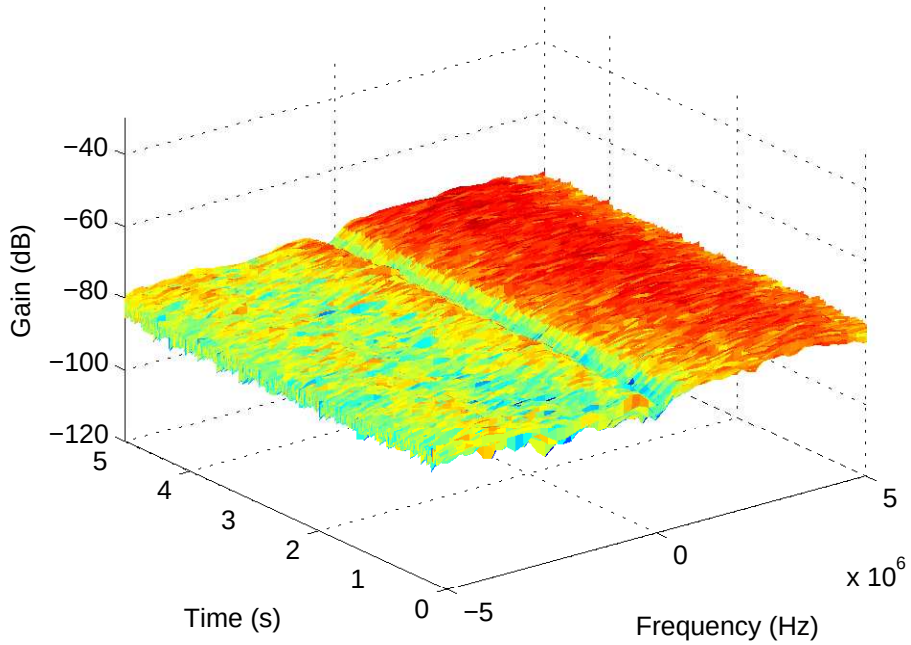

Figure 126: PSD at 2360 MHz: right wrist to off-body; Standing; 4 m separation; 90° orientation

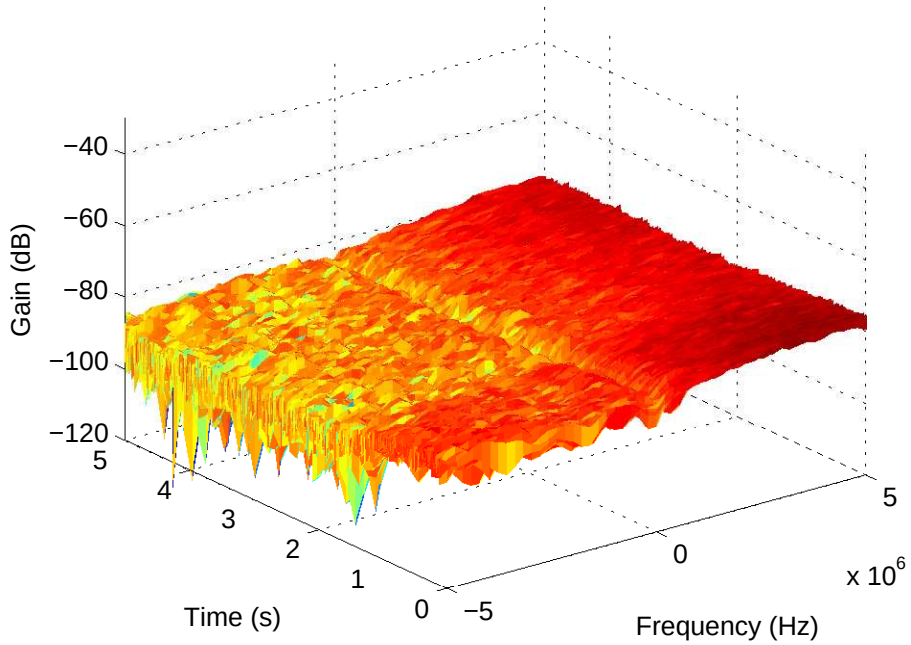

Figure 127: PSD at 2360 MHz: right wrist to off-body; Standing; 4 m separation; 180° orientation

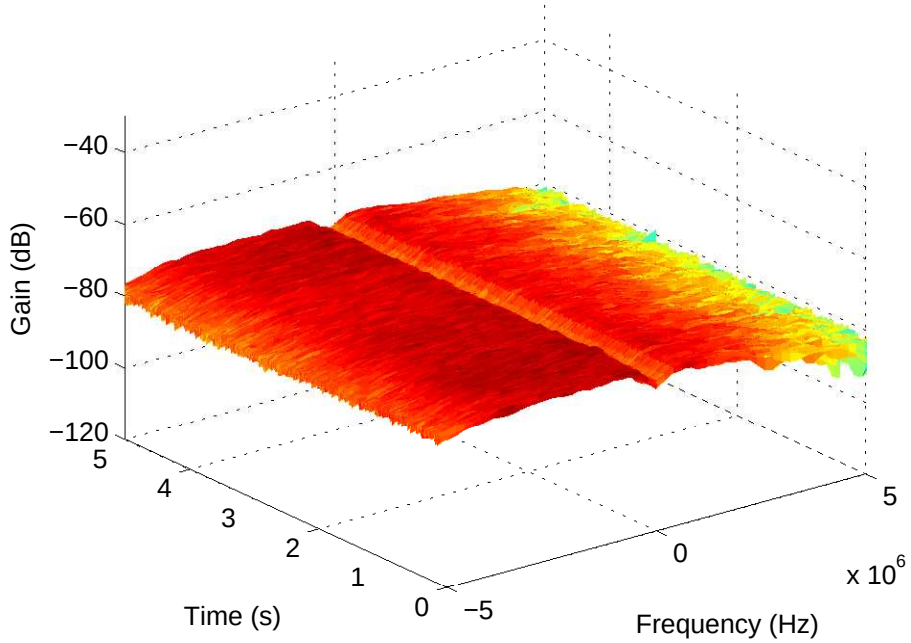

Figure 128: PSD at 2360 MHz: right wrist to off-body; Standing; 4 m separation; 270° orientation

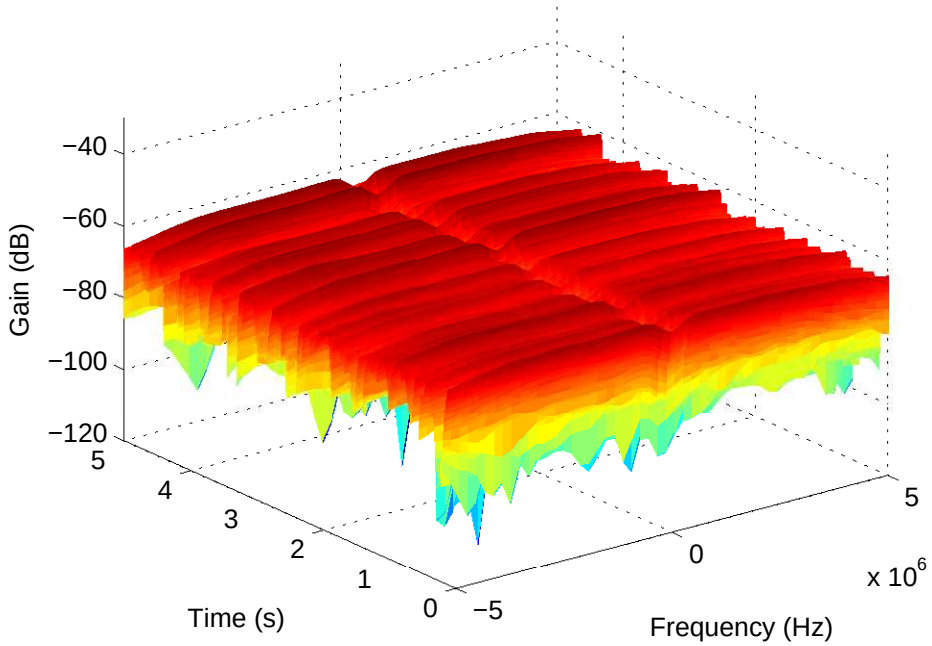

Figure 129: PSD at 2360 MHz: right wrist to off-body; Walking; 4 m separation; 0° orientation

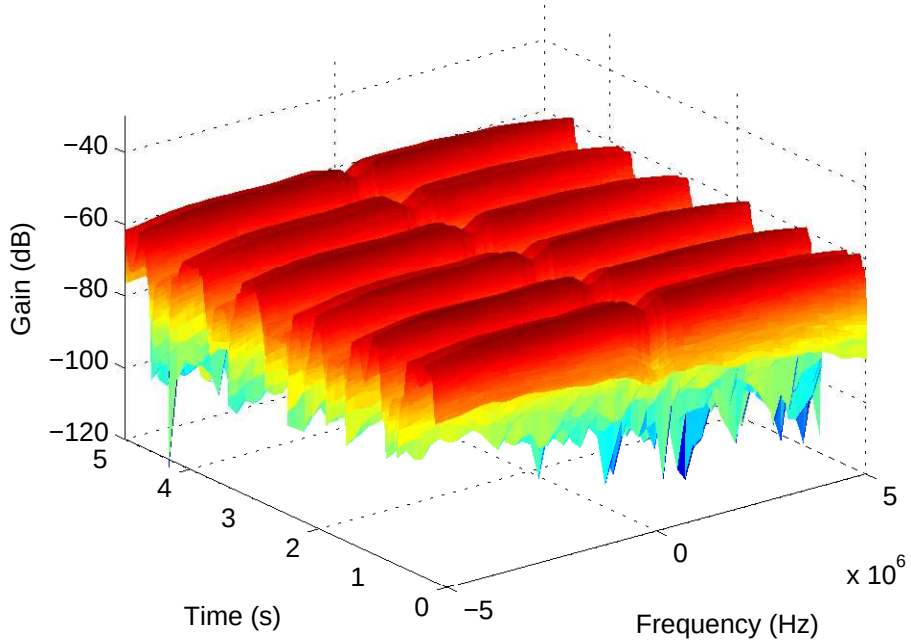

Figure 130: PSD at 2360 MHz: right wrist to off-body; Walking; 4 m separation; 90° orientation

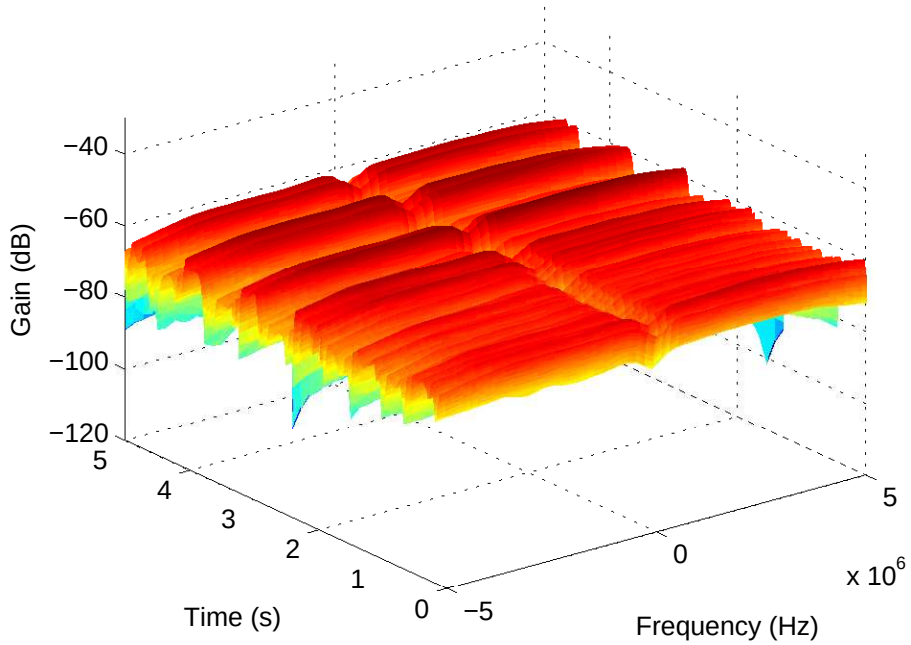

Figure 131: PSD at 2360 MHz: right wrist to off-body; Walking; 4 m separation; 180° orientation

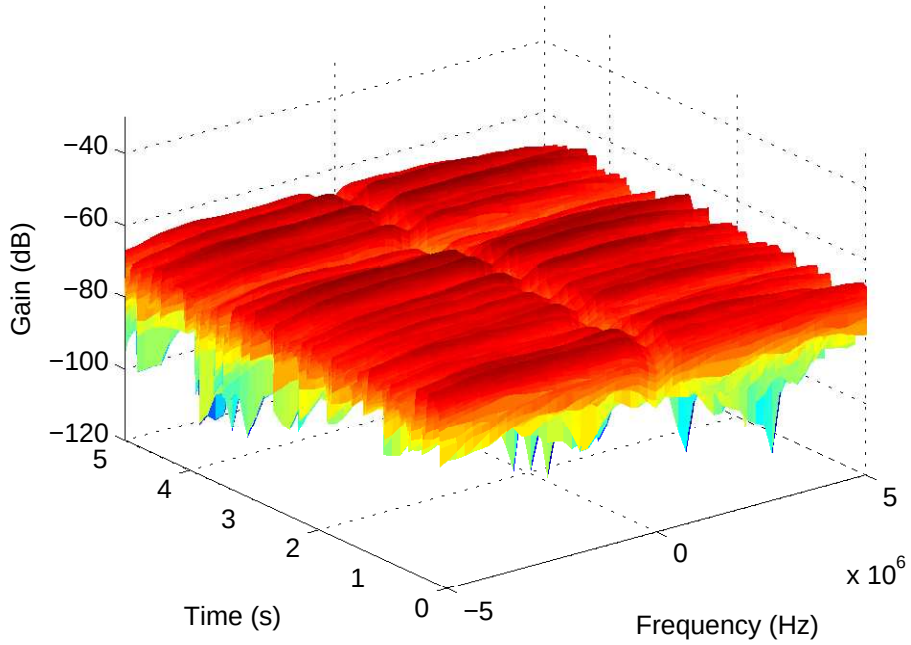

Figure 132: PSD at 2360 MHz: right wrist to off-body; Walking; 4 m separation; 270° orientation

A.2 Path Loss Characterization

A.2.1 820 MHz measurements

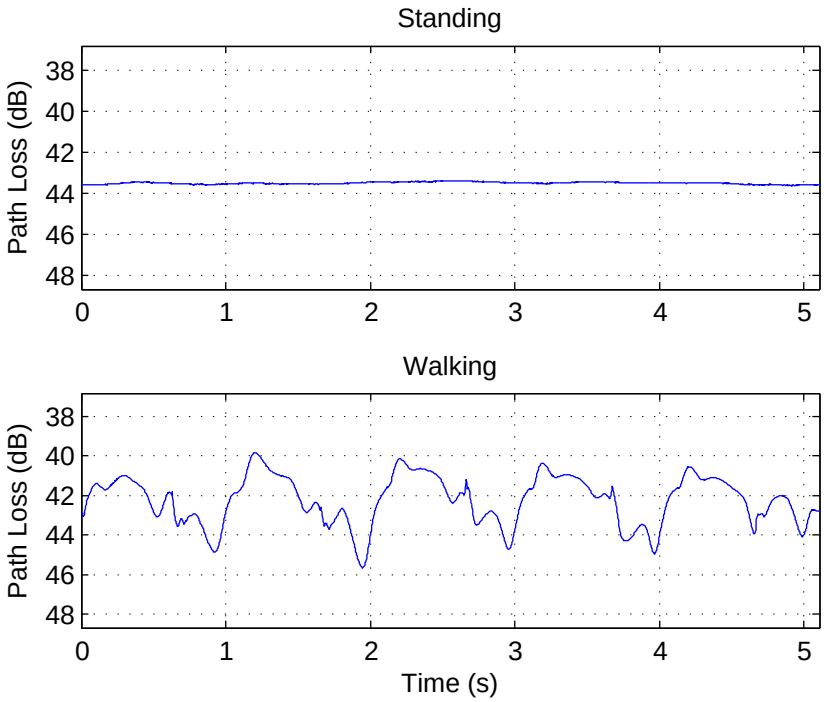

Figure 133: Path loss measurements over time at 820 MHz: chest to off-body; 1 m separation; 0° orientation

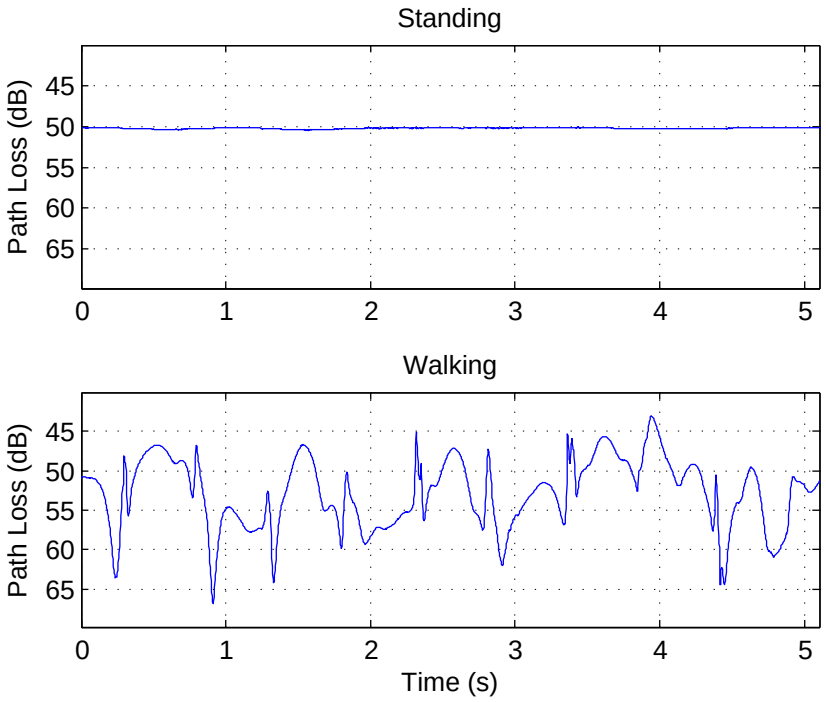

Figure 134: Path loss measurements over time at 820 MHz: chest to off-body; 1 m separation; 90° orientation

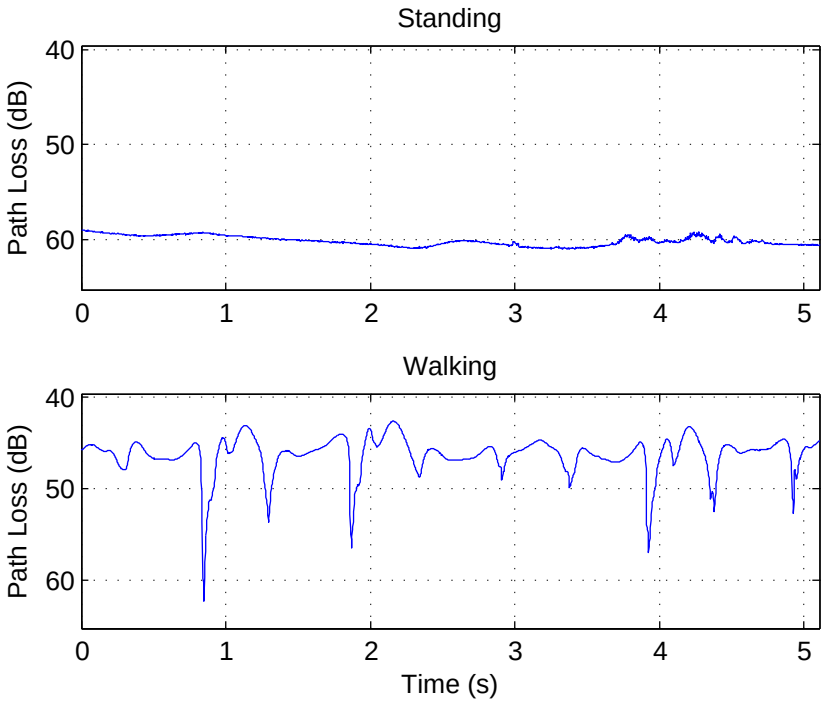

Figure 135: Path loss measurements over time at 820 MHz: chest to off-body; 1 m separation; 180° orientation

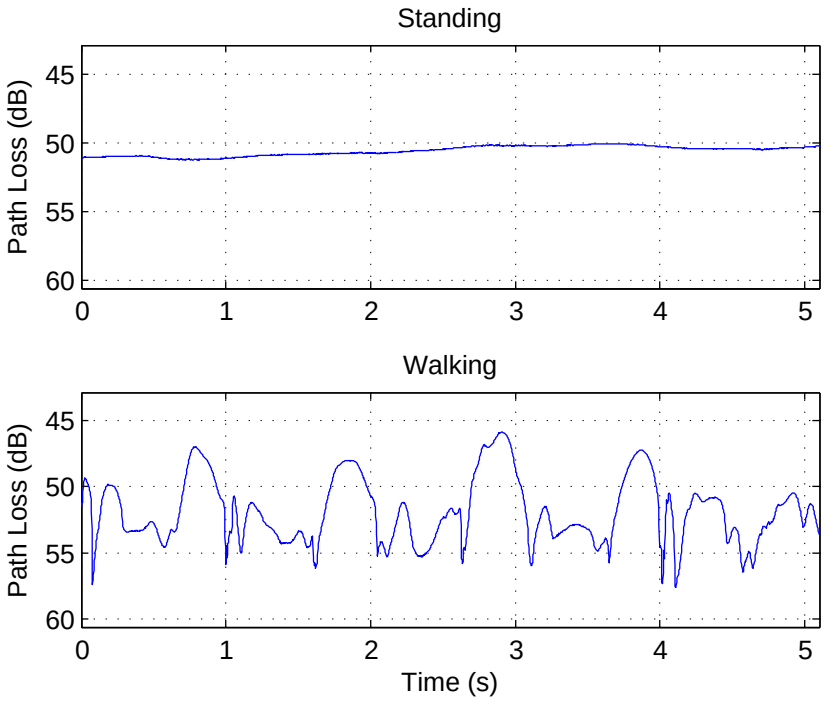

Figure 136: Path loss measurements over time at 820 MHz: chest to off-body; 1 m separation; 270° orientation

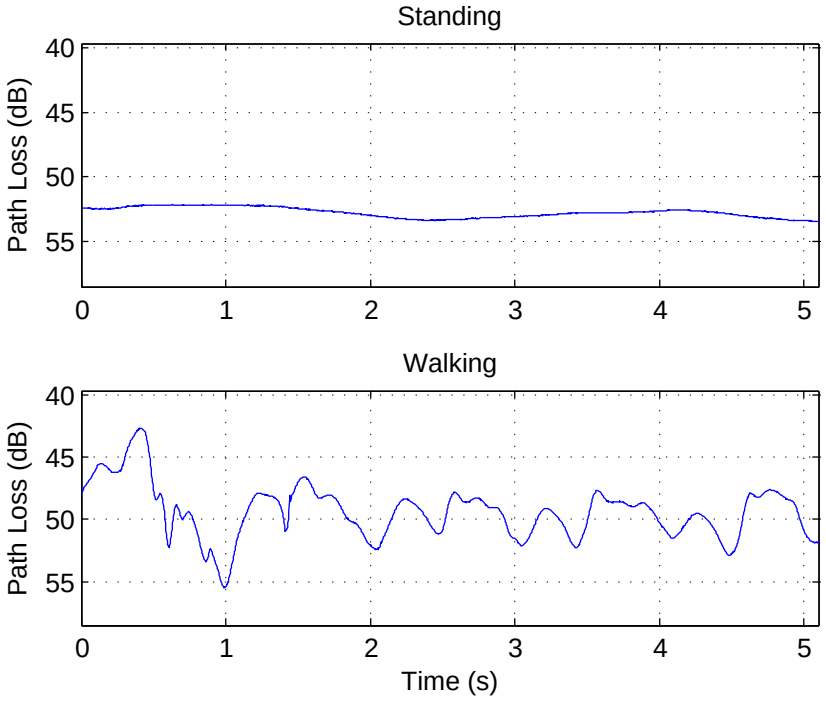

Figure 137: Path loss measurements over time at 820 MHz: chest to off-body; 2 m separation; 0° orientation

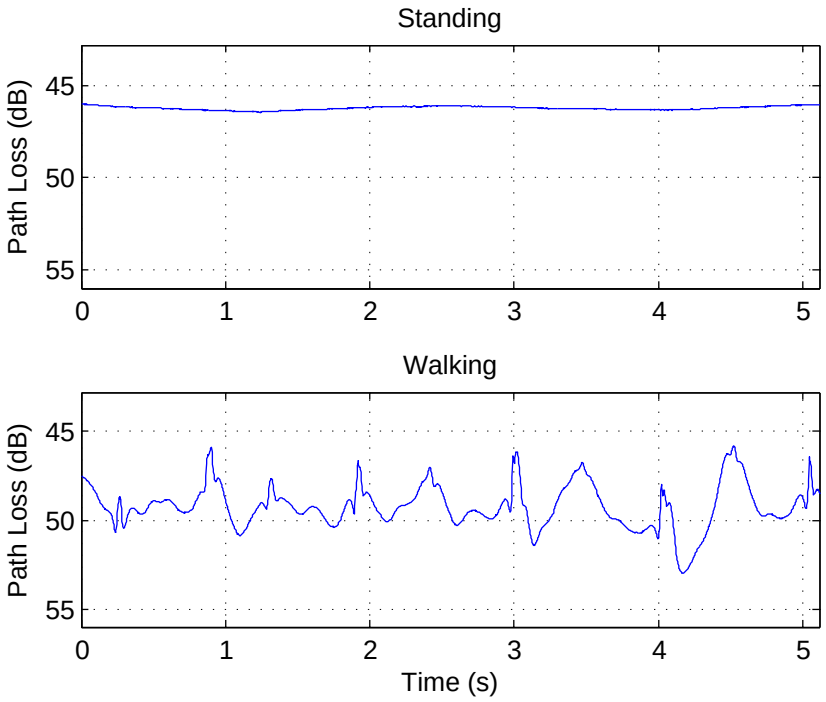

Figure 138: Path loss measurements over time at 820 MHz: chest to off-body; 2 m separation; 90° orientation

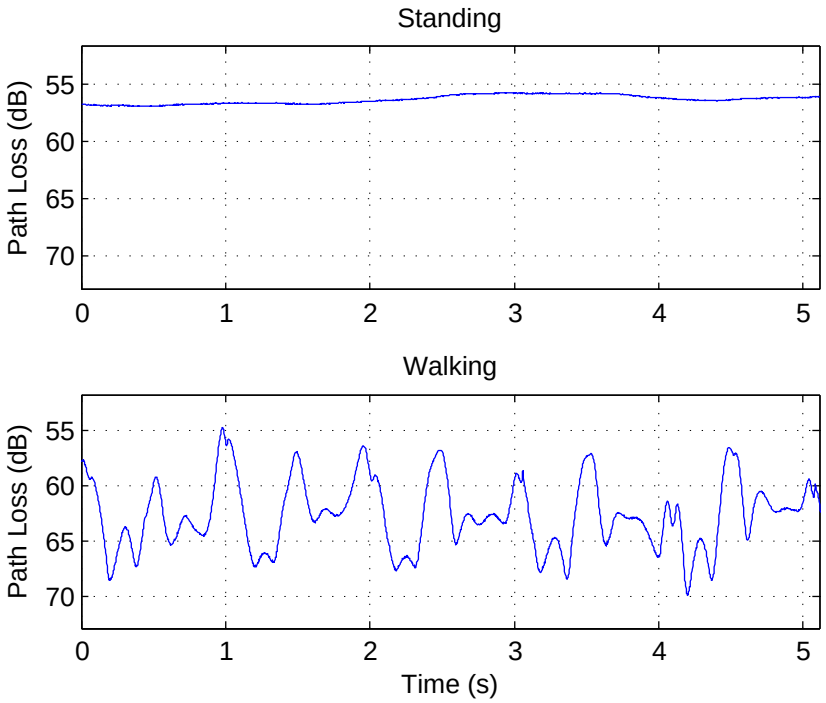

Figure 139: Path loss measurements over time at 820 MHz: chest to off-body; 2 m separation; 180° orientation

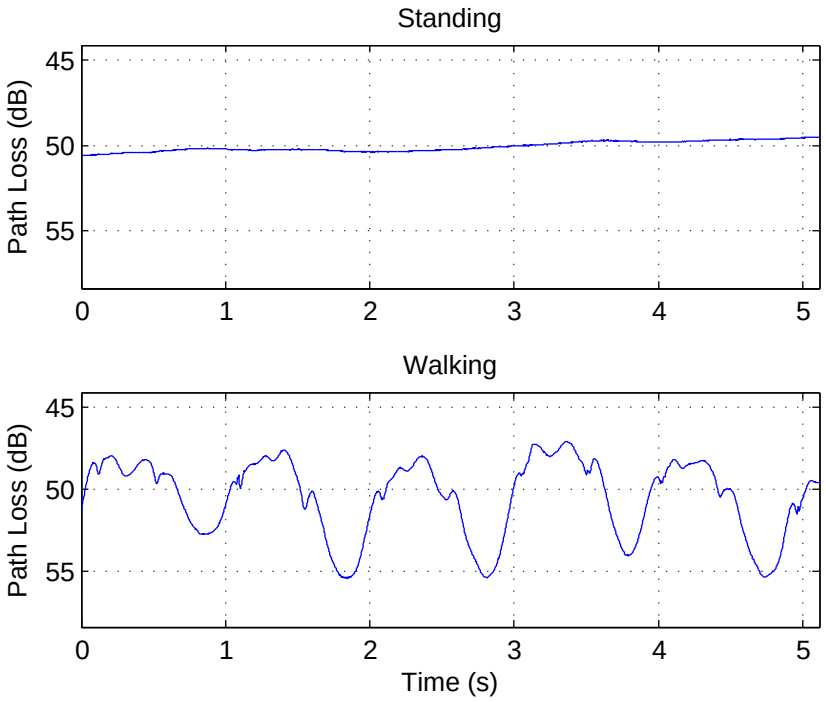

Figure 140: Path loss measurements over time at 820 MHz: chest to off-body; 2 m separation; 270° orientation

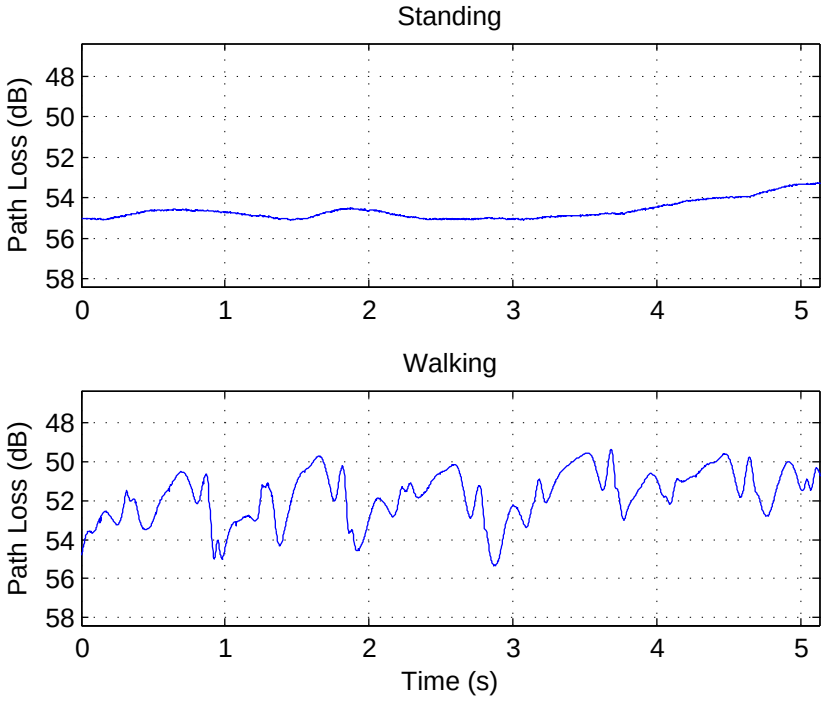

Figure 141: Path loss measurements over time at 820 MHz: chest to off-body; 3 m separation; 0° orientation

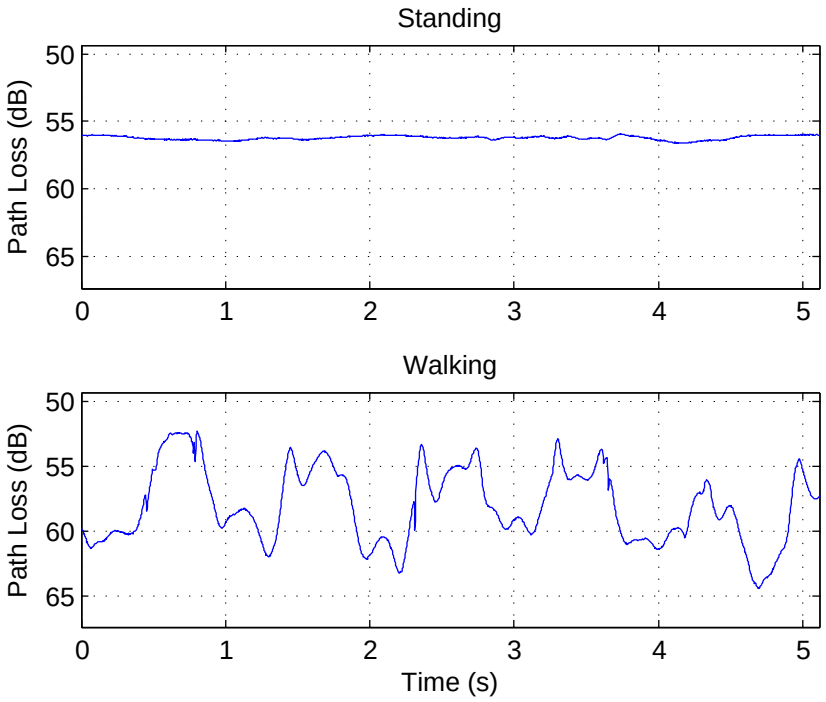

Figure 142: Path loss measurements over time at 820 MHz: chest to off-body; 3 m separation; 90° orientation

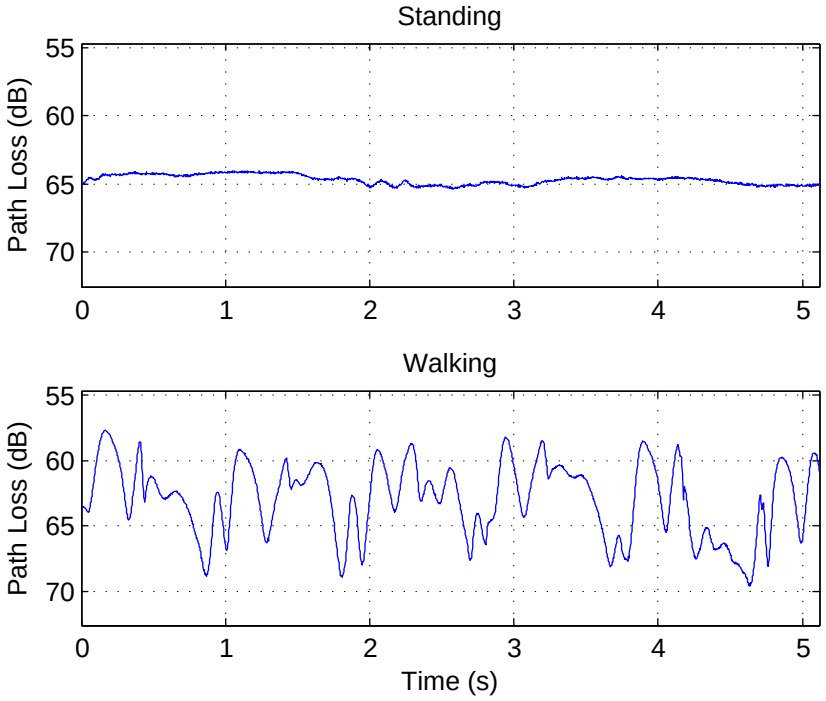

Figure 143: Path loss measurements over time at 820 MHz: chest to off-body; 3 m separation; 180° orientation

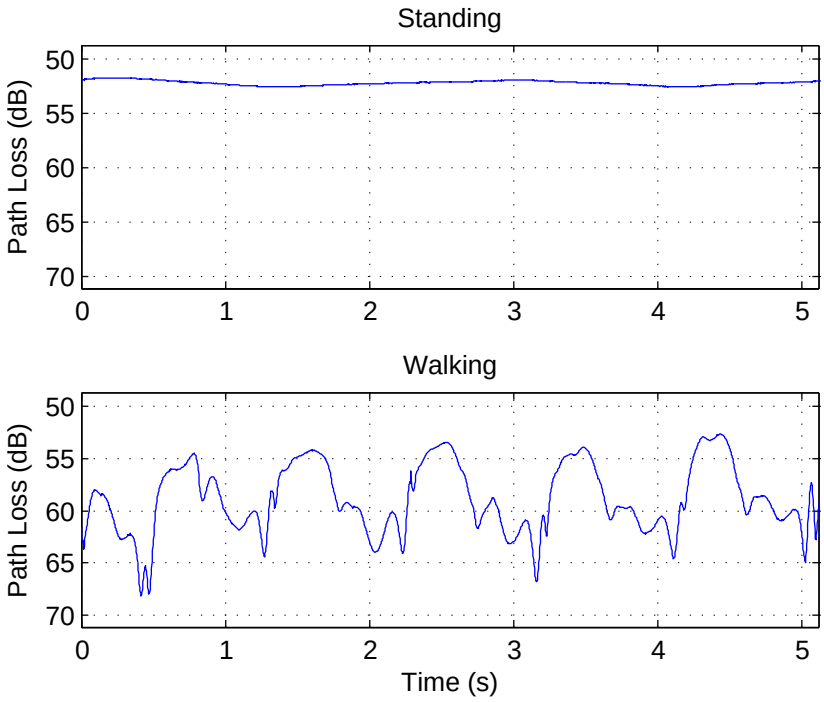

Figure 144: Path loss measurements over time at 820 MHz: chest to off-body; 3 m separation; 270° orientation

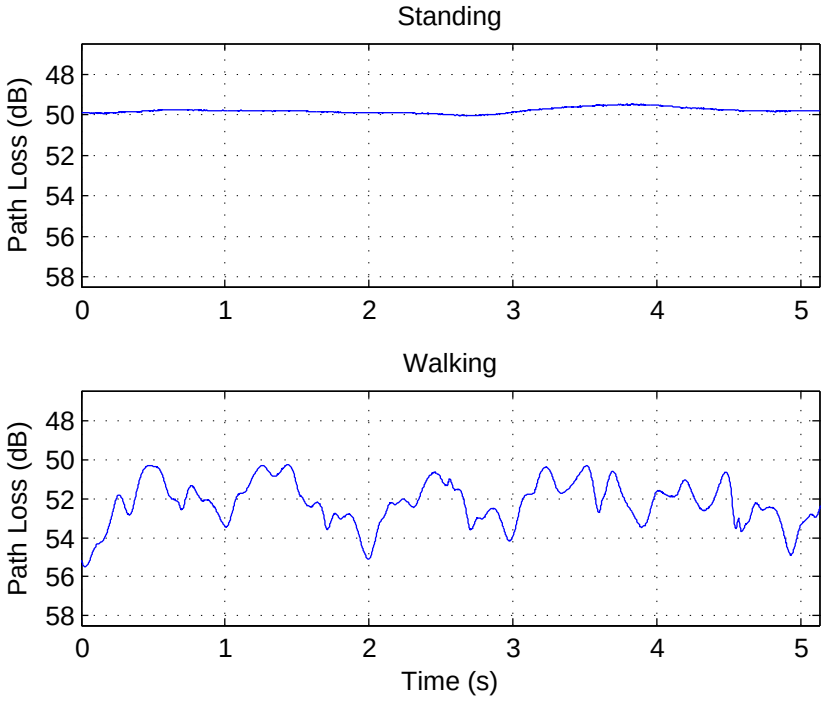

Figure 145: Path loss measurements over time at 820 MHz: chest to off-body; 4 m separation; 0° orientation

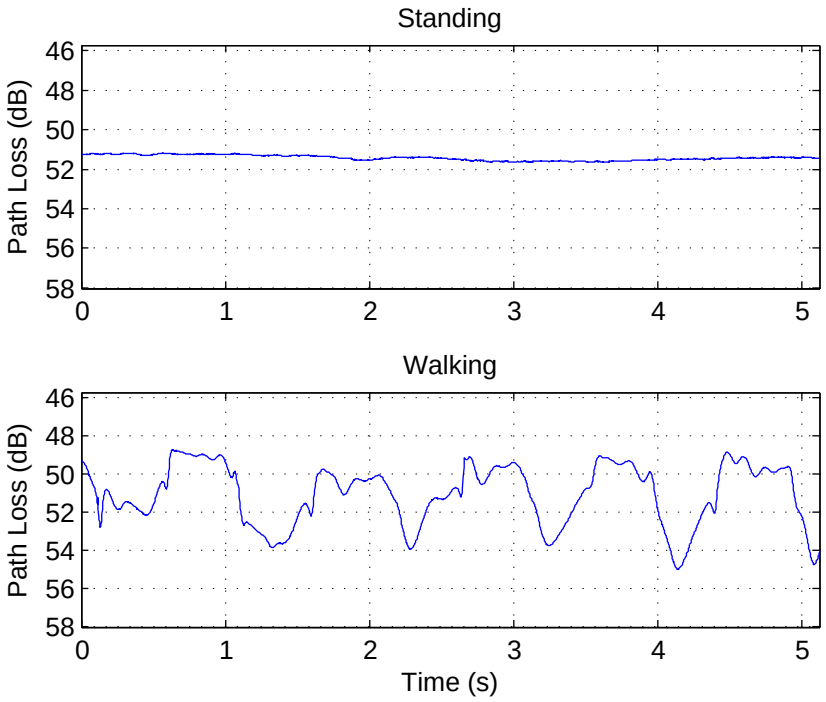

Figure 146: Path loss measurements over time at 820 MHz: chest to off-body; 4 m separation; 90° orientation

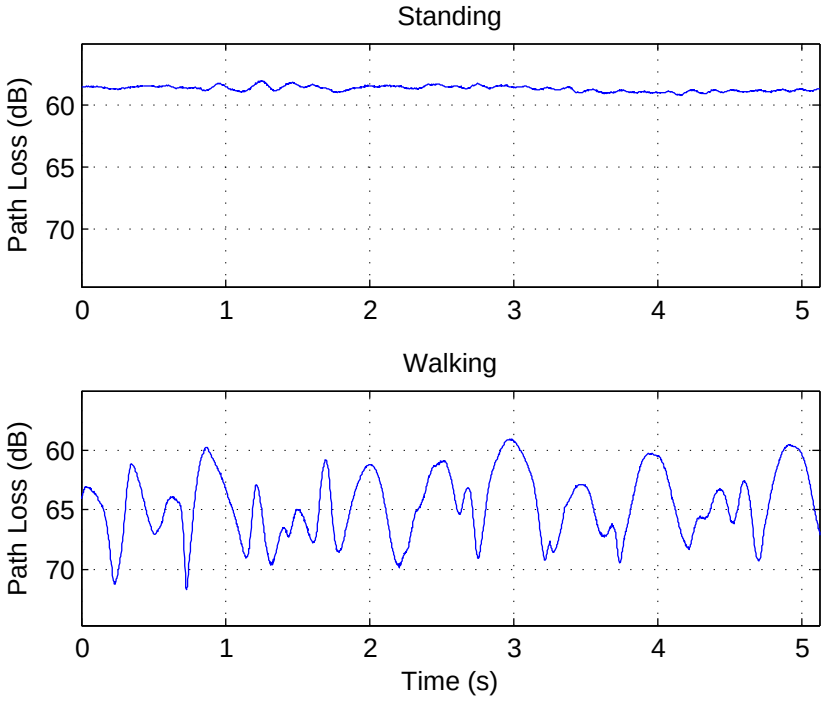

Figure 147: Path loss measurements over time at 820 MHz: chest to off-body; 4 m separation; 180° orientation

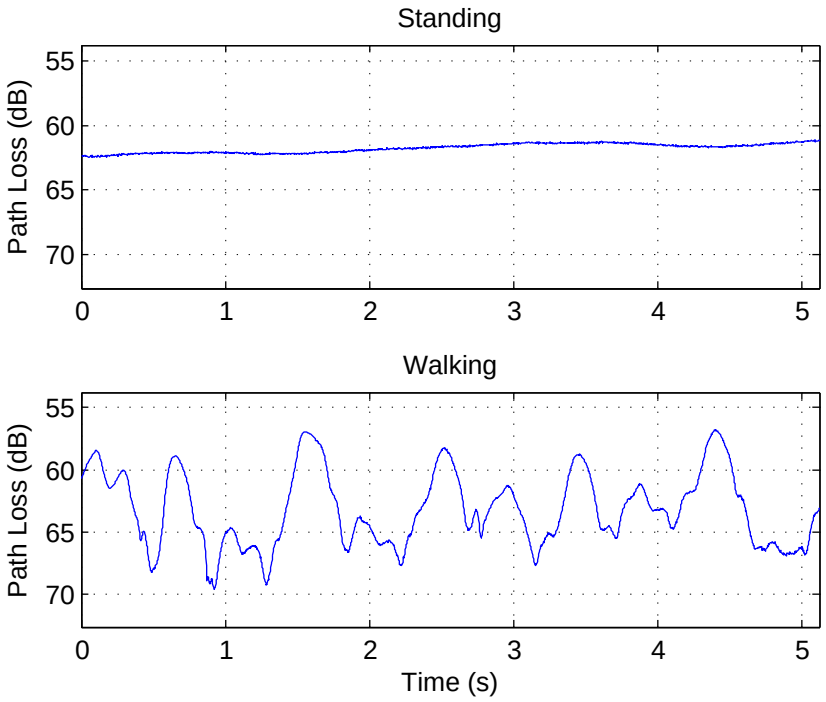

Figure 148: Path loss measurements over time at 820 MHz: chest to off-body; 4 m separation; 270° orientation

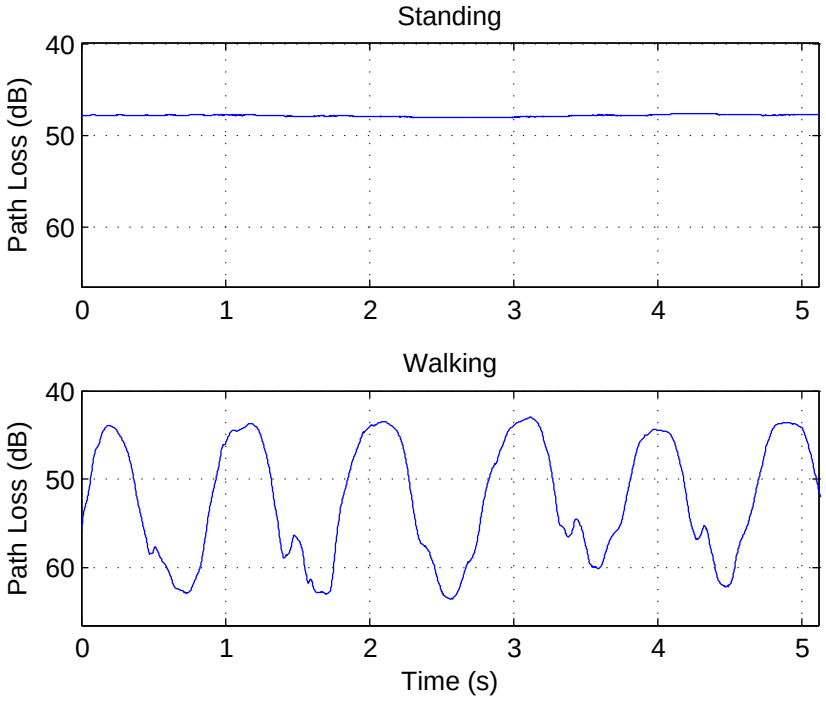

Figure 149: Path loss measurements over time at 820 MHz: right wrist to off-body; 1 m separation; 0° orientation

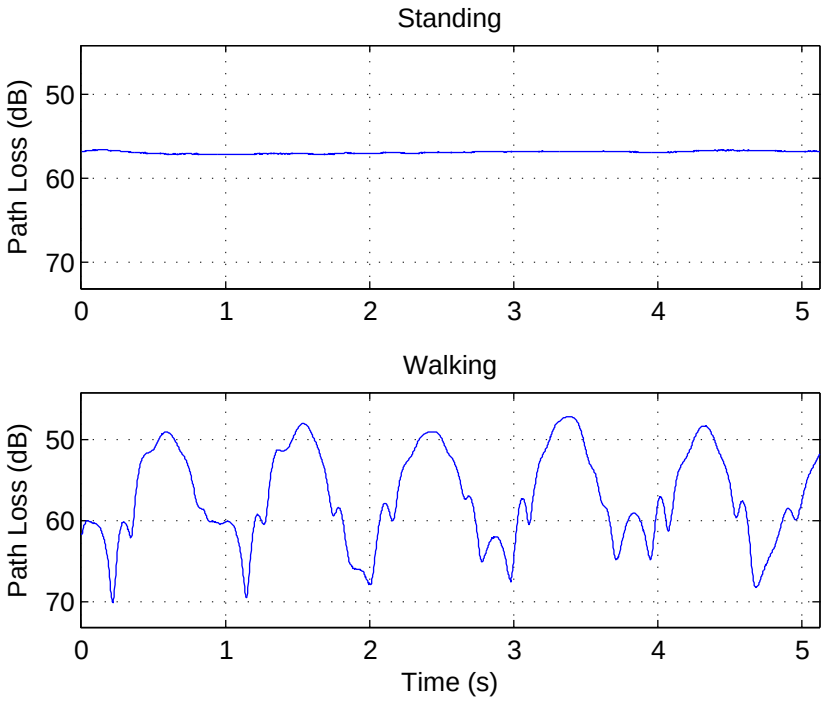

Figure 150: Path loss measurements over time at 820 MHz: right wrist to off-body; 1 m separation; 90° orientation

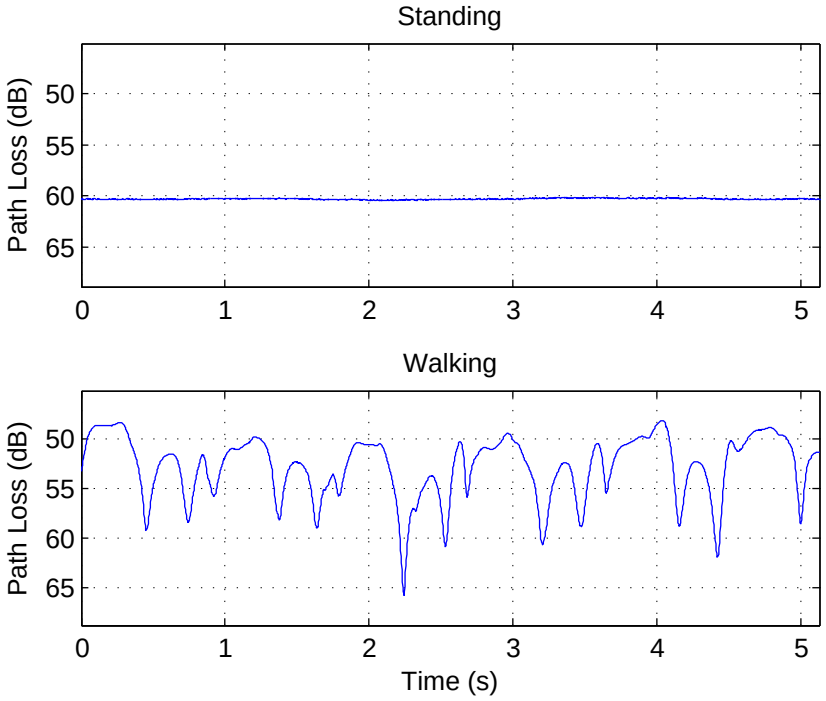

Figure 151: Path loss measurements over time at 820 MHz: right wrist to off-body; 1 m separation; 180° orientation

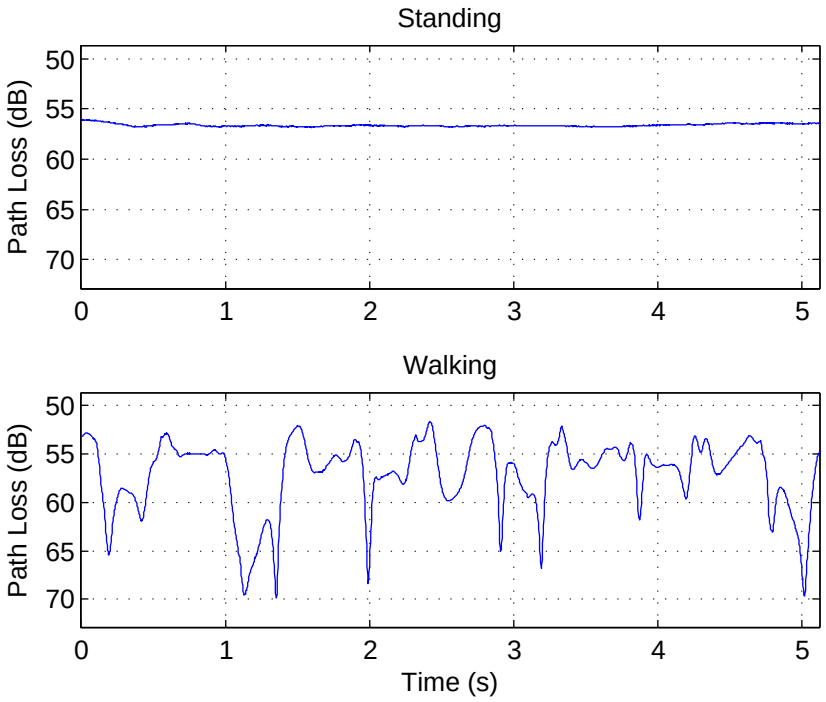

Figure 152: Path loss measurements over time at 820 MHz: right wrist to off-body; 1 m separation; 270° orientation

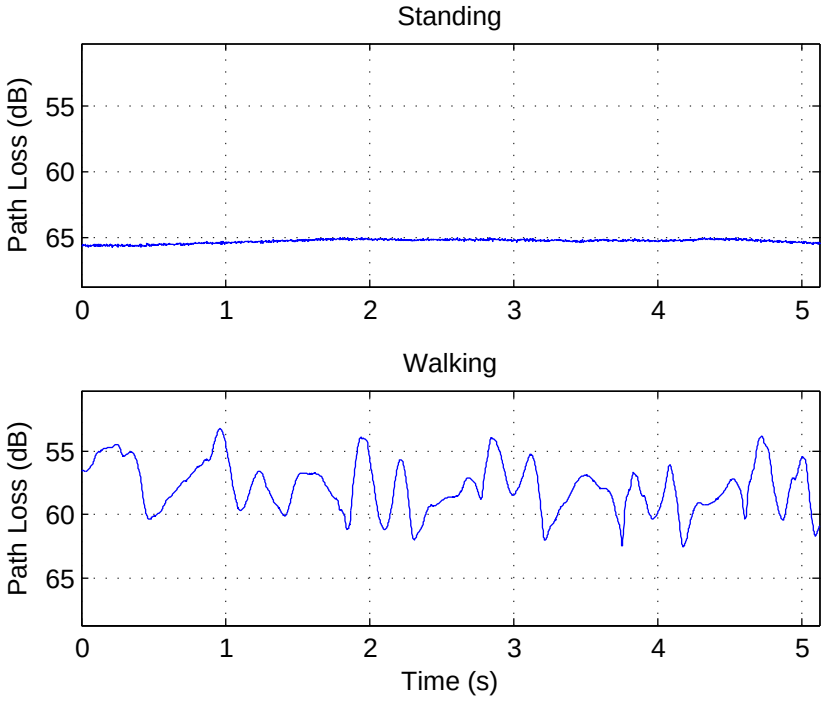

Figure 153: Path loss measurements over time at 820 MHz: right wrist to off-body; 2 m separation; 0° orientation

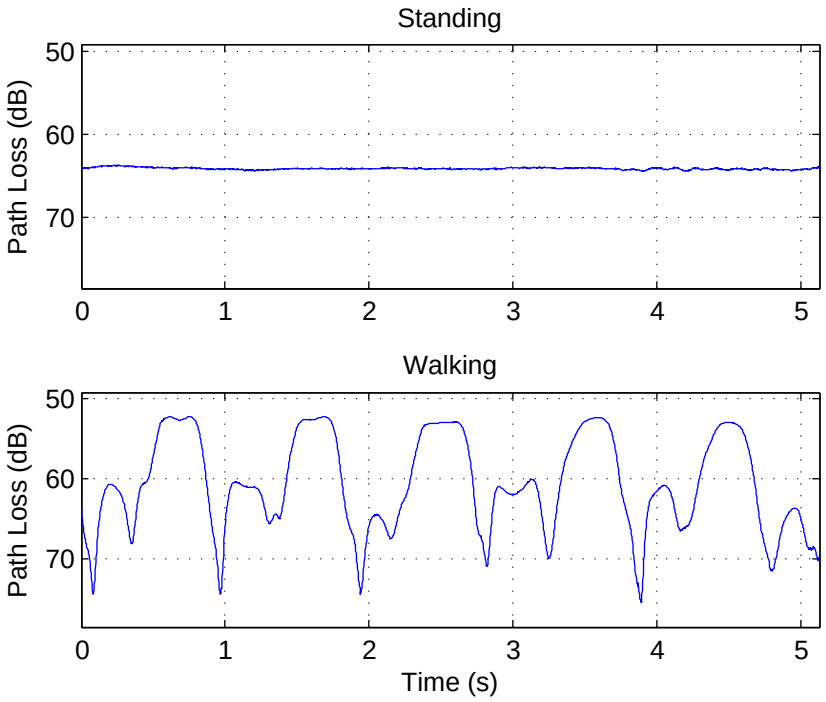

Figure 154: Path loss measurements over time at 820 MHz: right wrist to off-body; 2 m separation; 90° orientation

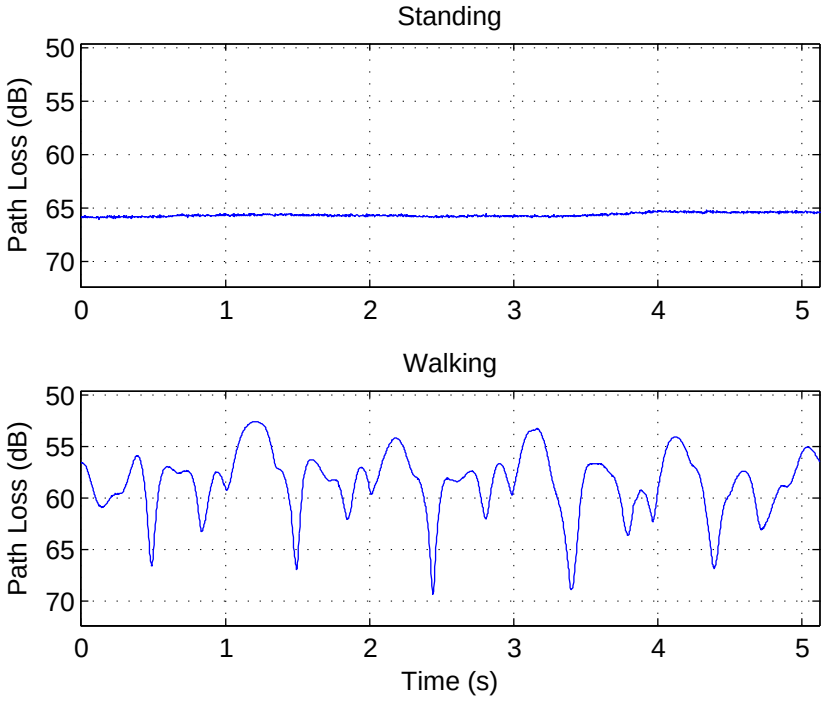

Figure 155: Path loss measurements over time at 820 MHz: right wrist to off-body; 2 m separation; 180° orientation

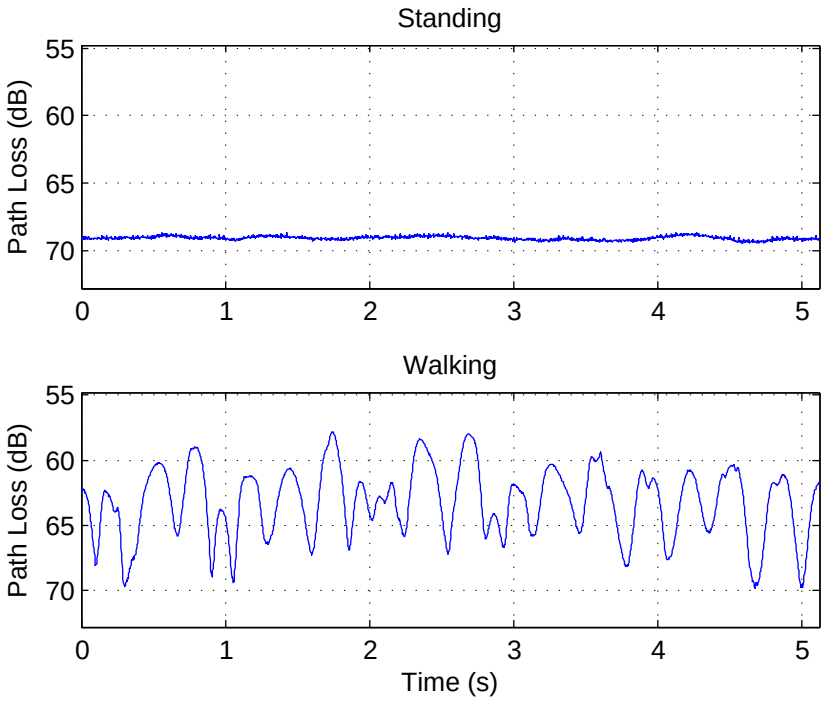

Figure 156: Path loss measurements over time at 820 MHz: right wrist to off-body; 2 m separation; 270° orientation

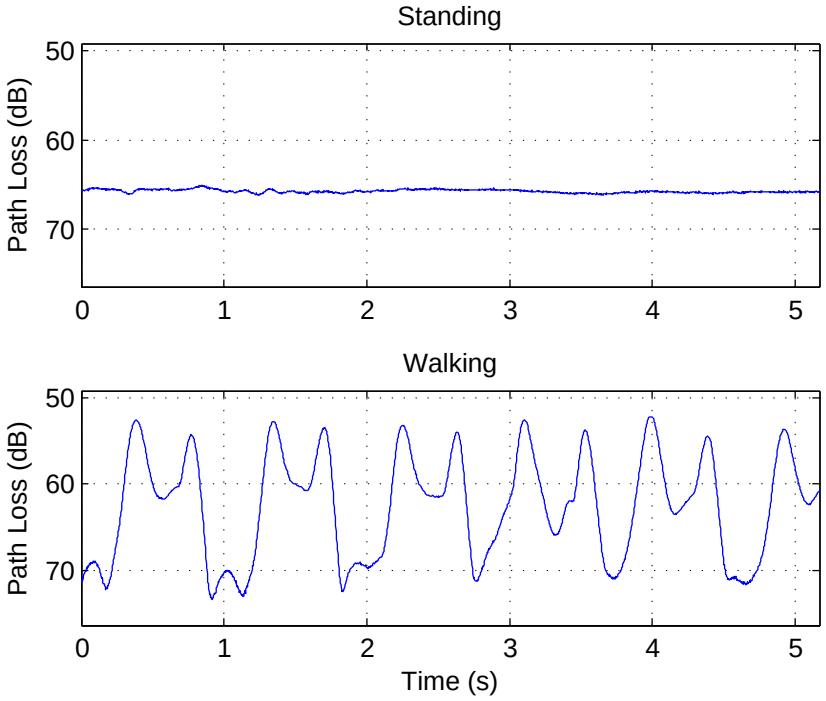

Figure 157: Path loss measurements over time at 820 MHz: right wrist to off-body; 3 m separation; 0° orientation

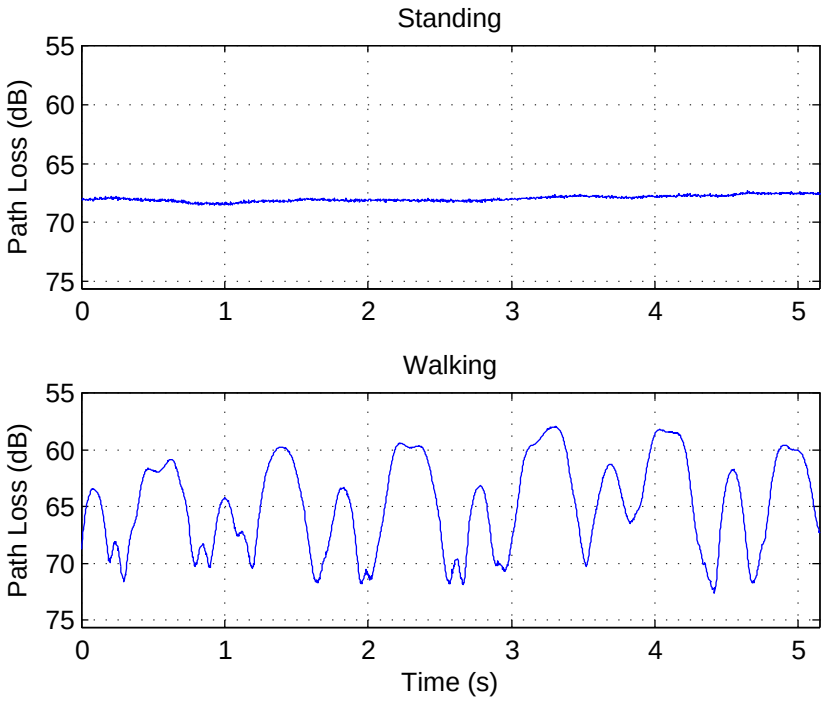

Figure 158: Path loss measurements over time at 820 MHz: right wrist to off-body; 3 m separation; 90° orientation

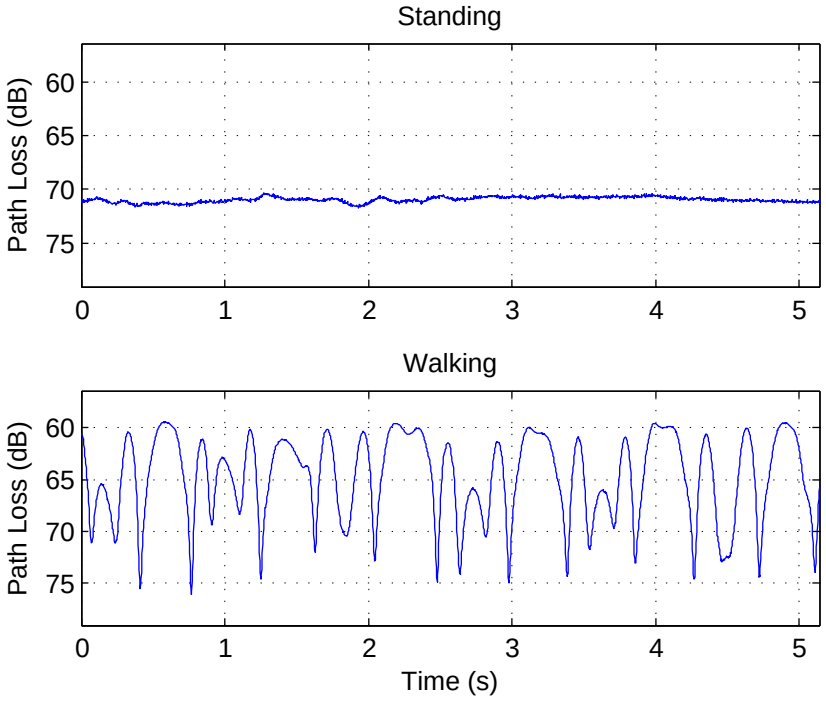

Figure 159: Path loss measurements over time at 820 MHz: right wrist to off-body; 3 m separation; 180° orientation

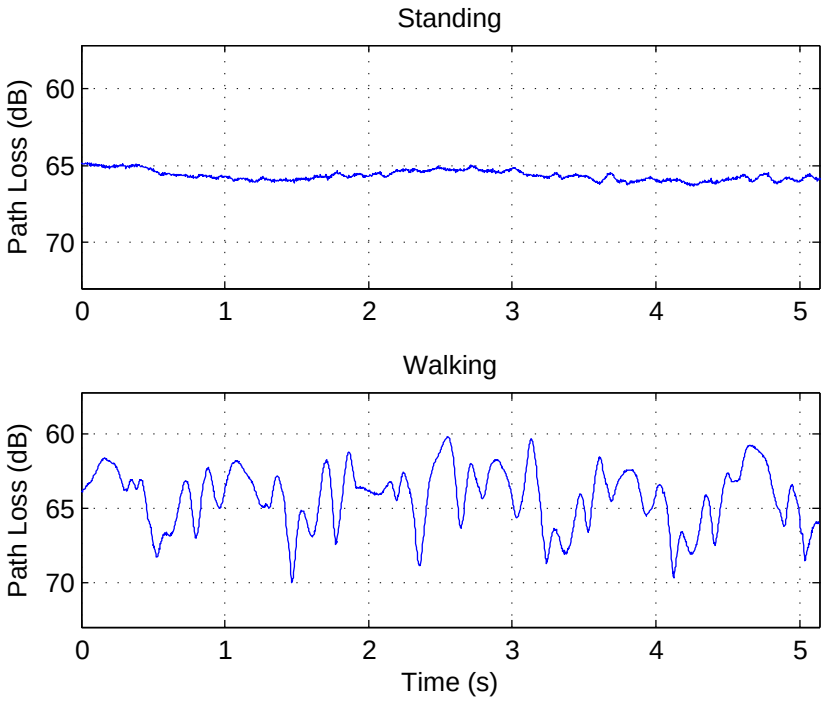

Figure 160: Path loss measurements over time at 820 MHz: right wrist to off-body; 3 m separation; 270° orientation

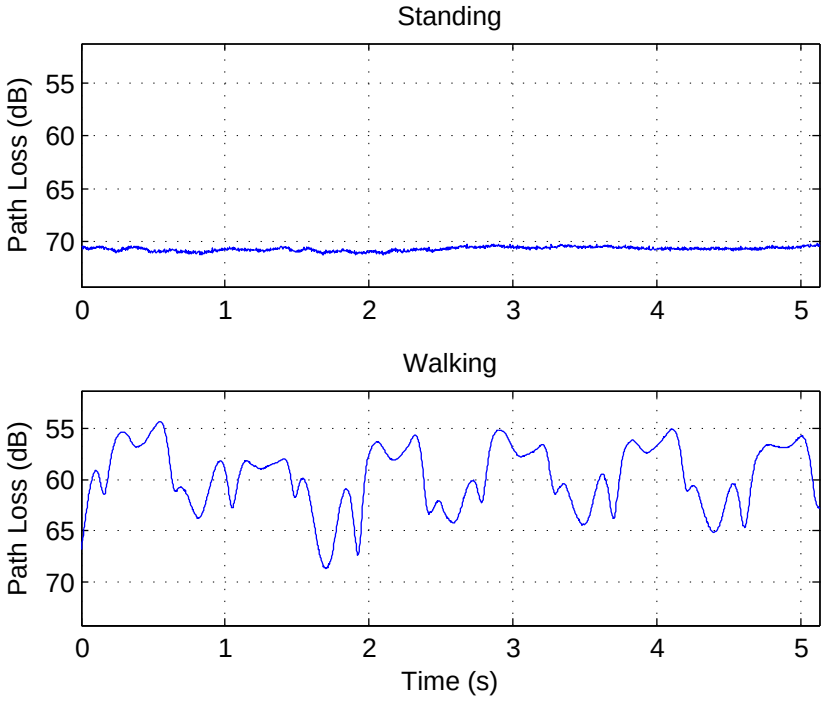

Figure 161: Path loss measurements over time at 820 MHz: right wrist to off-body; 4 m separation; 0° orientation

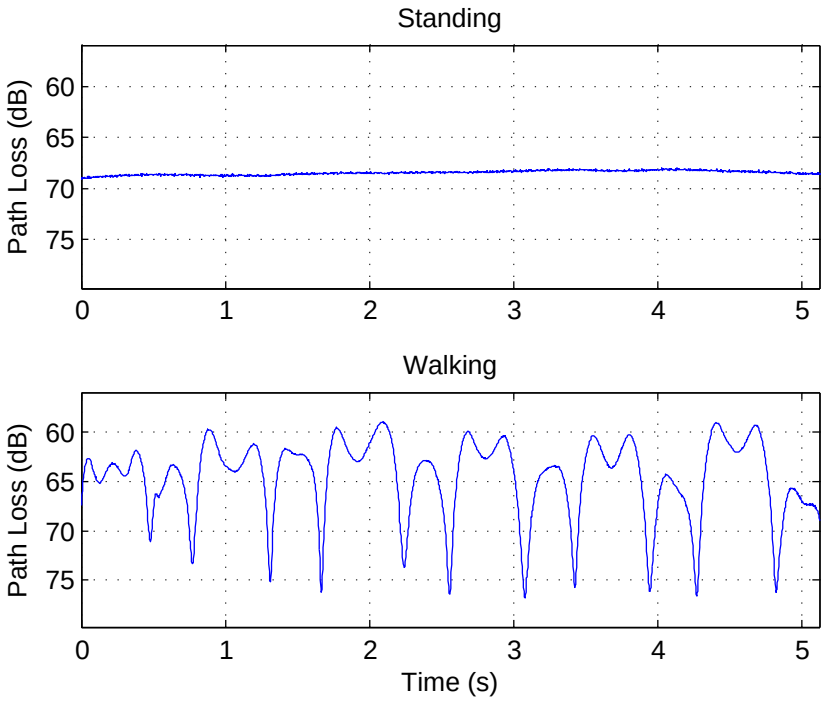

Figure 162: Path loss measurements over time at 820 MHz: right wrist to off-body; 4 m separation; 90° orientation

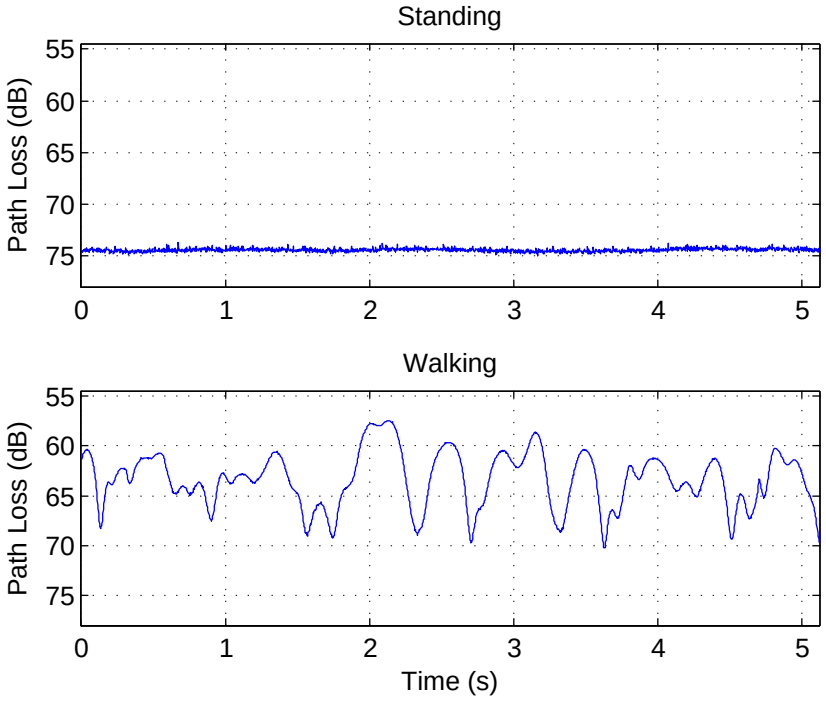

Figure 163: Path loss measurements over time at 820 MHz: right wrist to off-body; 4 m separation; 180° orientation

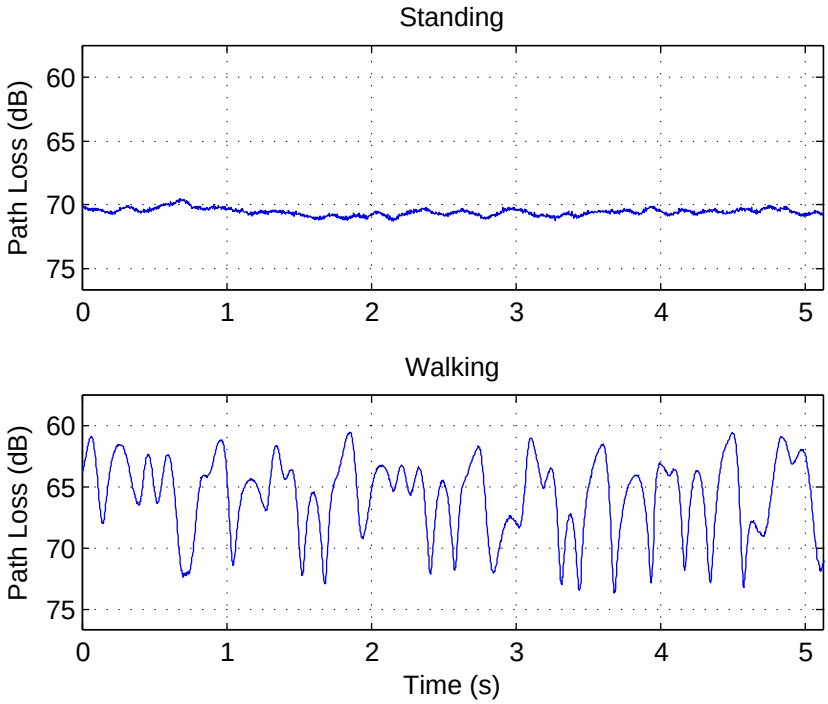

Figure 164: Path loss measurements over time at 820 MHz: right wrist to off-body; 4 m separation; 270° orientation

A.2.2 2.36 GHz measurements

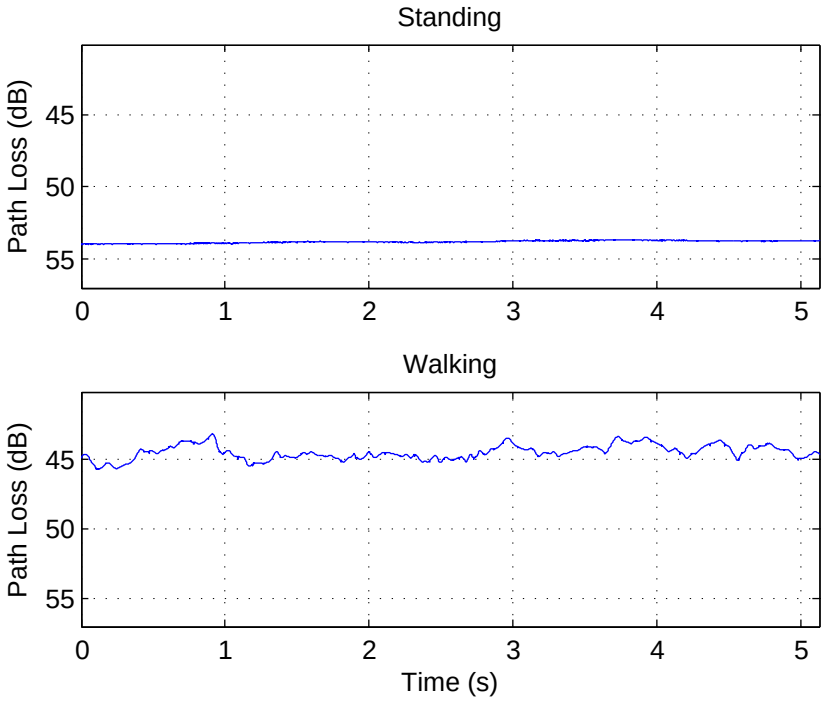

Figure 165: Path loss measurements over time at 2360 MHz: chest to off-body; 1 m separation; 0° orientation

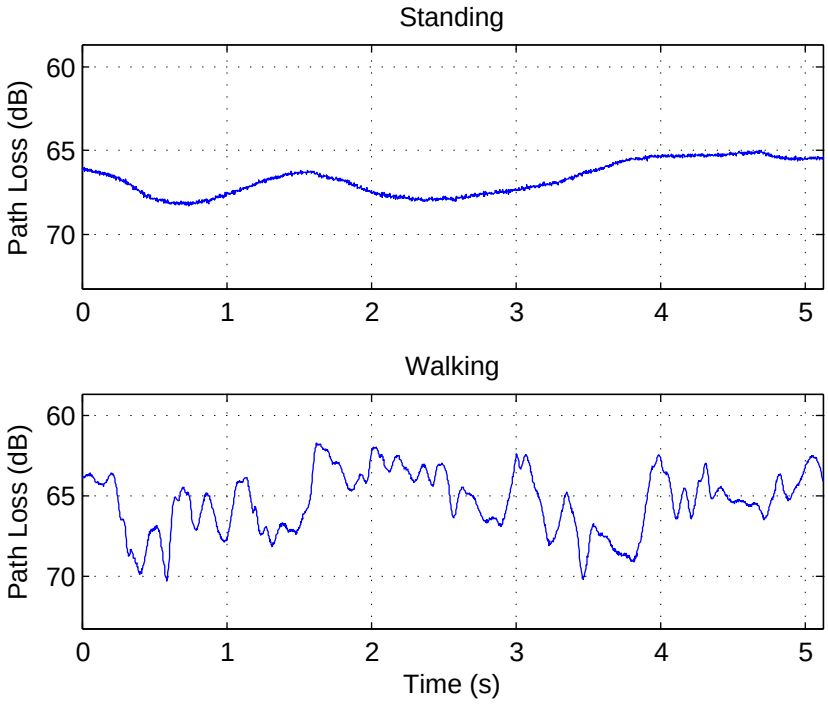

Figure 166: Path loss measurements over time at 2360 MHz: chest to off-body; 1 m separation; 90° orientation

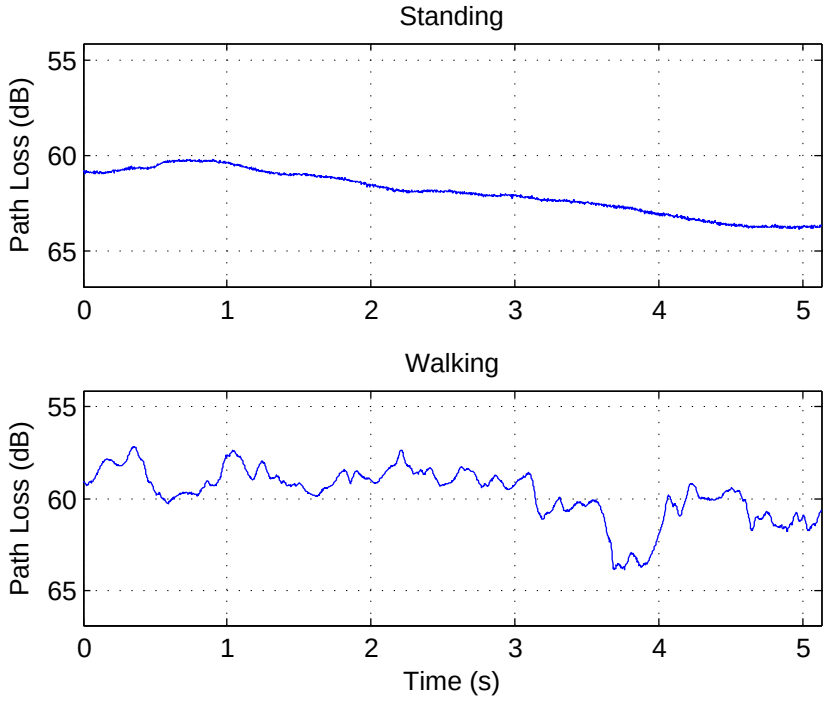

Figure 167: Path loss measurements over time at 2360 MHz: chest to off-body; 1 m separation; 180° orientation

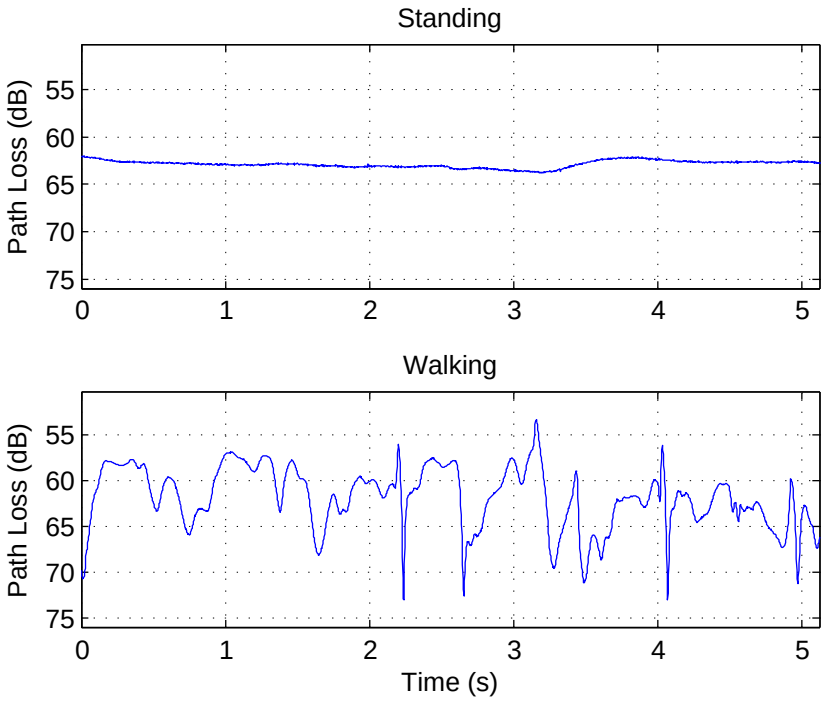

Figure 168: Path loss measurements over time at 2360 MHz: chest to off-body; 1 m separation; 270° orientation

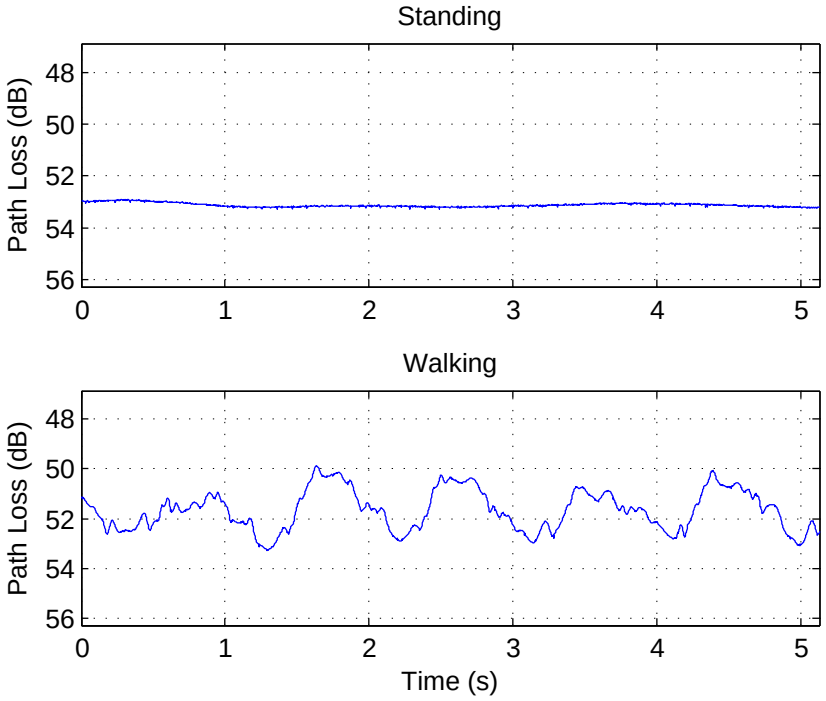

Figure 169: Path loss measurements over time at 2360 MHz: chest to off-body; 2 m separation; 0° orientation

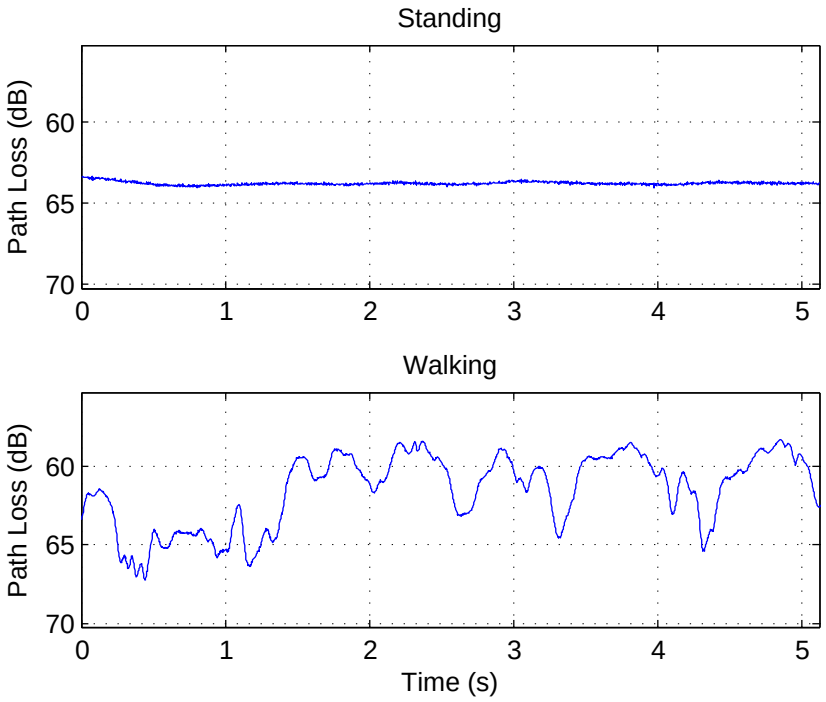

Figure 170: Path loss measurements over time at 2360 MHz: chest to off-body; 2 m separation; 90° orientation

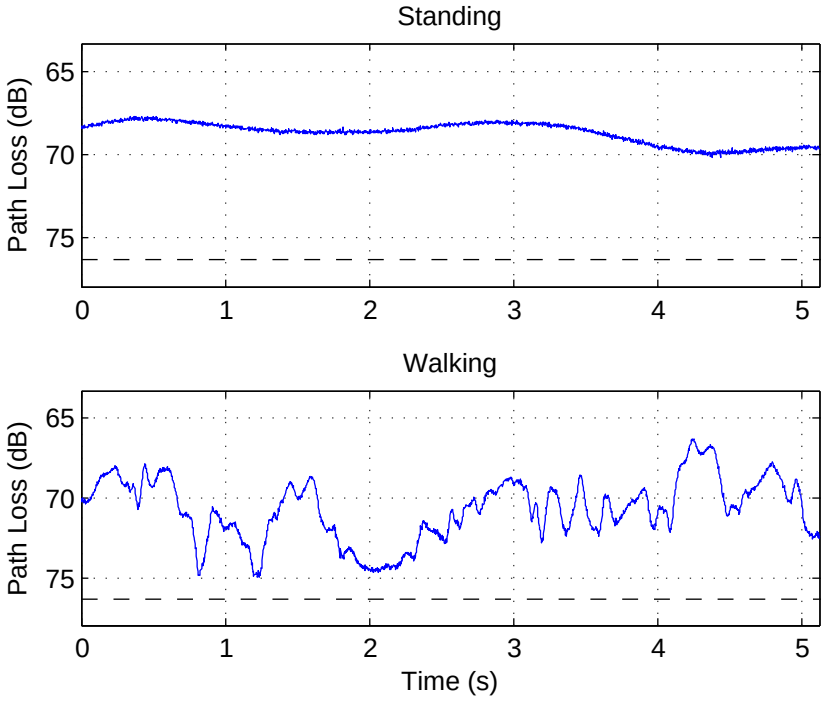

Figure 171: Path loss measurements over time at 2360 MHz: chest to off-body; 2 m separation; 180° orientation

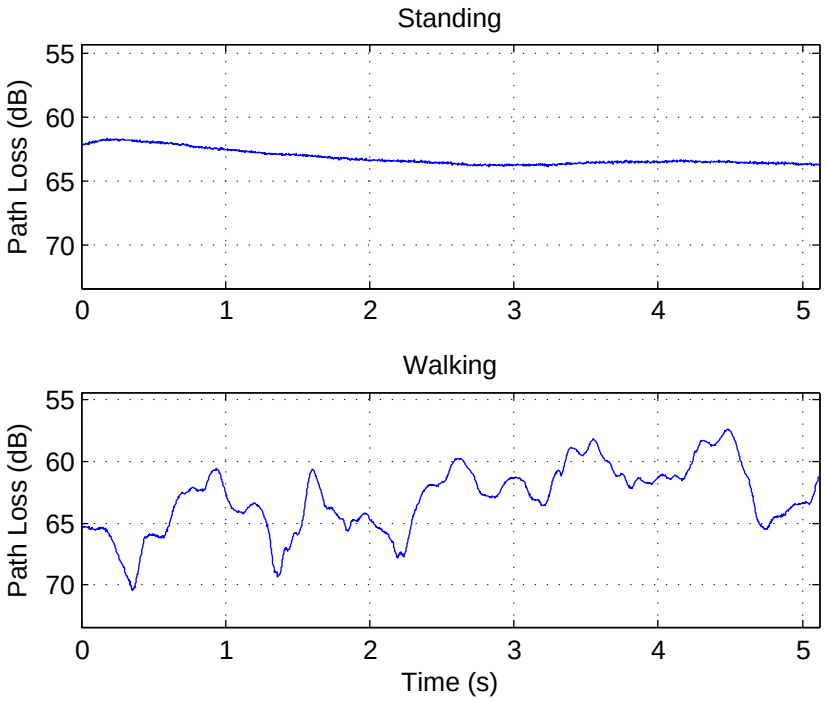

Figure 172: Path loss measurements over time at 2360 MHz: chest to off-body; 2 m separation; 270° orientation

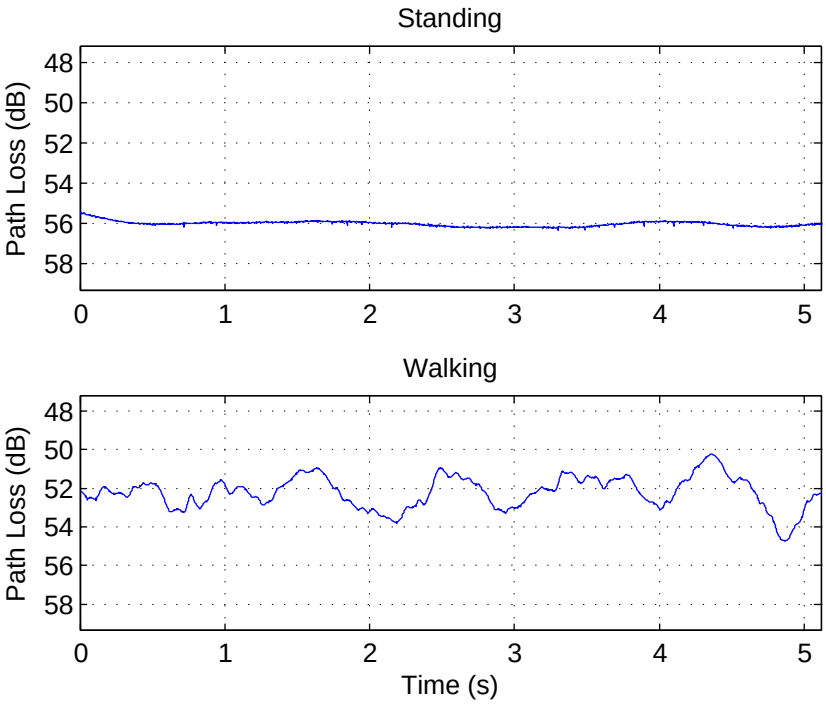

Figure 173: Path loss measurements over time at 2360 MHz: chest to off-body; 3 m separation; 0° orientation

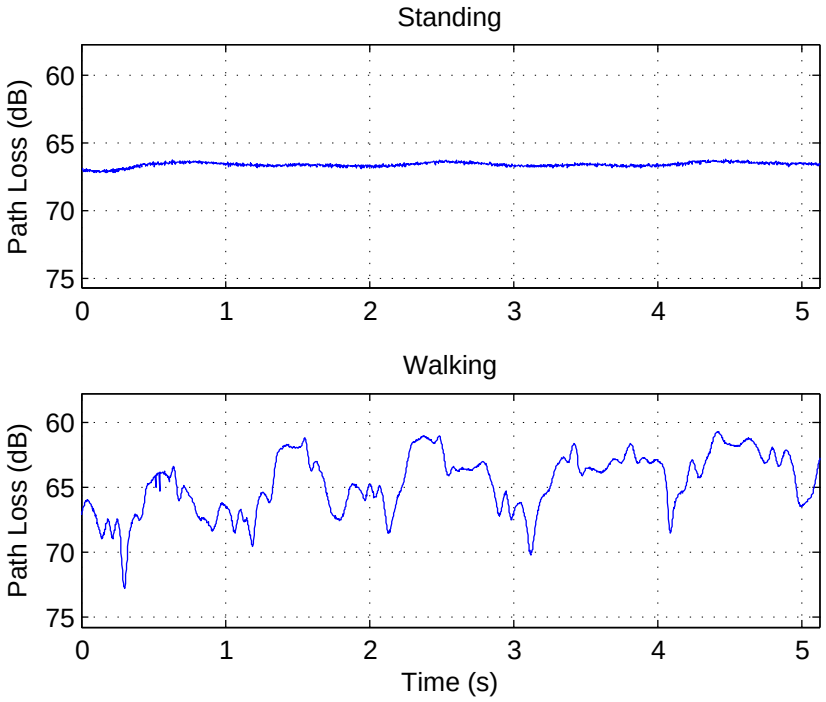

Figure 174: Path loss measurements over time at 2360 MHz: chest to off-body; 3 m separation; 90° orientation

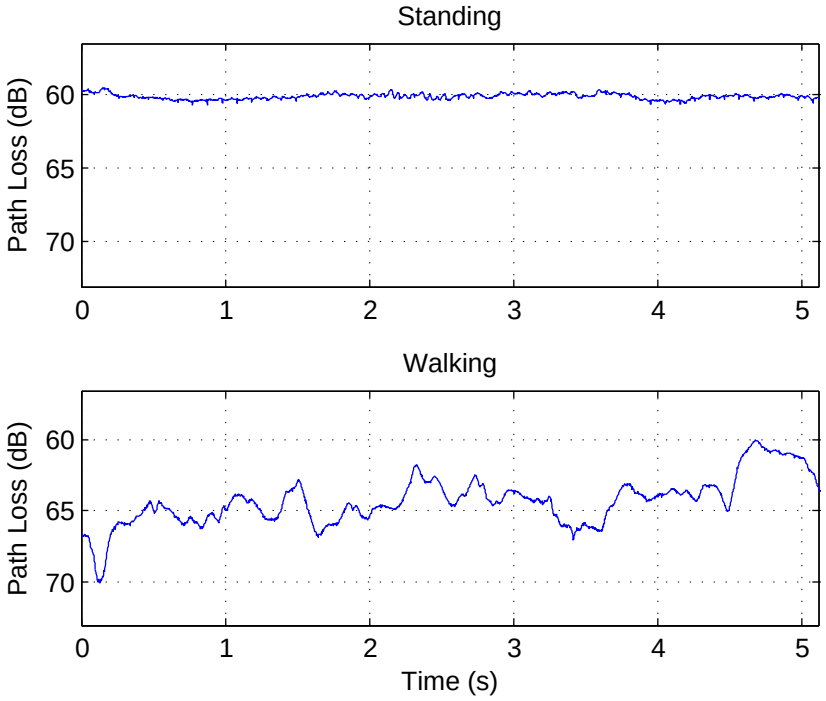

Figure 175: Path loss measurements over time at 2360 MHz: chest to off-body; 3 m separation; 180° orientation

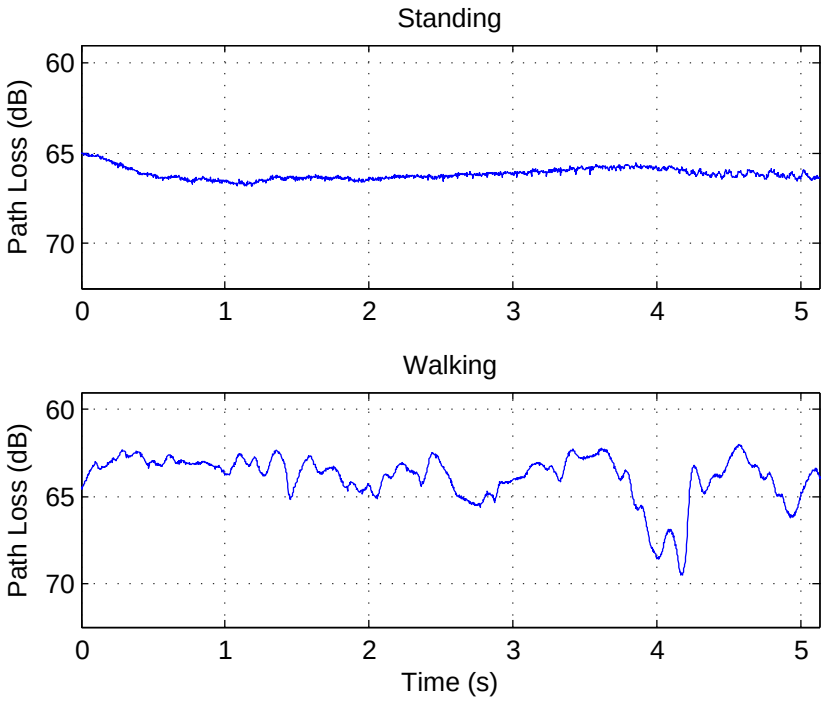

Figure 176: Path loss measurements over time at 2360 MHz: chest to off-body; 3 m separation; 270° orientation

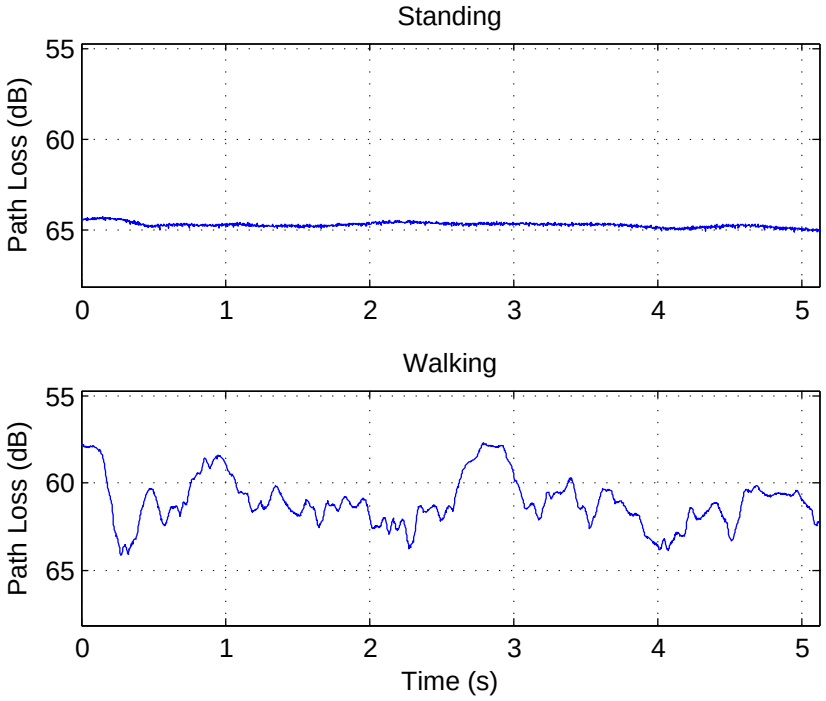

Figure 177: Path loss measurements over time at 2360 MHz: chest to off-body; 4 m separation; 0° orientation

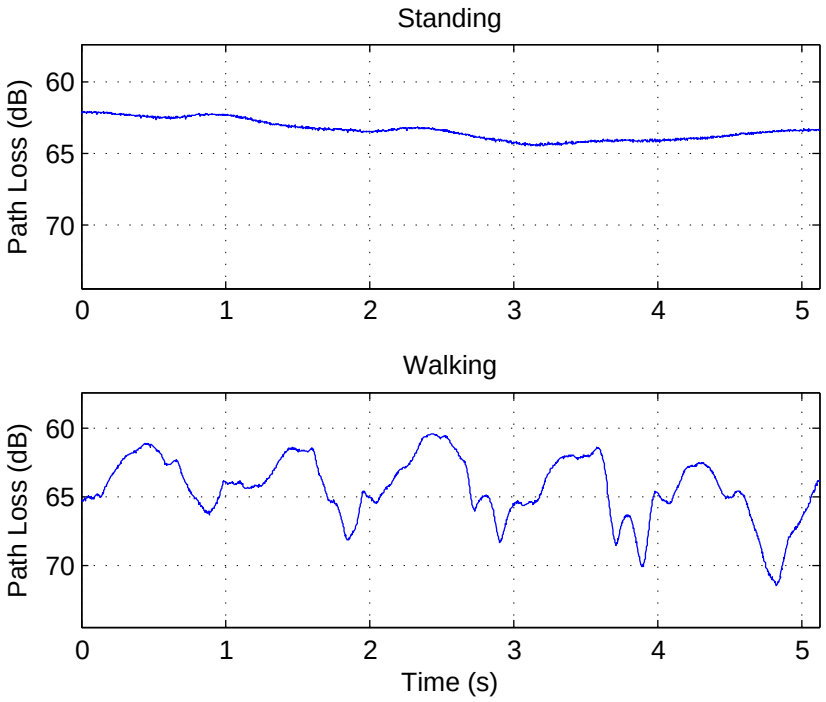

Figure 178: Path loss measurements over time at 2360 MHz: chest to off-body; 4 m separation; 90° orientation

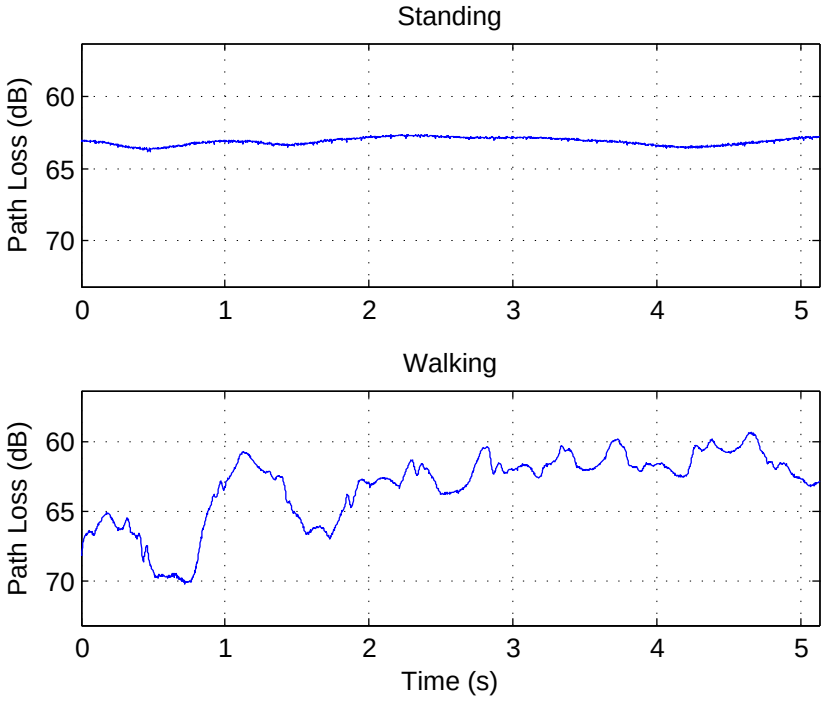

Figure 179: Path loss measurements over time at 2360 MHz: chest to off-body; 4 m separation; 180° orientation

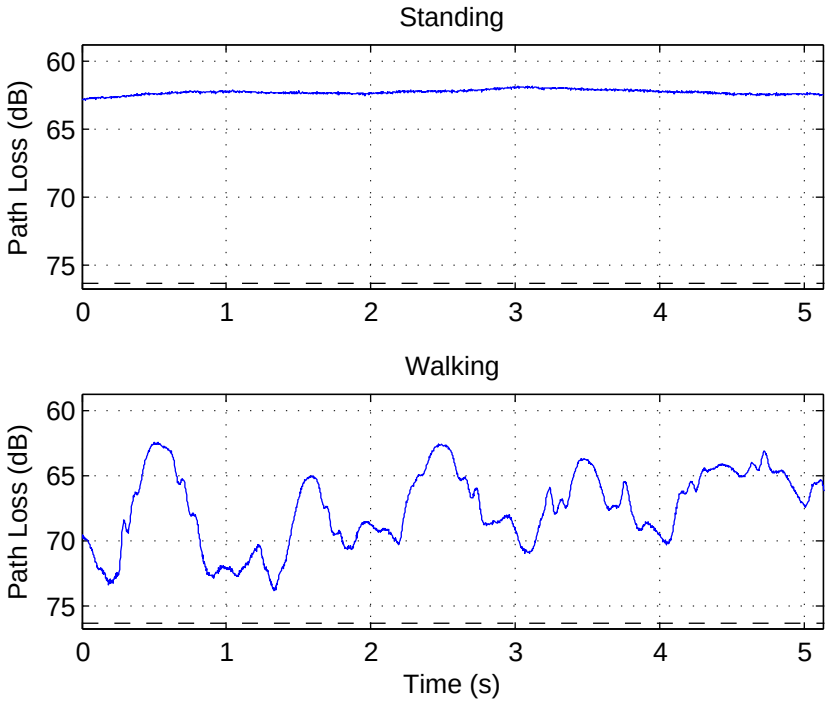

Figure 180: Path loss measurements over time at 2360 MHz: chest to off-body; 4 m separation; 270° orientation

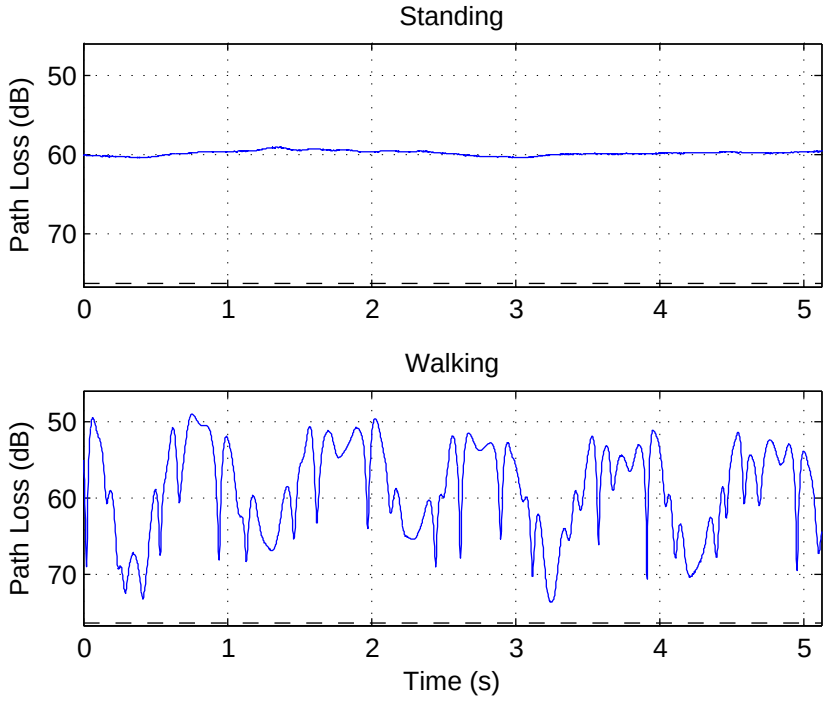

Figure 181: Path loss measurements over time at 2360 MHz: right wrist to off-body; 1 m separation; 0° orientation

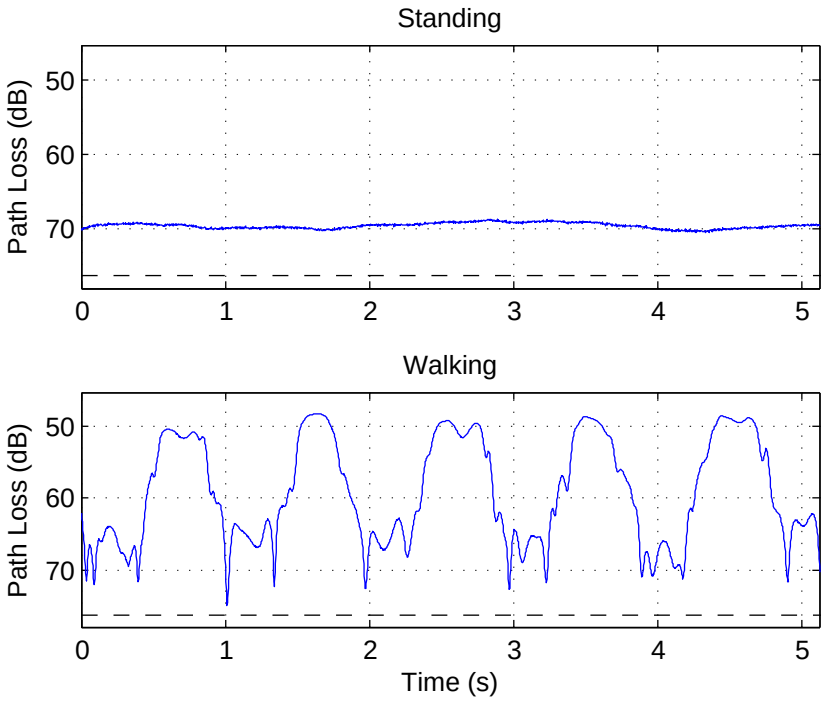

Figure 182: Path loss measurements over time at 2360 MHz: right wrist to off-body; 1 m separation; 90° orientation

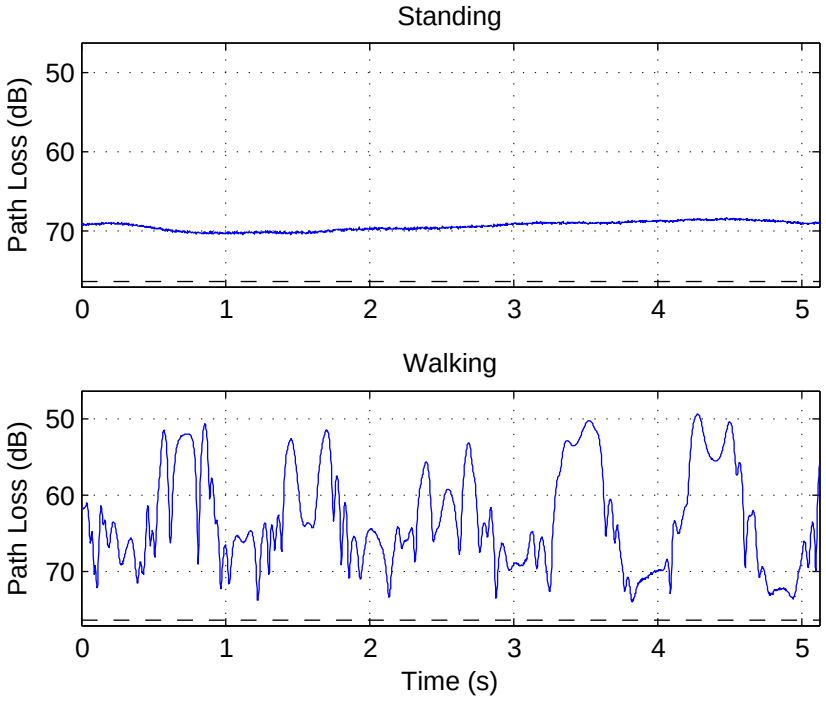

Figure 183: Path loss measurements over time at 2360 MHz: right wrist to off-body; 1 m separation; 180° orientation

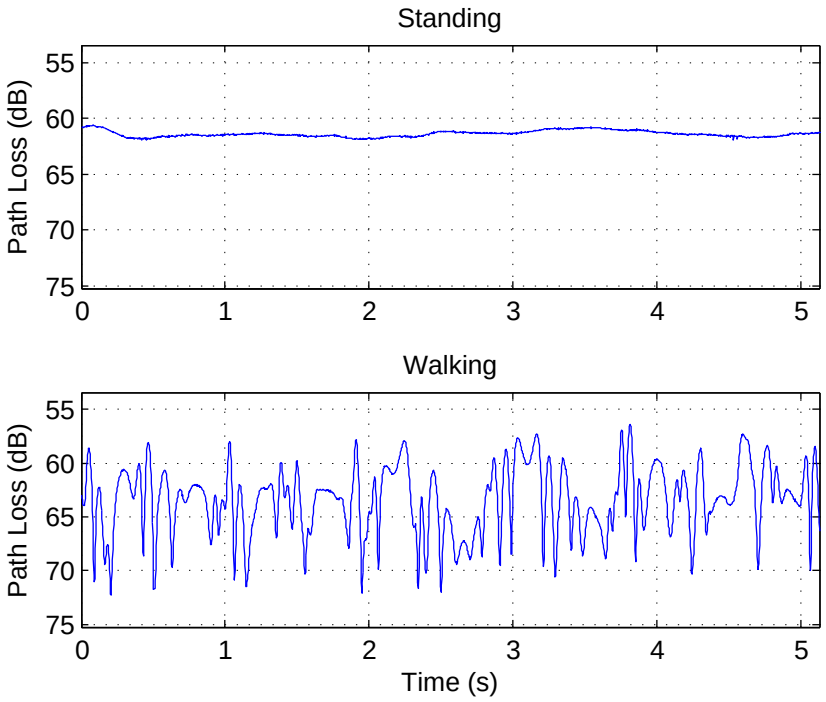

Figure 184: Path loss measurements over time at 2360 MHz: right wrist to off-body; 1 m separation; 270° orientation

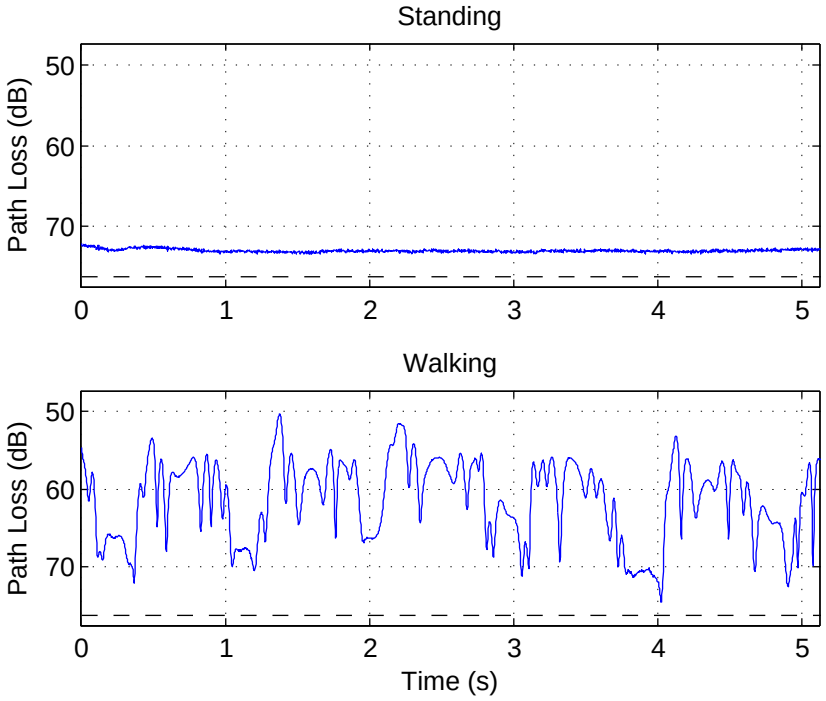

Figure 185: Path loss measurements over time at 2360 MHz: right wrist to off-body; 2 m separation; 0° orientation

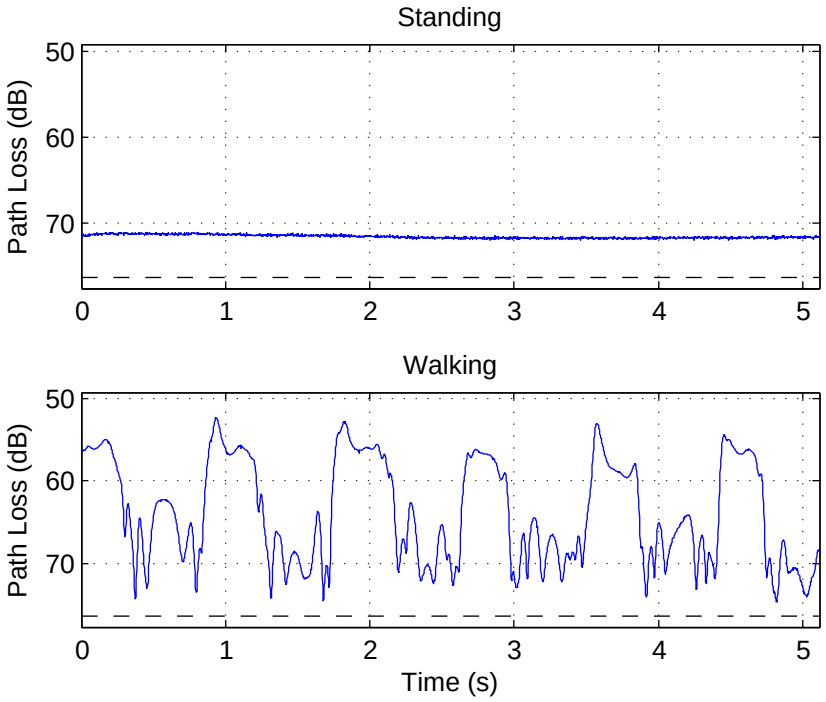

Figure 186: Path loss measurements over time at 2360 MHz: right wrist to off-body; 2 m separation; 90° orientation

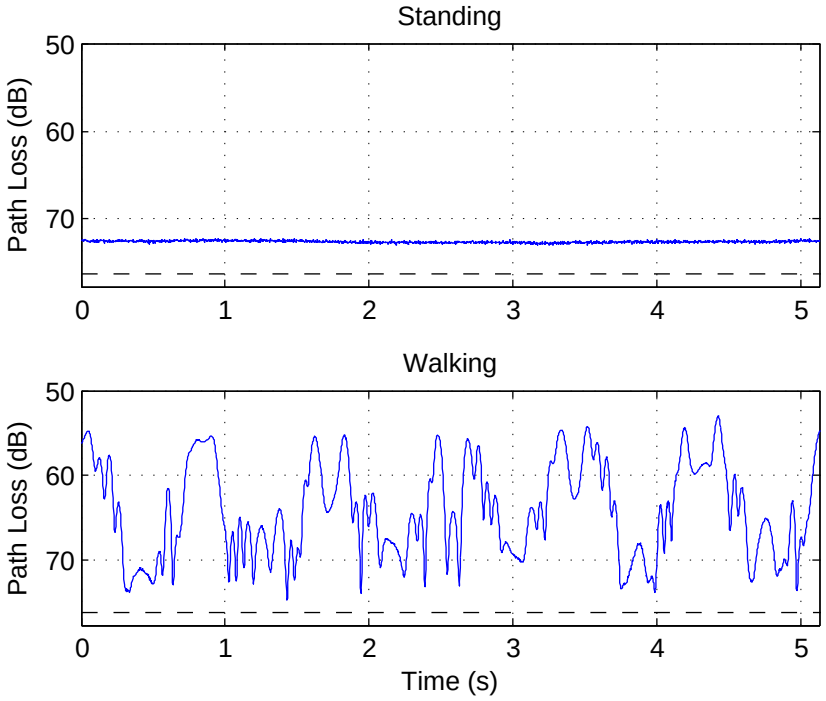

Figure 187: Path loss measurements over time at 2360 MHz: right wrist to off-body; 2 m separation; 180° orientation

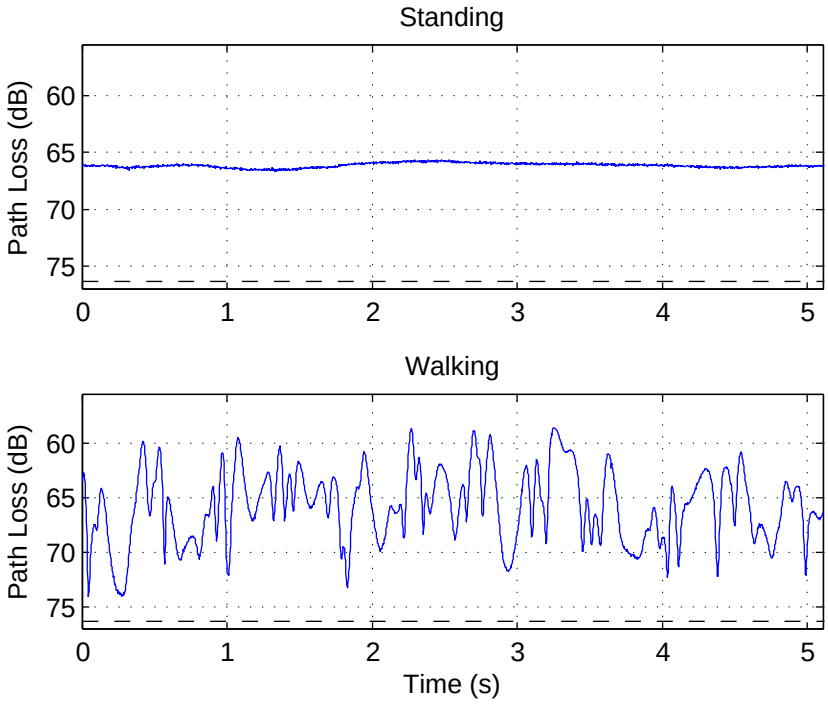

Figure 188: Path loss measurements over time at 2360 MHz: right wrist to off-body; 2 m separation; 270° orientation

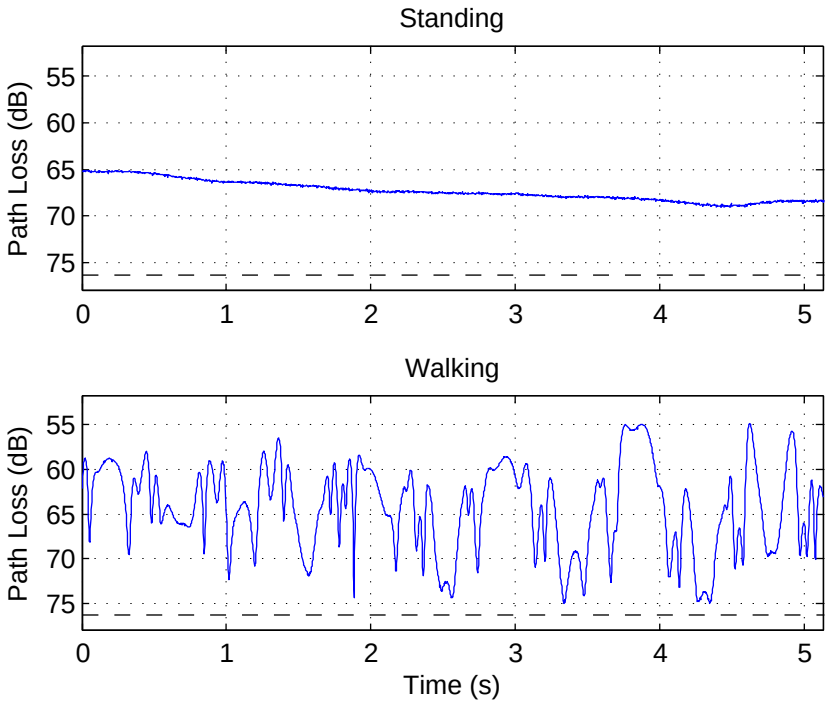

Figure 189: Path loss measurements over time at 2360 MHz: right wrist to off-body; 3 m separation; 0° orientation

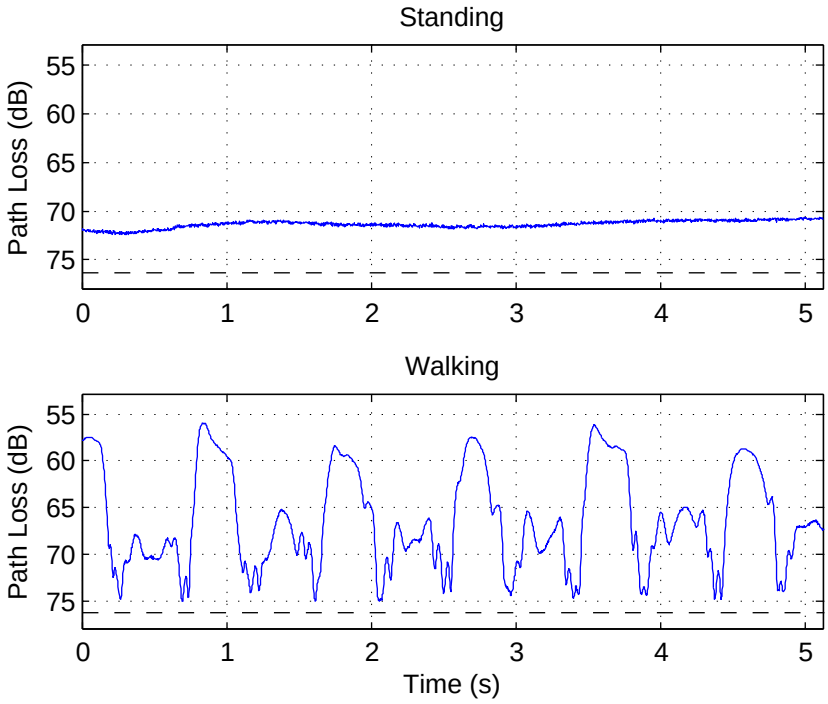

Figure 190: Path loss measurements over time at 2360 MHz: right wrist to off-body; 3 m separation; 90° orientation

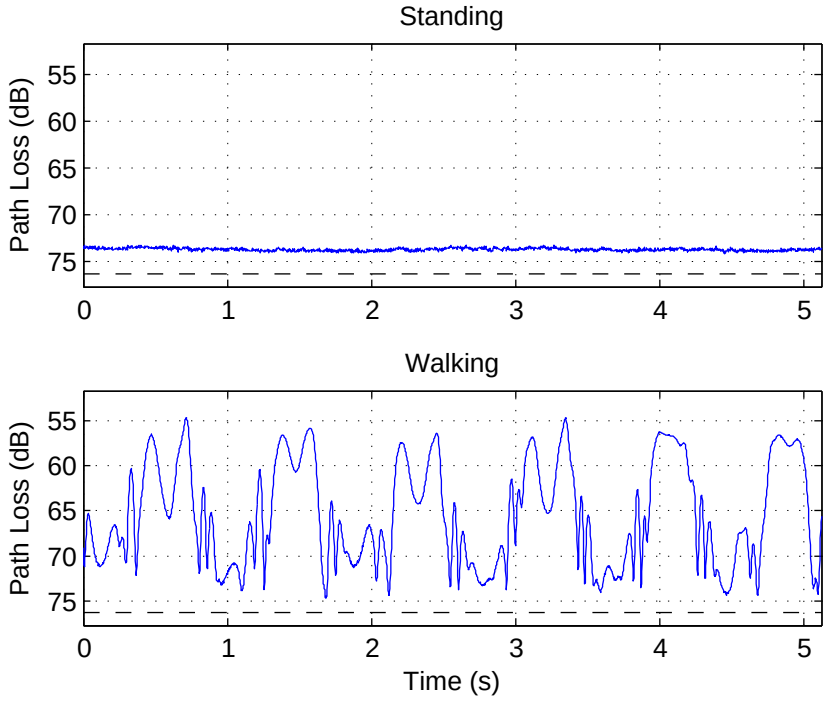

Figure 191: Path loss measurements over time at 2360 MHz: right wrist to off-body; 3 m separation; 180° orientation

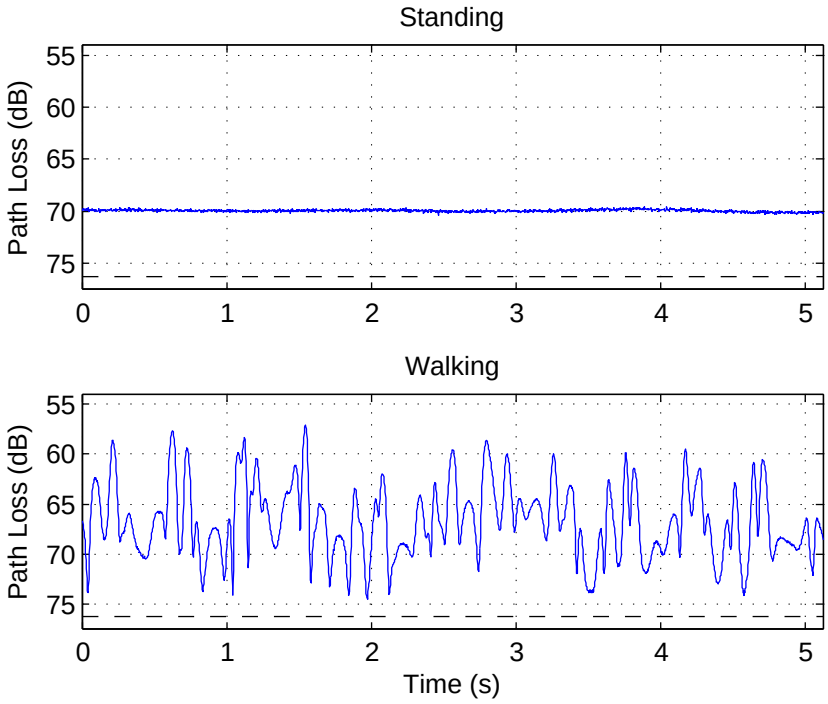

Figure 192: Path loss measurements over time at 2360 MHz: right wrist to off-body; 3 m separation; 270° orientation

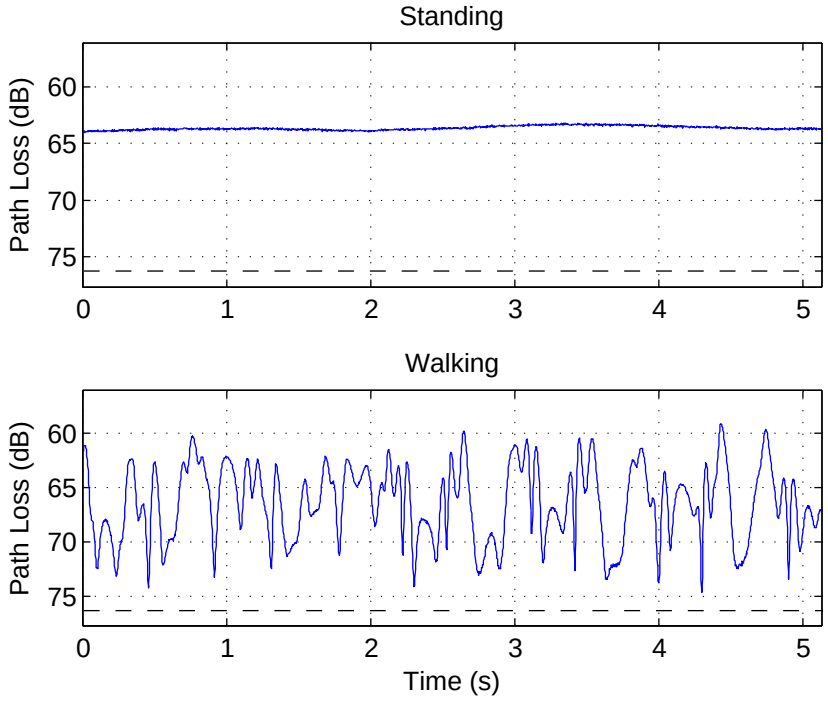

Figure 193: Path loss measurements over time at 2360 MHz: right wrist to off-body; 4 m separation; 0° orientation

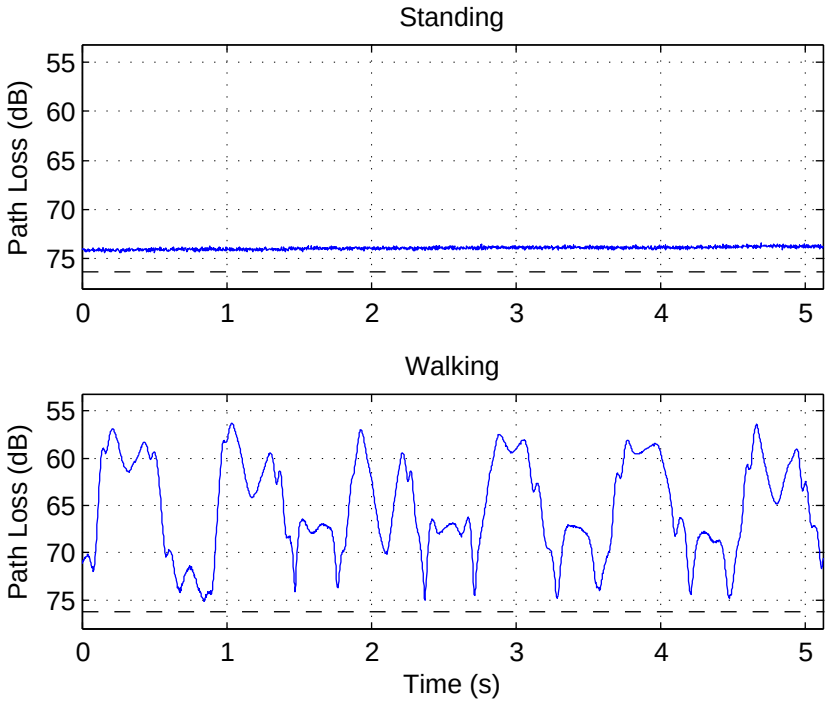

Figure 194: Path loss measurements over time at 2360 MHz: right wrist to off-body; 4 m separation; 90° orientation

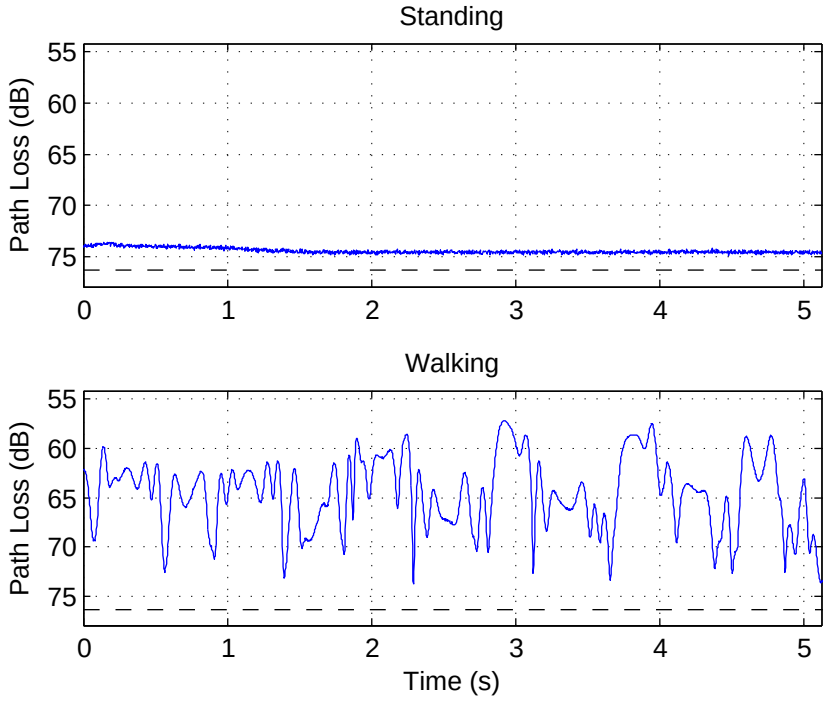

Figure 195: Path loss measurements over time at 2360 MHz: right wrist to off-body; 4 m separation; 180° orientation

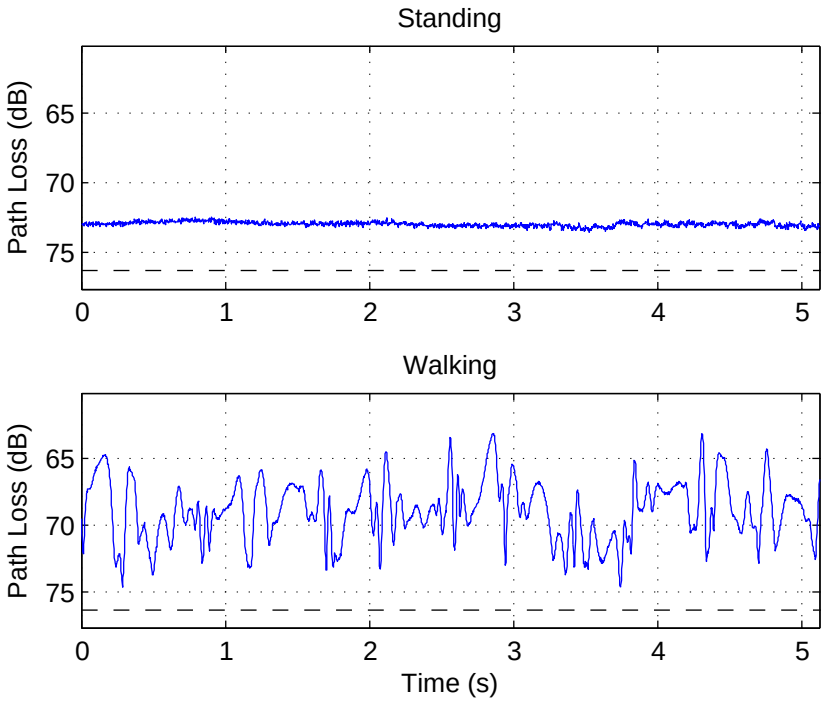

Figure 196: Path loss measurements over time at 2360 MHz: right wrist to off-body; 4 m separation; 270° orientation

A.3 Statistical Description of Received Power

A.3.1 PDFs at 820 MHz

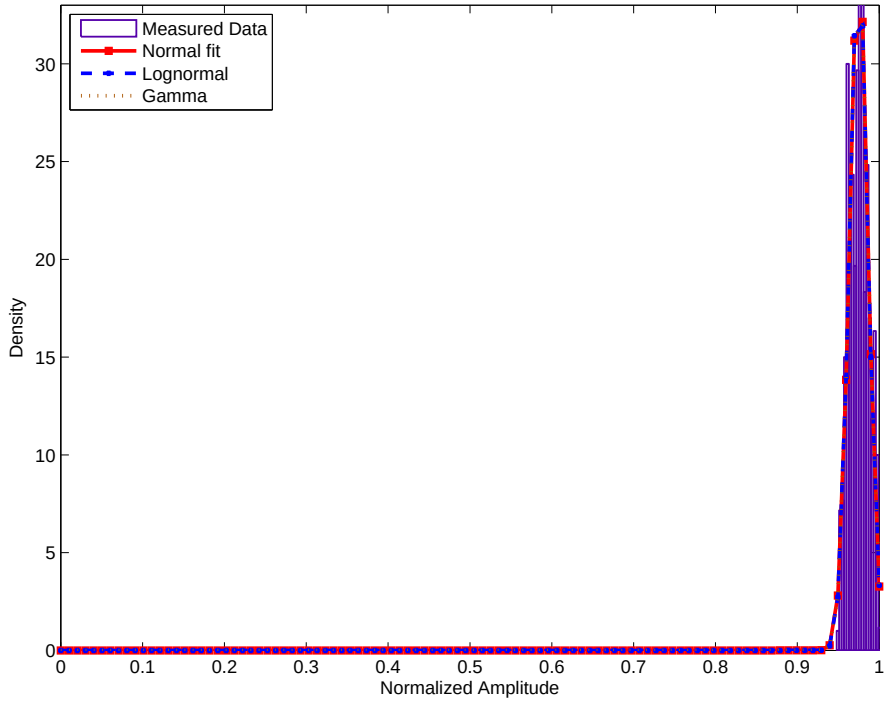

Figure 197: PDF of received power at 820 MHz: chest to off-body; Standing; 1 m separation; 0° orientation

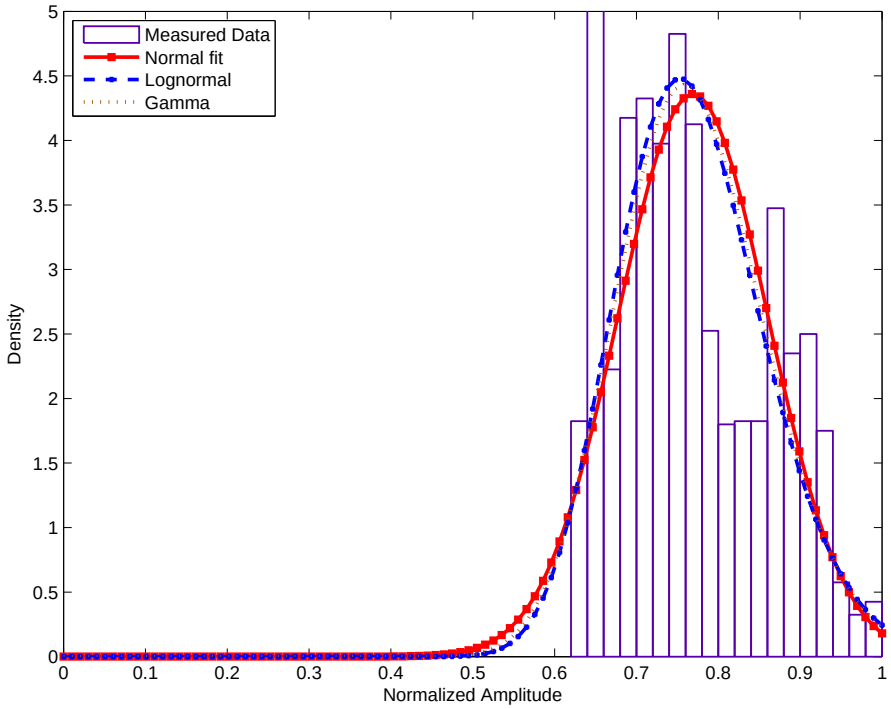

Figure 198: PDF of received power at 820 MHz: chest to off-body; Standing; 1 m separation; 180° orientation

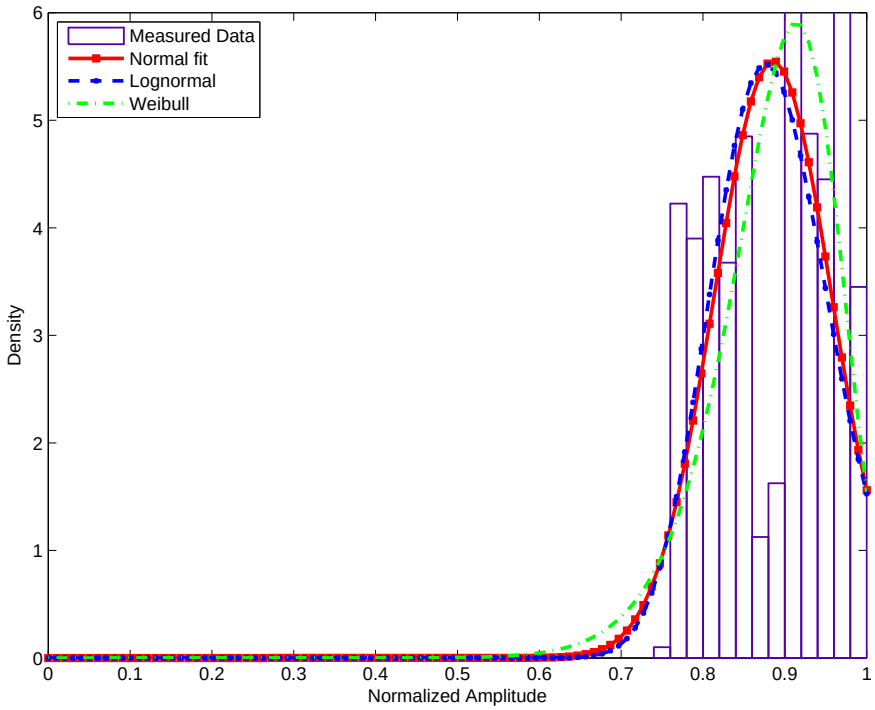

Figure 199: PDF of received power at 820 MHz: chest to off-body; Standing; 1 m separation; 270° orientation

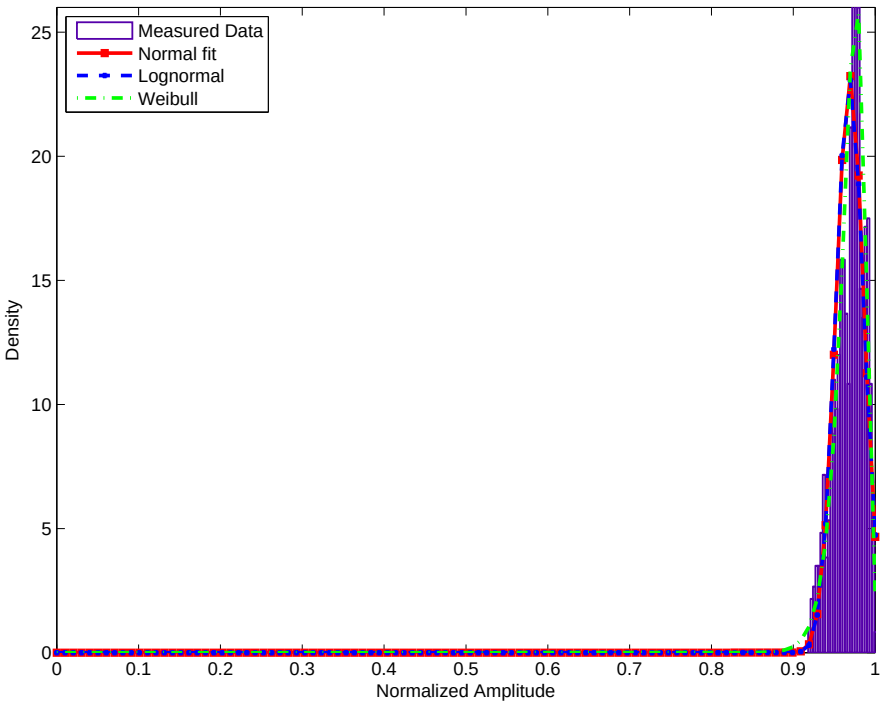

Figure 200: PDF of received power at 820 MHz: chest to off-body; Standing; 1 m separation; 90° orientation

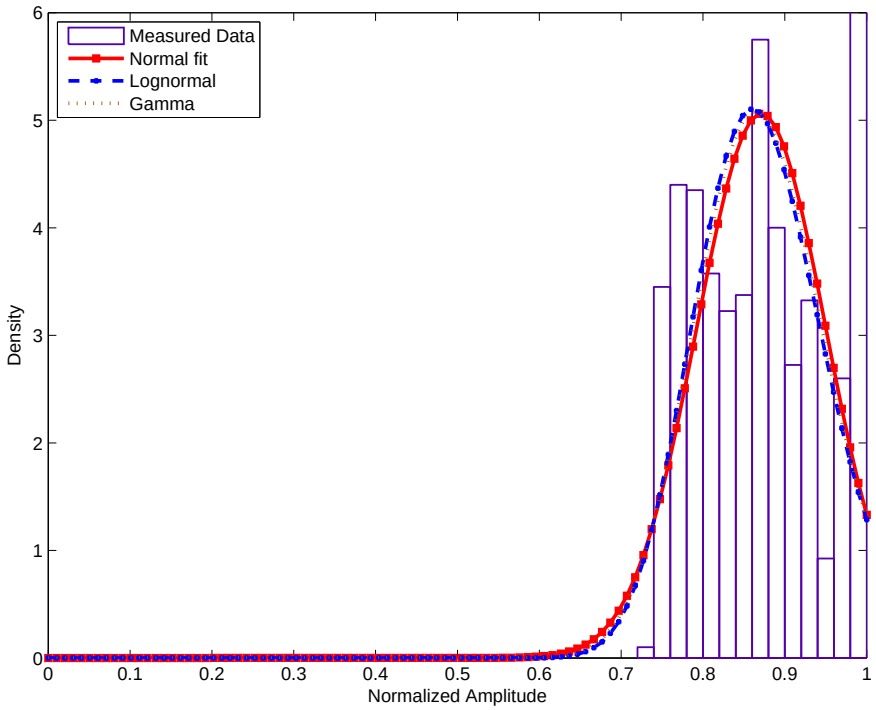

Figure 201: PDF of received power at 820 MHz: chest to off-body; Standing; 2 m separation; 0° orientation

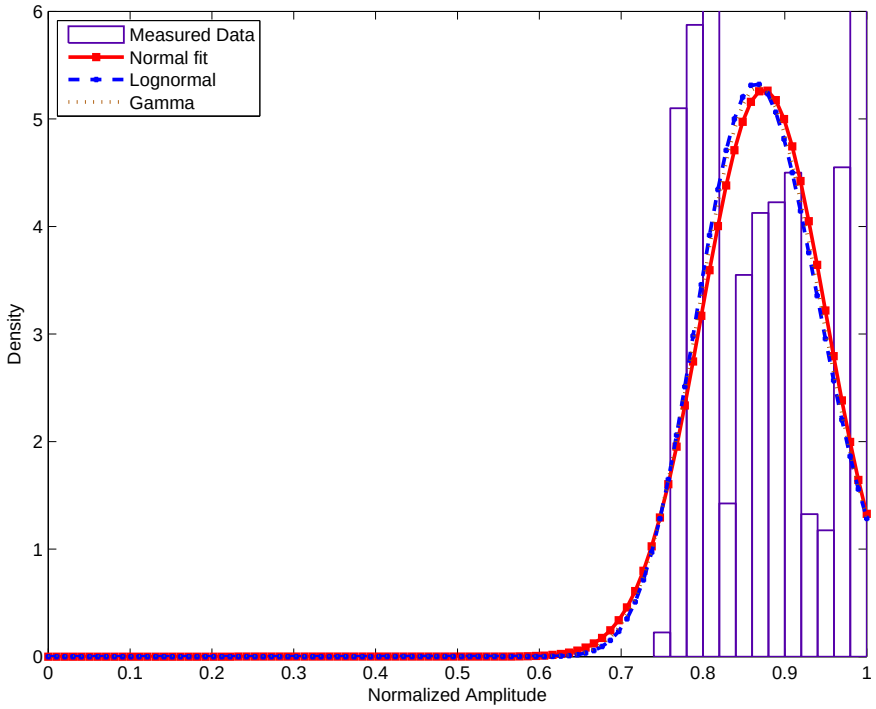

Figure 202: PDF of received power at 820 MHz: chest to off-body; Standing; 2 m separation; 180° orientation

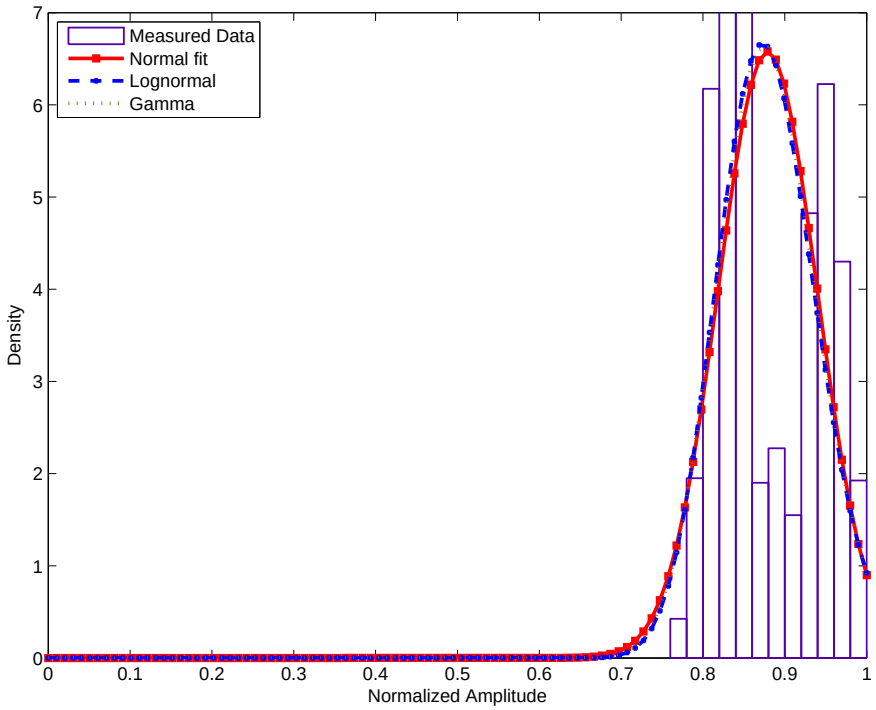

Figure 203: PDF of received power at 820 MHz: chest to off-body; Standing; 2 m separation; 270° orientation

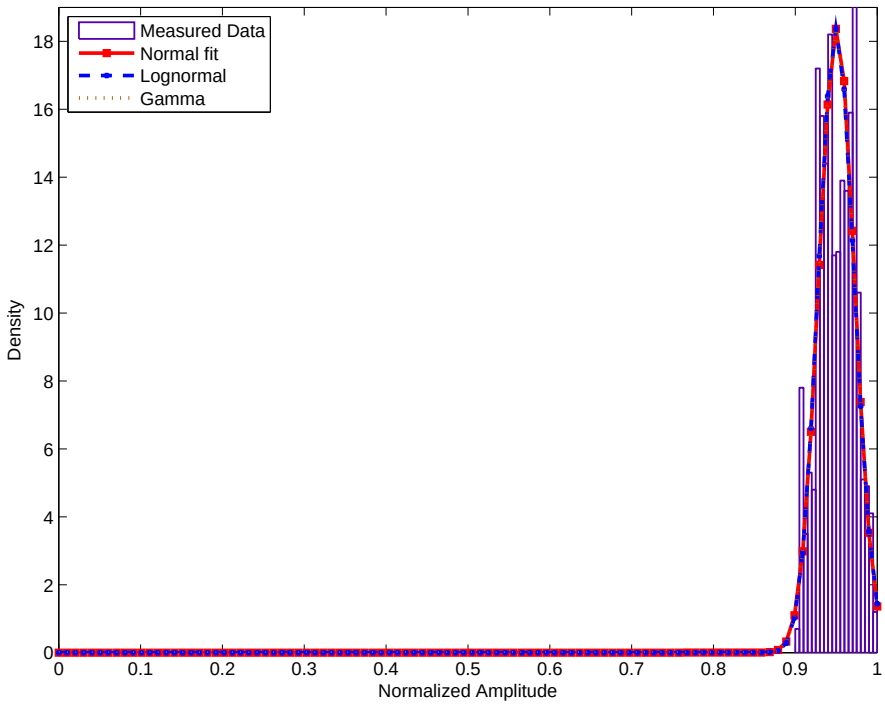

Figure 204: PDF of received power at 820 MHz: chest to off-body; Standing; 2 m separation; 90° orientation

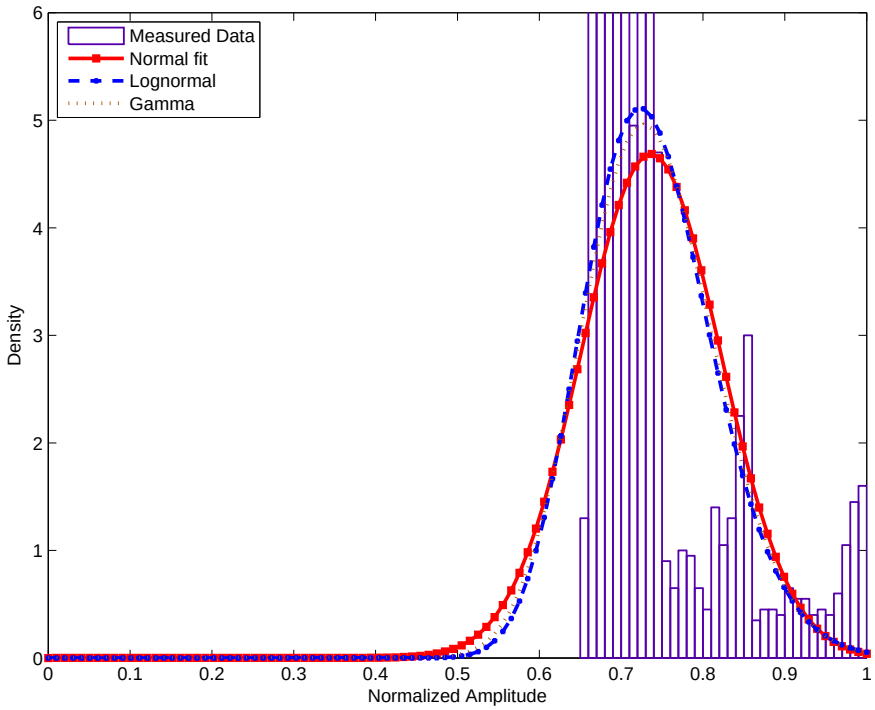

Figure 205: PDF of received power at 820 MHz: chest to off-body; Standing; 3 m separation; 0° orientation

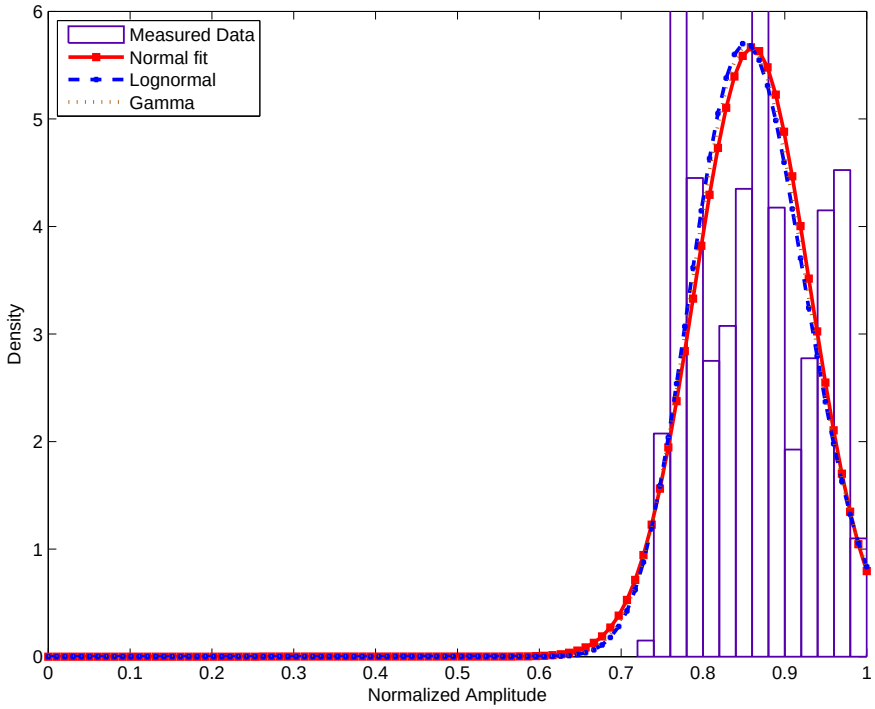

Figure 206: PDF of received power at 820 MHz: chest to off-body; Standing; 3 m separation; 180° orientation

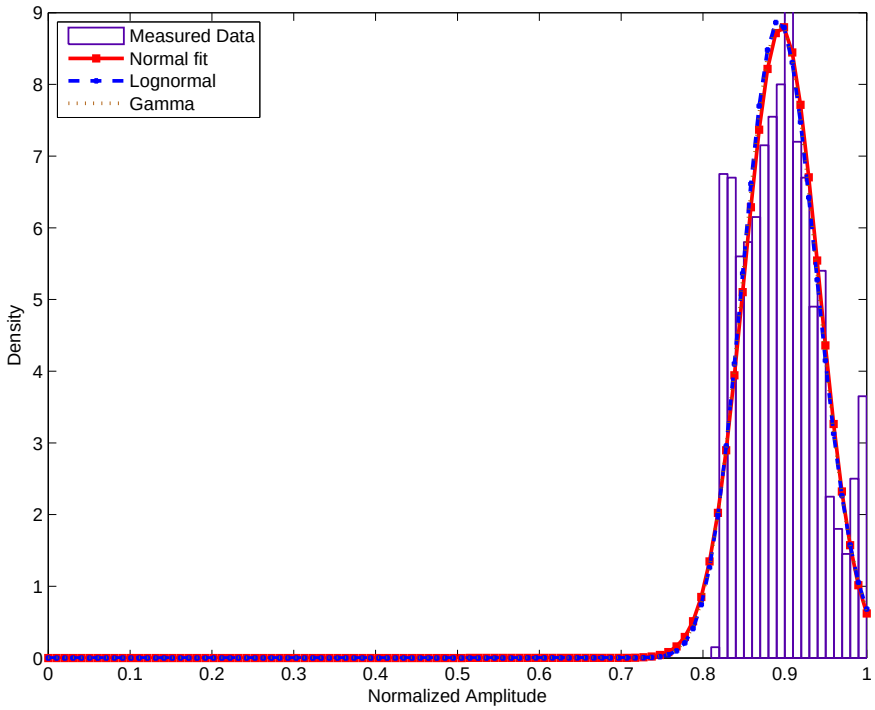

Figure 207: PDF of received power at 820 MHz: chest to off-body; Standing; 3 m separation; 270° orientation

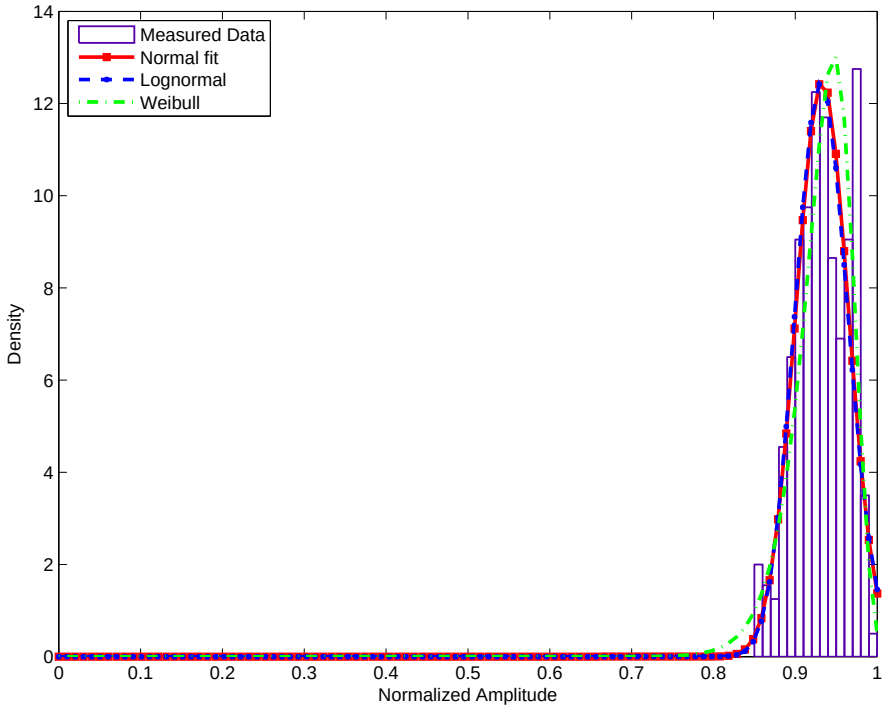

Figure 208: PDF of received power at 820 MHz: chest to off-body; Standing; 3 m separation; 90° orientation

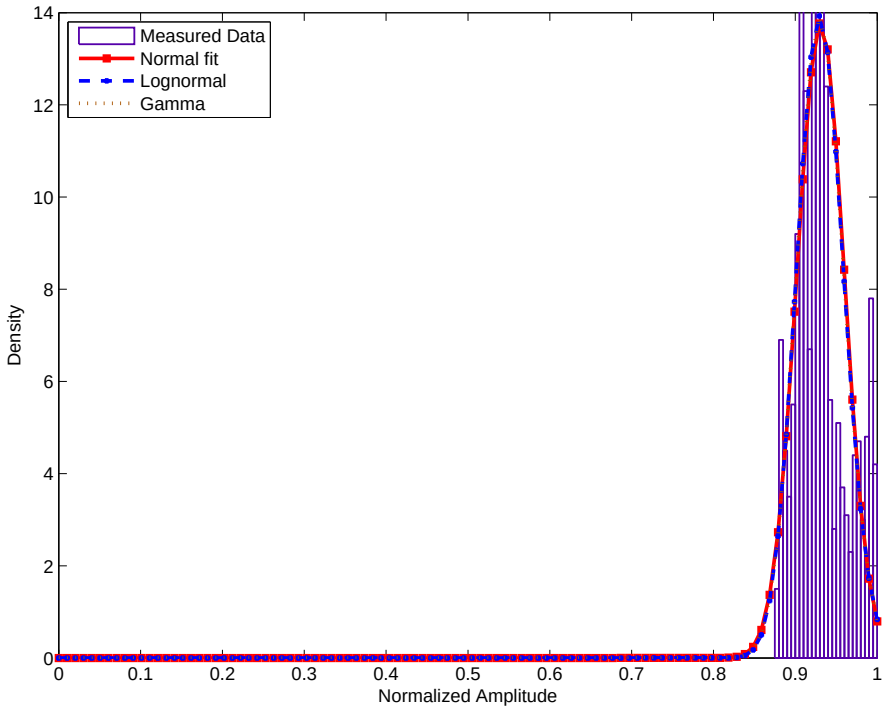

Figure 209: PDF of received power at 820 MHz: chest to off-body; Standing; 4 m separation; 0° orientation

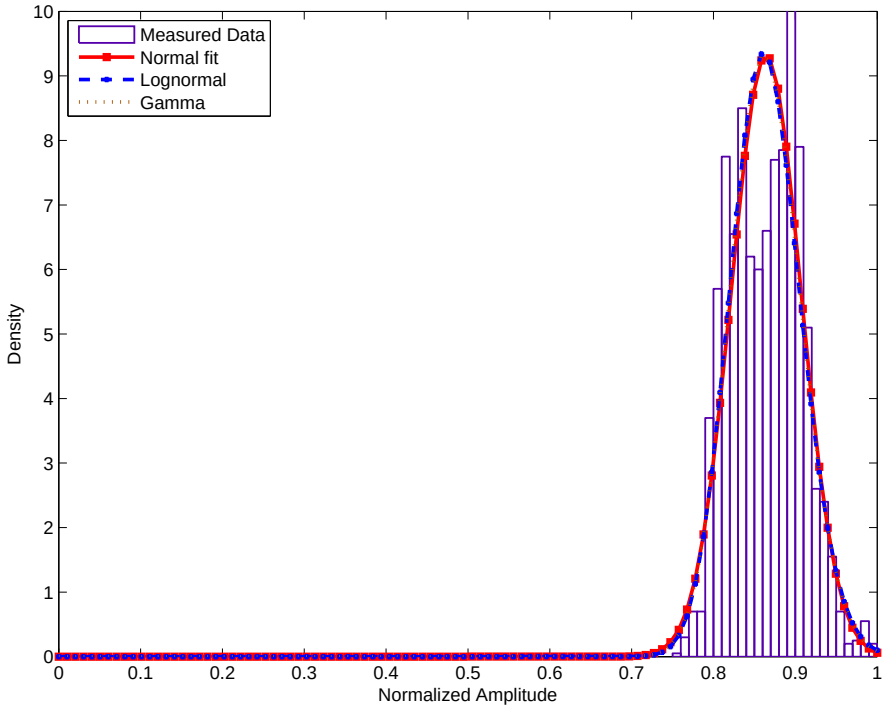

Figure 210: PDF of received power at 820 MHz: chest to off-body; Standing; 4 m separation; 180° orientation

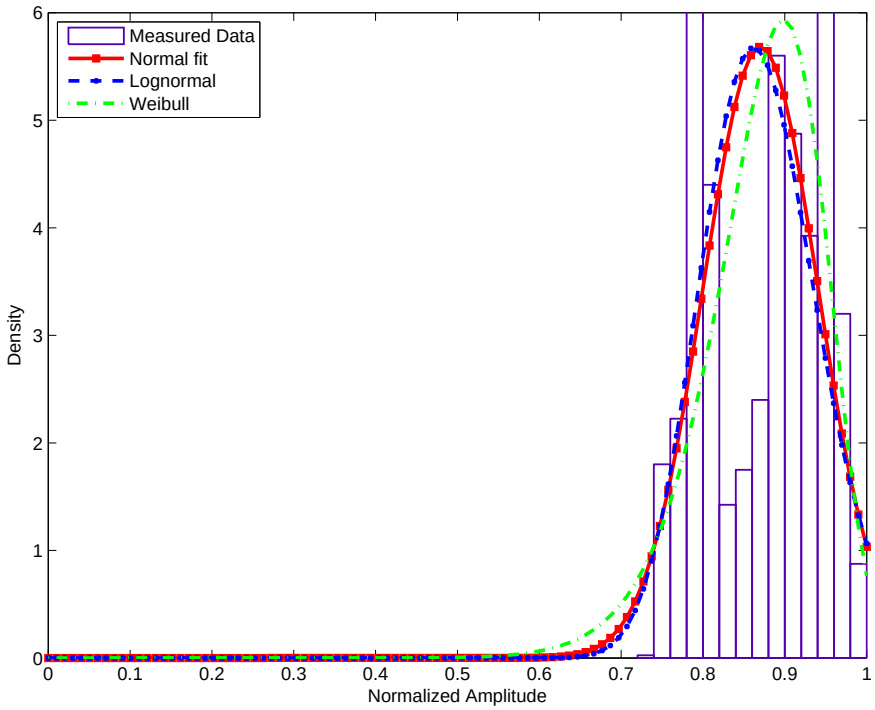

Figure 211: PDF of received power at 820 MHz: chest to off-body; Standing; 4 m separation; 270° orientation

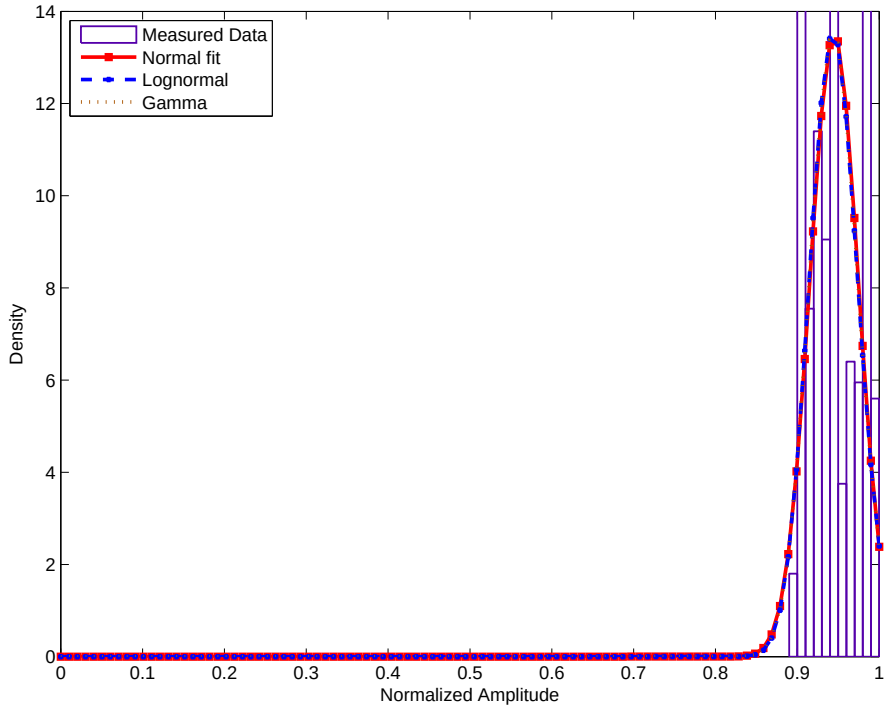

Figure 212: PDF of received power at 820 MHz: chest to off-body; Standing; 4 m separation; 90° orientation

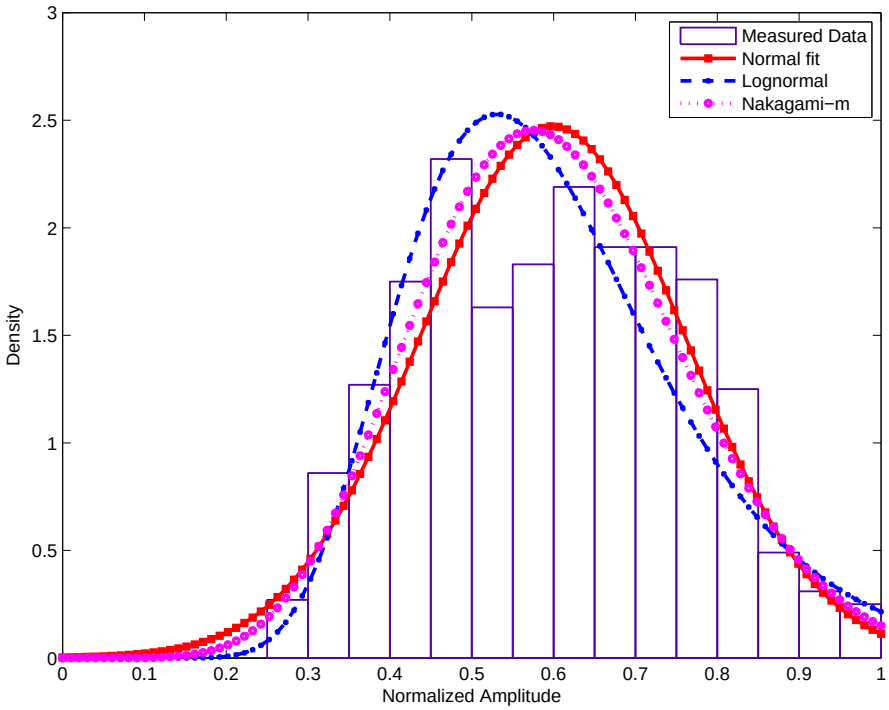

Figure 213: PDF of received power at 820 MHz: chest to off-body; Walking; 1 m separation; 0° orientation

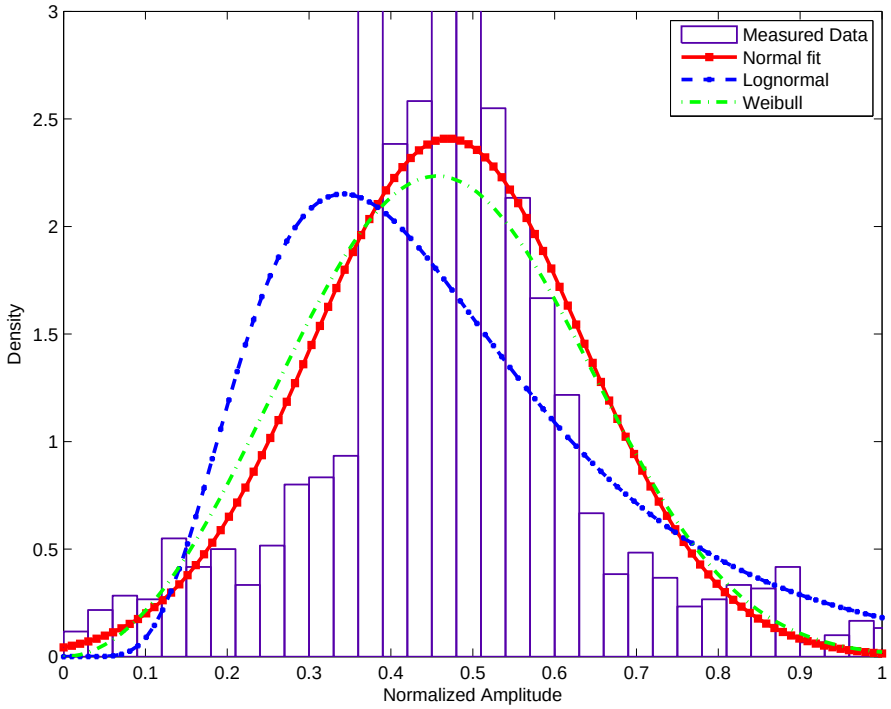

Figure 214: PDF of received power at 820 MHz: chest to off-body; Walking; 1 m separation; 180° orientation

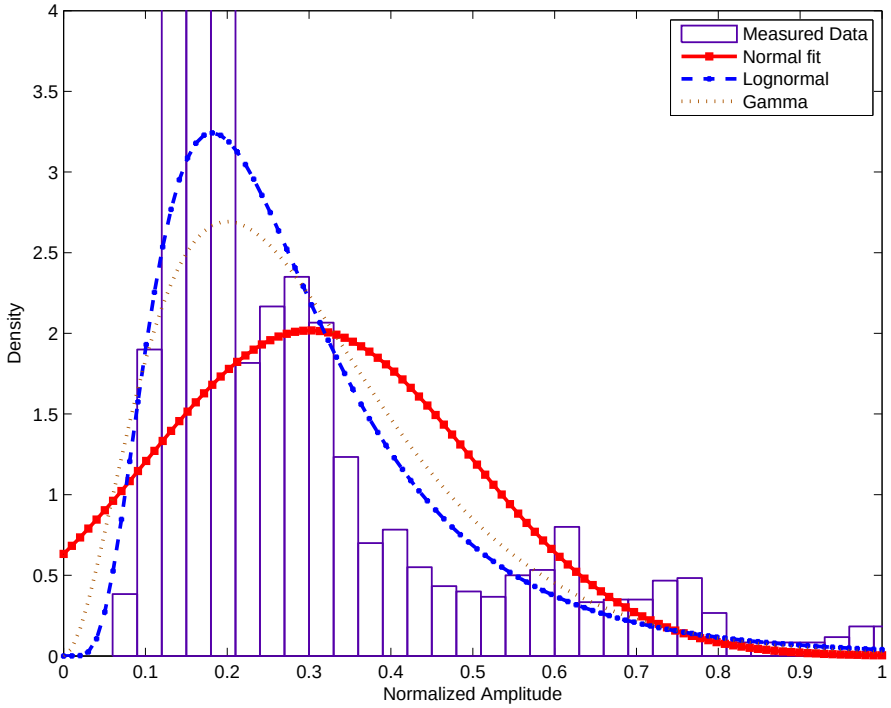

Figure 215: PDF of received power at 820 MHz: chest to off-body; Walking; 1 m separation; 270° orientation

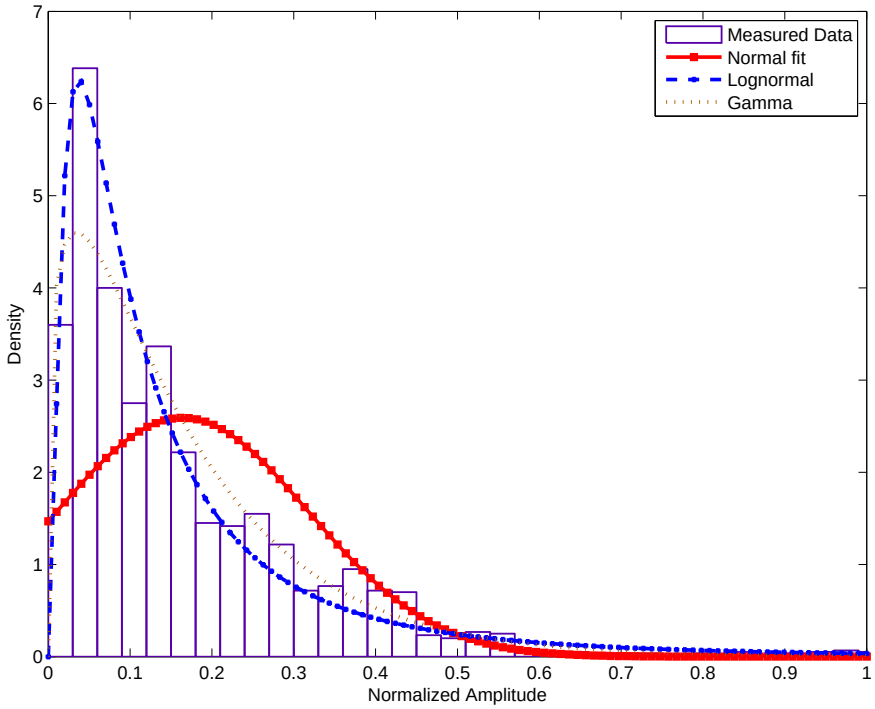

Figure 216: PDF of received power at 820 MHz: chest to off-body; Walking; 1 m separation; 90° orientation

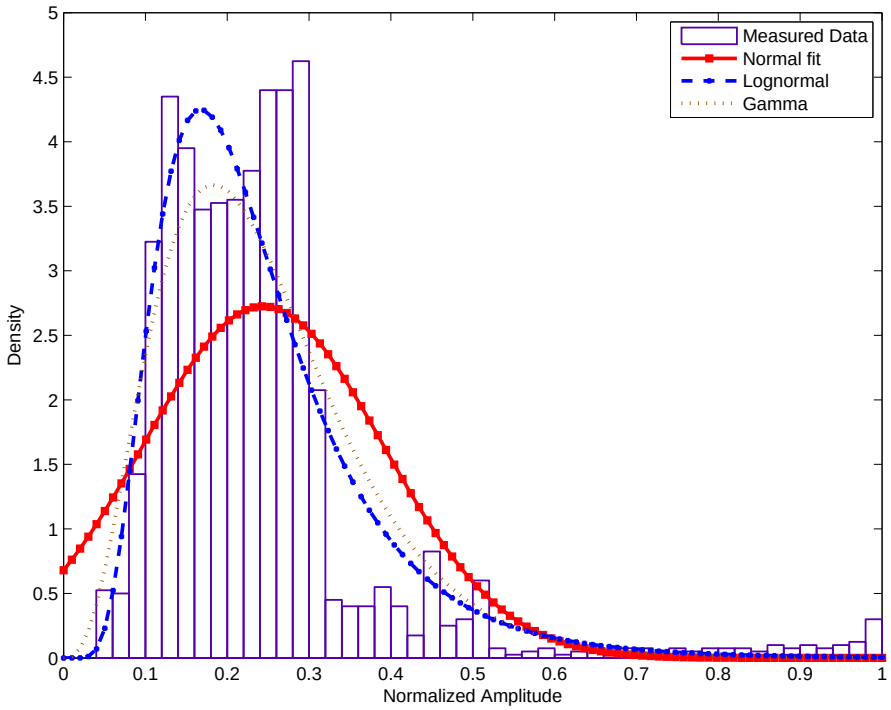

Figure 217: PDF of received power at 820 MHz: chest to off-body; Walking; 2 m separation; 0° orientation

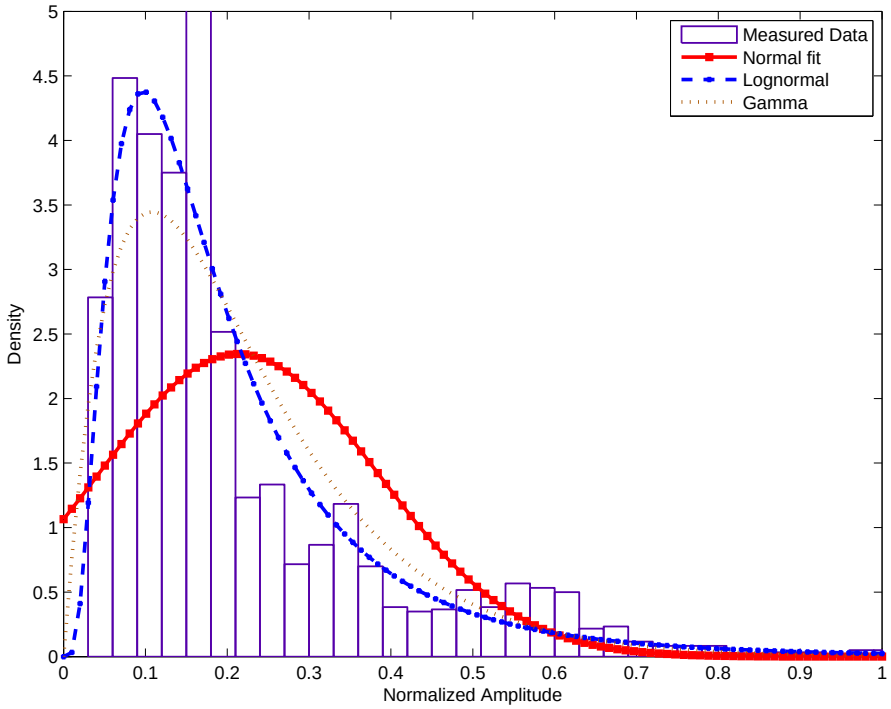

Figure 218: PDF of received power at 820 MHz: chest to off-body; Walking; 2 m separation; 180° orientation

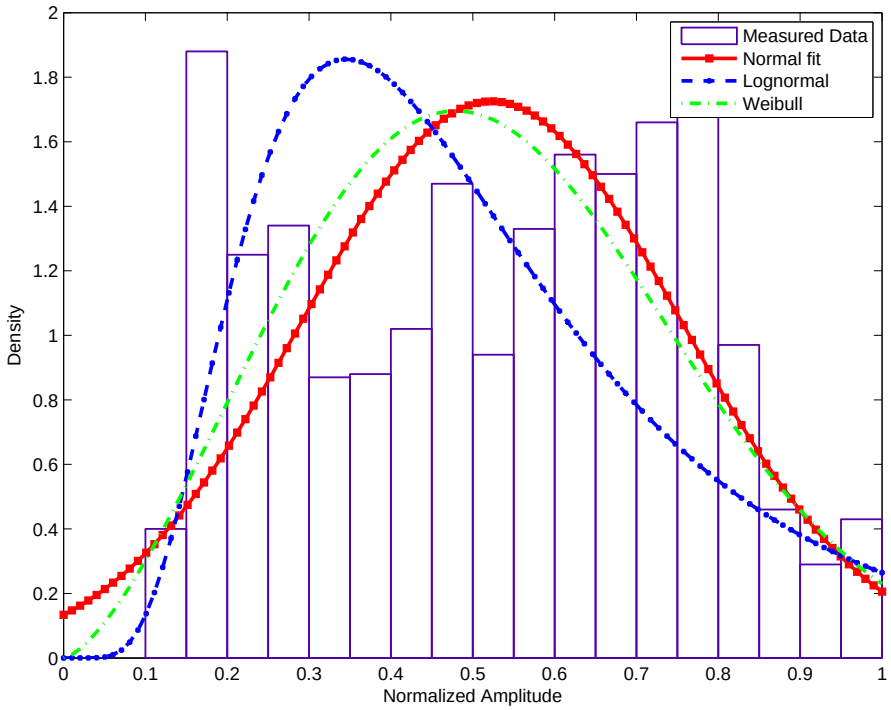

Figure 219: PDF of received power at 820 MHz: chest to off-body; Walking; 2 m separation; 270° orientation

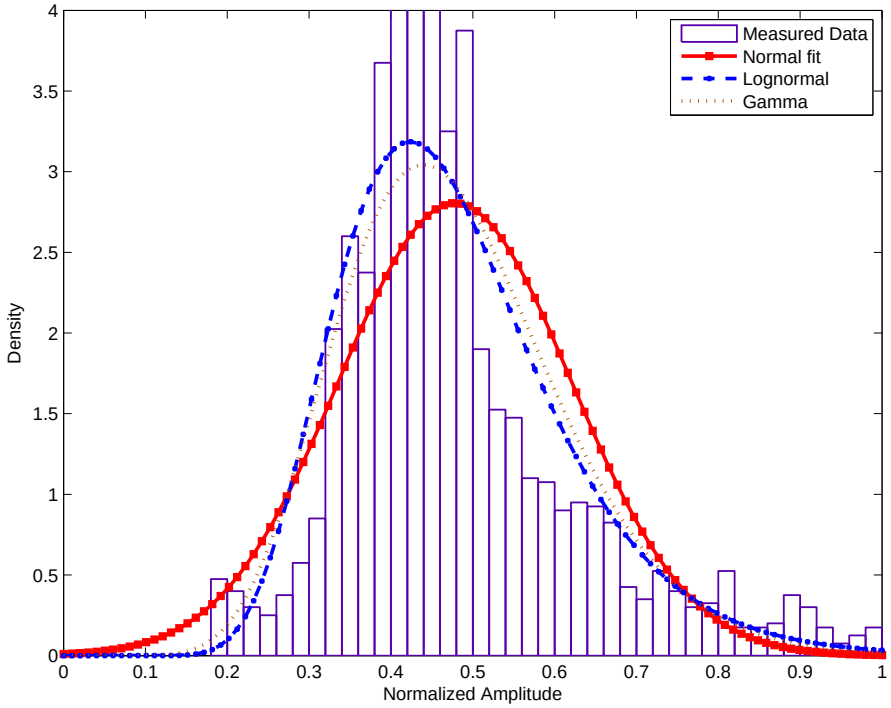

Figure 220: PDF of received power at 820 MHz: chest to off-body; Walking; 2 m separation; 90° orientation

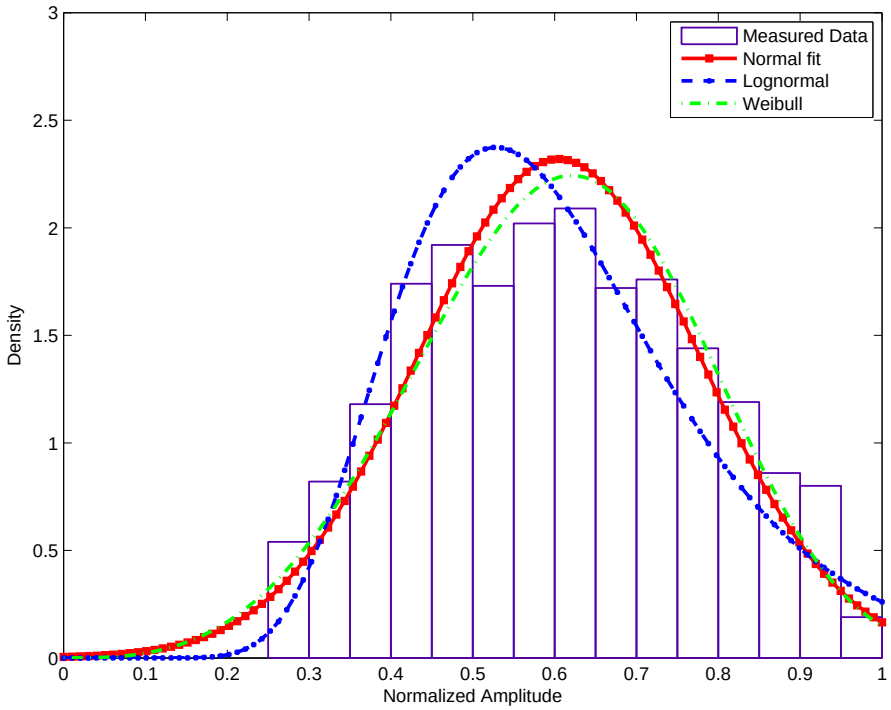

Figure 221: PDF of received power at 820 MHz: chest to off-body; Walking; 3 m separation; 0° orientation

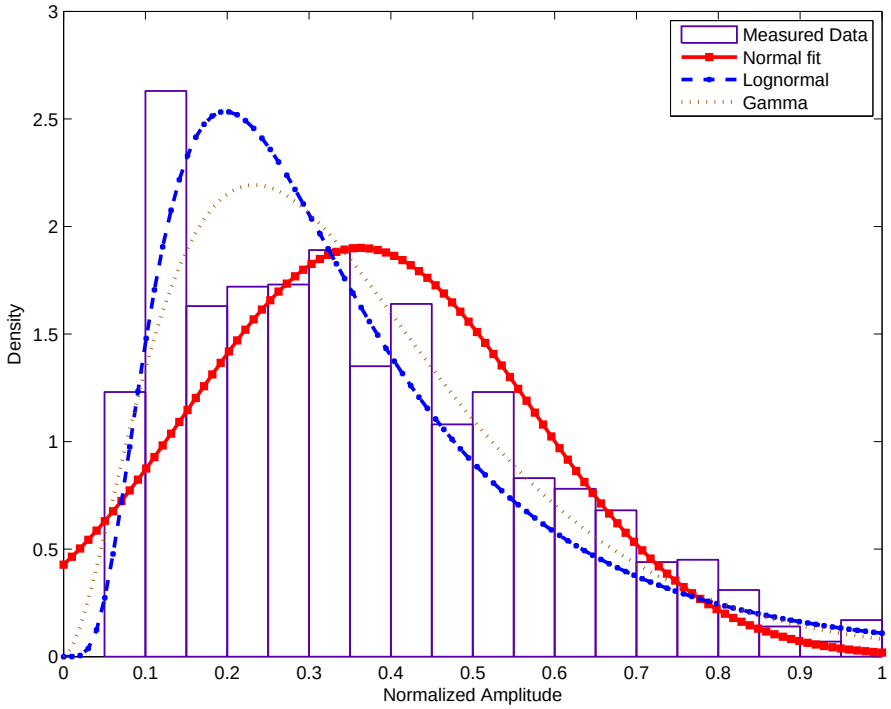

Figure 222: PDF of received power at 820 MHz: chest to off-body; Walking; 3 m separation; 180° orientation

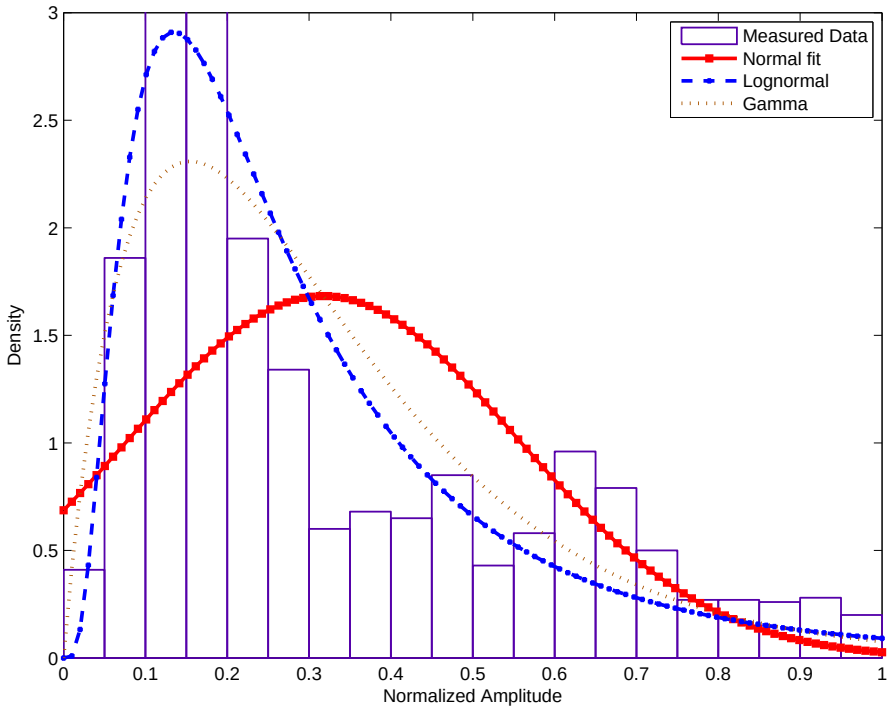

Figure 223: PDF of received power at 820 MHz: chest to off-body; Walking; 3 m separation; 270° orientation

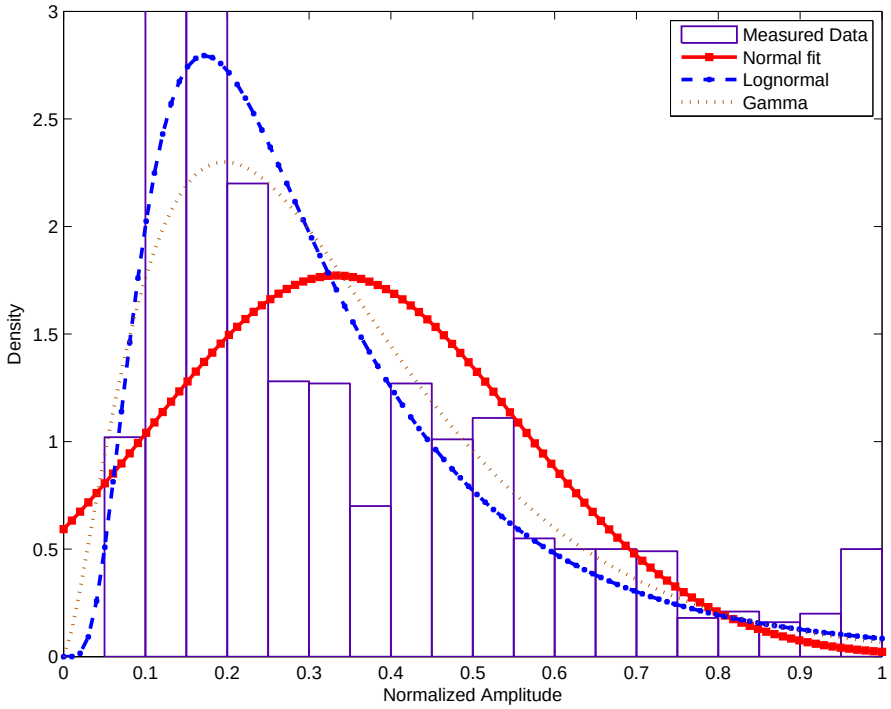

Figure 224: PDF of received power at 820 MHz: chest to off-body; Walking; 3 m separation; 90° orientation

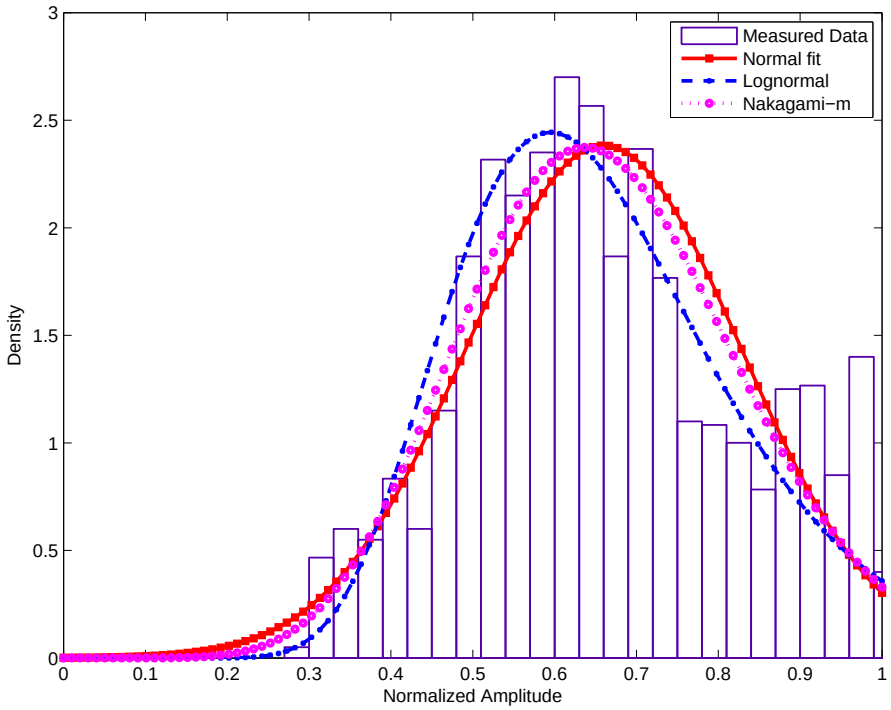

Figure 225: PDF of received power at 820 MHz: chest to off-body; Walking; 4 m separation; 0° orientation

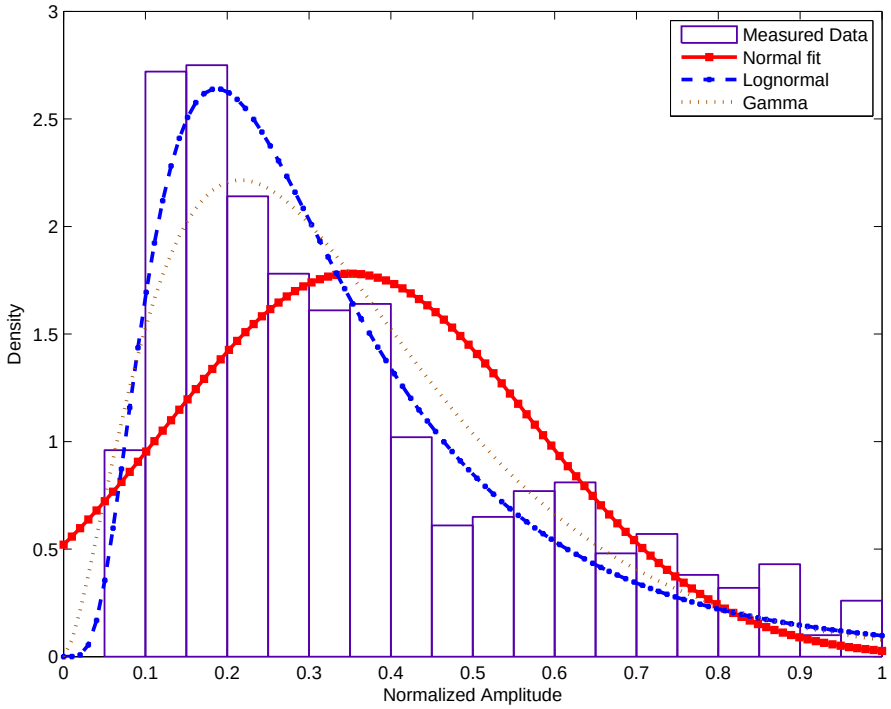

Figure 226: PDF of received power at 820 MHz: chest to off-body; Walking; 4 m separation; 180° orientation

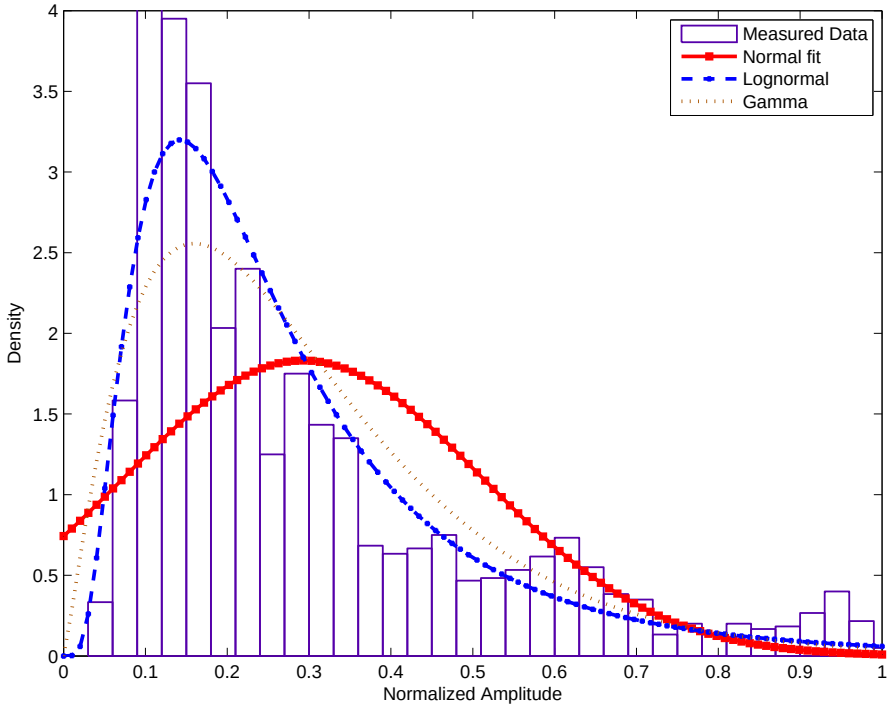

Figure 227: PDF of received power at 820 MHz: chest to off-body; Walking; 4 m separation; 270° orientation

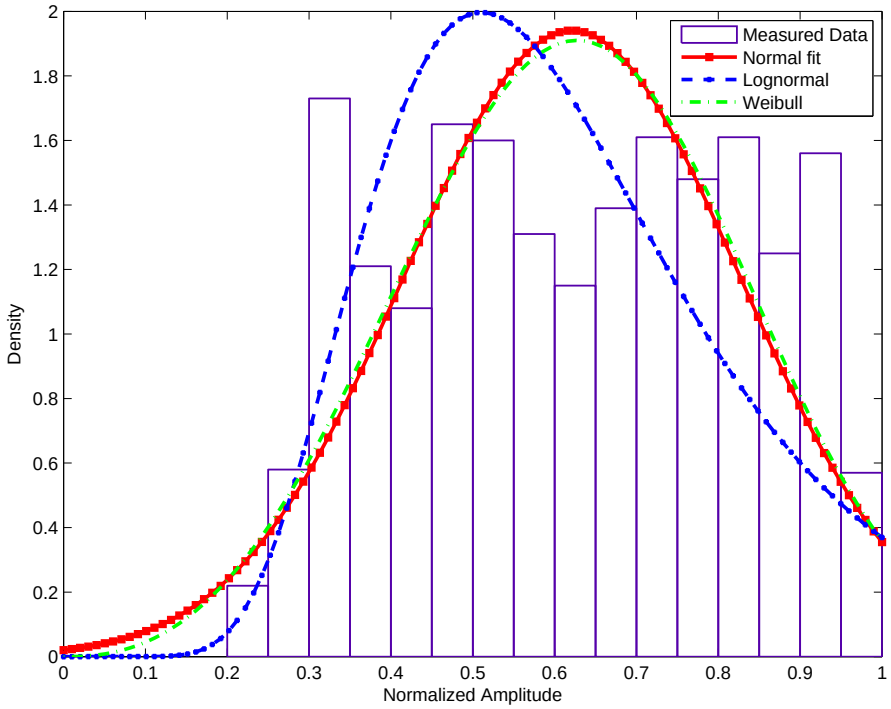

Figure 228: PDF of received power at 820 MHz: chest to off-body; Walking; 4 m separation; 90° orientation

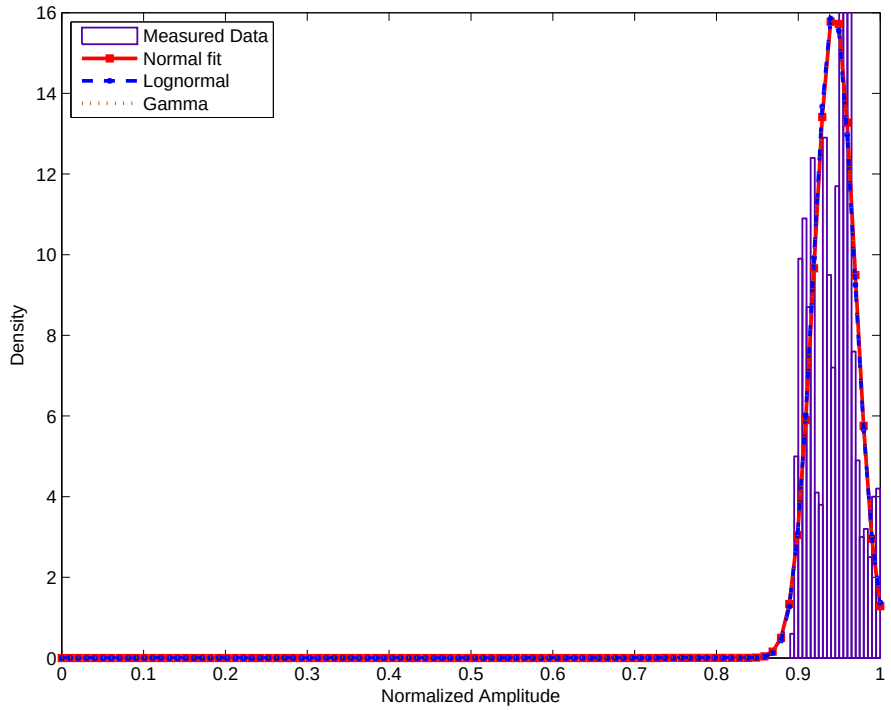

Figure 229: PDF of received power at 820 MHz: right wrist to off-body; Standing; 1 m separation; 0° orientation

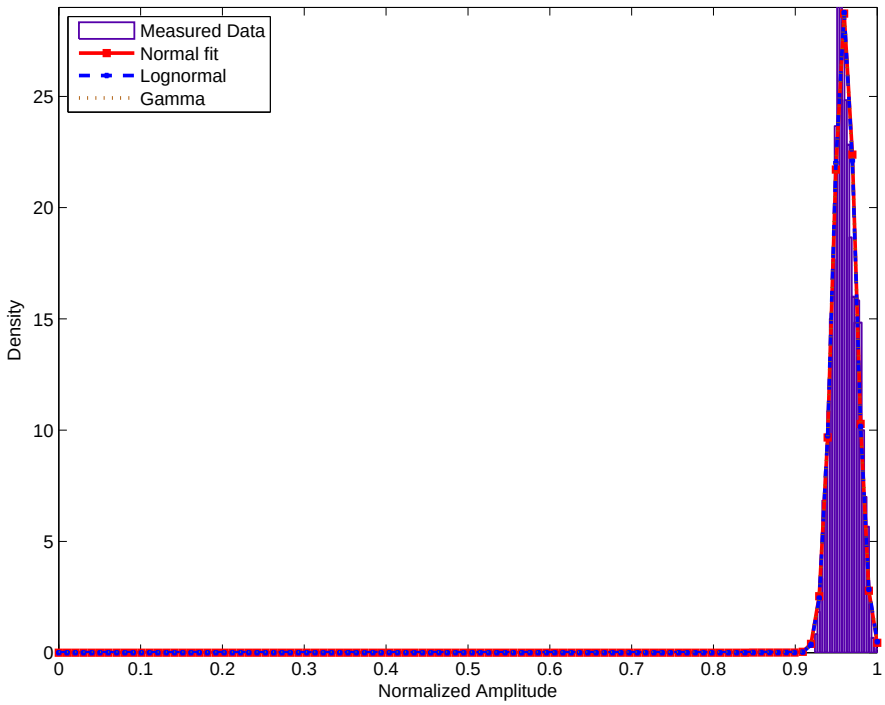

Figure 230: PDF of received power at 820 MHz: right wrist to off-body; Standing; 1 m separation; 180° orientation

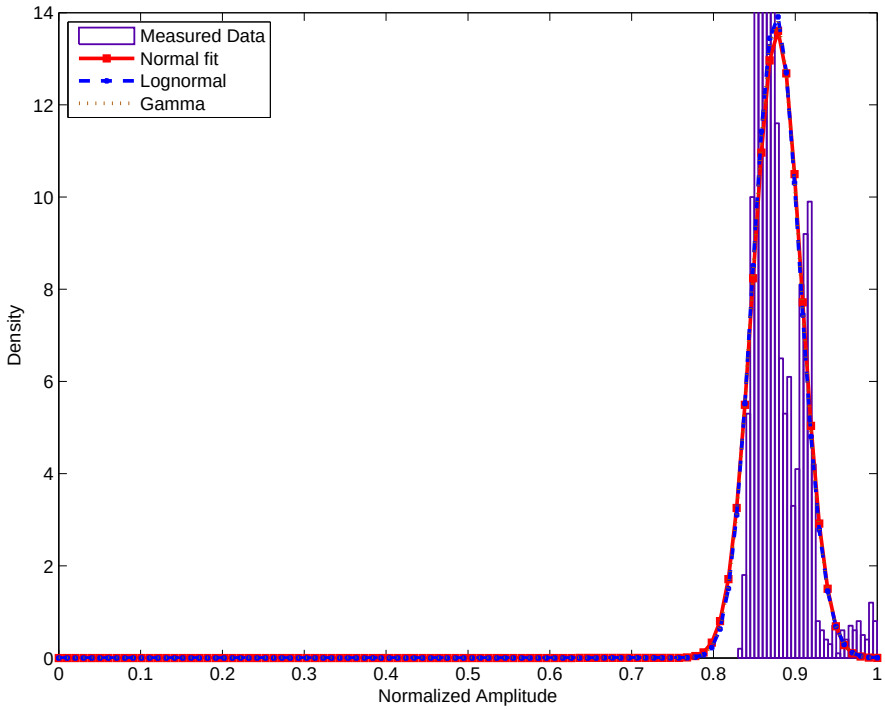

Figure 231: PDF of received power at 820 MHz: right wrist to off-body; Standing; 1 m separation; 270° orientation

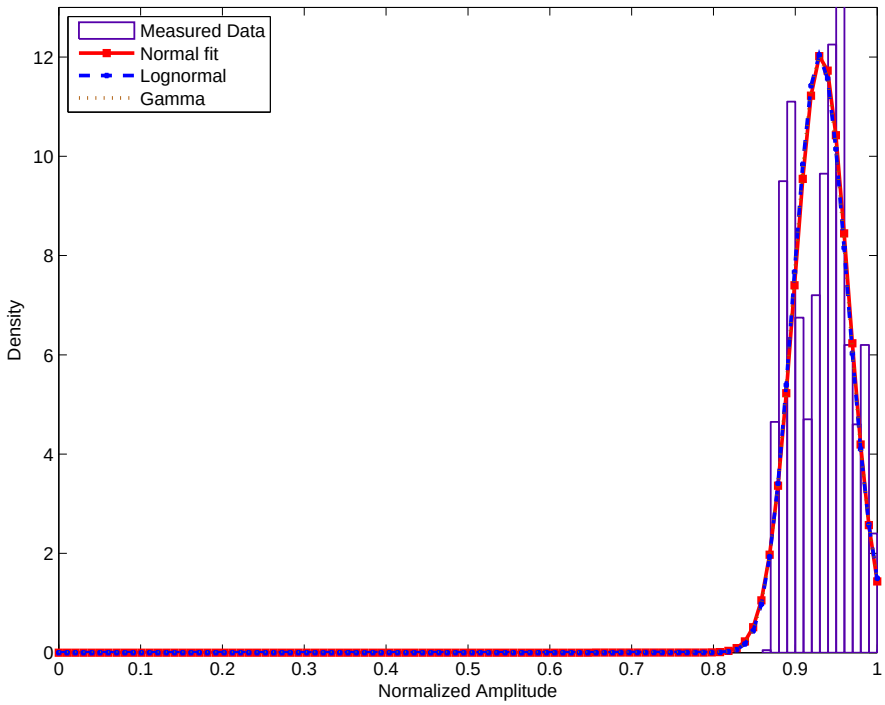

Figure 232: PDF of received power at 820 MHz: right wrist to off-body; Standing; 1 m separation; 90° orientation

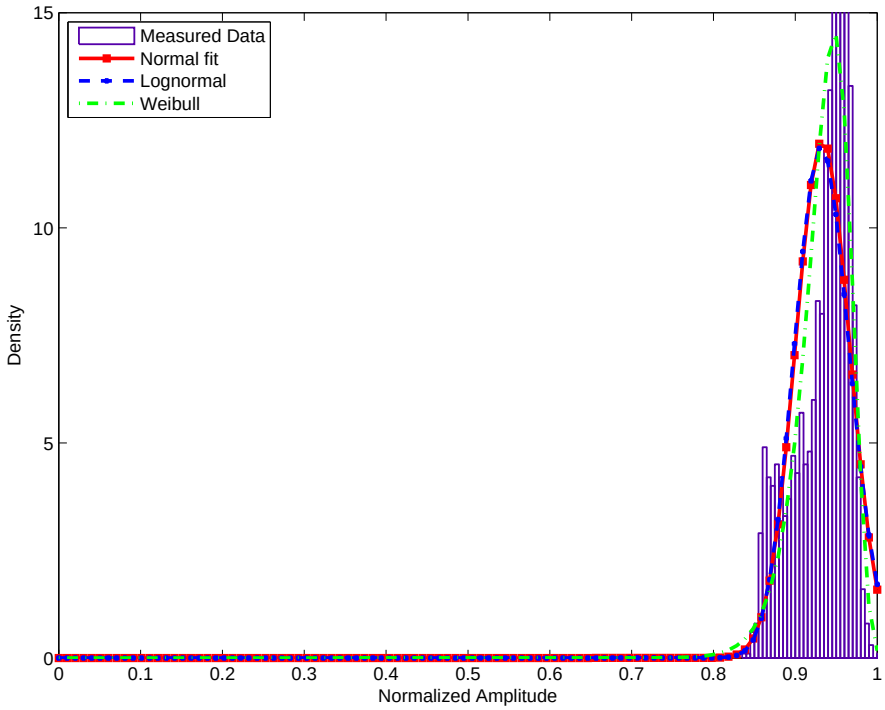

Figure 233: PDF of received power at 820 MHz: right wrist to off-body; Standing; 2 m separation; 0° orientation

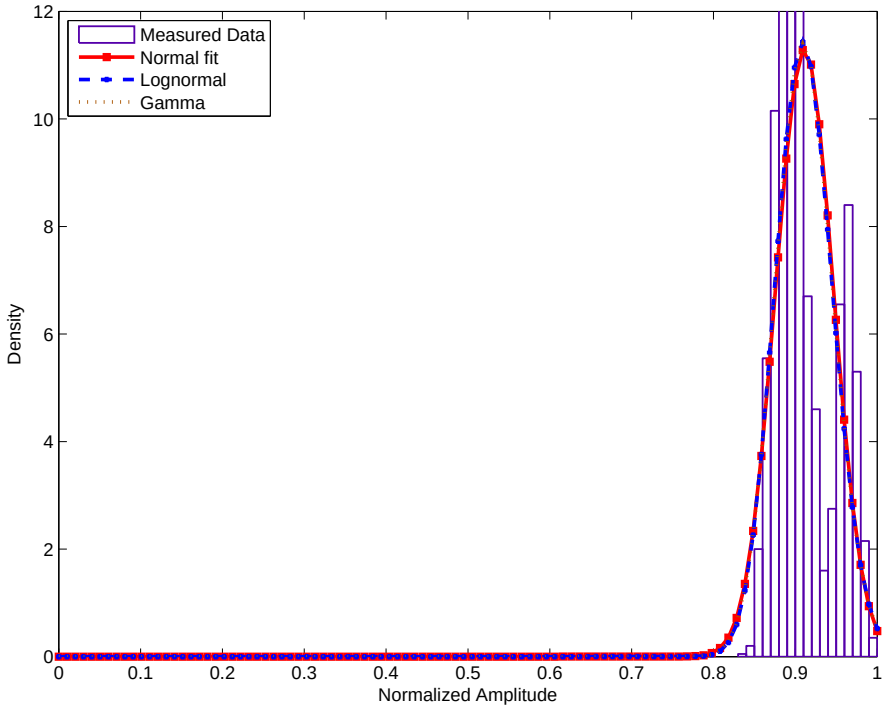

Figure 234: PDF of received power at 820 MHz: right wrist to off-body; Standing; 2 m separation; 180° orientation

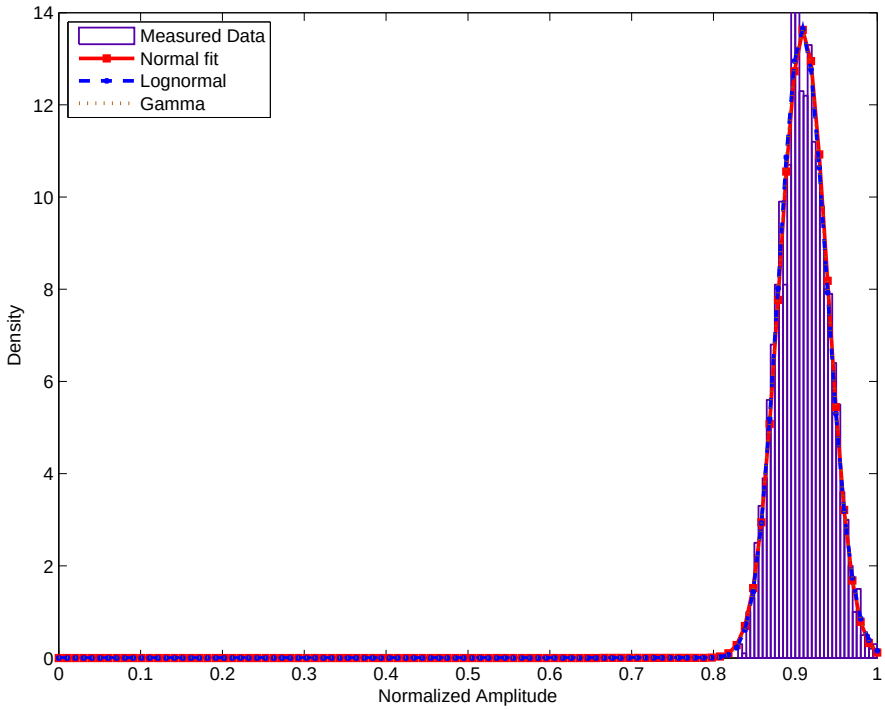

Figure 235: PDF of received power at 820 MHz: right wrist to off-body; Standing; 2 m separation; 270° orientation

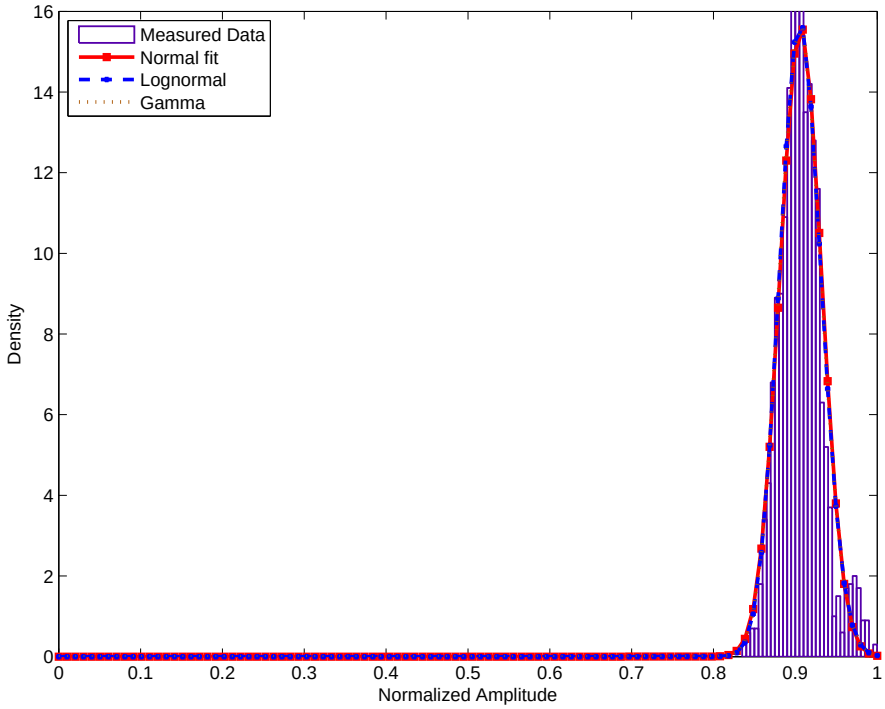

Figure 236: PDF of received power at 820 MHz: right wrist to off-body; Standing; 2 m separation; 90° orientation

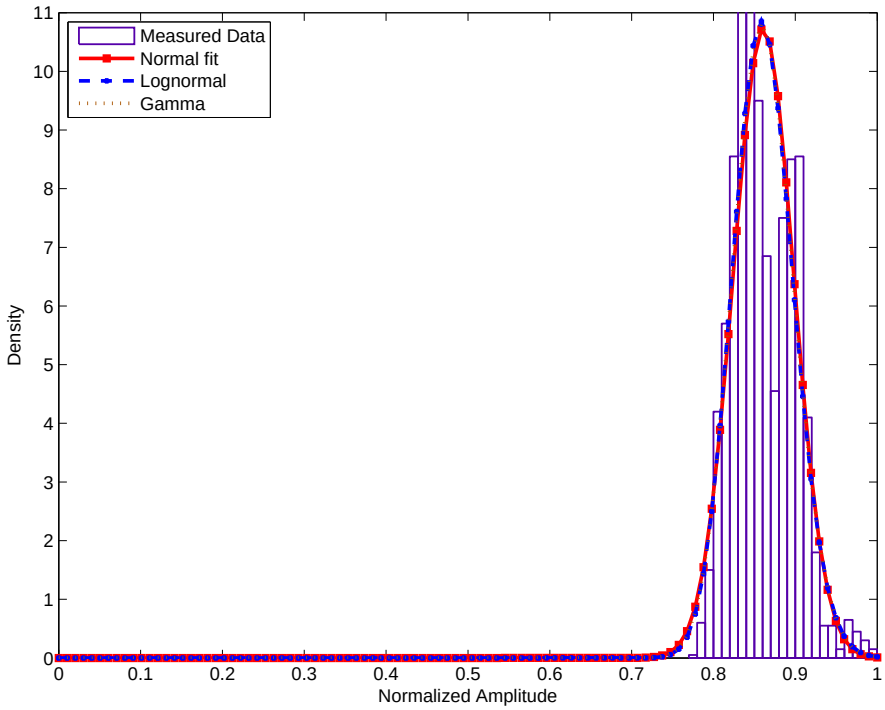

Figure 237: PDF of received power at 820 MHz: right wrist to off-body; Standing; 3 m separation; 0° orientation

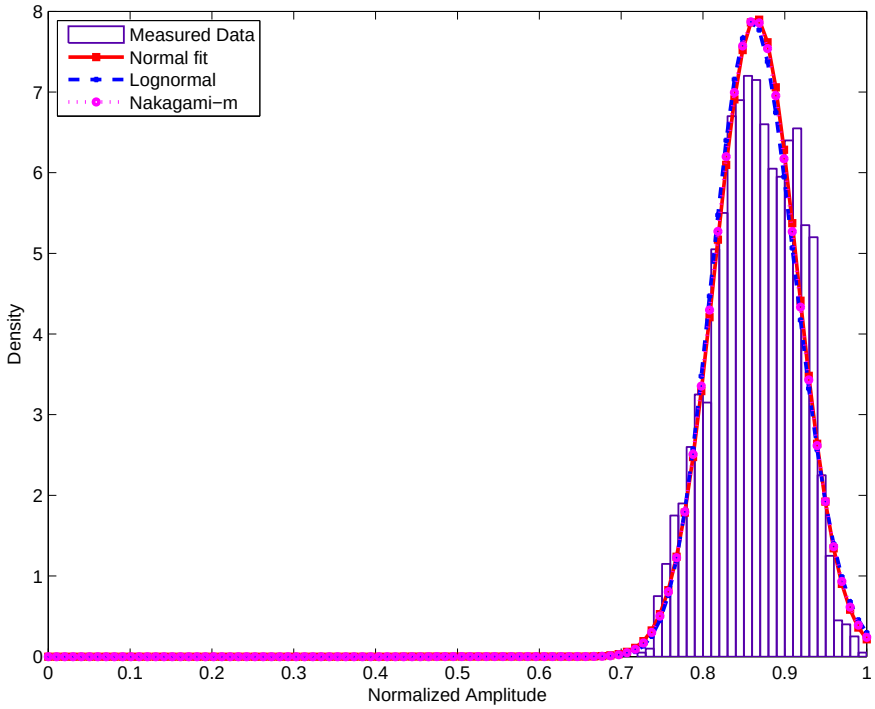

Figure 238: PDF of received power at 820 MHz: right wrist to off-body; Standing; 3 m separation; 180° orientation

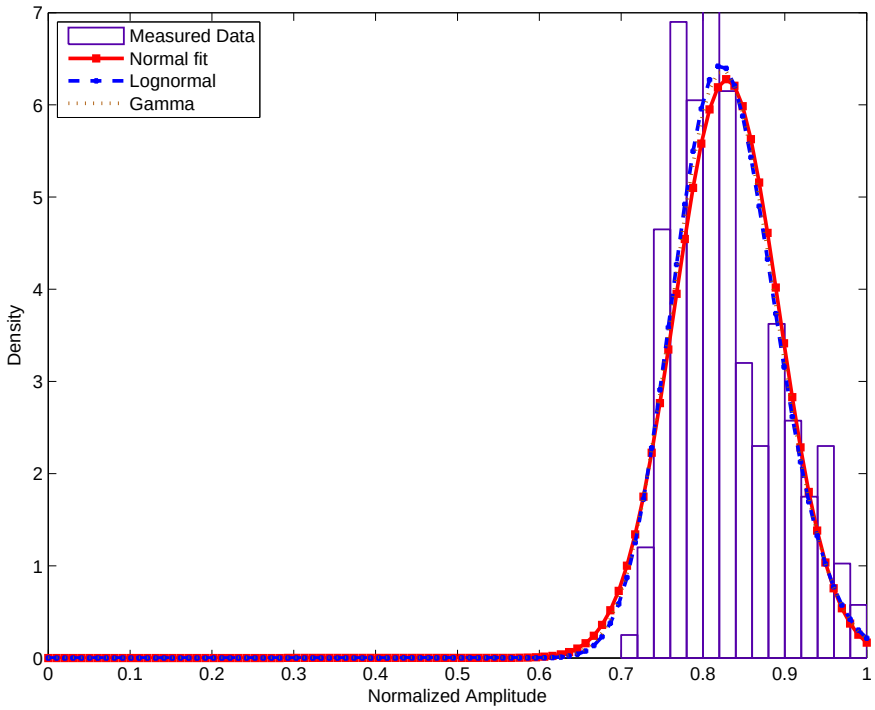

Figure 239: PDF of received power at 820 MHz: right wrist to off-body; Standing; 3 m separation; 270° orientation

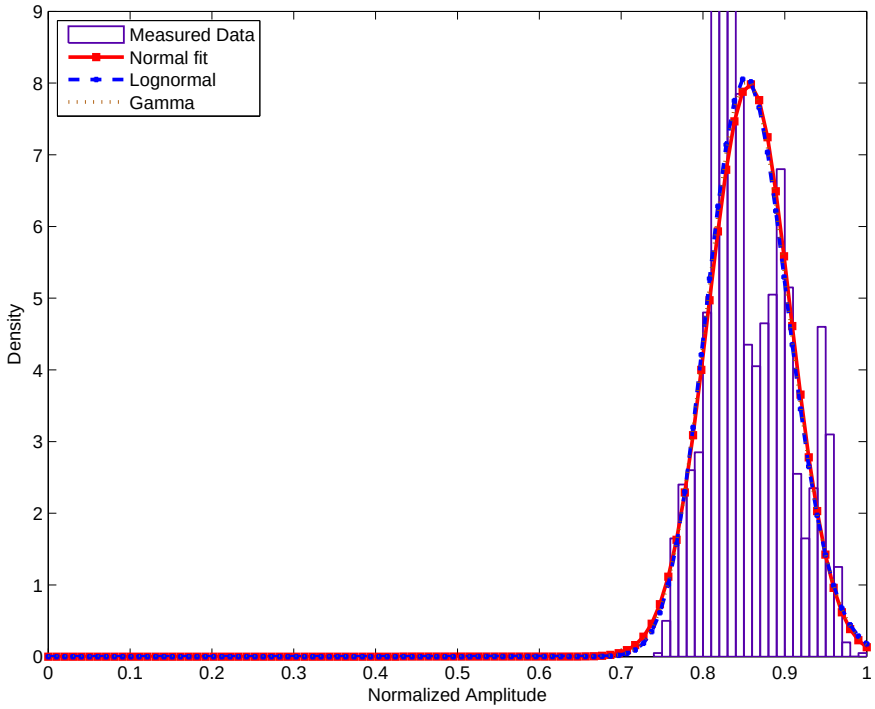

Figure 240: PDF of received power at 820 MHz: right wrist to off-body; Standing; 3 m separation; 90° orientation

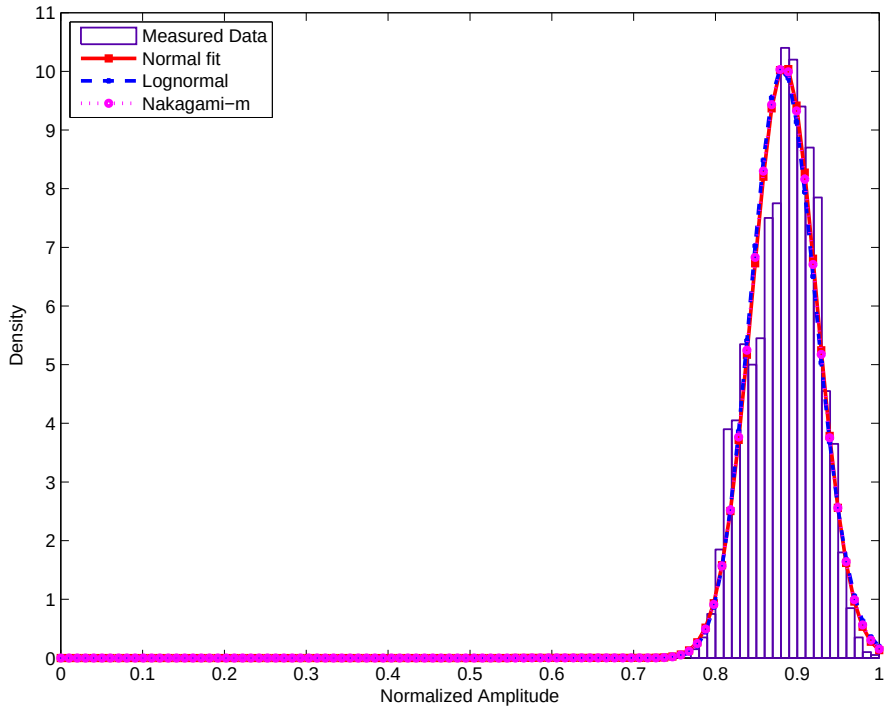

Figure 241: PDF of received power at 820 MHz: right wrist to off-body; Standing; 4 m separation; 0° orientation

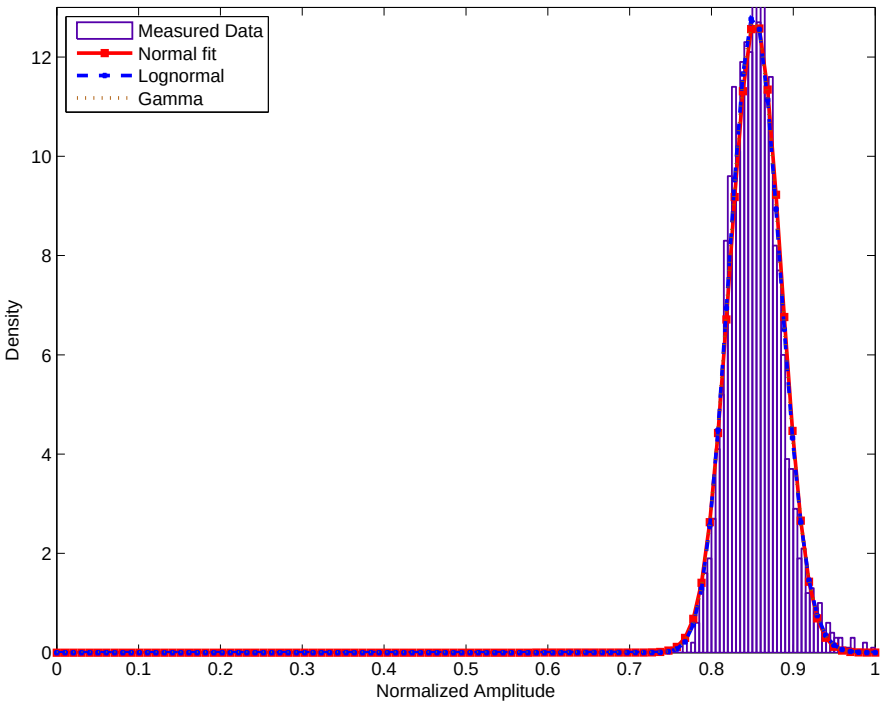

Figure 242: PDF of received power at 820 MHz: right wrist to off-body; Standing; 4 m separation; 180° orientation

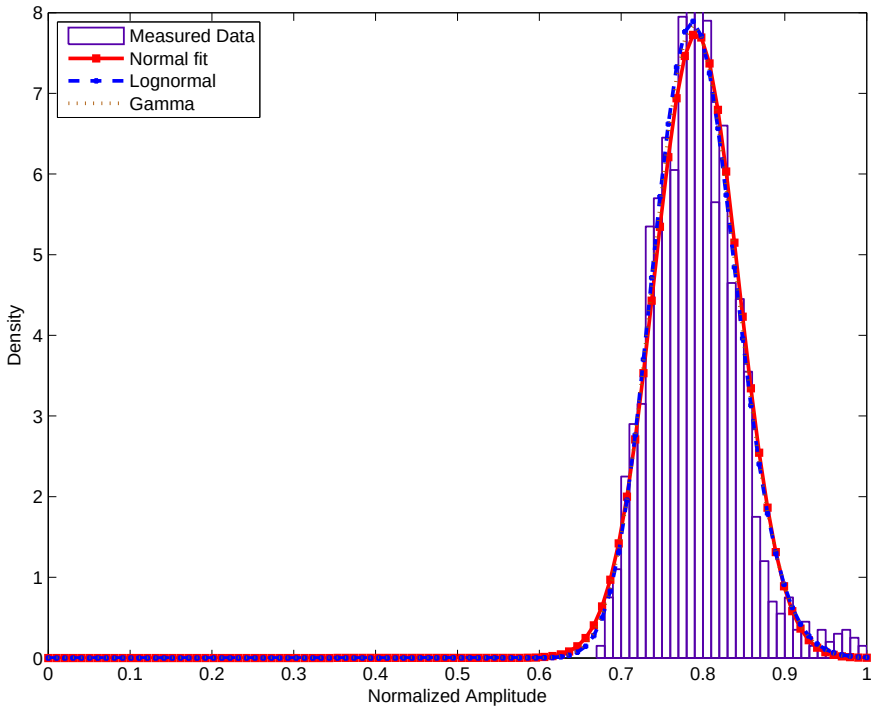

Figure 243: PDF of received power at 820 MHz: right wrist to off-body; Standing; 4 m separation; 270° orientation

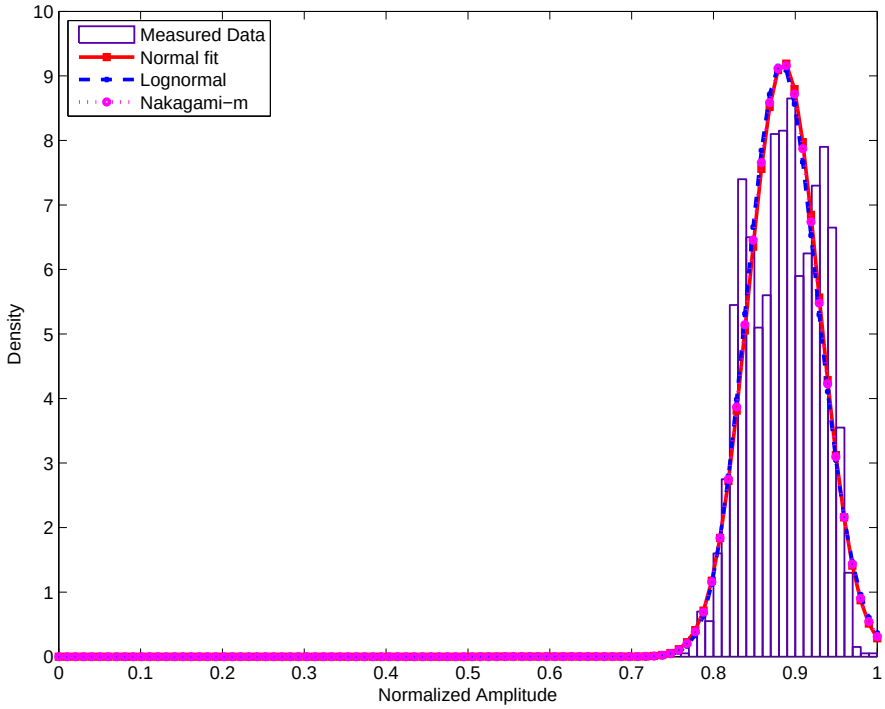

Figure 244: PDF of received power at 820 MHz: right wrist to off-body; Standing; 4 m separation; 90° orientation

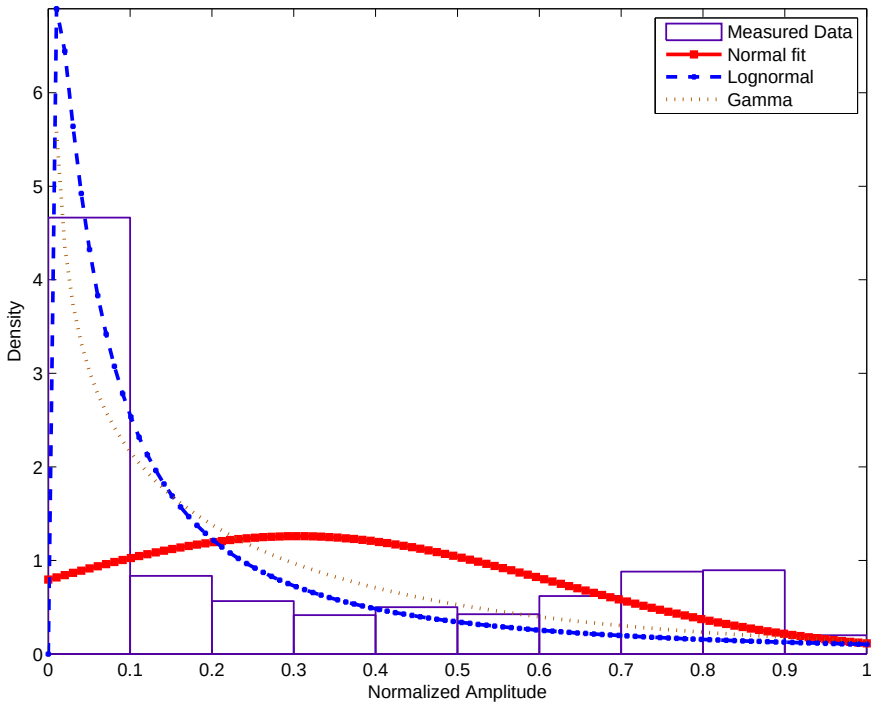

Figure 245: PDF of received power at 820 MHz: right wrist to off-body; Walking; 1 m separation; 0° orientation

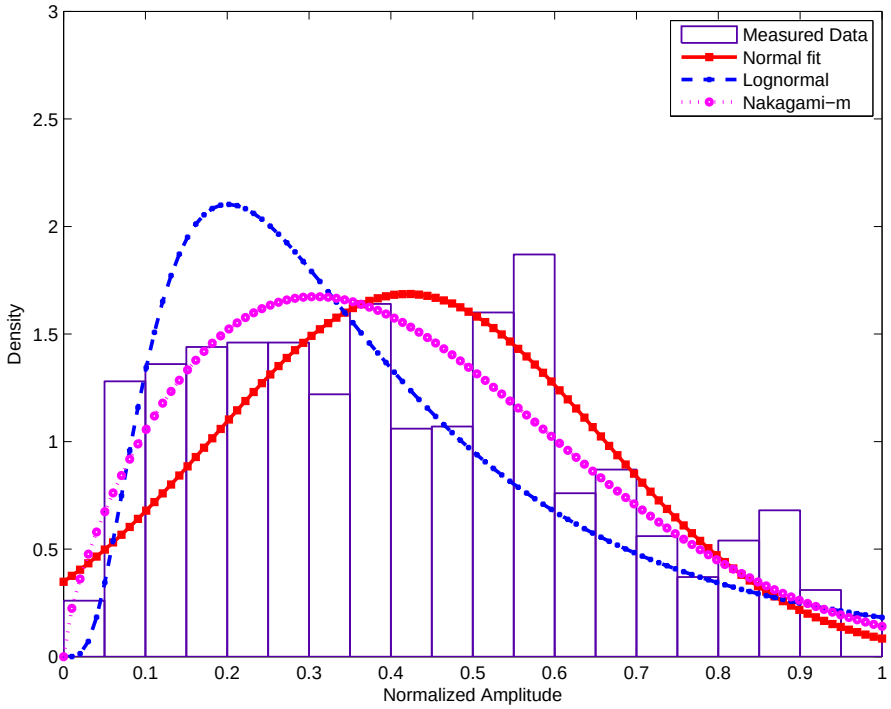

Figure 246: PDF of received power at 820 MHz: right wrist to off-body; Walking; 1 m separation; 180° orientation

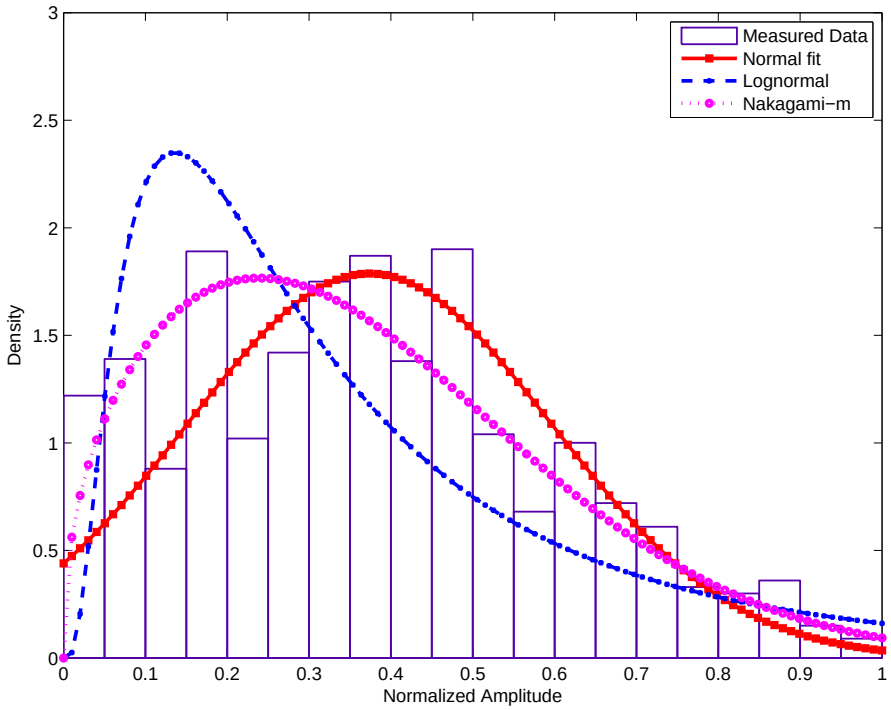

Figure 247: PDF of received power at 820 MHz: right wrist to off-body; Walking; 1 m separation; 270° orientation

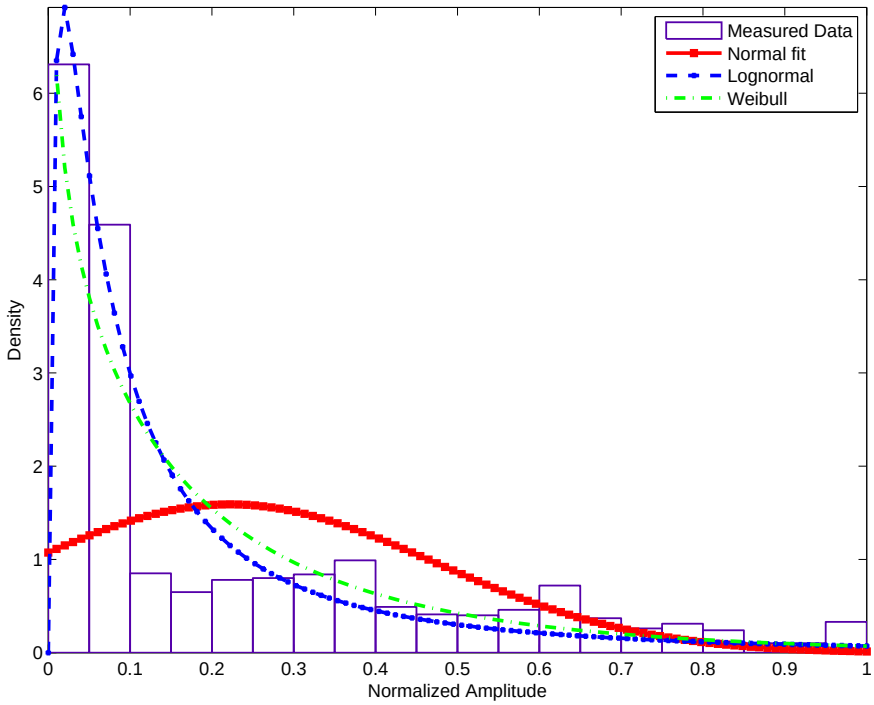

Figure 248: PDF of received power at 820 MHz: right wrist to off-body; Walking; 1 m separation; 90° orientation

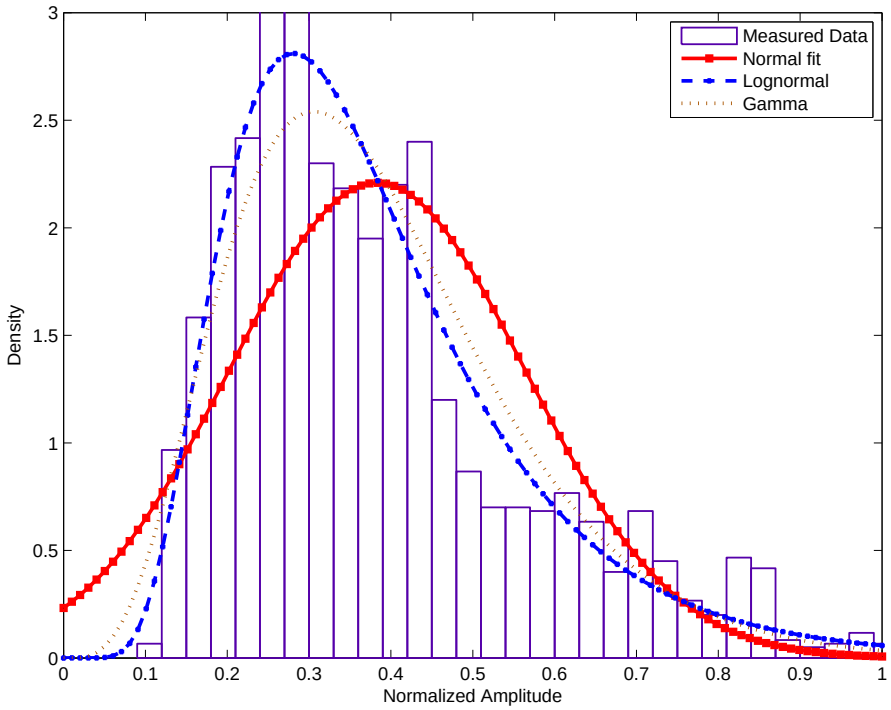

Figure 249: PDF of received power at 820 MHz: right wrist to off-body; Walking; 2 m separation; 0° orientation

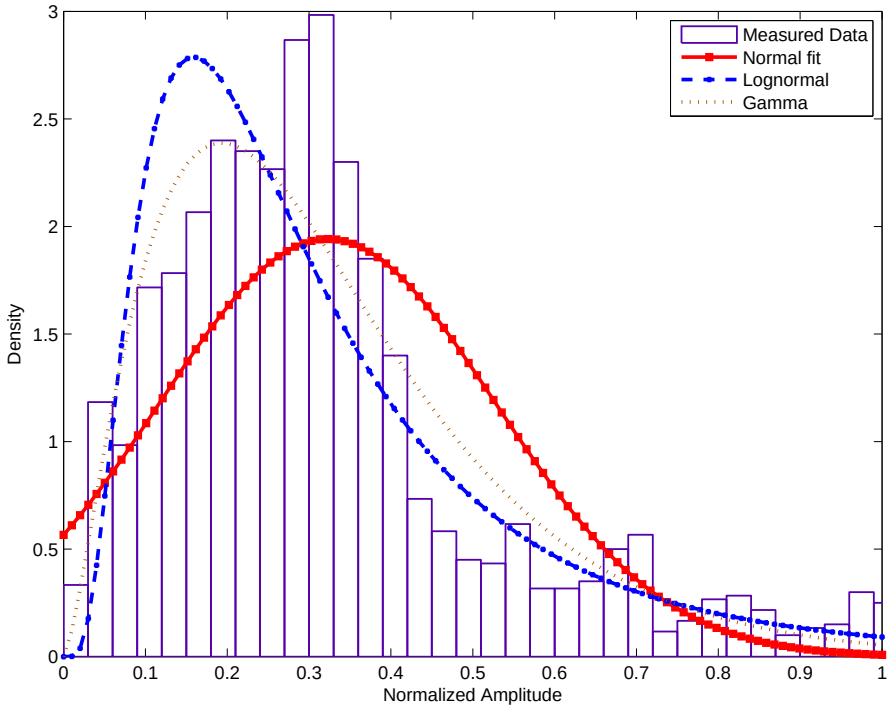

Figure 250: PDF of received power at 820 MHz: right wrist to off-body; Walking; 2 m separation; 180° orientation

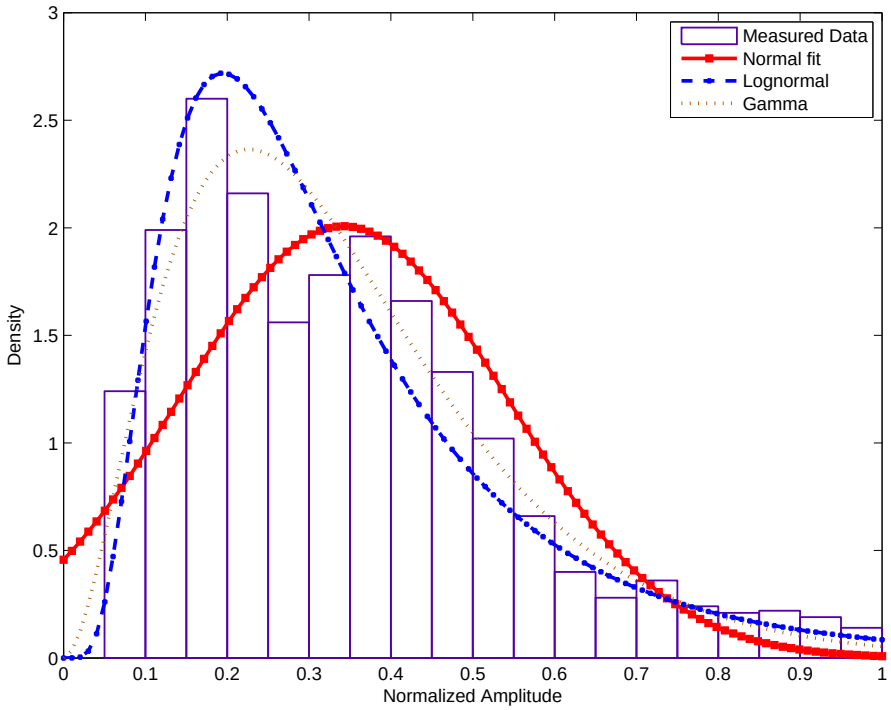

Figure 251: PDF of received power at 820 MHz: right wrist to off-body; Walking; 2 m separation; 270° orientation

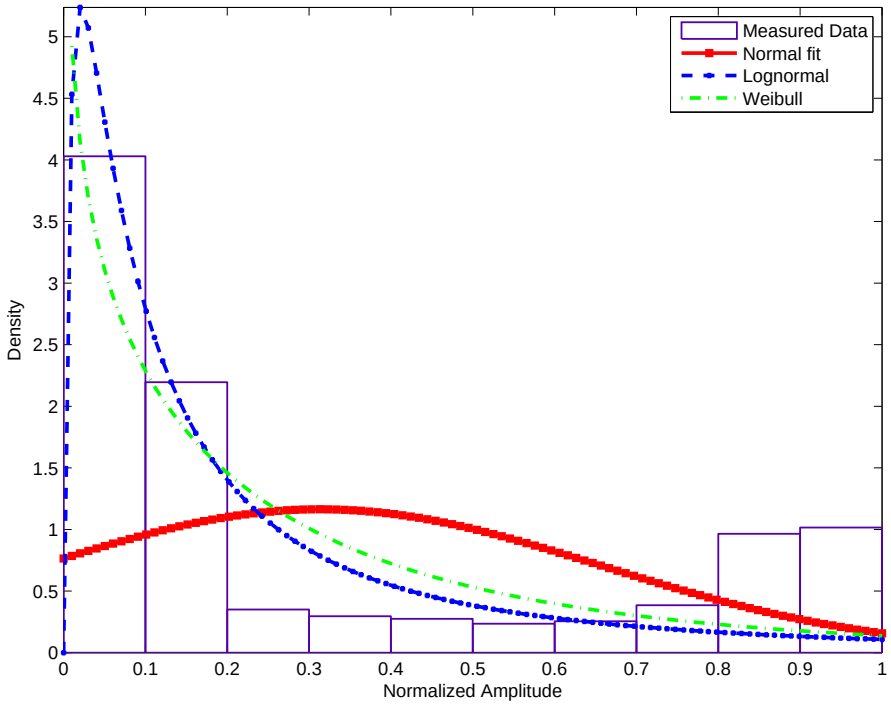

Figure 252: PDF of received power at 820 MHz: right wrist to off-body; Walking; 2 m separation; 90° orientation

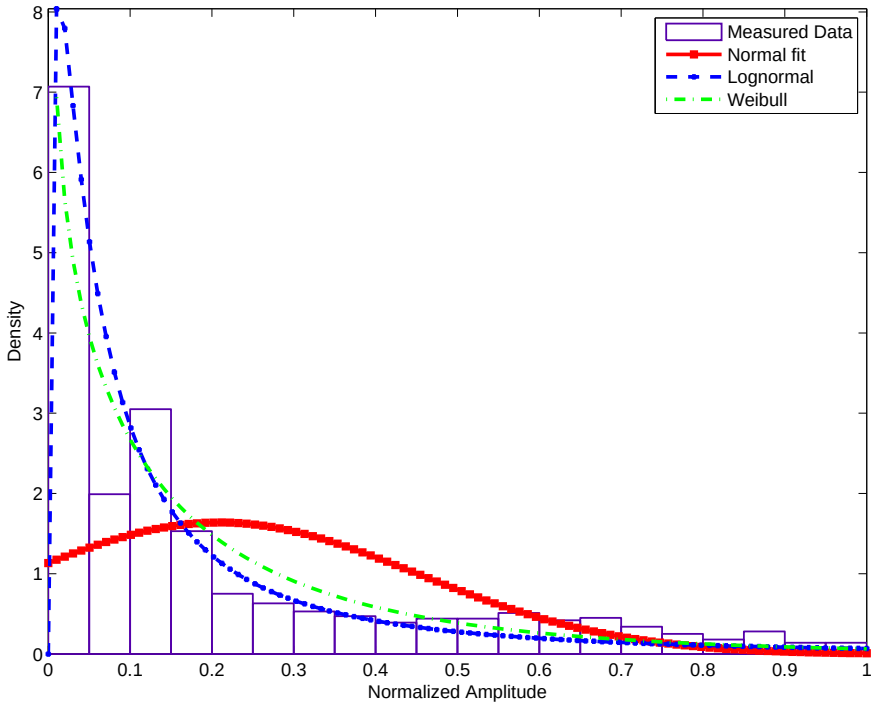

Figure 253: PDF of received power at 820 MHz: right wrist to off-body; Walking; 3 m separation; 0° orientation

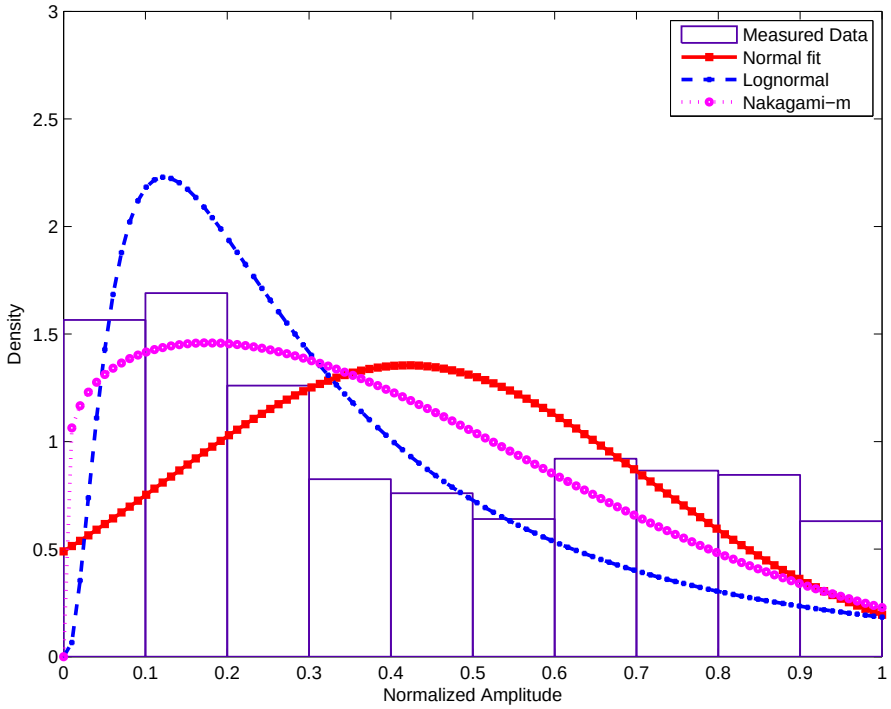

Figure 254: PDF of received power at 820 MHz: right wrist to off-body; Walking; 3 m separation; 180° orientation

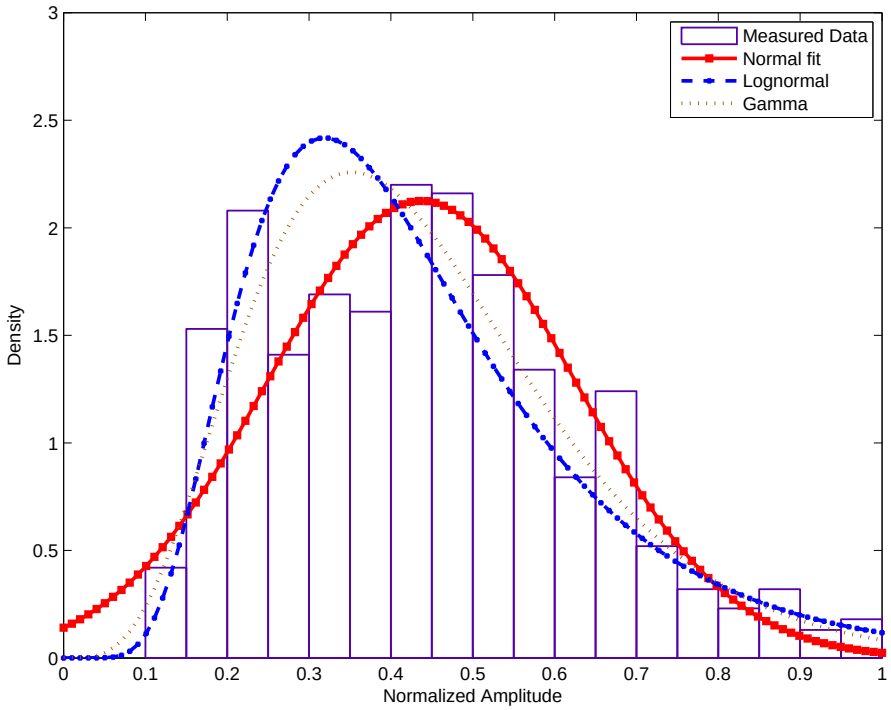

Figure 255: PDF of received power at 820 MHz: right wrist to off-body; Walking; 3 m separation; 270° orientation

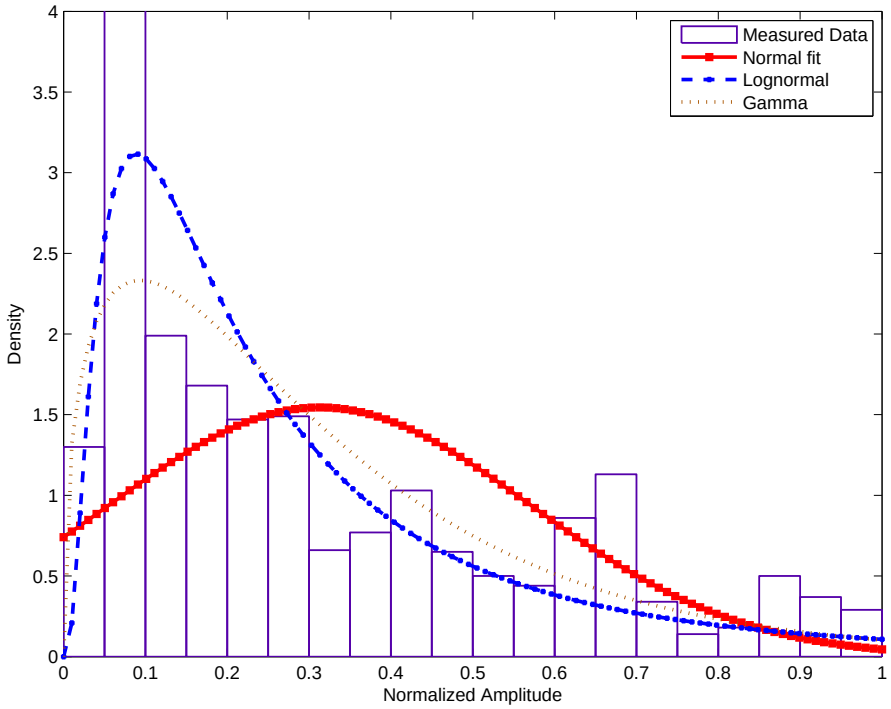

Figure 256: PDF of received power at 820 MHz: right wrist to off-body; Walking; 3 m separation; 90° orientation

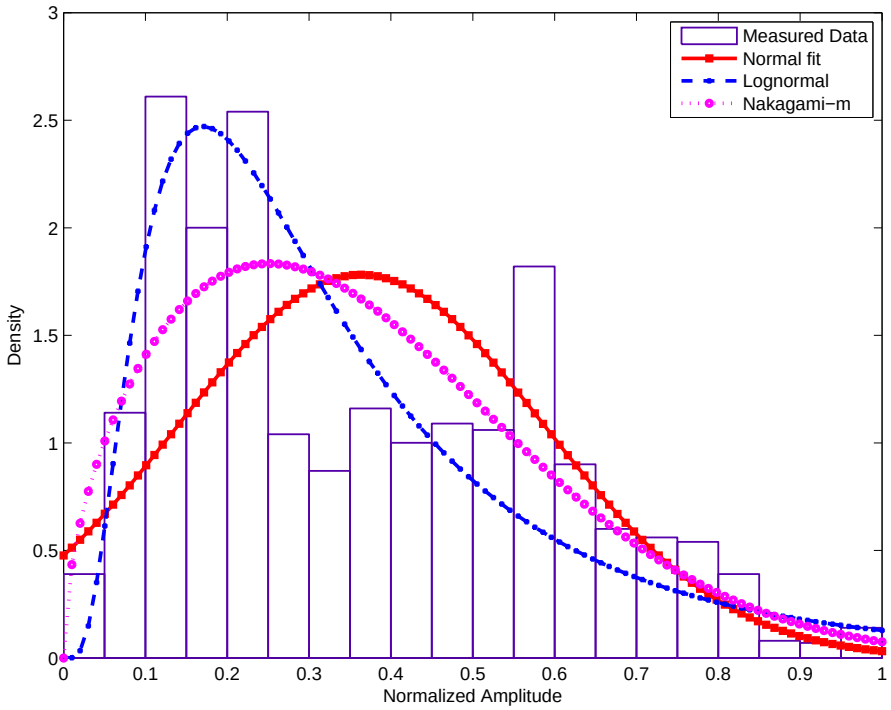

Figure 257: PDF of received power at 820 MHz: right wrist to off-body; Walking; 4 m separation; 0° orientation

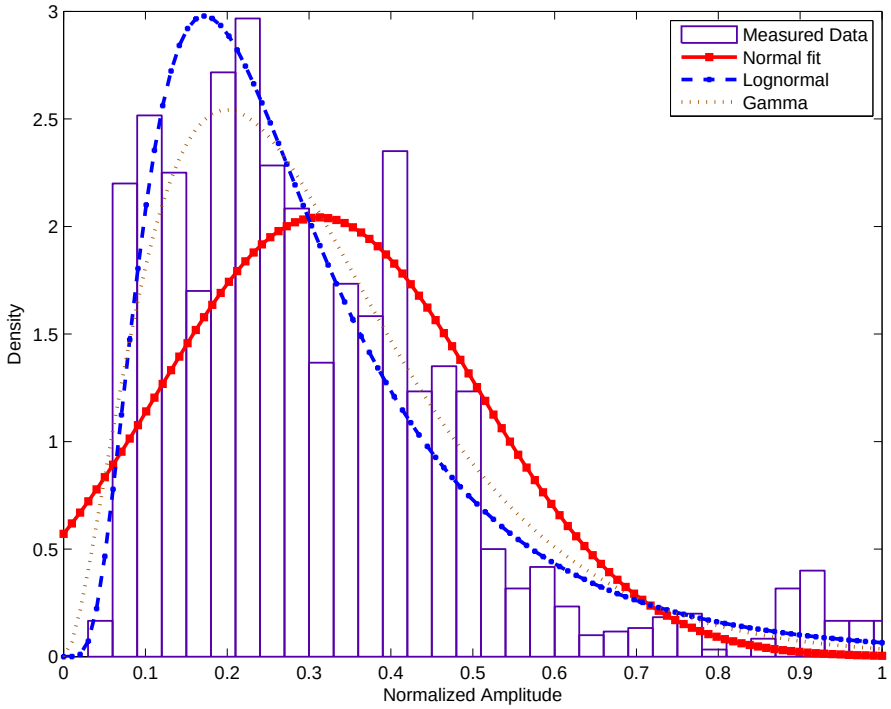

Figure 258: PDF of received power at 820 MHz: right wrist to off-body; Walking; 4 m separation; 180° orientation

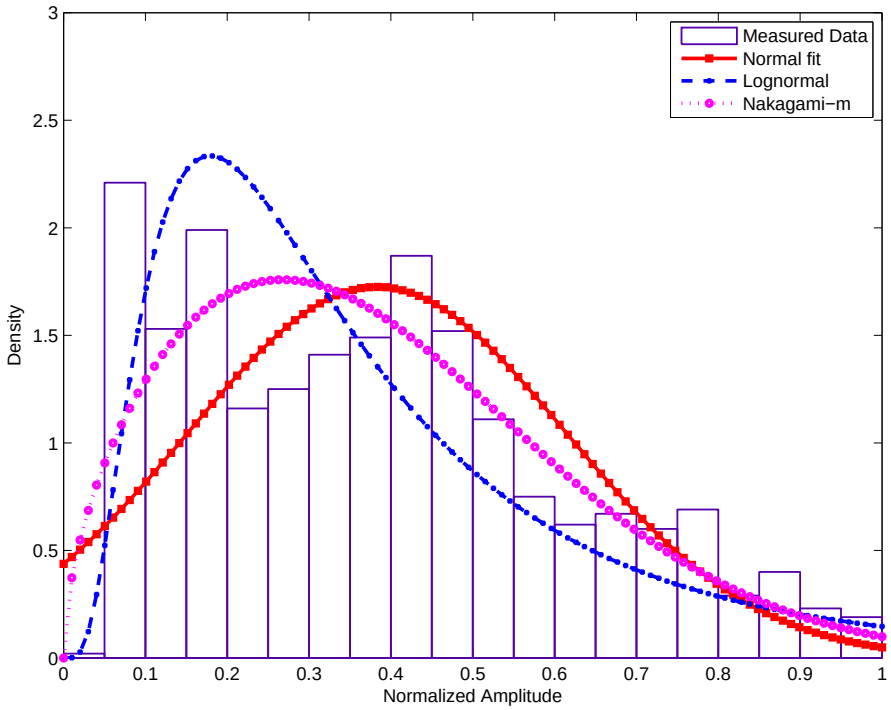

Figure 259: PDF of received power at 820 MHz: right wrist to off-body; Walking; 4 m separation; 270° orientation

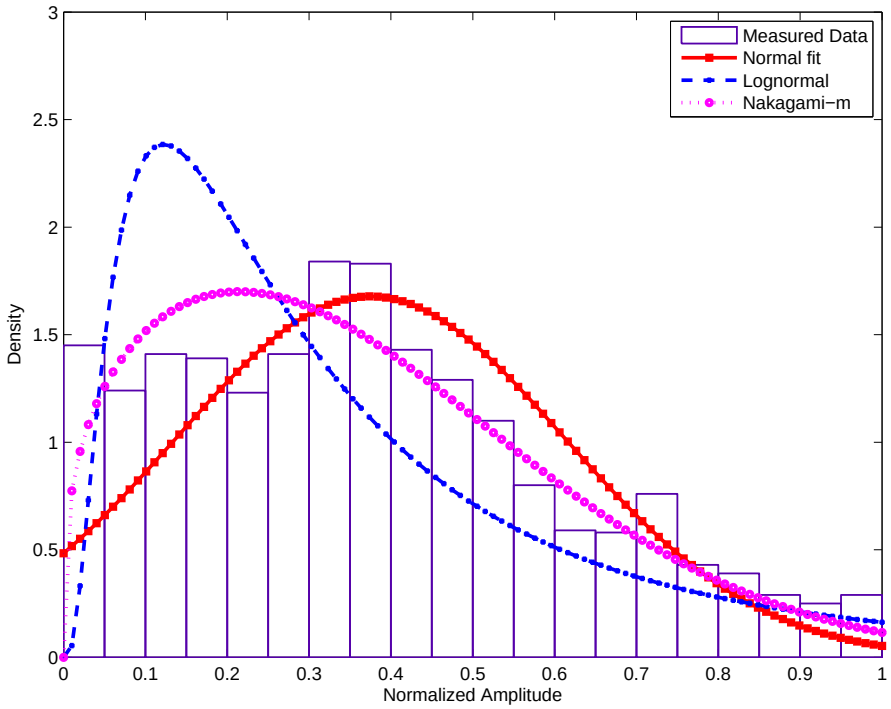

Figure 260: PDF of received power at 820 MHz: right wrist to off-body; Walking; 4 m separation; 90° orientation

A.3.2 PDFs at 2.36 GHz

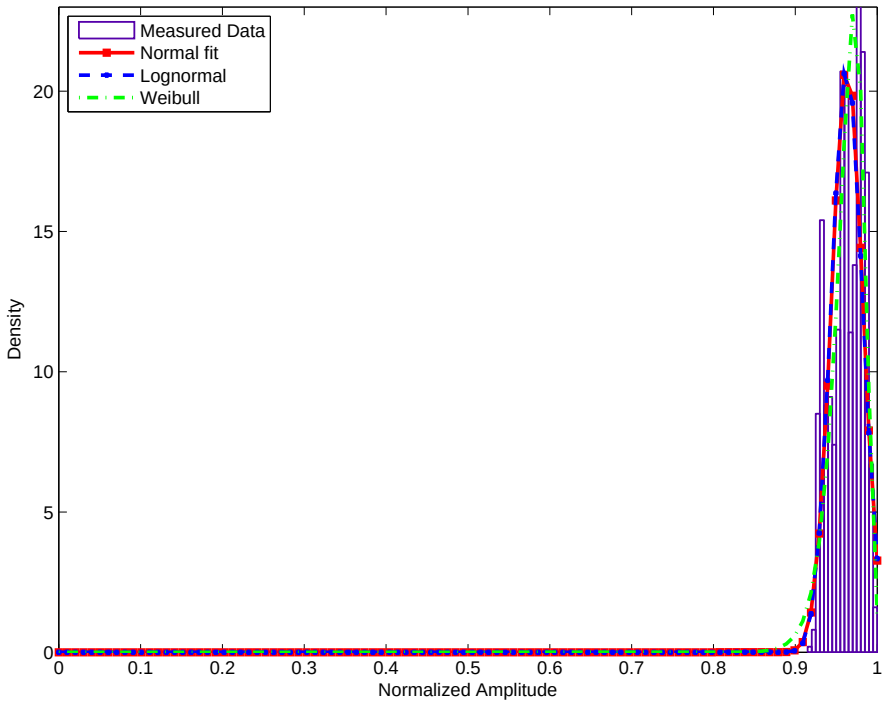

Figure 261: PDF of received power at 2360 MHz: chest to off-body; Standing; 1 m separation; 0° orientation

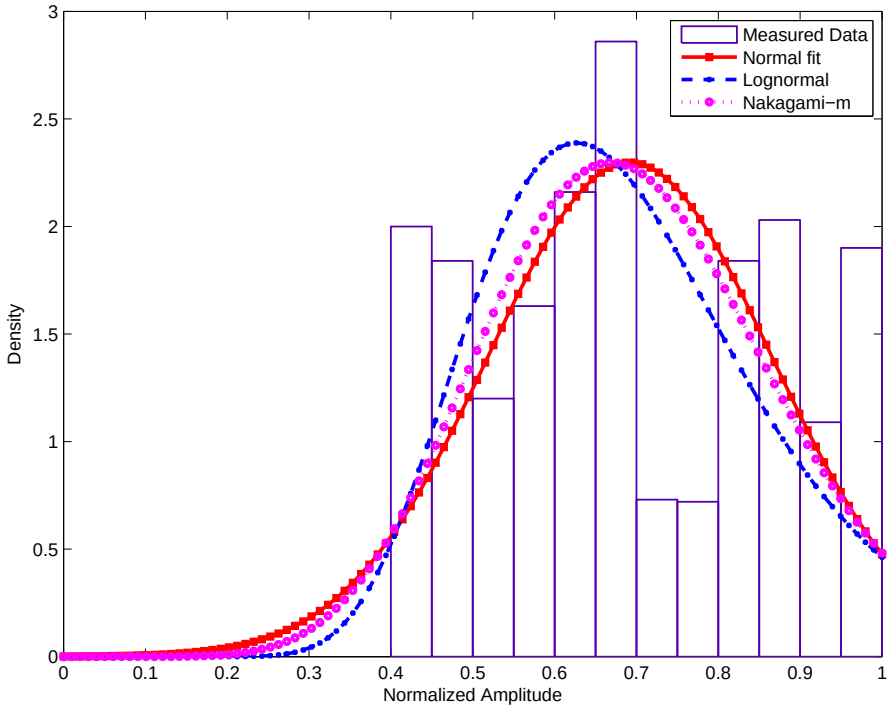

Figure 262: PDF of received power at 2360 MHz: chest to off-body; Standing; 1 m separation; 180° orientation

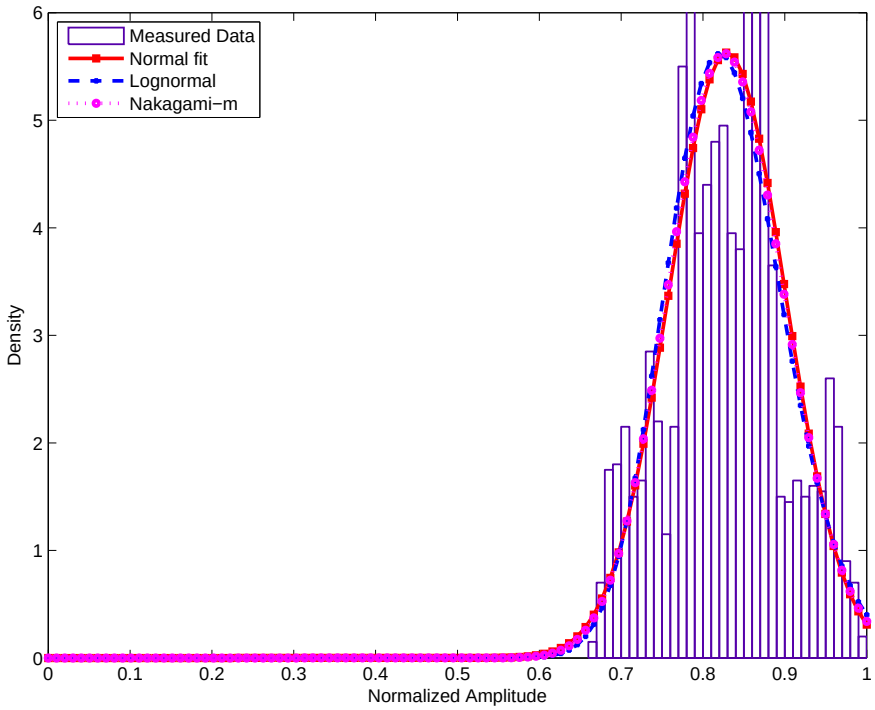

Figure 263: PDF of received power at 2360 MHz: chest to off-body; Standing; 1 m separation; 270° orientation

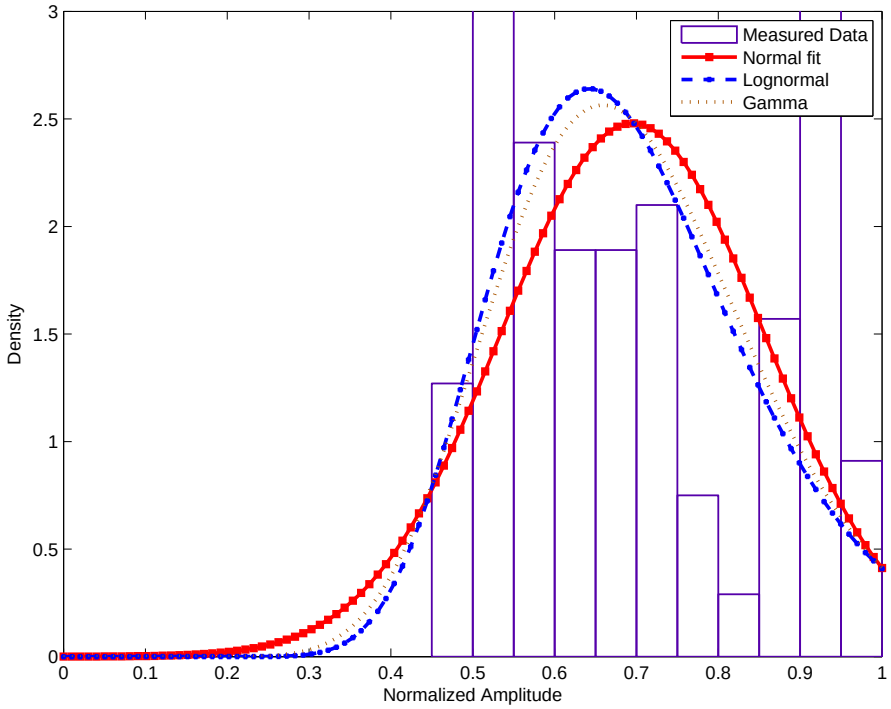

Figure 264: PDF of received power at 2360 MHz: chest to off-body; Standing; 1 m separation; 90° orientation

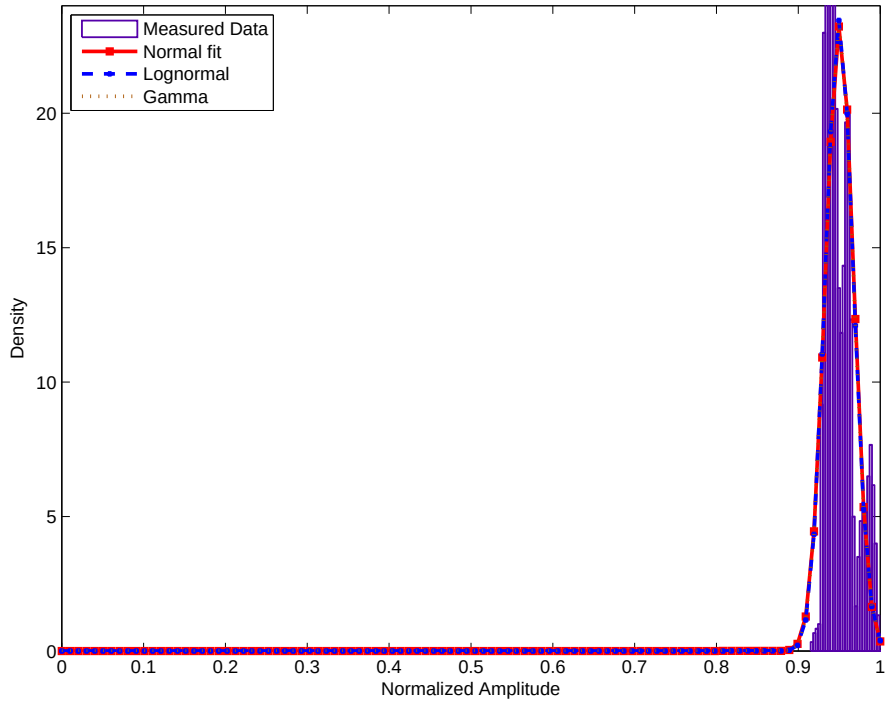

Figure 265: PDF of received power at 2360 MHz: chest to off-body; Standing; 2 m separation; 0° orientation

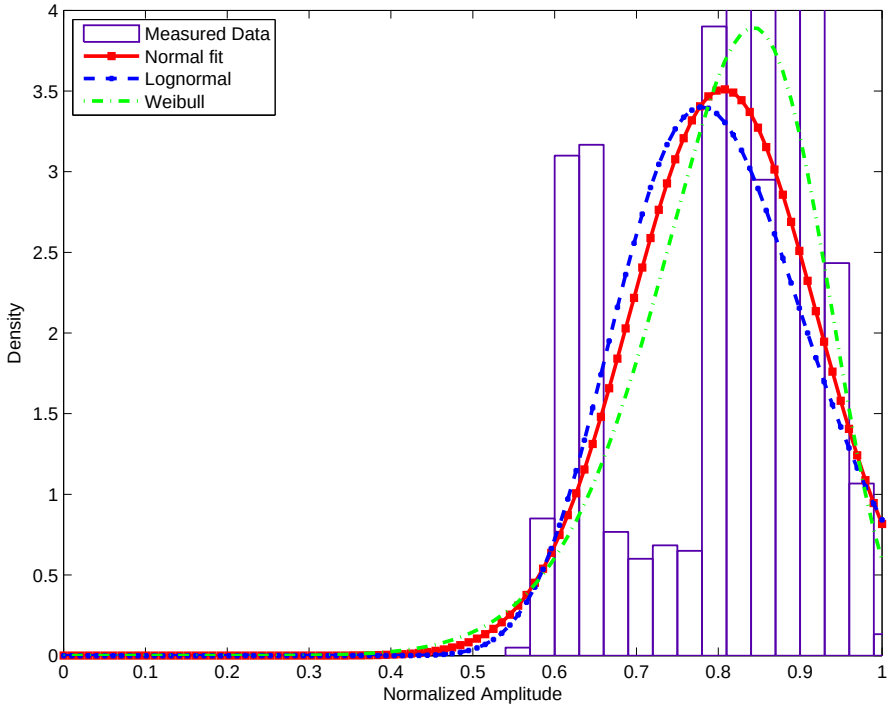

Figure 266: PDF of received power at 2360 MHz: chest to off-body; Standing; 2 m separation; 180° orientation

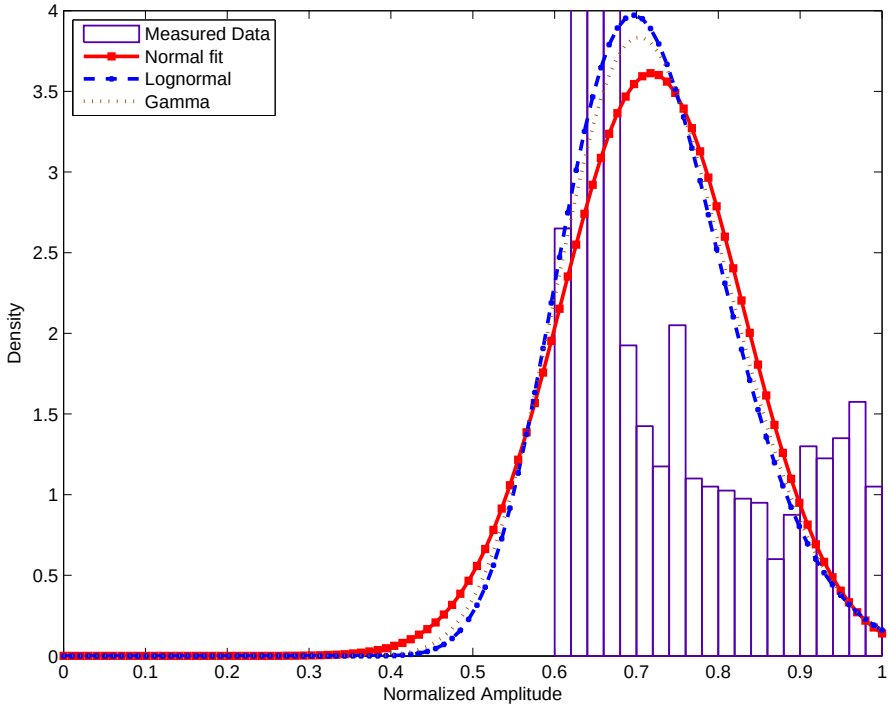

Figure 267: PDF of received power at 2360 MHz: chest to off-body; Standing; 2 m separation; 270° orientation

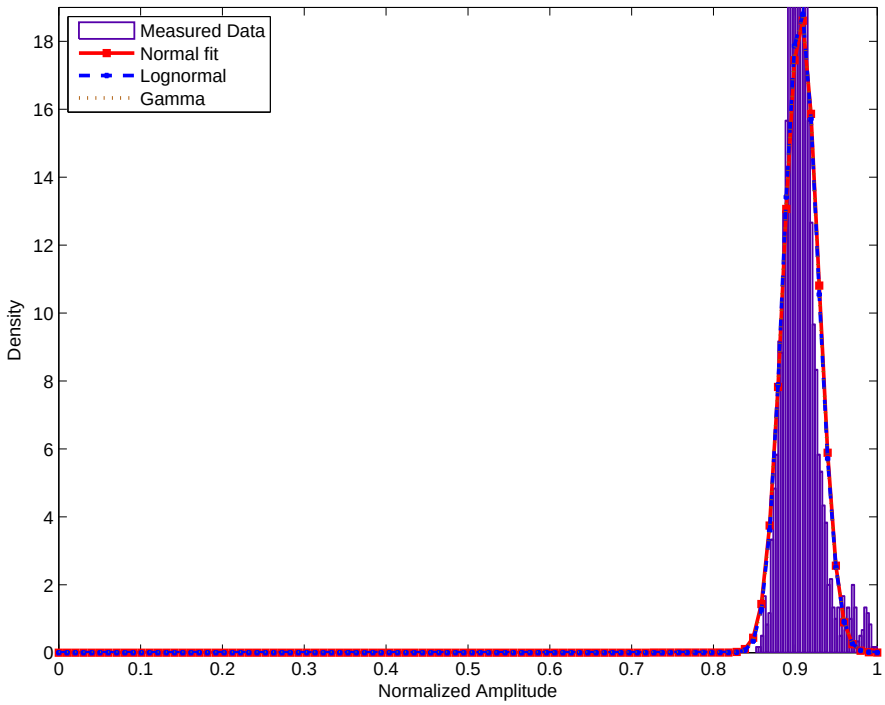

Figure 268: PDF of received power at 2360 MHz: chest to off-body; Standing; 2 m separation; 90° orientation

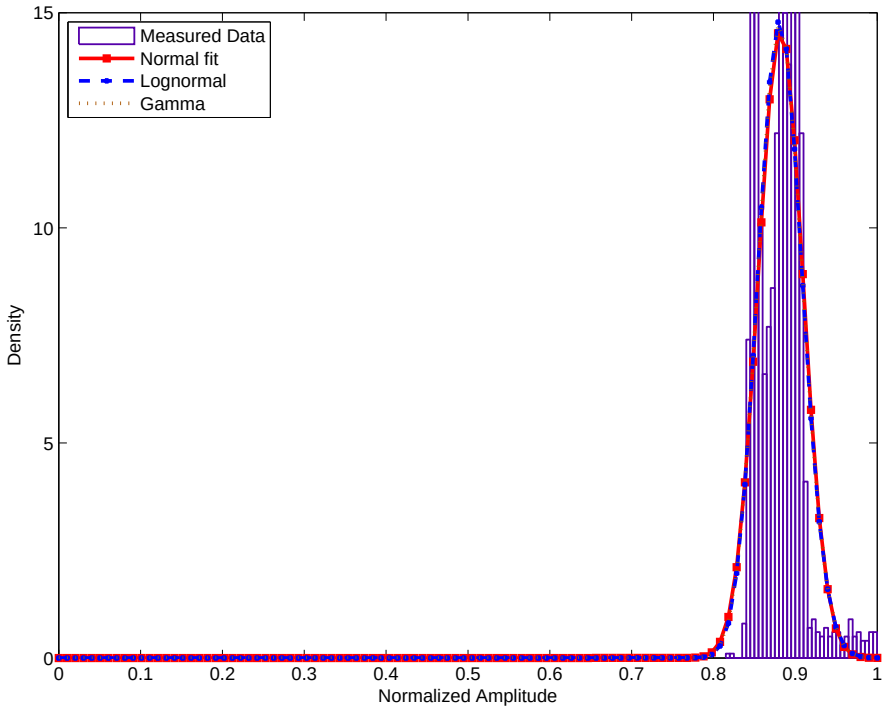

Figure 269: PDF of received power at 2360 MHz: chest to off-body; Standing; 3 m separation; 0° orientation

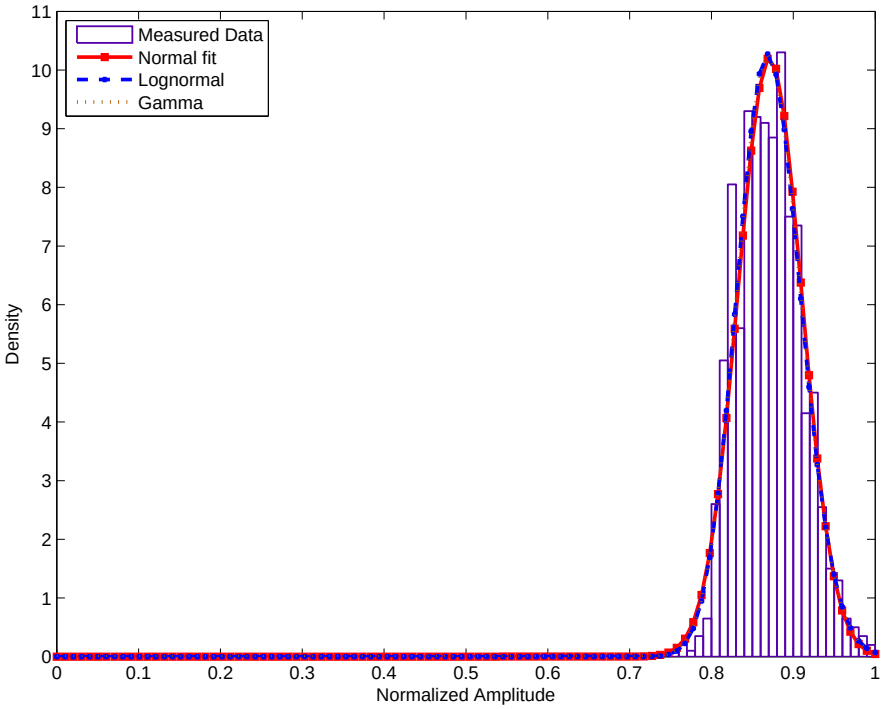

Figure 270: PDF of received power at 2360 MHz: chest to off-body; Standing; 3 m separation; 180° orientation

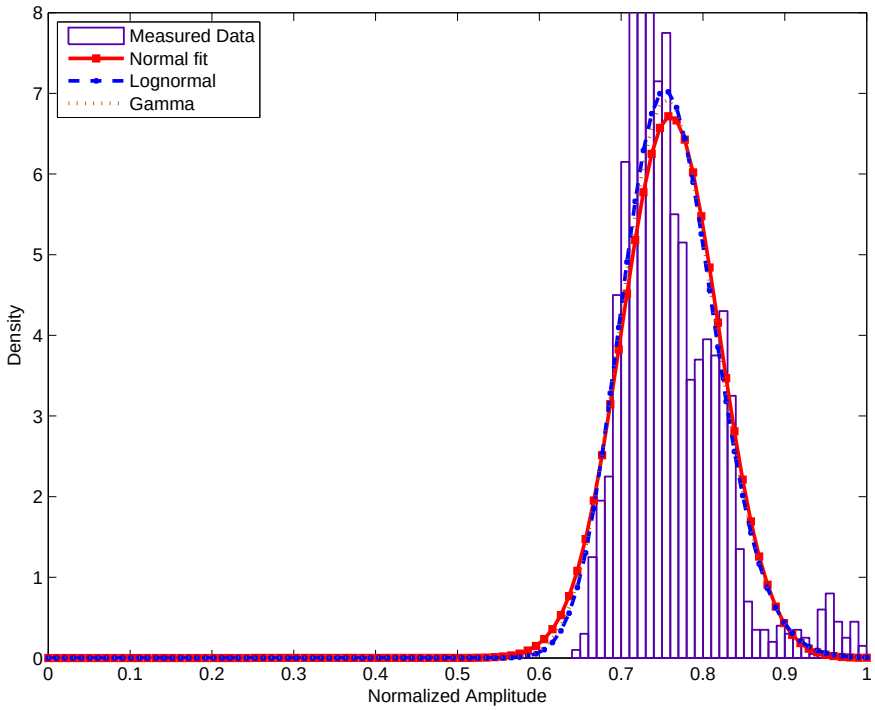

Figure 271: PDF of received power at 2360 MHz: chest to off-body; Standing; 3 m separation; 270° orientation

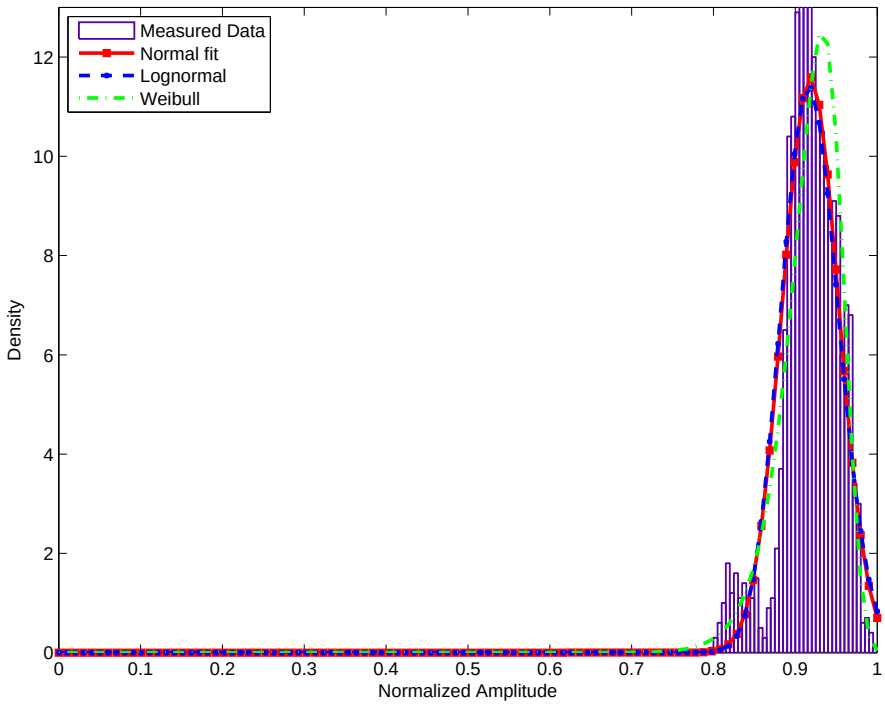

Figure 272: PDF of received power at 2360 MHz: chest to off-body; Standing; 3 m separation; 90° orientation

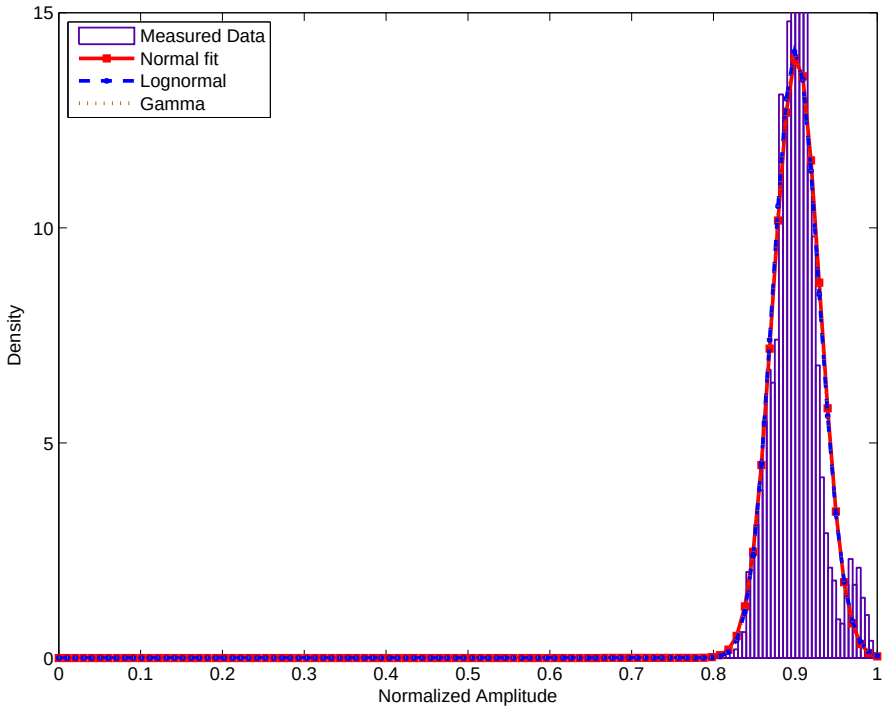

Figure 273: PDF of received power at 2360 MHz: chest to off-body; Standing; 4 m separation; 0° orientation

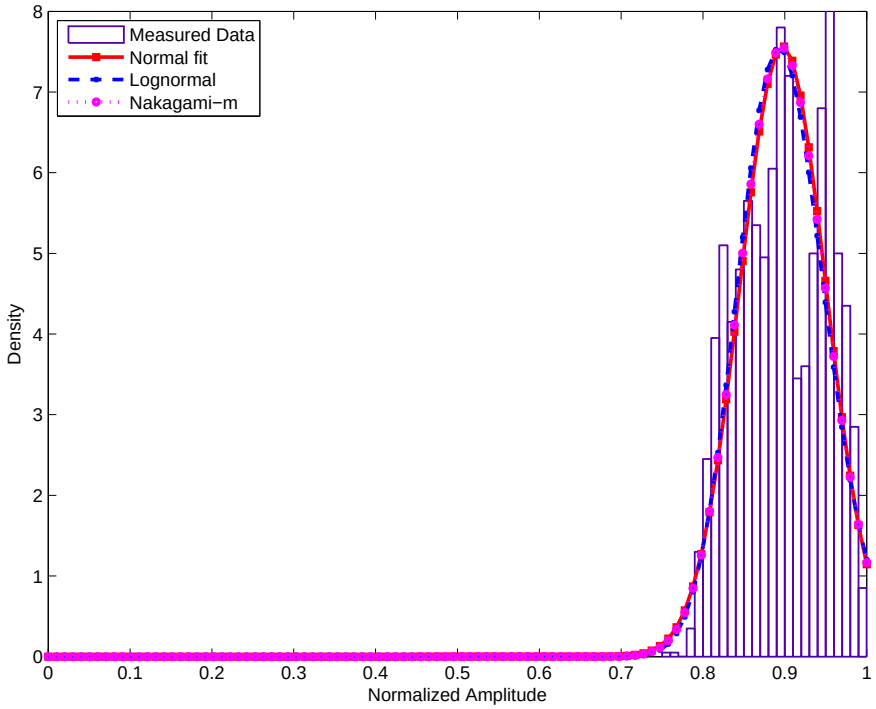

Figure 274: PDF of received power at 2360 MHz: chest to off-body; Standing; 4 m separation; 180° orientation

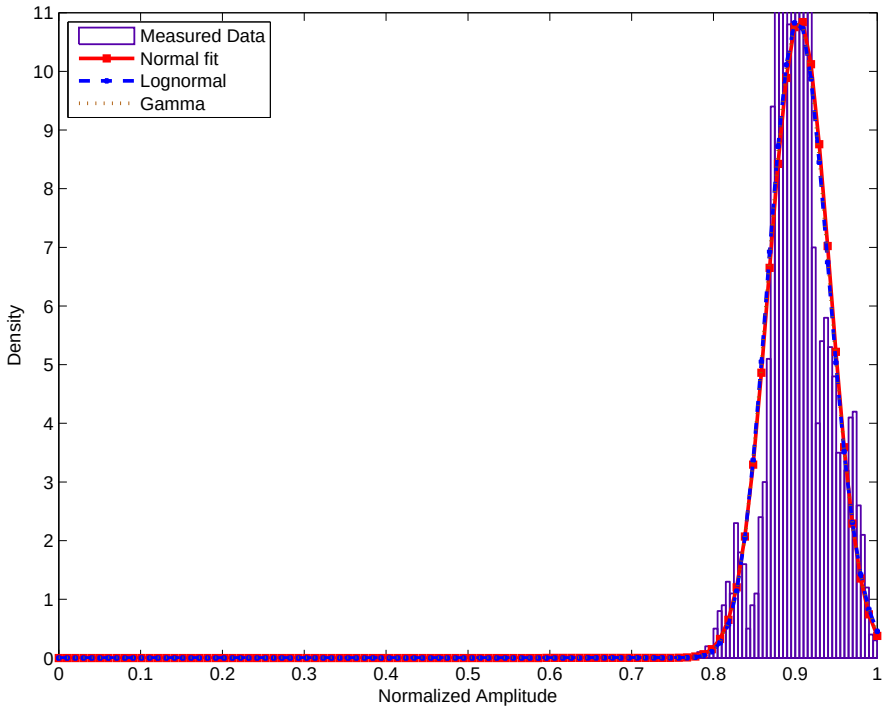

Figure 275: PDF of received power at 2360 MHz: chest to off-body; Standing; 4 m separation; 270° orientation

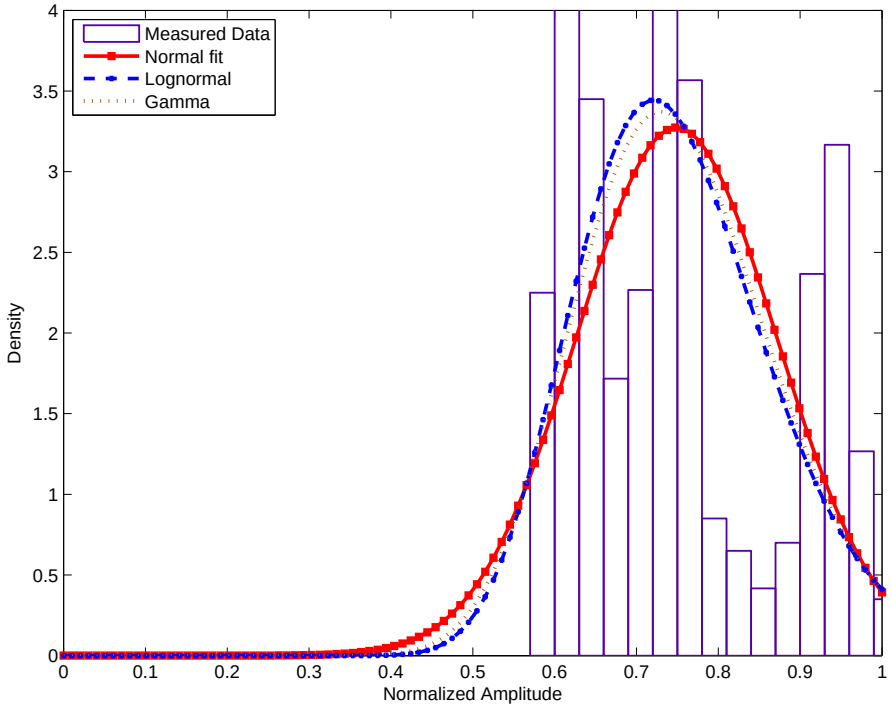

Figure 276: PDF of received power at 2360 MHz: chest to off-body; Standing; 4 m separation; 90° orientation

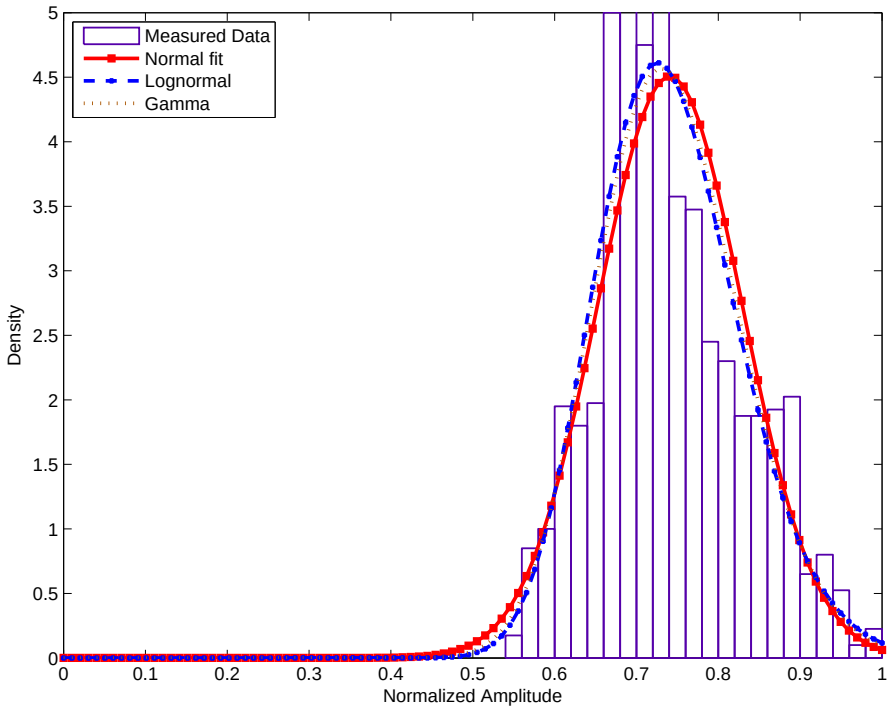

Figure 277: PDF of received power at 2360 MHz: chest to off-body; Walking; 1 m separation; 0° orientation

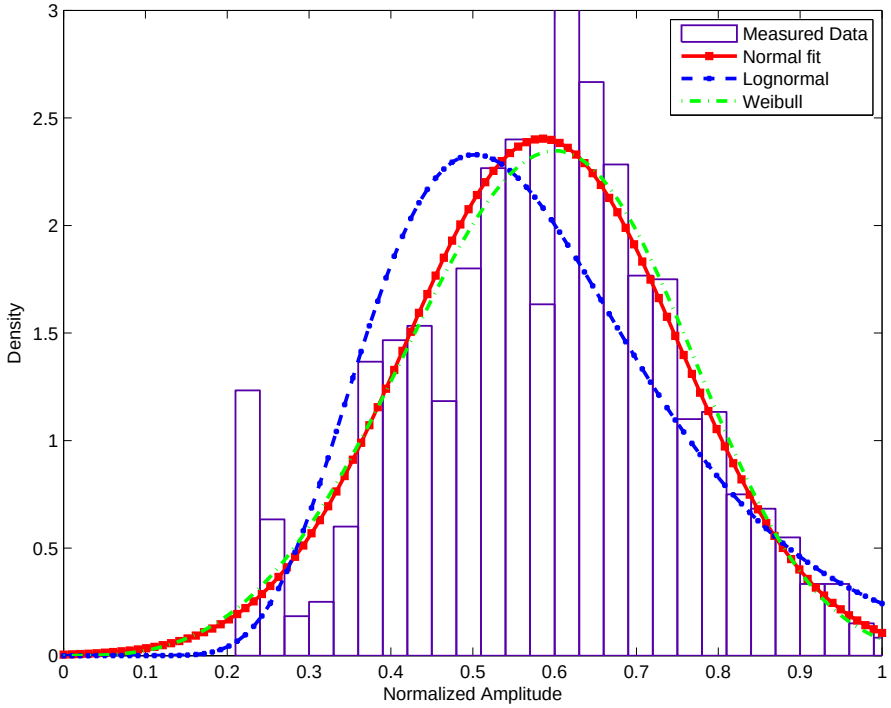

Figure 278: PDF of received power at 2360 MHz: chest to off-body; Walking; 1 m separation; 180° orientation

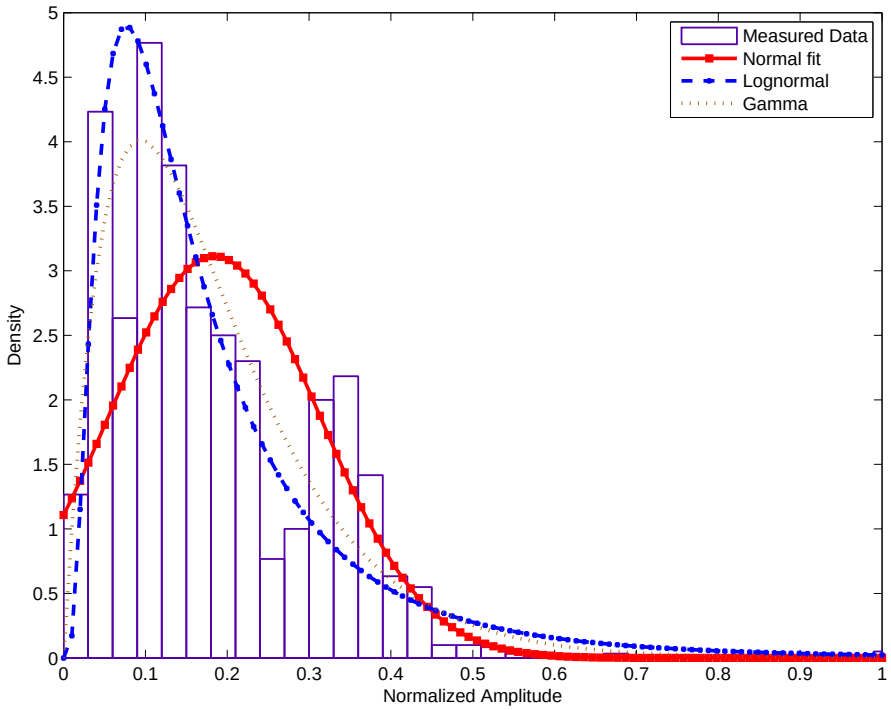

Figure 279: PDF of received power at 2360 MHz: chest to off-body; Walking; 1 m separation; 270° orientation

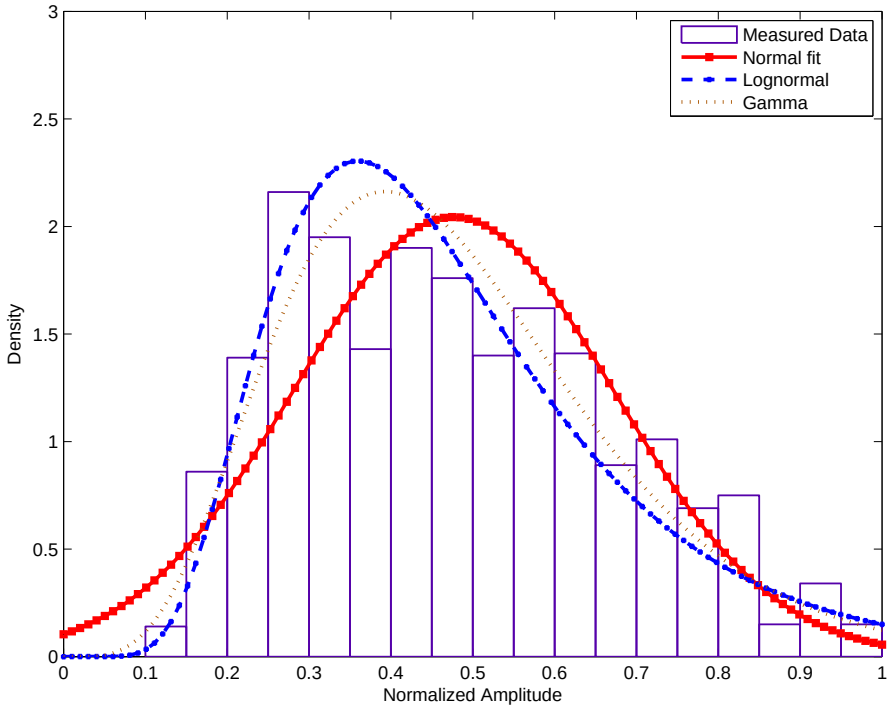

Figure 280: PDF of received power at 2360 MHz: chest to off-body; Walking; 1 m separation; 90° orientation

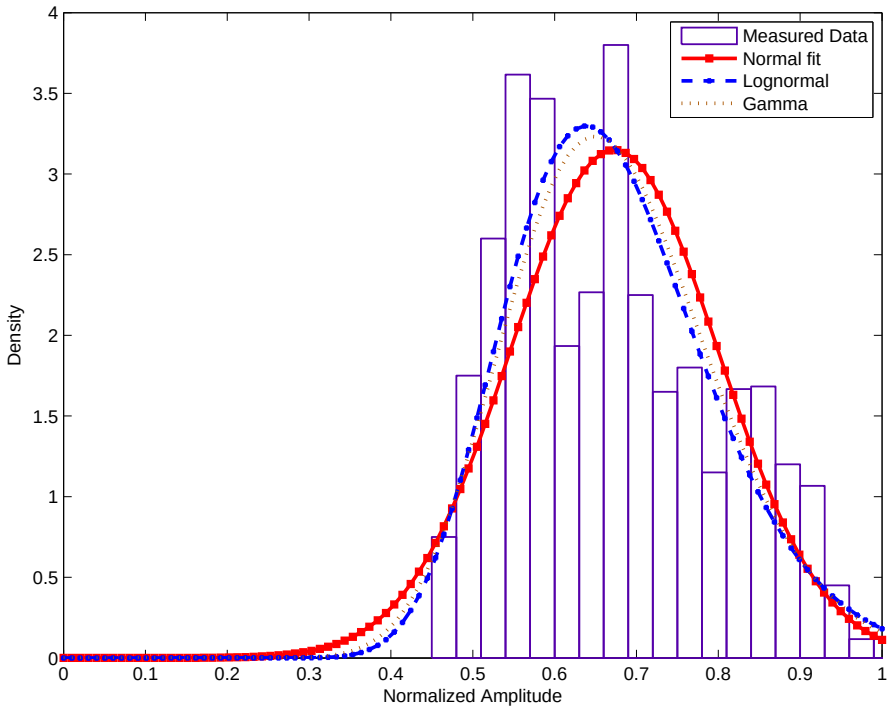

Figure 281: PDF of received power at 2360 MHz: chest to off-body; Walking; 2 m separation; 0° orientation

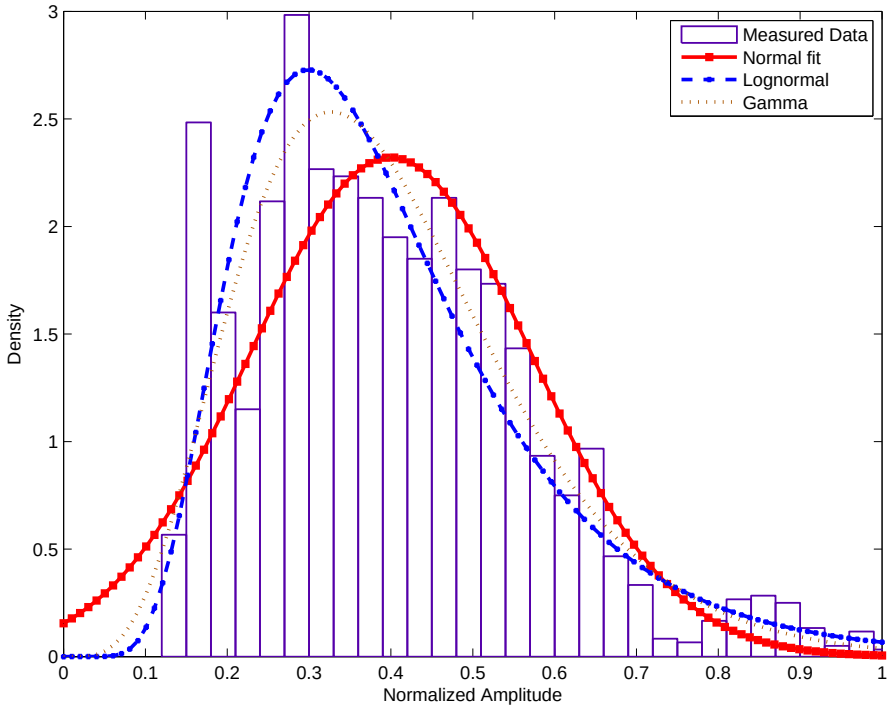

Figure 282: PDF of received power at 2360 MHz: chest to off-body; Walking; 2 m separation; 180° orientation

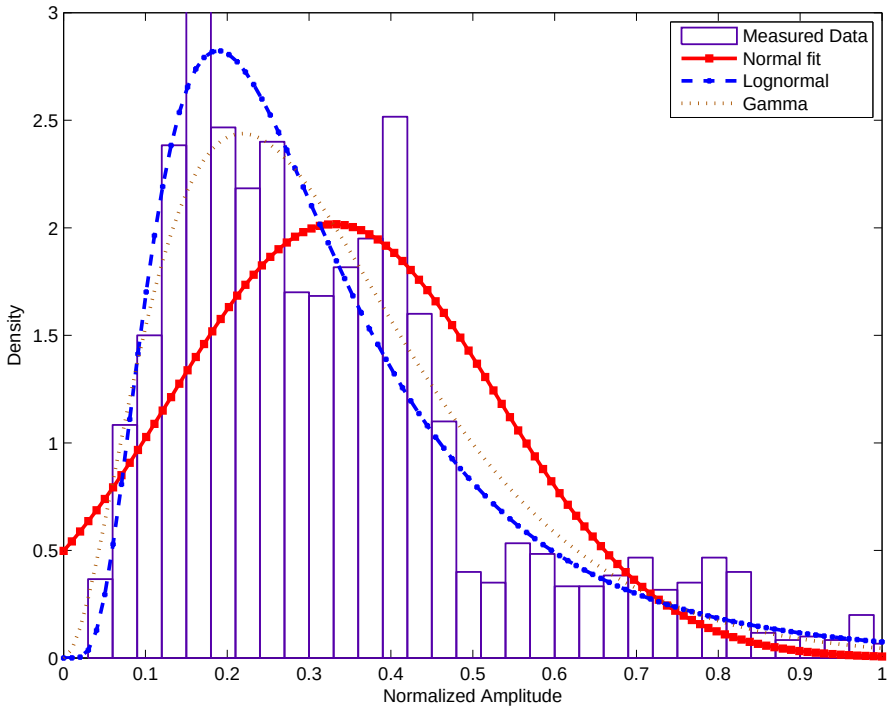

Figure 283: PDF of received power at 2360 MHz: chest to off-body; Walking; 2 m separation; 270° orientation

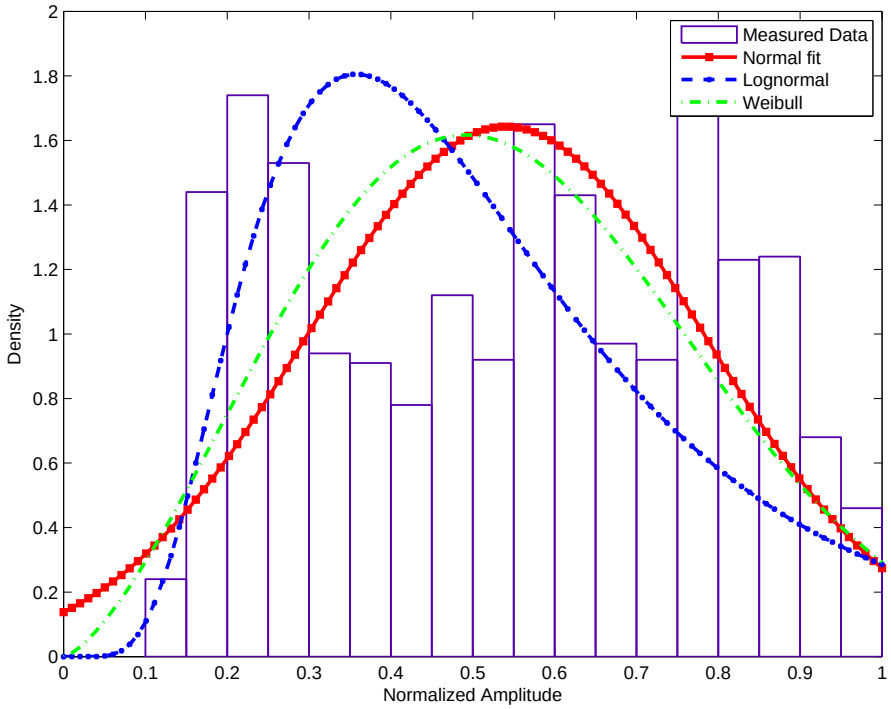

Figure 284: PDF of received power at 2360 MHz: chest to off-body; Walking; 2 m separation; 90° orientation

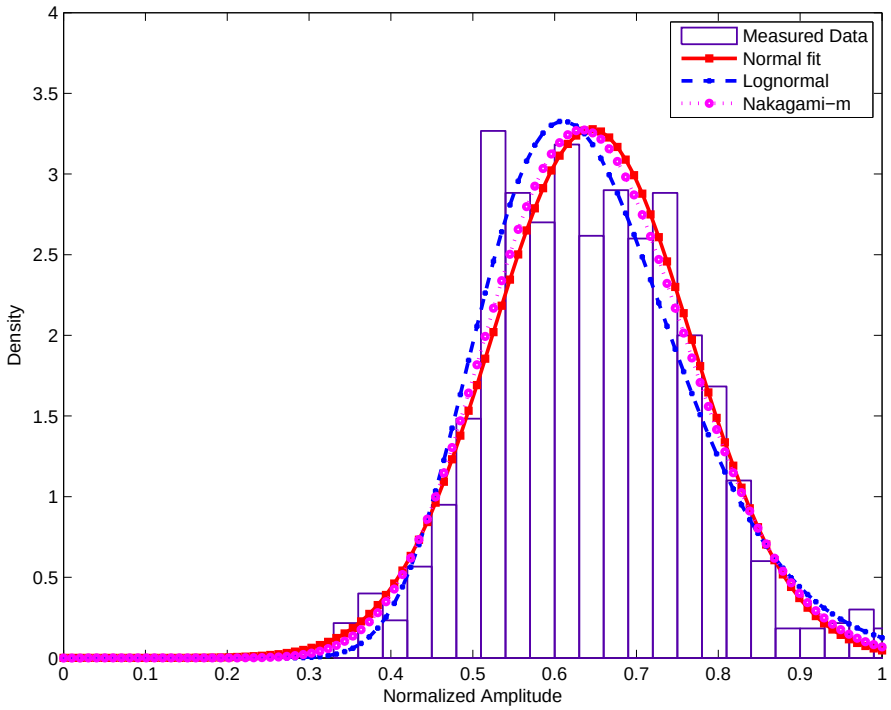

Figure 285: PDF of received power at 2360 MHz: chest to off-body; Walking; 3 m separation; 0° orientation

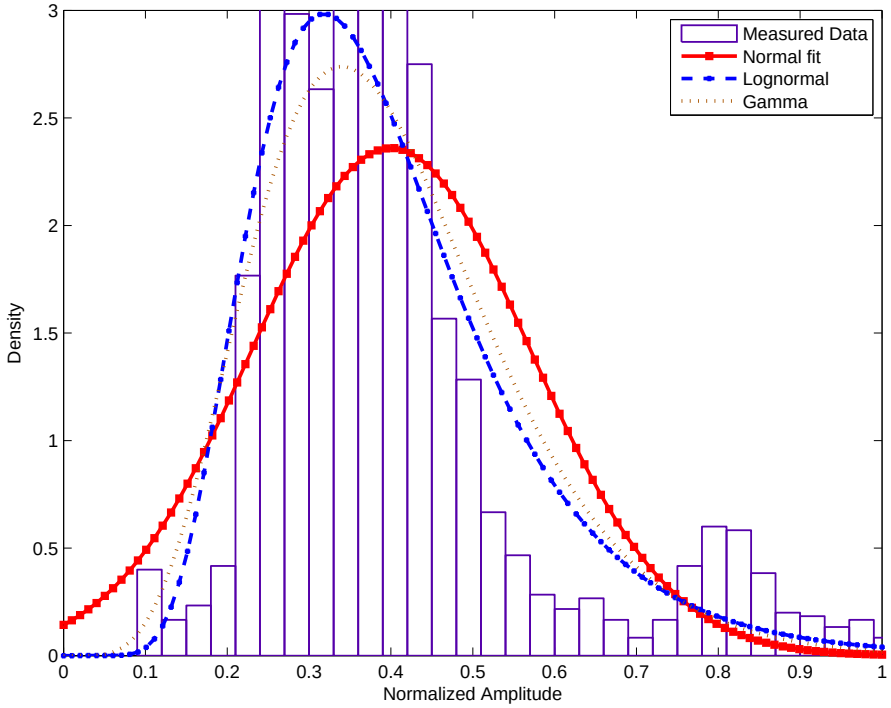

Figure 286: PDF of received power at 2360 MHz: chest to off-body; Walking; 3 m separation; 180° orientation

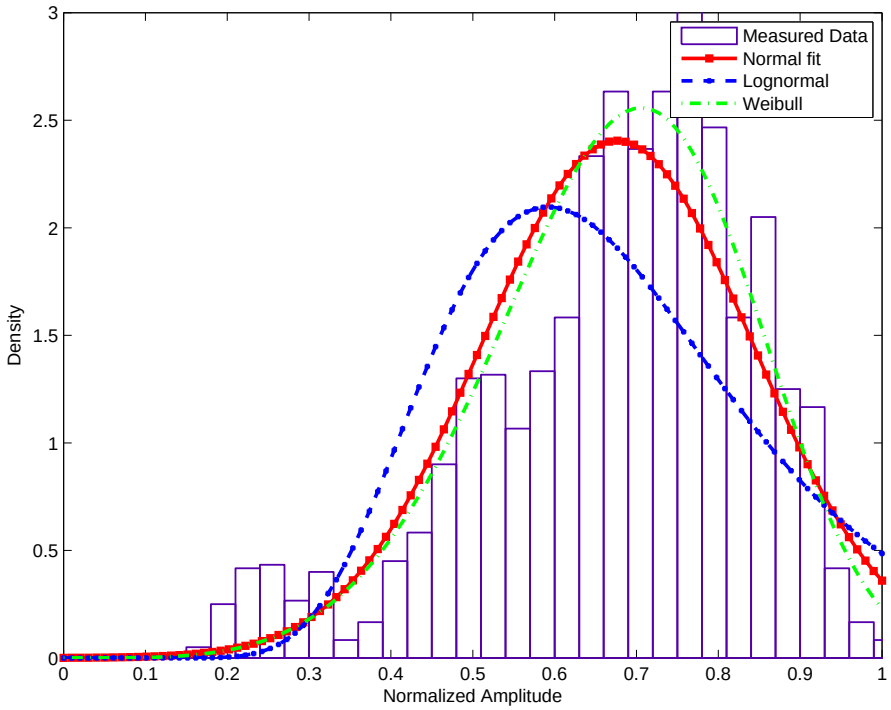

Figure 287: PDF of received power at 2360 MHz: chest to off-body; Walking; 3 m separation; 270° orientation

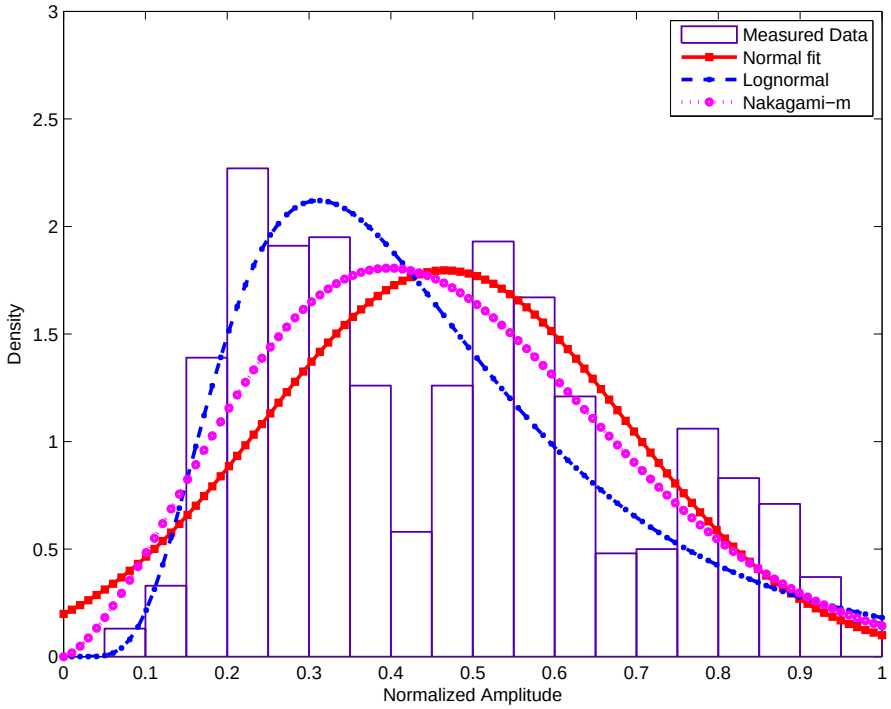

Figure 288: PDF of received power at 2360 MHz: chest to off-body; Walking; 3 m separation; 90° orientation

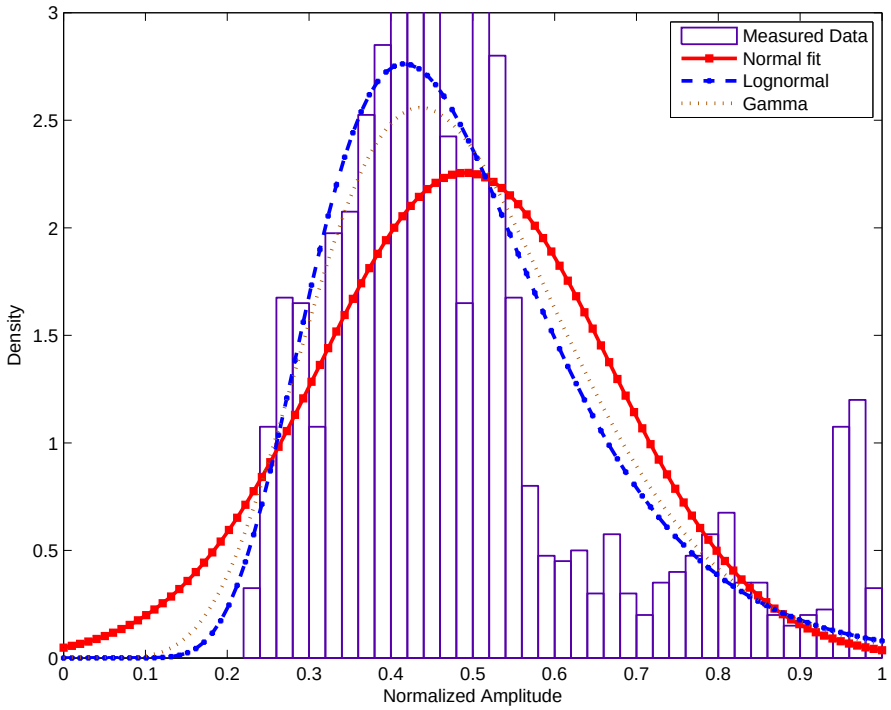

Figure 289: PDF of received power at 2360 MHz: chest to off-body; Walking; 4 m separation; 0° orientation

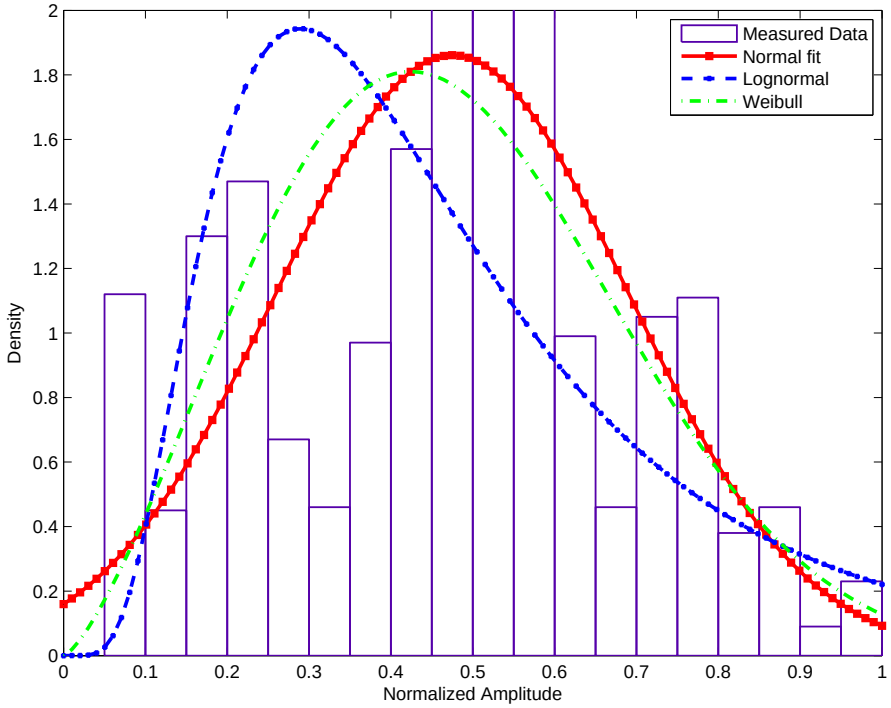

Figure 290: PDF of received power at 2360 MHz: chest to off-body; Walking; 4 m separation; 180° orientation

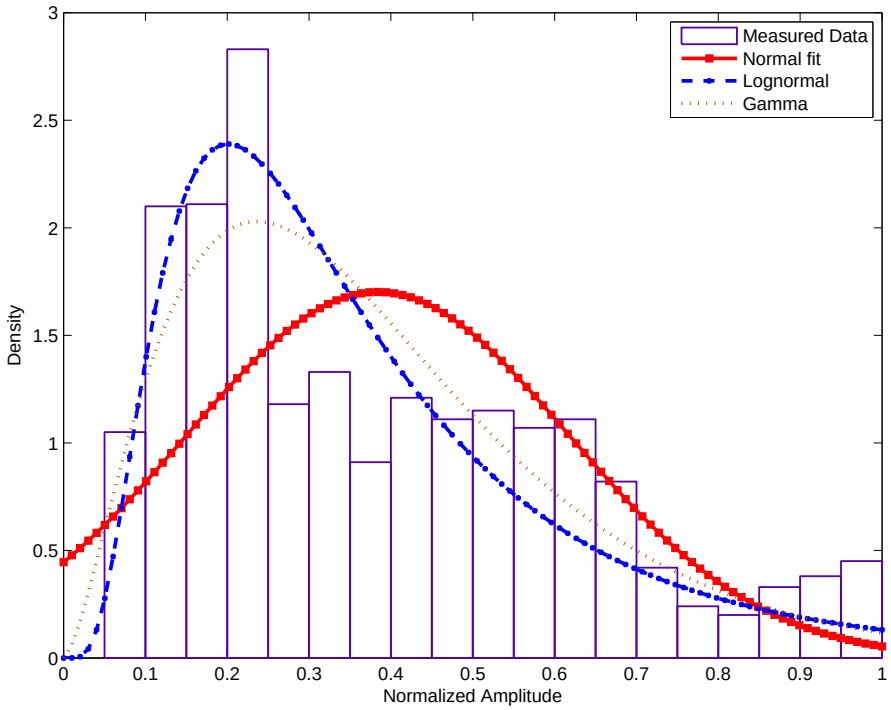

Figure 291: PDF of received power at 2360 MHz: chest to off-body; Walking; 4 m separation; 270° orientation

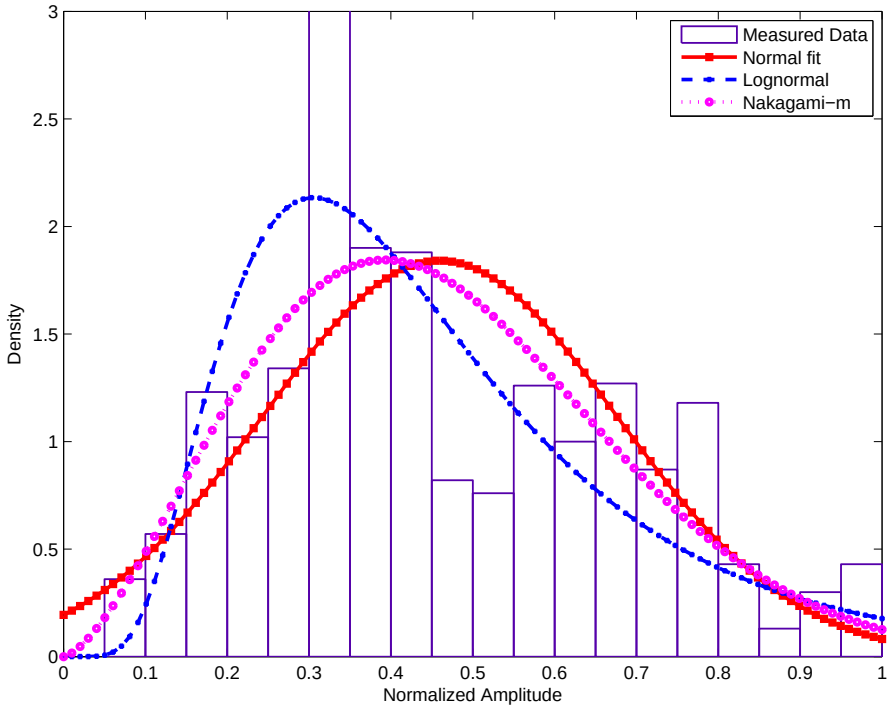

Figure 292: PDF of received power at 2360 MHz: chest to off-body; Walking; 4 m separation; 90° orientation

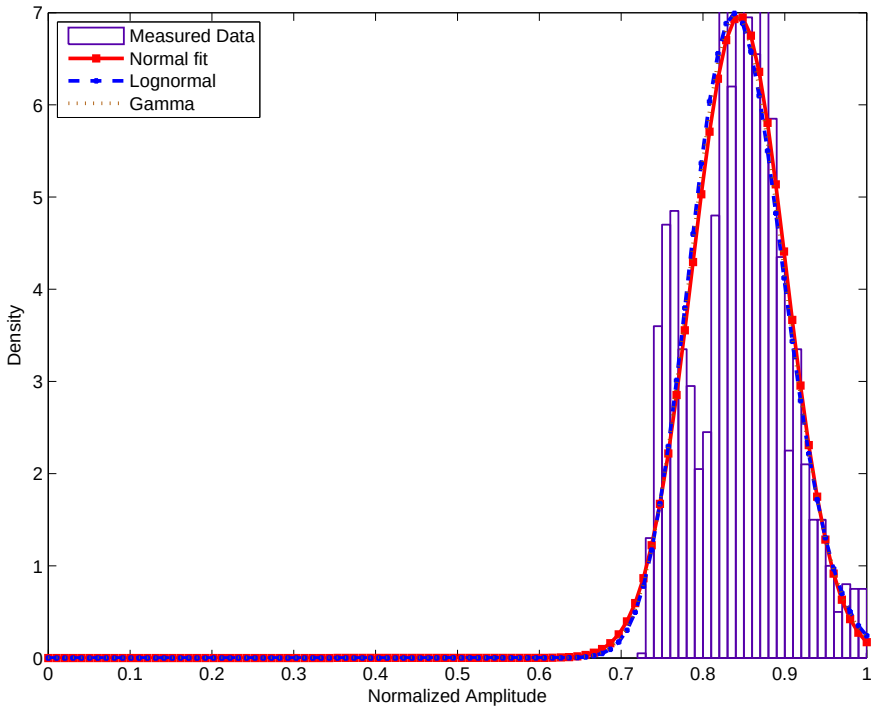

Figure 293: PDF of received power at 2360 MHz: right wrist to off-body; Standing; 1 m separation; 0° orientation

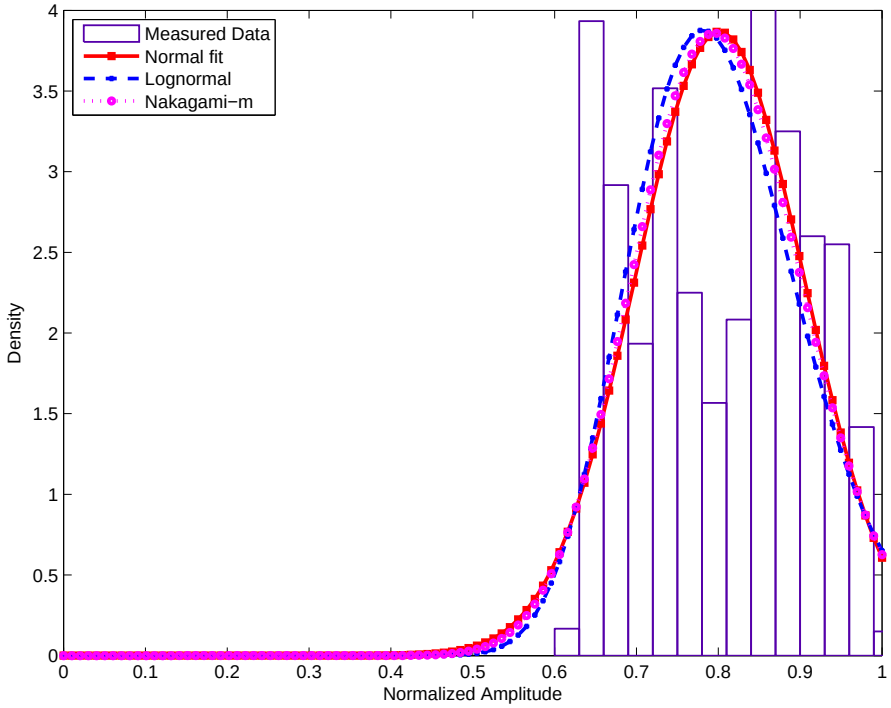

Figure 294: PDF of received power at 2360 MHz: right wrist to off-body; Standing; 1 m separation; 180° orientation

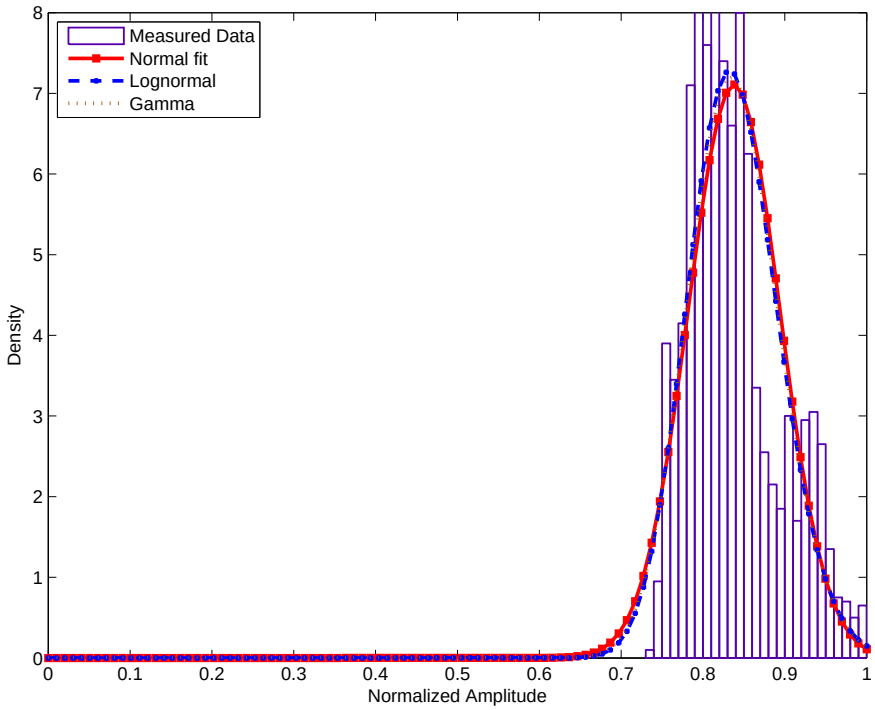

Figure 295: PDF of received power at 2360 MHz: right wrist to off-body; Standing; 1 m separation; 270° orientation

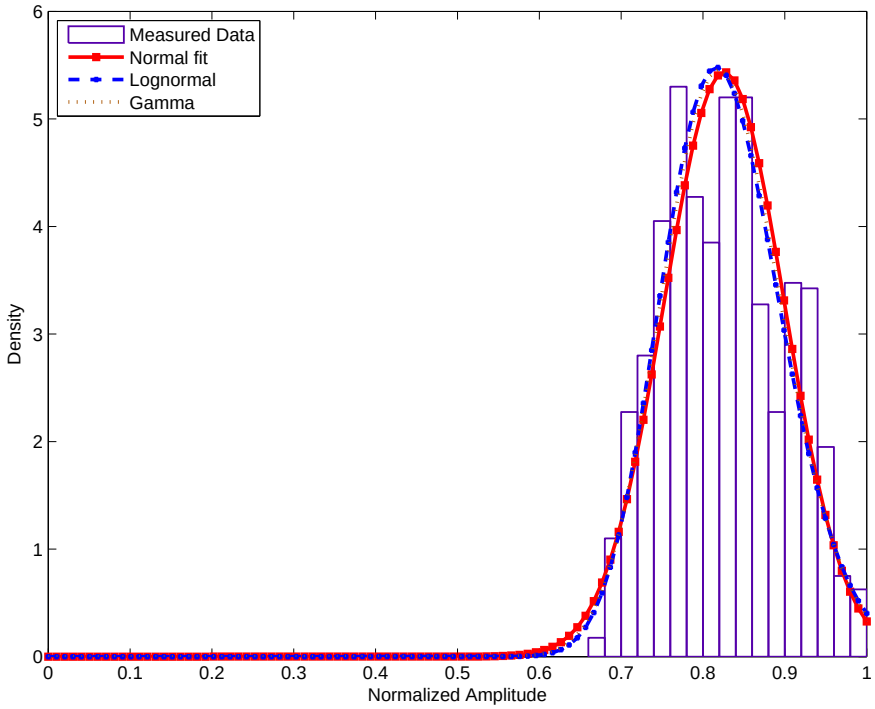

Figure 296: PDF of received power at 2360 MHz: right wrist to off-body; Standing; 1 m separation; 90° orientation

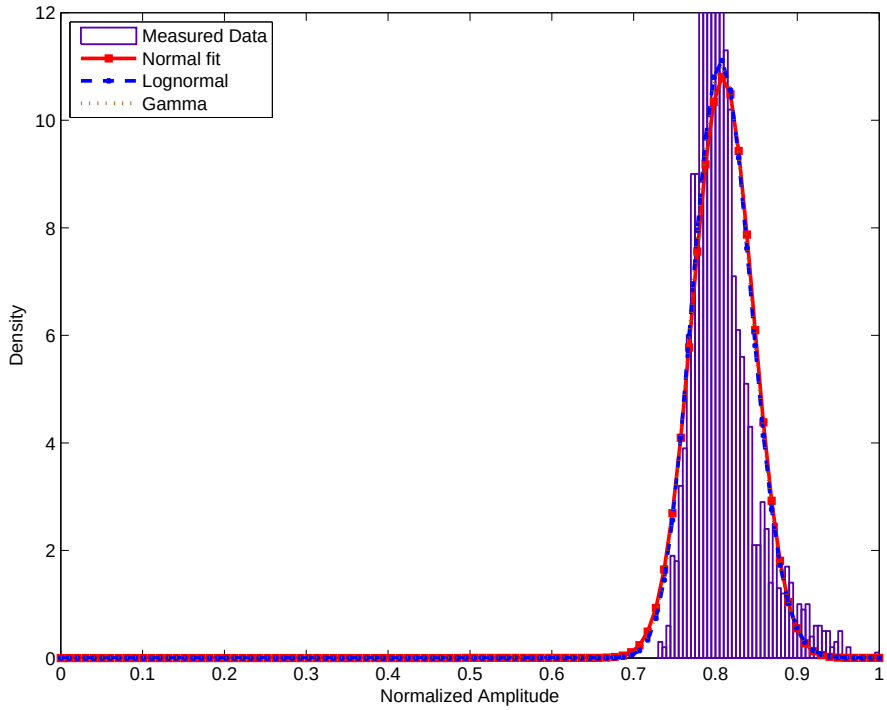

Figure 297: PDF of received power at 2360 MHz: right wrist to off-body; Standing; 2 m separation; 0° orientation

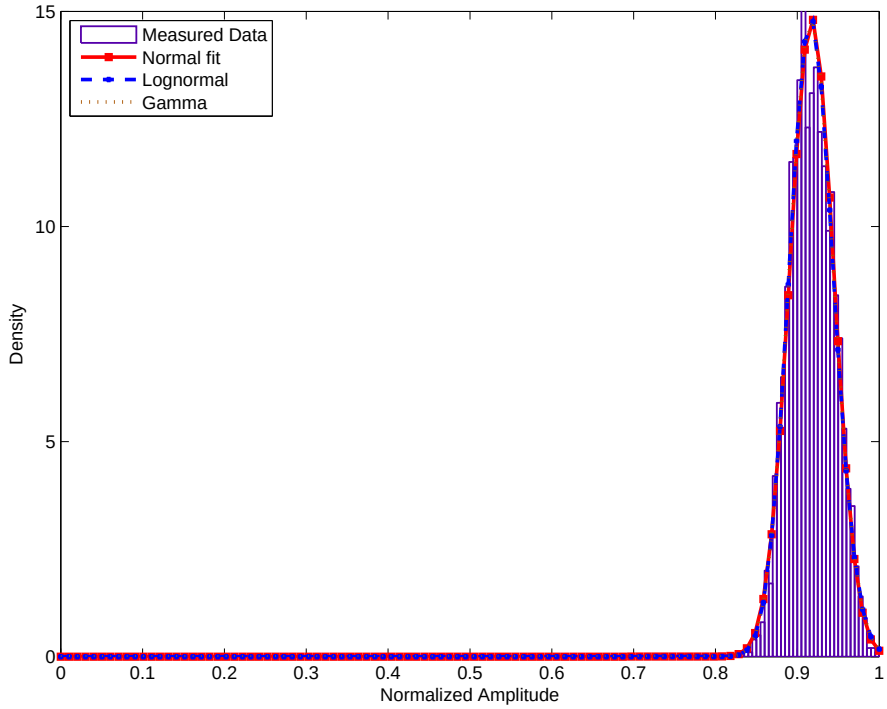

Figure 298: PDF of received power at 2360 MHz: right wrist to off-body; Standing; 2 m separation; 180° orientation

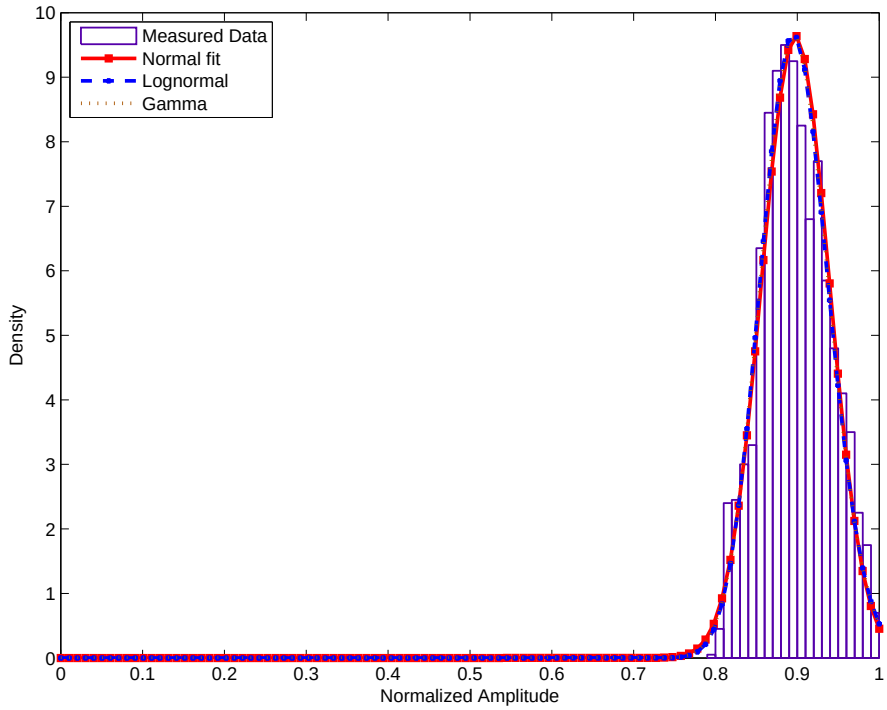

Figure 299: PDF of received power at 2360 MHz: right wrist to off-body; Standing; 2 m separation; 270° orientation

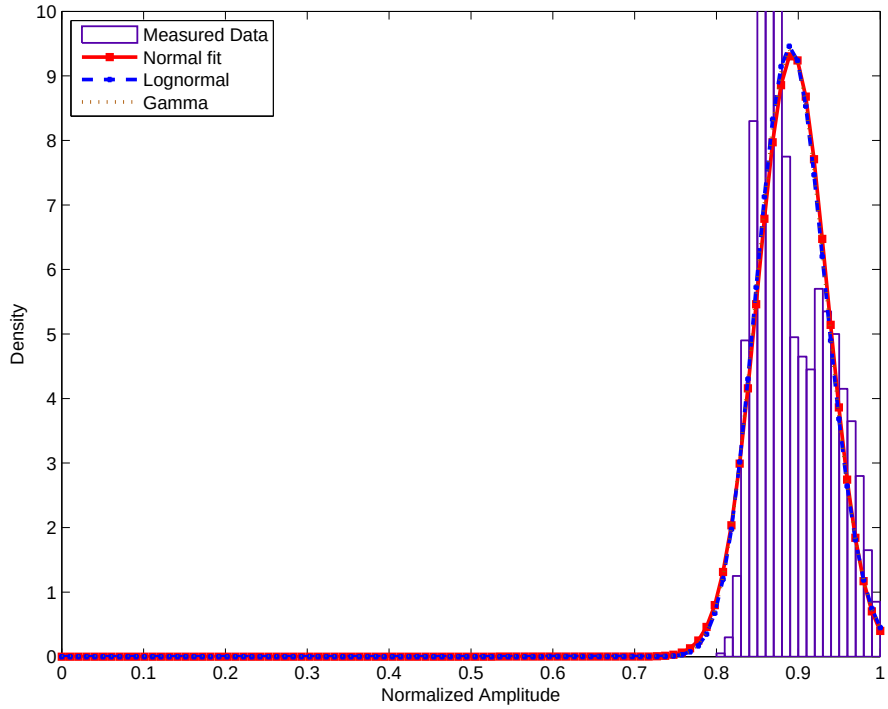

Figure 300: PDF of received power at 2360 MHz: right wrist to off-body; Standing; 2 m separation; 90° orientation

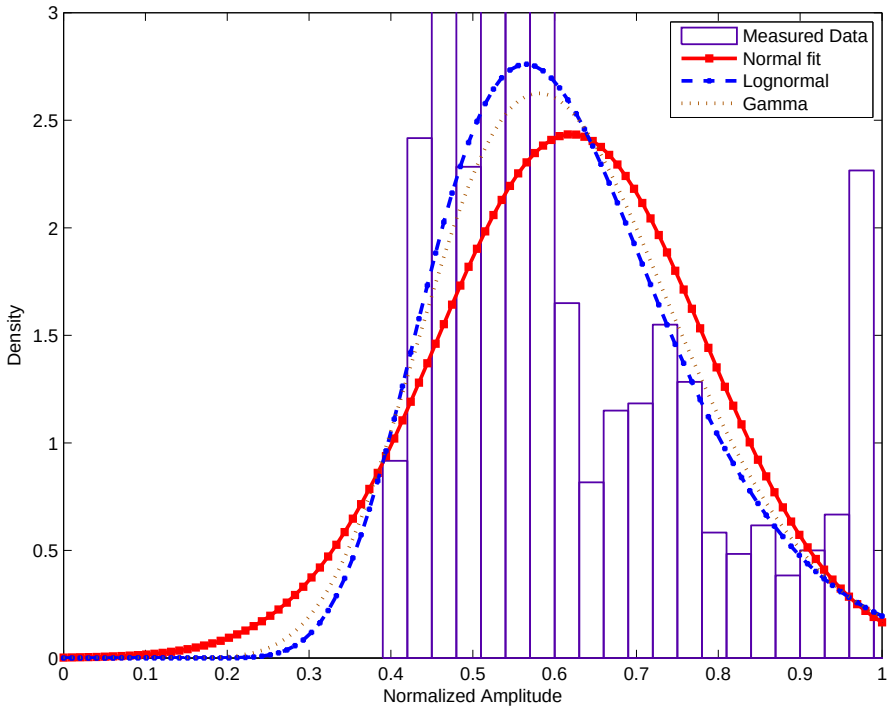

Figure 301: PDF of received power at 2360 MHz: right wrist to off-body; Standing; 3 m separation; 0° orientation

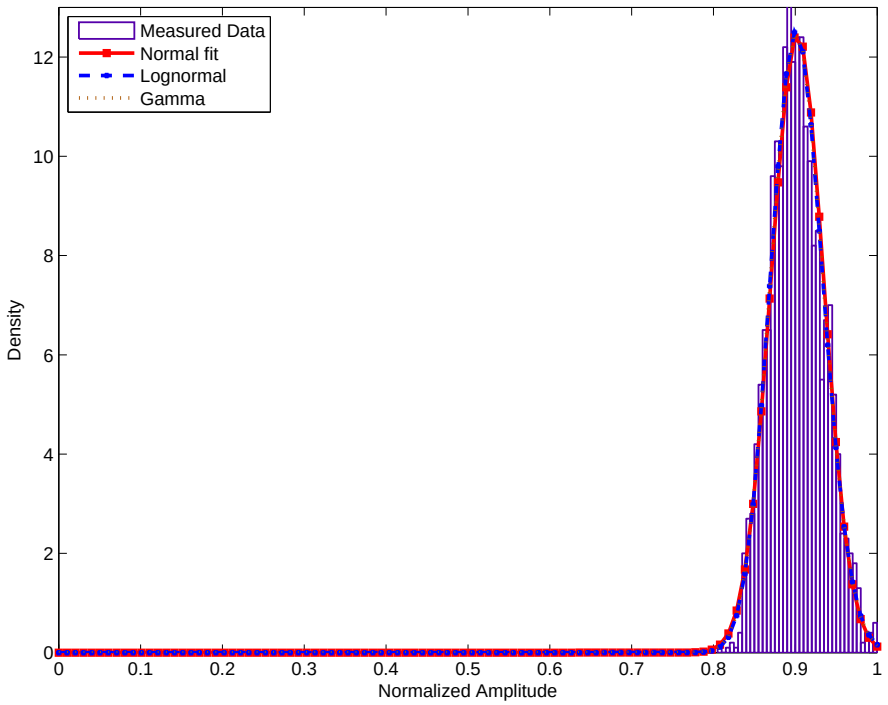

Figure 302: PDF of received power at 2360 MHz: right wrist to off-body; Standing; 3 m separation; 180° orientation

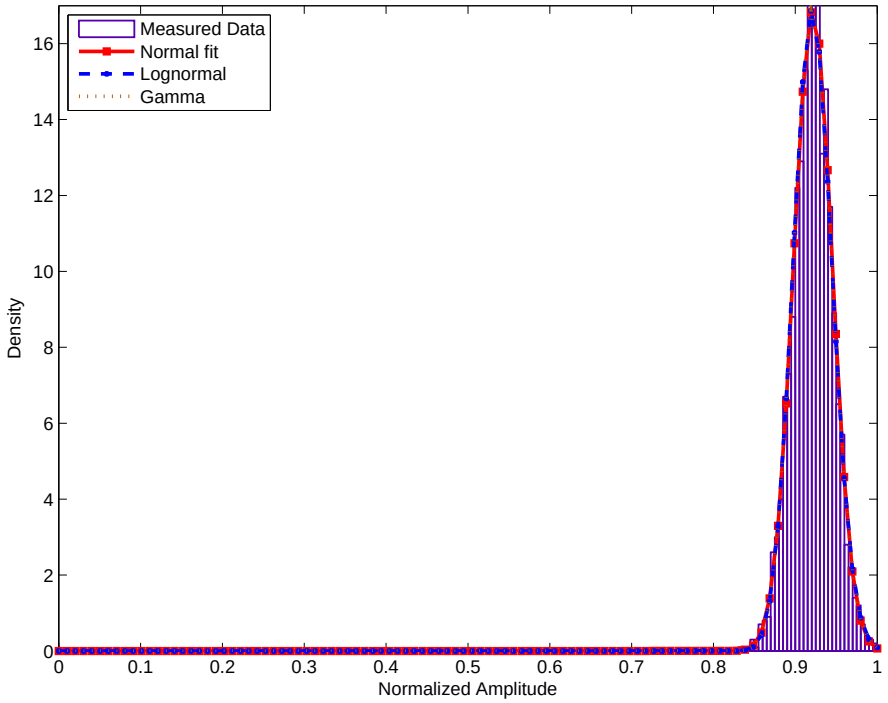

Figure 303: PDF of received power at 2360 MHz: right wrist to off-body; Standing; 3 m separation; 270° orientation

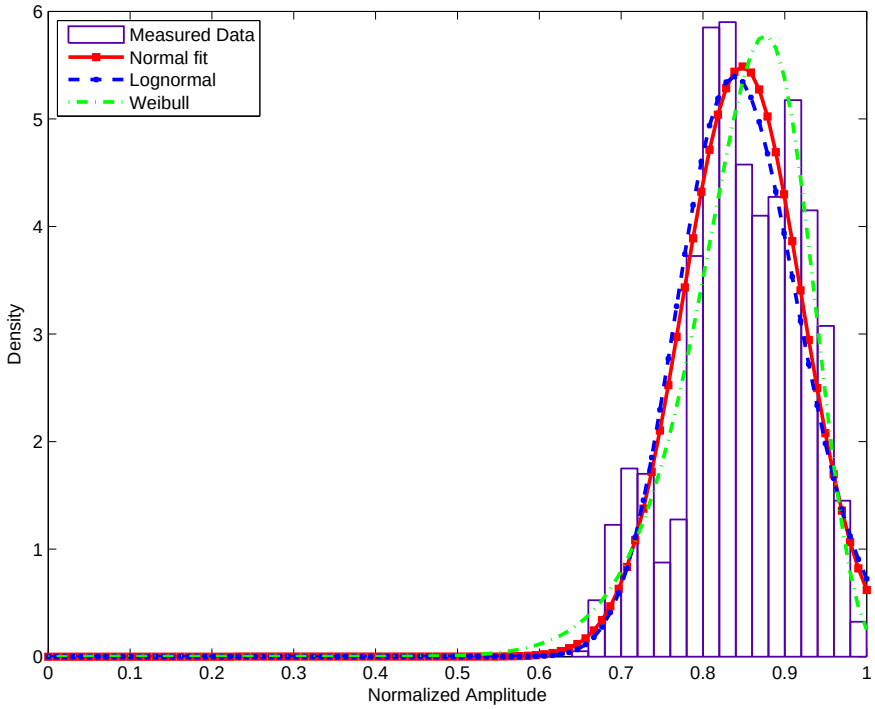

Figure 304: PDF of received power at 2360 MHz: right wrist to off-body; Standing; 3 m separation; 90° orientation

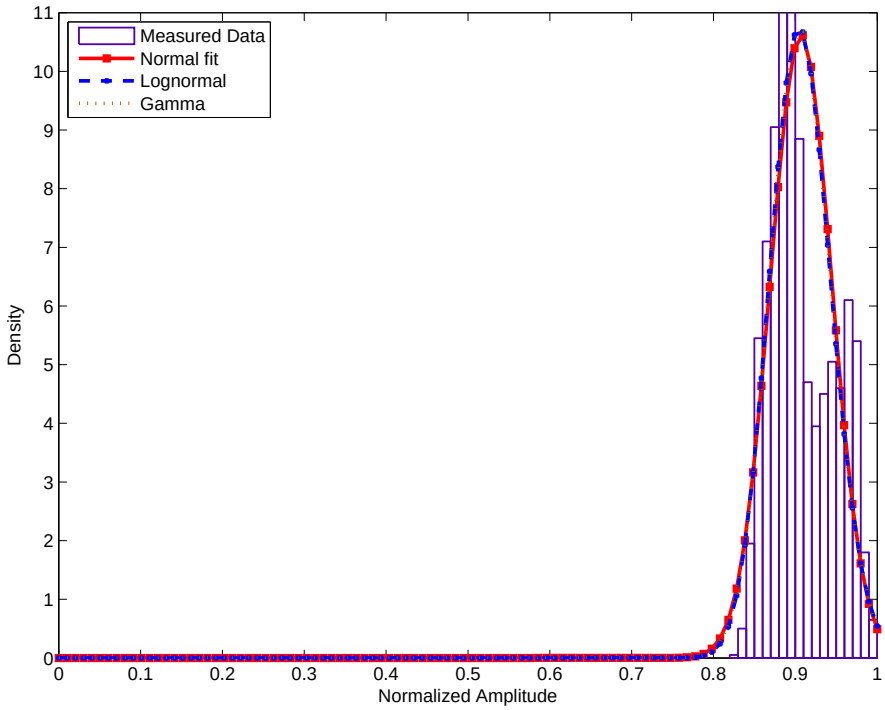

Figure 305: PDF of received power at 2360 MHz: right wrist to off-body; Standing; 4 m separation; 0° orientation

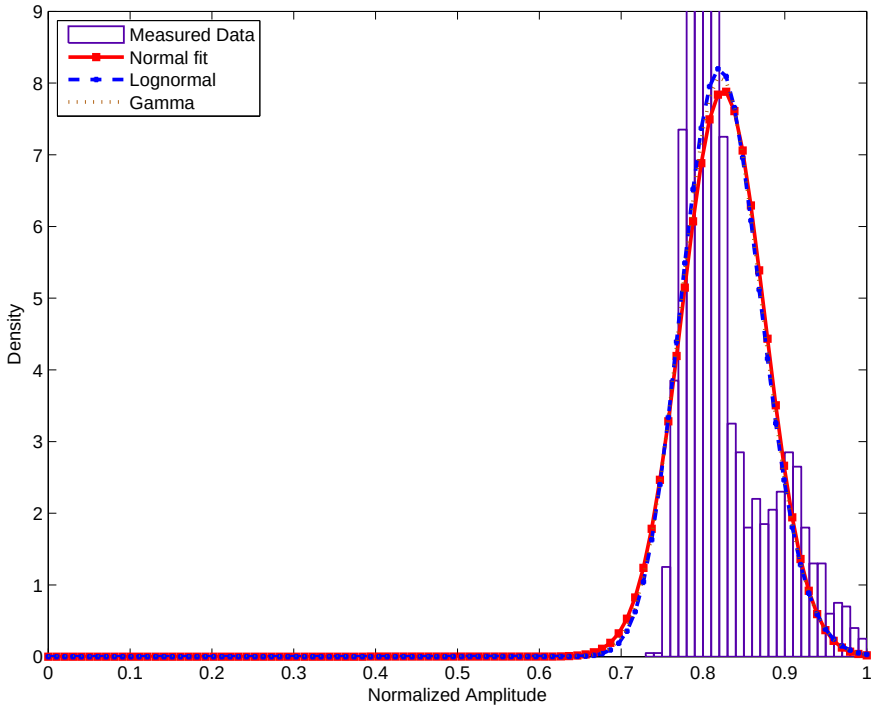

Figure 306: PDF of received power at 2360 MHz: right wrist to off-body; Standing; 4 m separation; 180° orientation

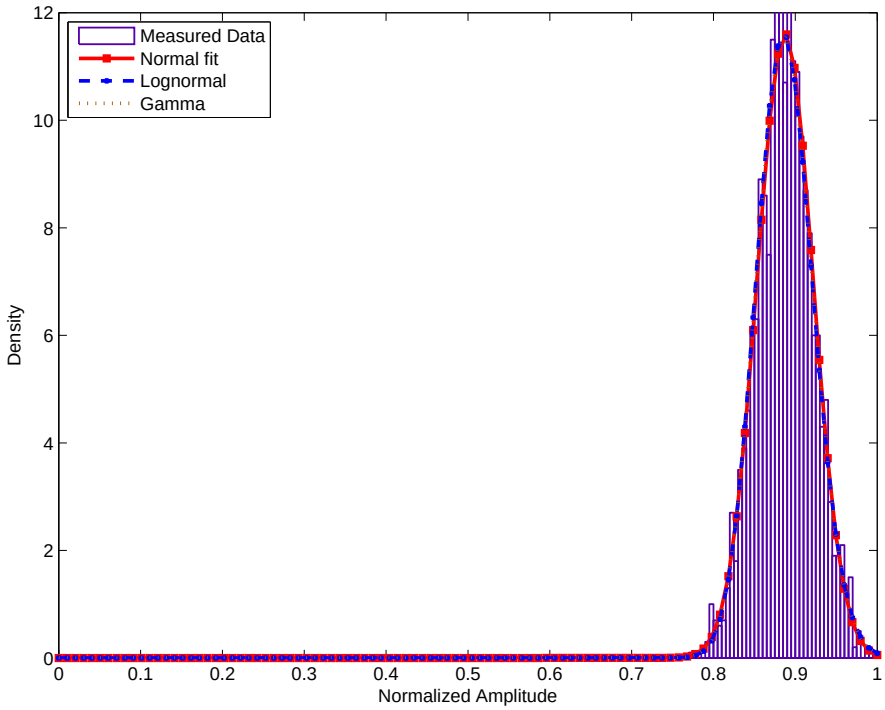

Figure 307: PDF of received power at 2360 MHz: right wrist to off-body; Standing; 4 m separation; 270° orientation

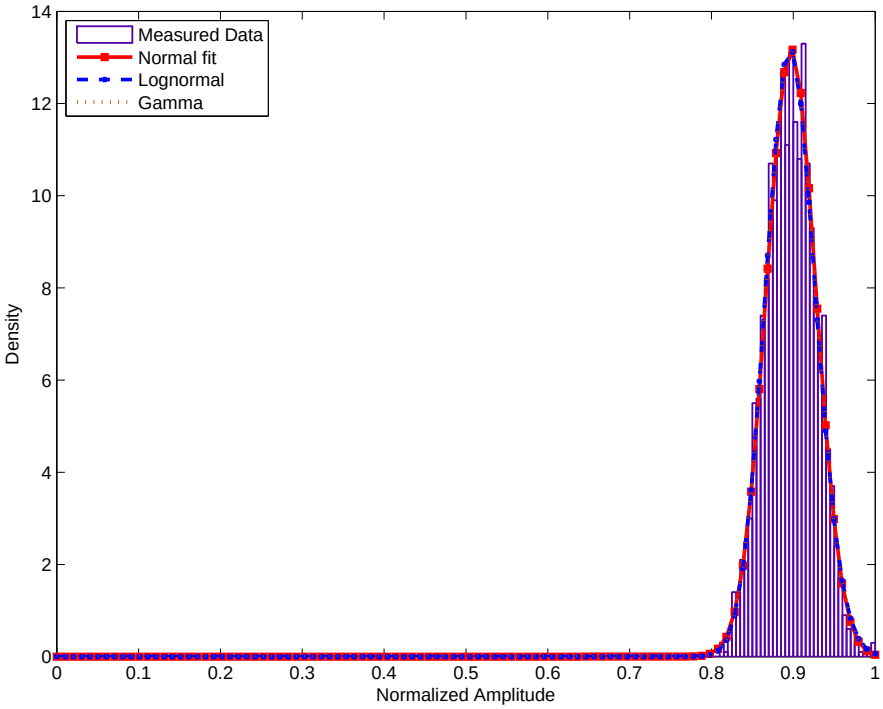

Figure 308: PDF of received power at 2360 MHz: right wrist to off-body; Standing; 4 m separation; 90° orientation

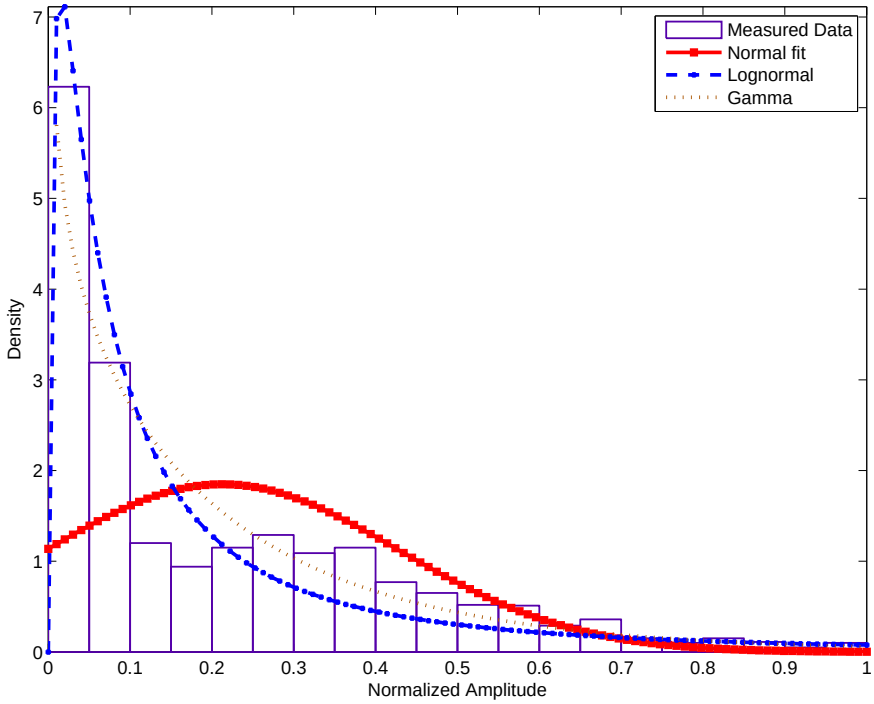

Figure 309: PDF of received power at 2360 MHz: right wrist to off-body; Walking; 1 m separation; 0° orientation

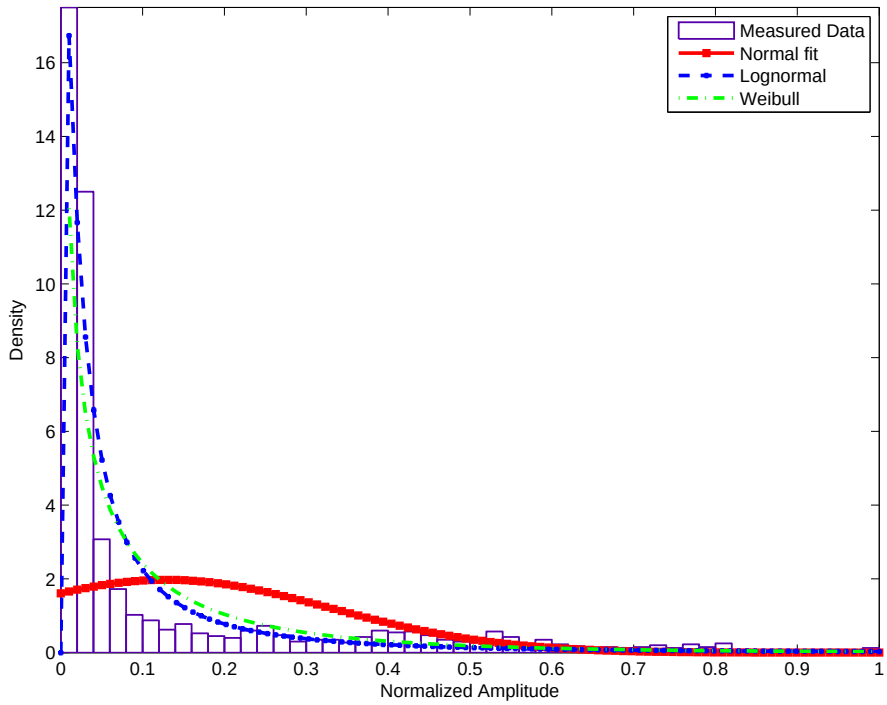

Figure 310: PDF of received power at 2360 MHz: right wrist to off-body; Walking; 1 m separation; 180° orientation

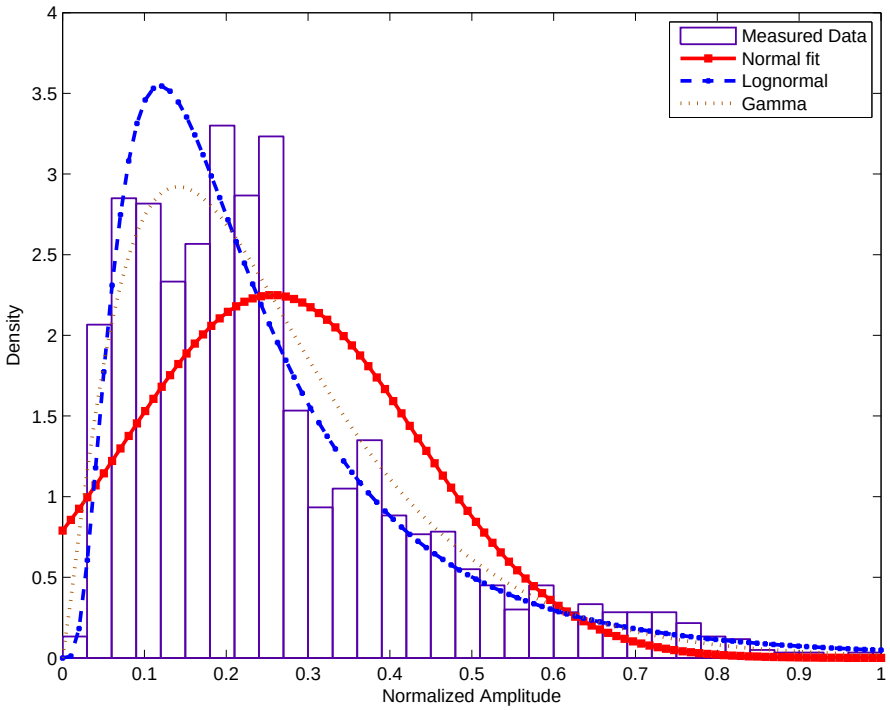

Figure 311: PDF of received power at 2360 MHz: right wrist to off-body; Walking; 1 m separation; 270° orientation

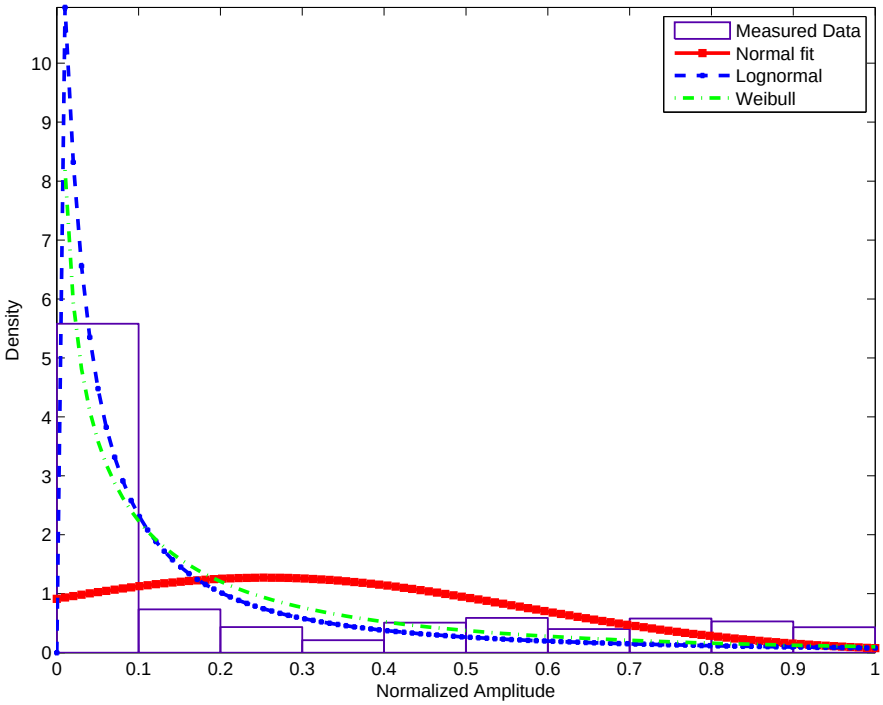

Figure 312: PDF of received power at 2360 MHz: right wrist to off-body; Walking; 1 m separation; 90° orientation

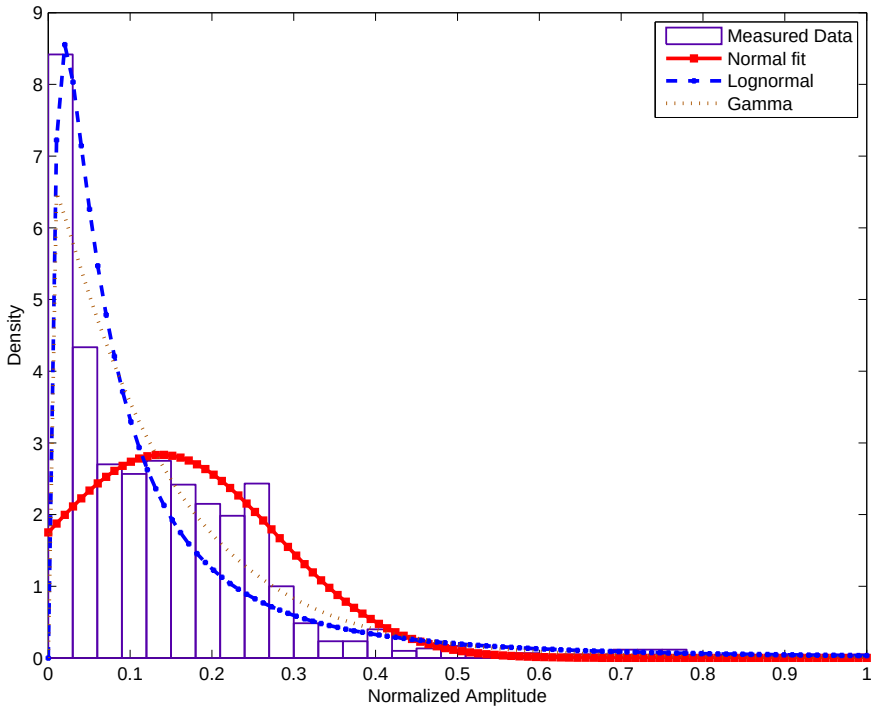

Figure 313: PDF of received power at 2360 MHz: right wrist to off-body; Walking; 2 m separation; 0° orientation

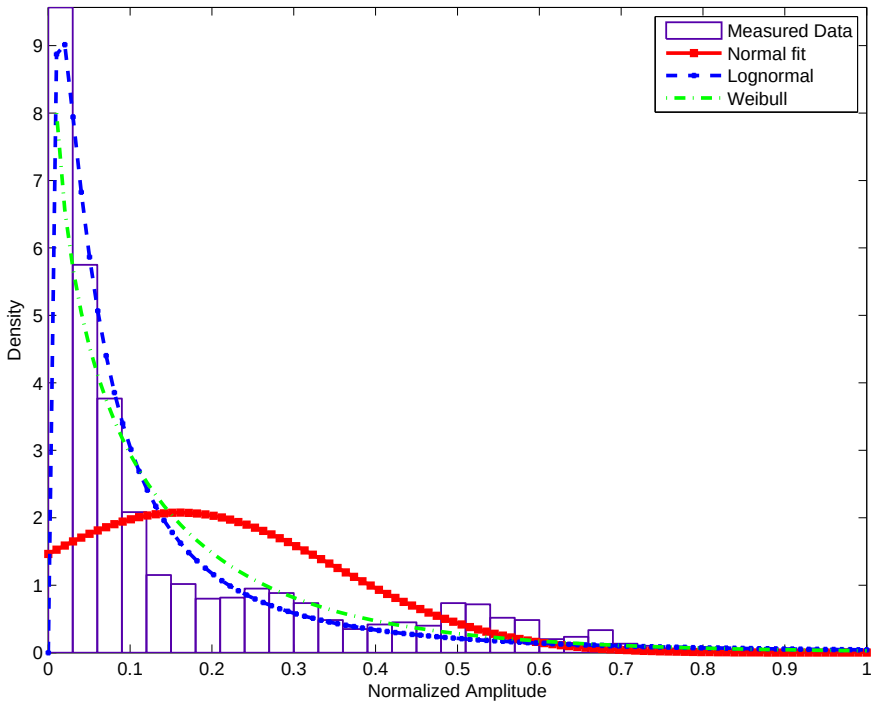

Figure 314: PDF of received power at 2360 MHz: right wrist to off-body; Walking; 2 m separation; 180° orientation

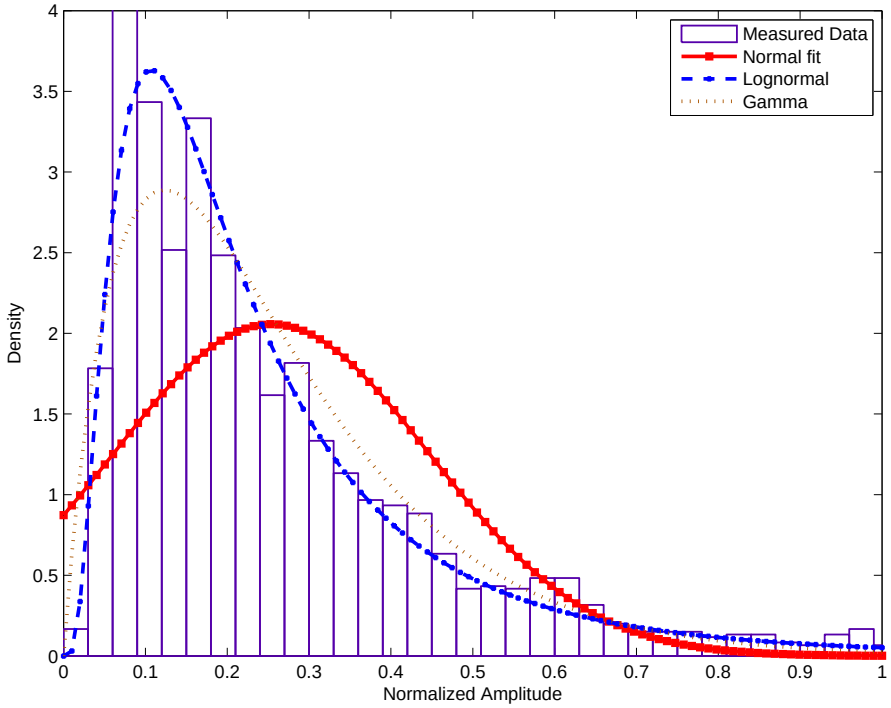

Figure 315: PDF of received power at 2360 MHz: right wrist to off-body; Walking; 2 m separation; 270° orientation

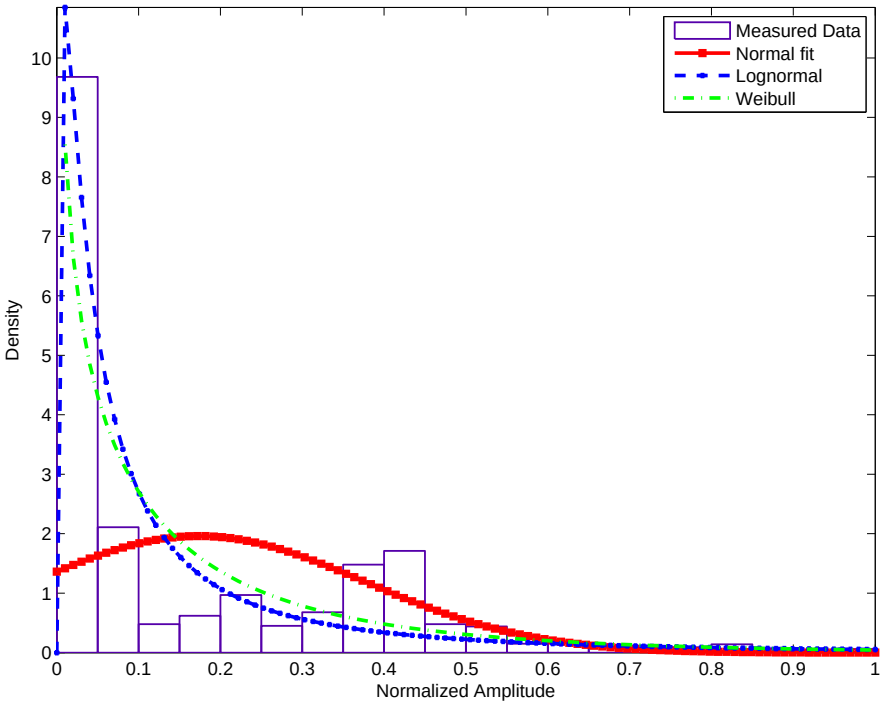

Figure 316: PDF of received power at 2360 MHz: right wrist to off-body; Walking; 2 m separation; 90° orientation

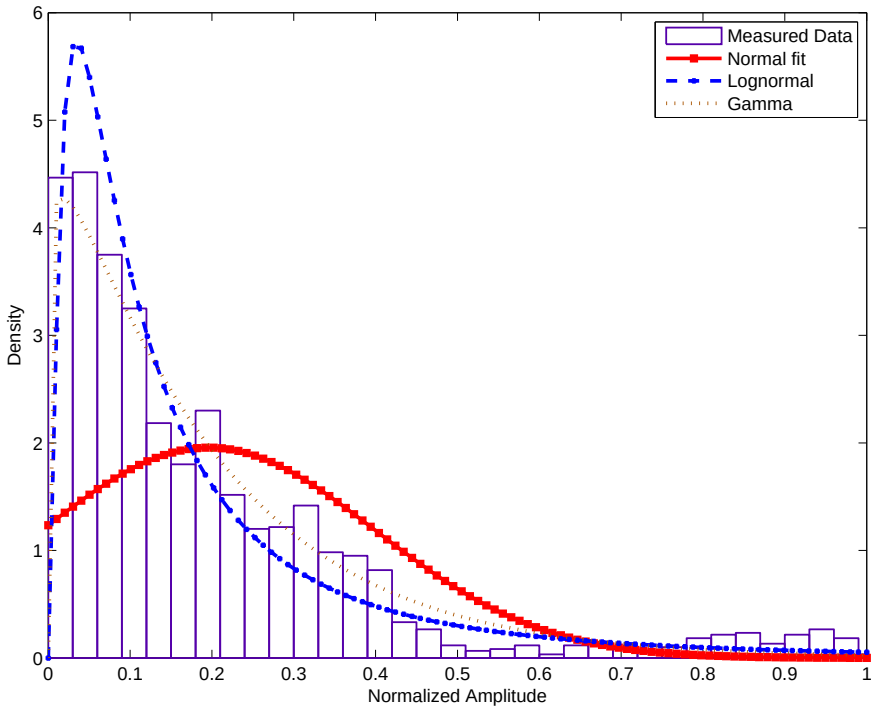

Figure 317: PDF of received power at 2360 MHz: right wrist to off-body; Walking; 3 m separation; 0° orientation

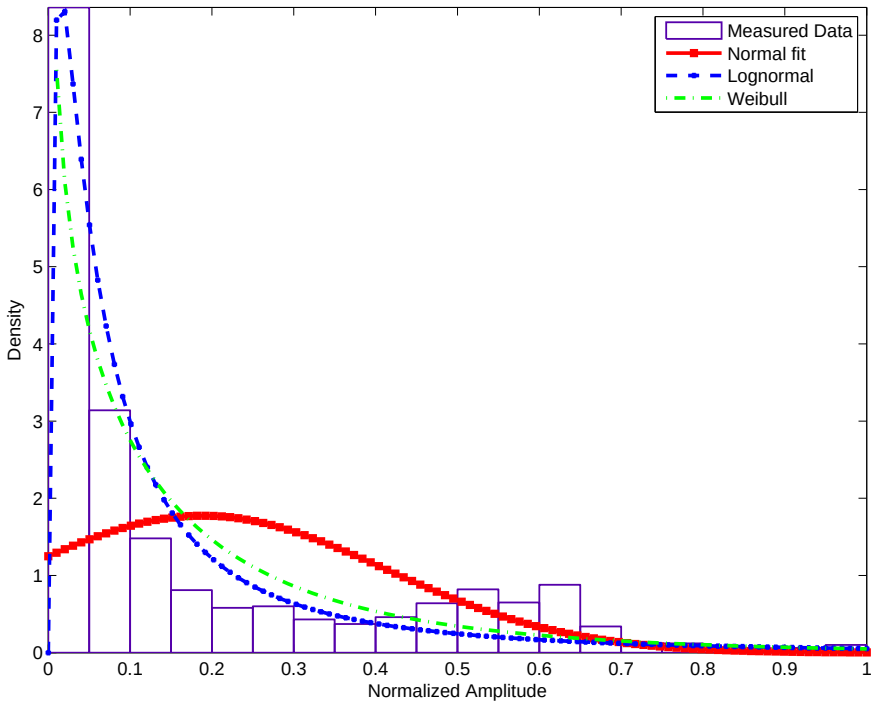

Figure 318: PDF of received power at 2360 MHz: right wrist to off-body; Walking; 3 m separation; 180° orientation

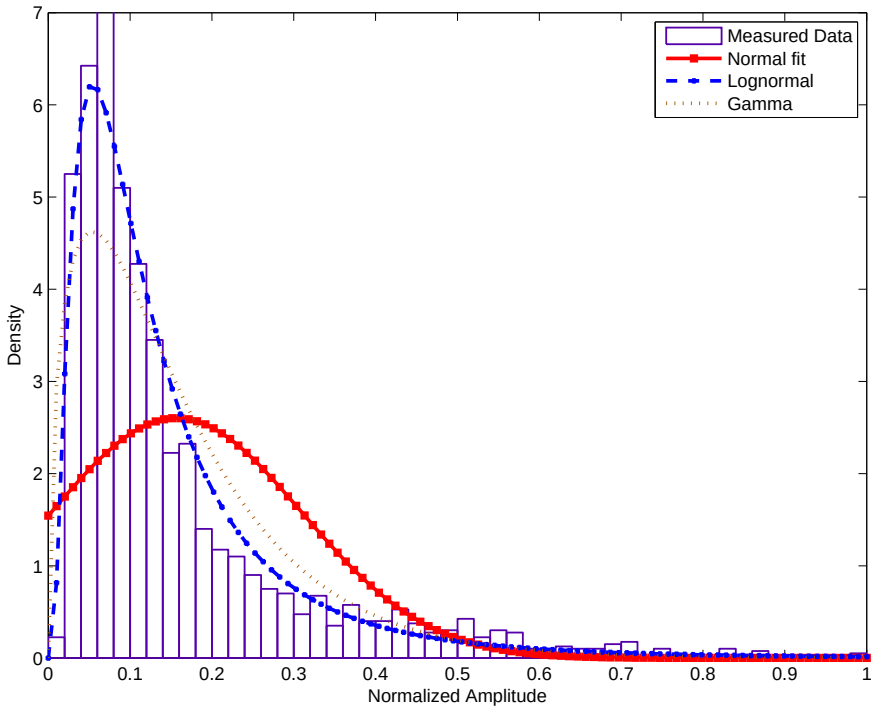

Figure 319: PDF of received power at 2360 MHz: right wrist to off-body; Walking; 3 m separation; 270° orientation

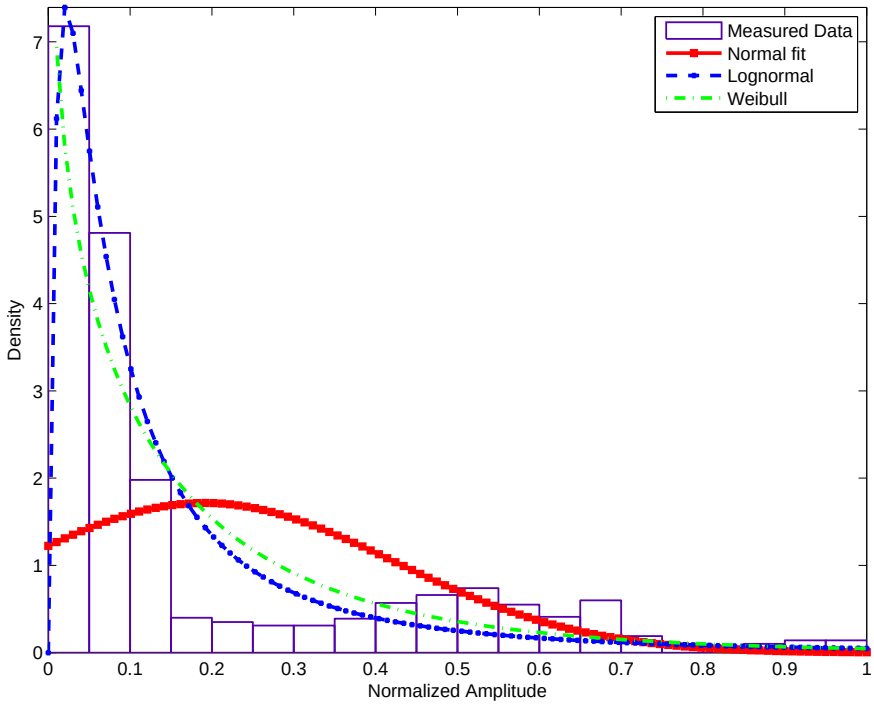

Figure 320: PDF of received power at 2360 MHz: right wrist to off-body; Walking; 3 m separation; 90° orientation

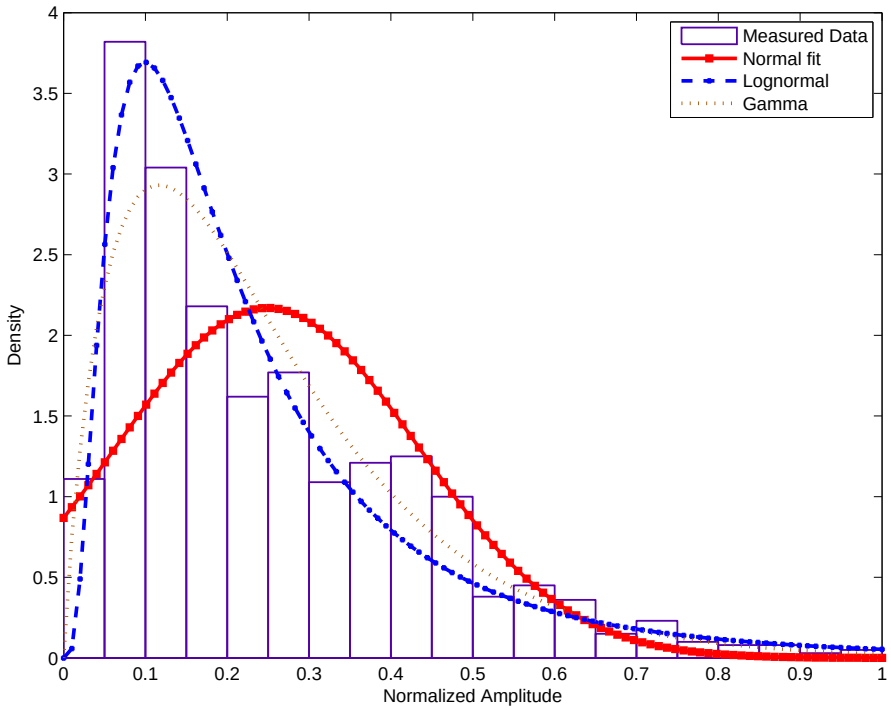

Figure 321: PDF of received power at 2360 MHz: right wrist to off-body; Walking; 4 m separation; 0° orientation

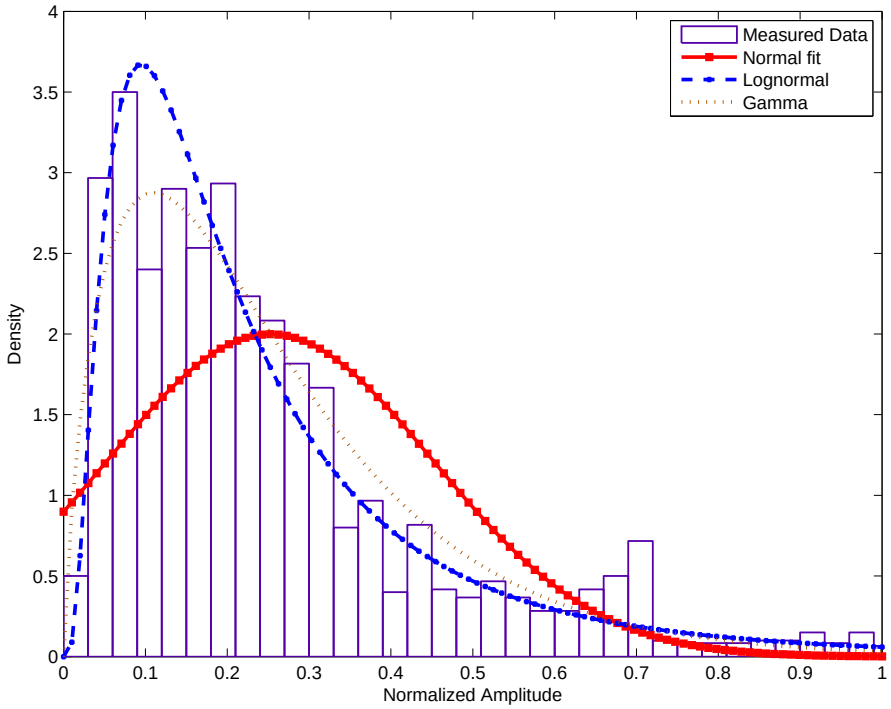

Figure 322: PDF of received power at 2360 MHz: right wrist to off-body; Walking; 4 m separation; 180° orientation

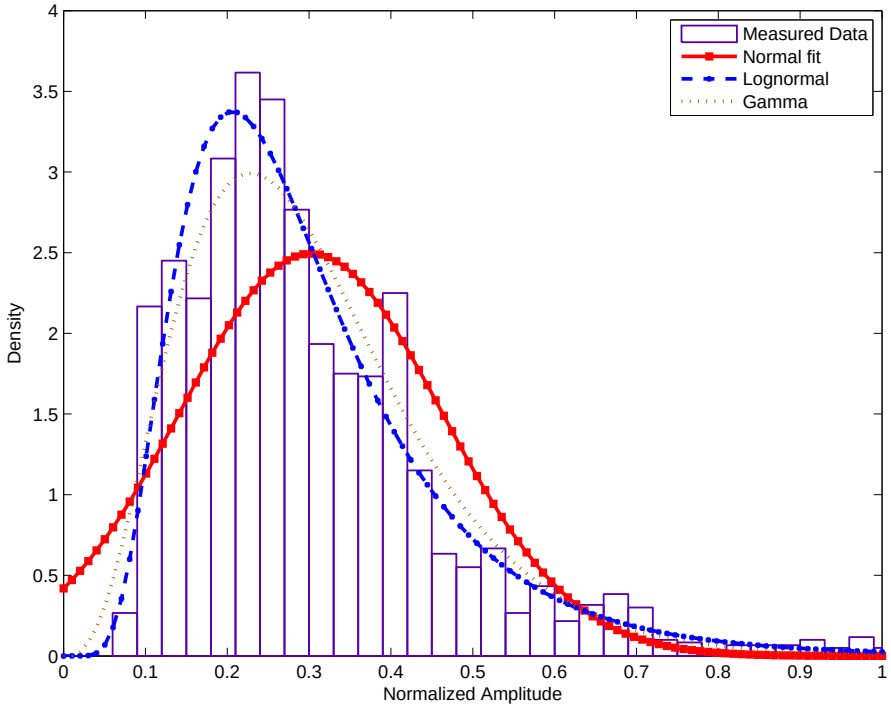

Figure 323: PDF of received power at 2360 MHz: right wrist to off-body; Walking; 4 m separation; 270° orientation

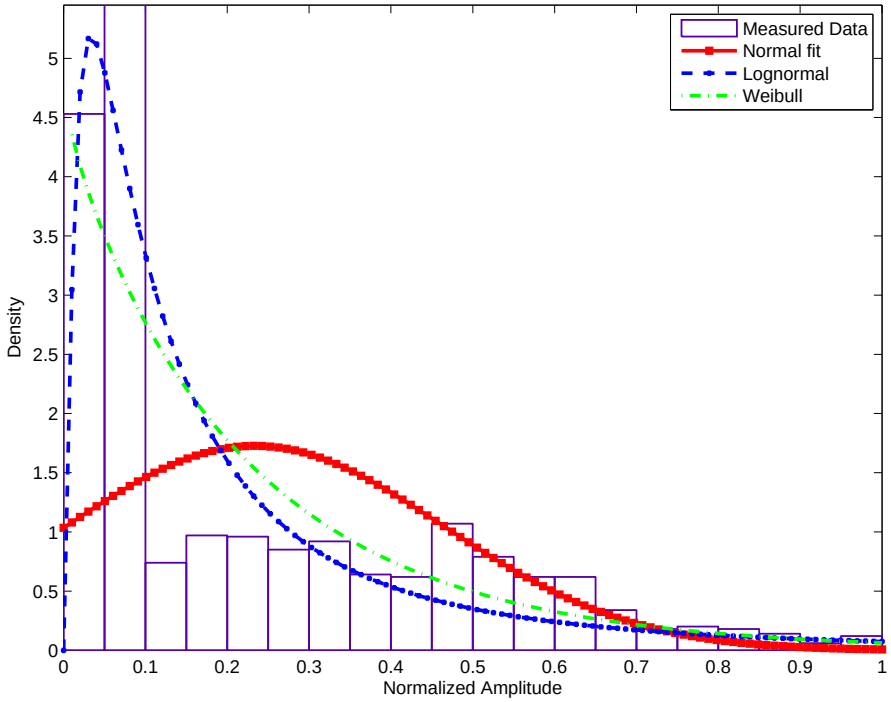

Figure 324: PDF of received power at 2360 MHz: right wrist to off-body; Walking; 4 m separation; 90° orientation

A.4 Channel Time-Coherence

A.4.1 820 MHz Measurements

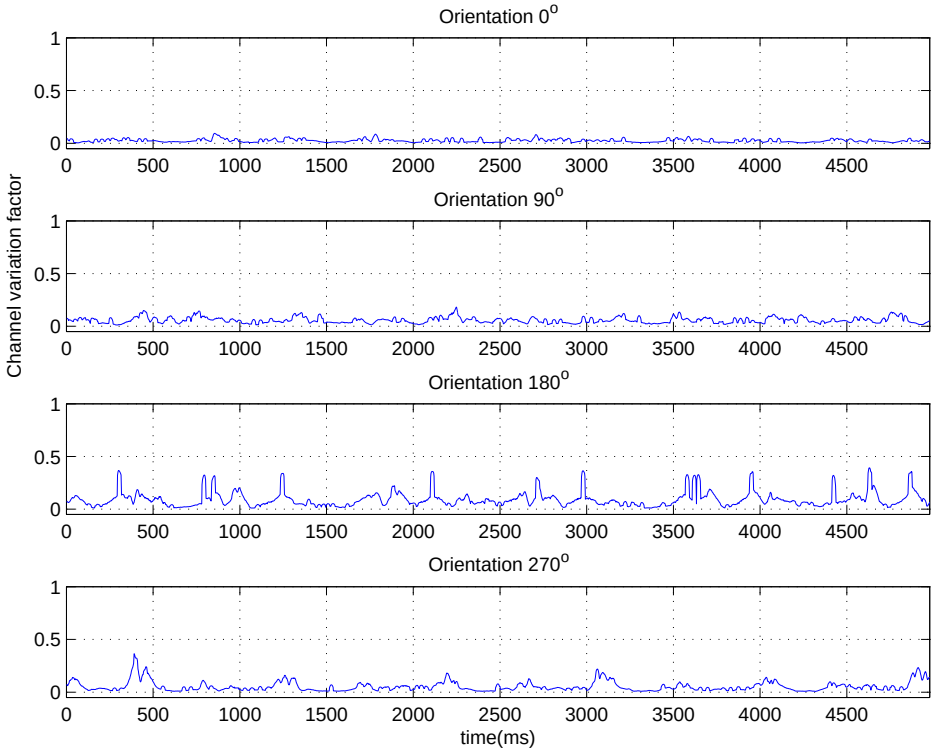

Figure 325: Channel variation factor for a time varying period of 25ms, Chest to off body, subject walking, Rx Distance 3m, orientations, 0^o, 90^o, 180^o and 270^o - 820 MHz

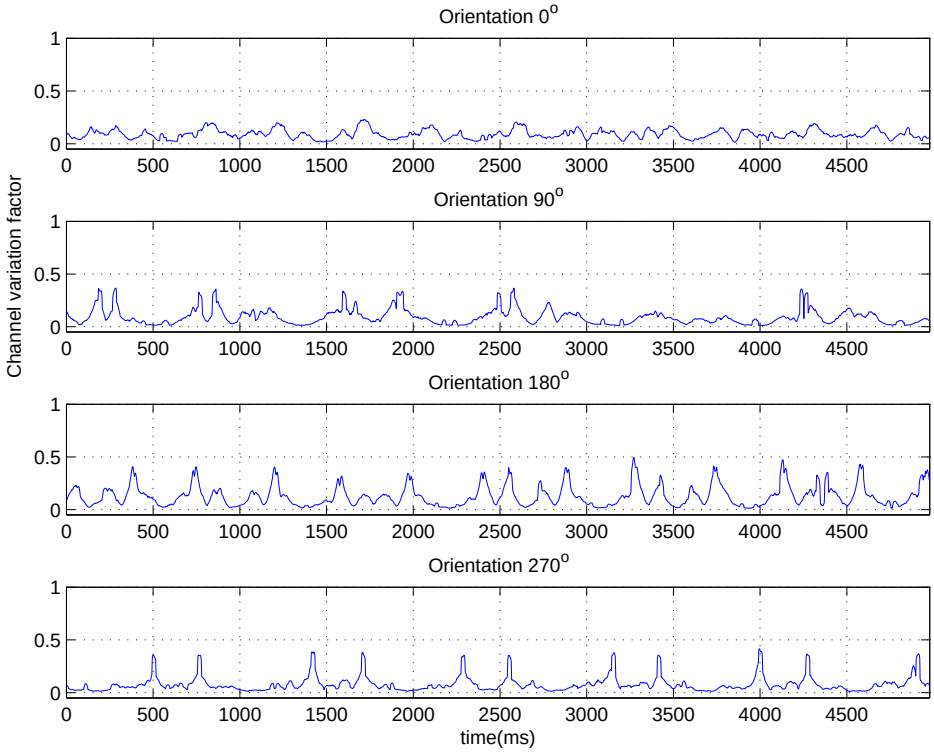

Figure 326: Channel variation factor for a time varying period of 25ms, Right wrist to off body, subject walking, Rx Distance 3m, orientations, 0^o, 90^o, 180^o and 270^o - 820 MHz

A.4.2 2.36 GHz Measurements

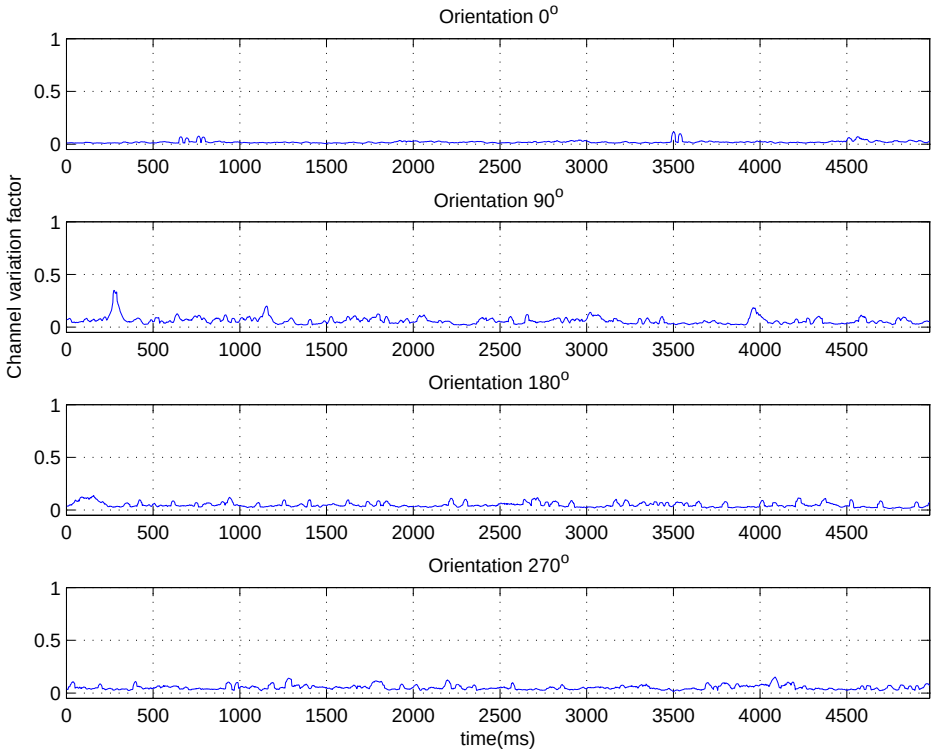

Figure 327: Channel variation factor for a time varying period of 25ms, Chest to off body, subject walking, Rx Distance 3m,orientations, 0^o, 90^o, 180^o and 270^o - 2360 MHz

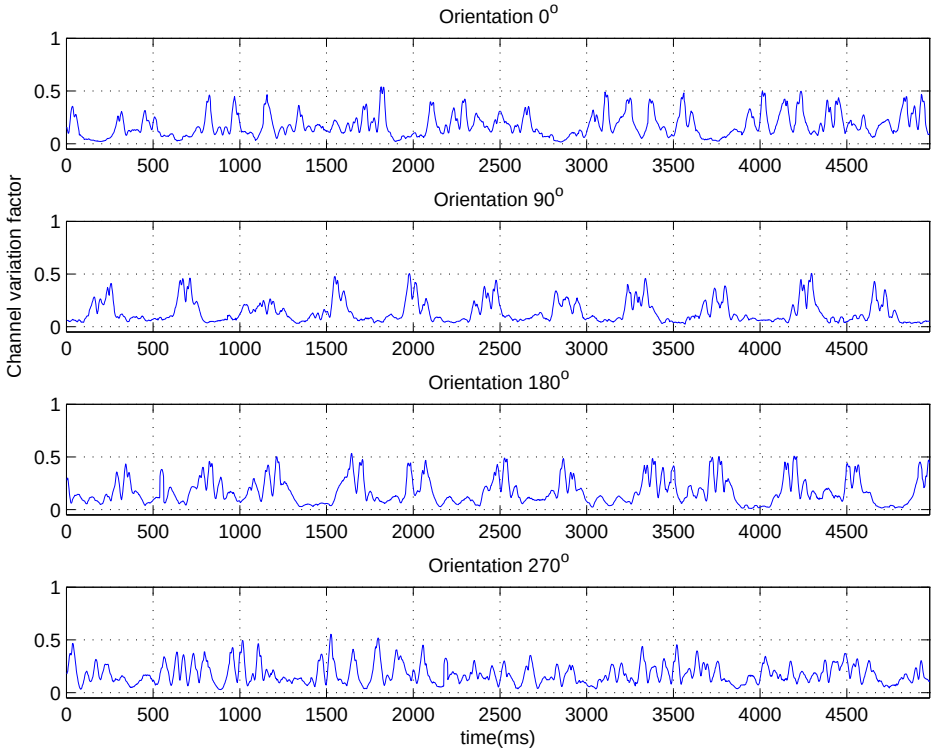

Figure 328: Channel variation factor for a time varying period of 25ms, Right wrist to off body, subject walking, Rx Distance 3m, orientations, 0^o, 90^o, 180^o and 270^o - 2360 MHz

A.4.3 Channel Variation CDFs for 820 MHz and 2.36 GHz

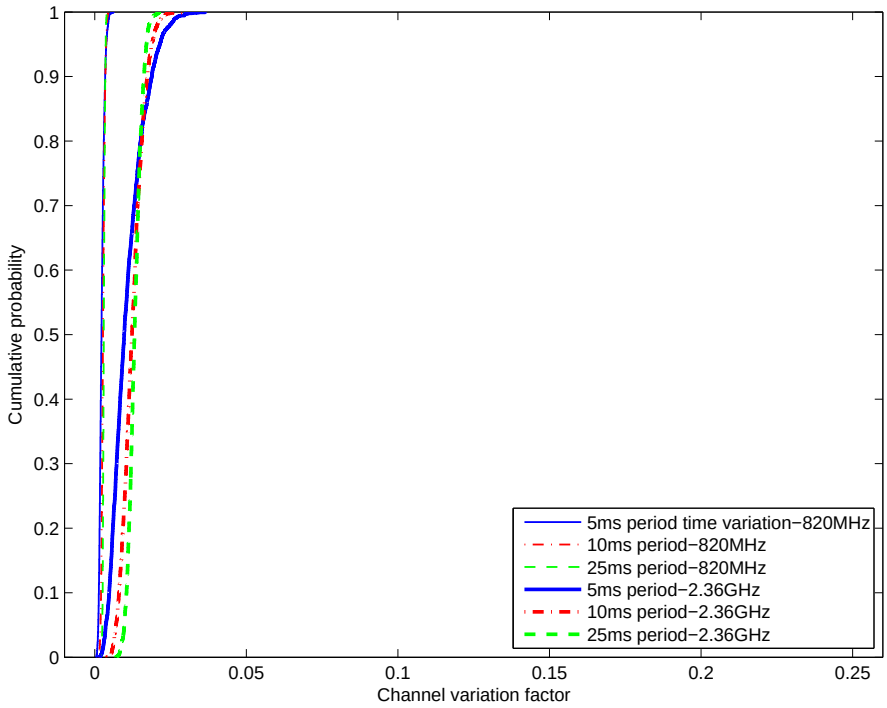

Figure 329: CDF of channel variation factor at 820 MHz and 2.36 GHz: chest to off-body; Standing; 1 m separation; 0° orientation

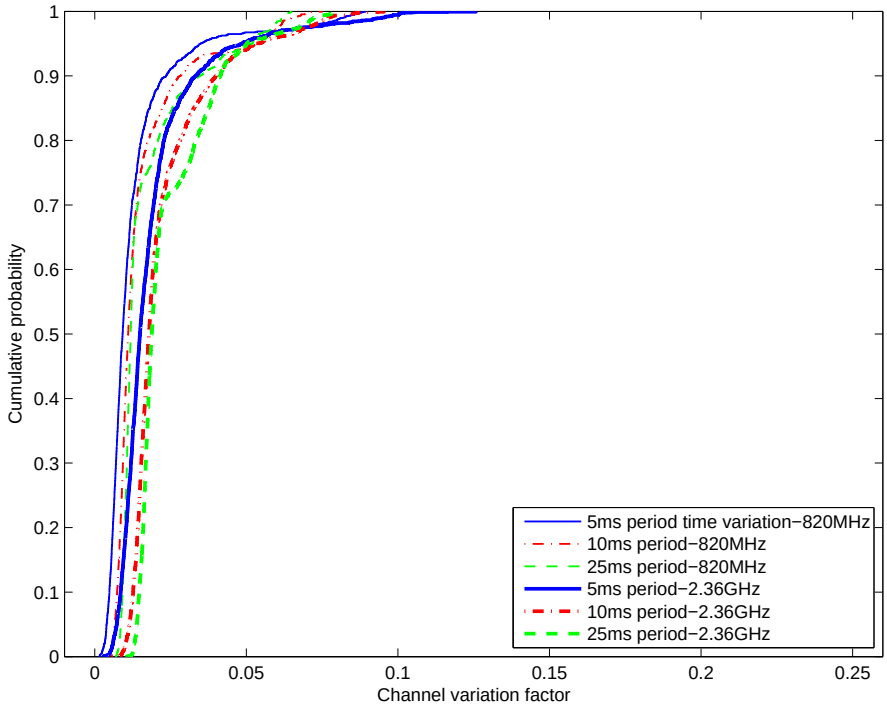

Figure 330: CDF of channel variation factor at 820 MHz and 2.36 GHz: chest to off-body; Standing; 1 m separation; 180° orientation

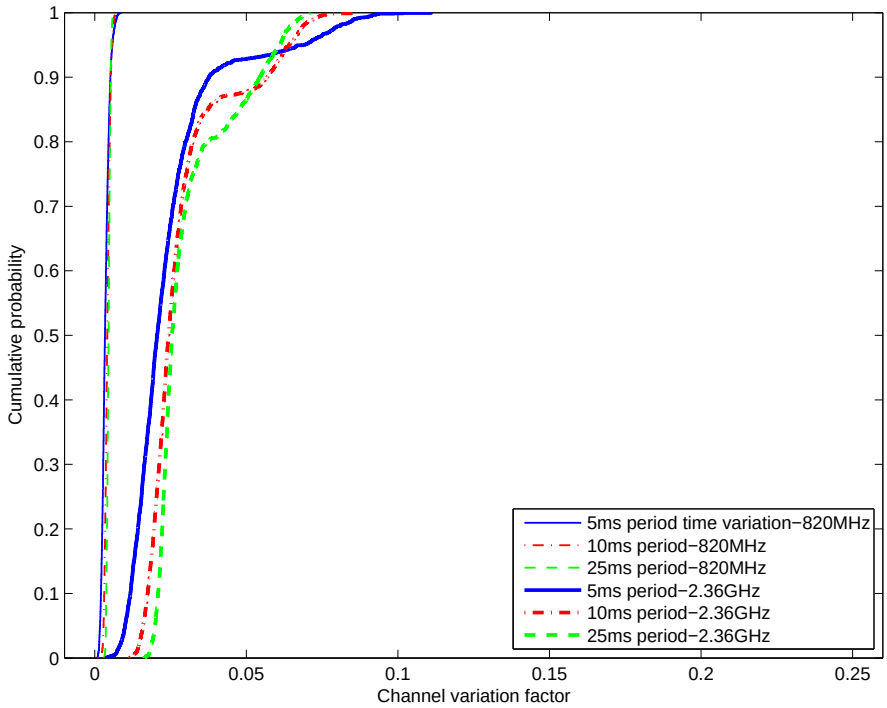

Figure 331: CDF of channel variation factor at 820 MHz and 2.36 GHz: chest to off-body; Standing; 1 m separation; 270° orientation

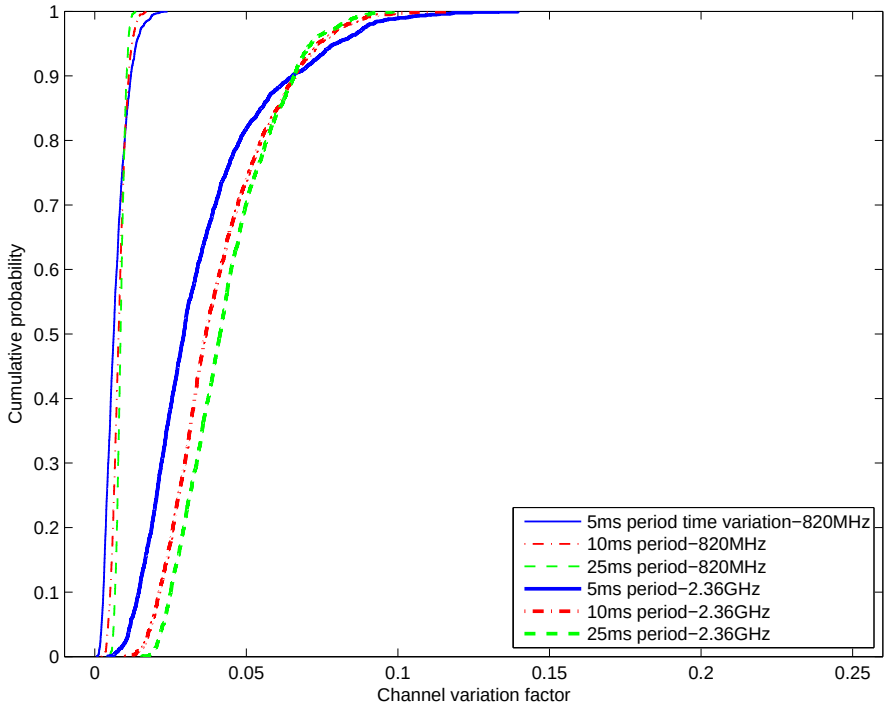

Figure 332: CDF of channel variation factor at 820 MHz and 2.36 GHz: chest to off-body; Standing; 1 m separation; 90° orientation

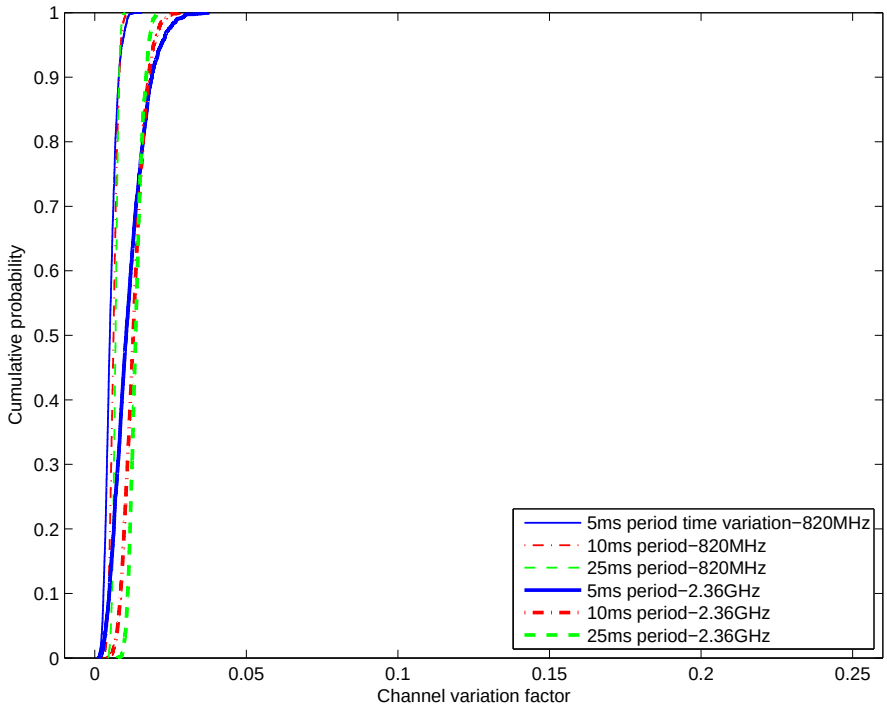

Figure 333: CDF of channel variation factor at 820 MHz and 2.36 GHz: chest to off-body; Standing; 2 m separation; 0° orientation

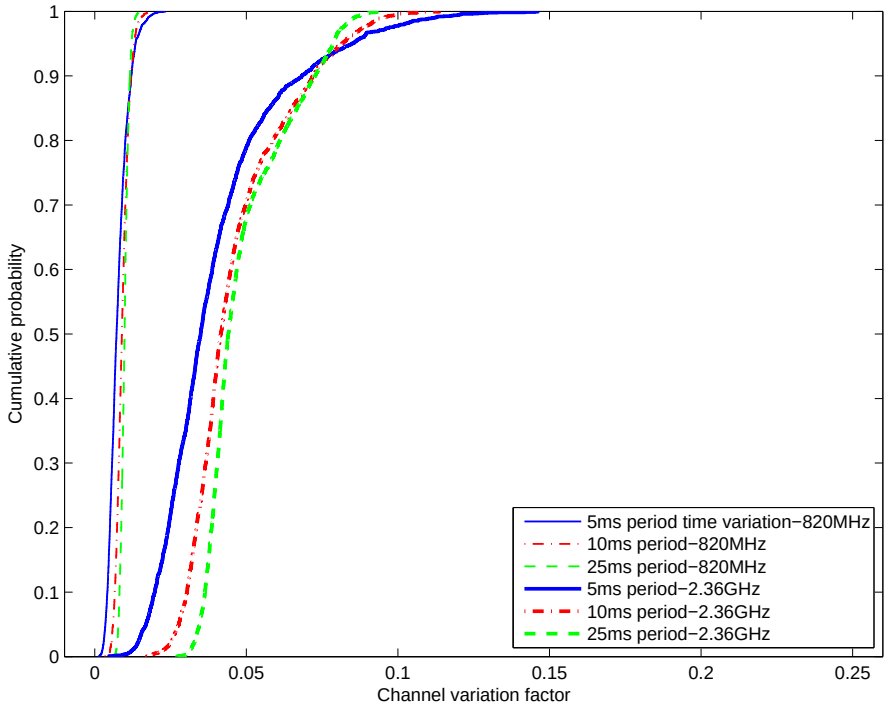

Figure 334: CDF of channel variation factor at 820 MHz and 2.36 GHz: chest to off-body; Standing; 2 m separation; 180° orientation

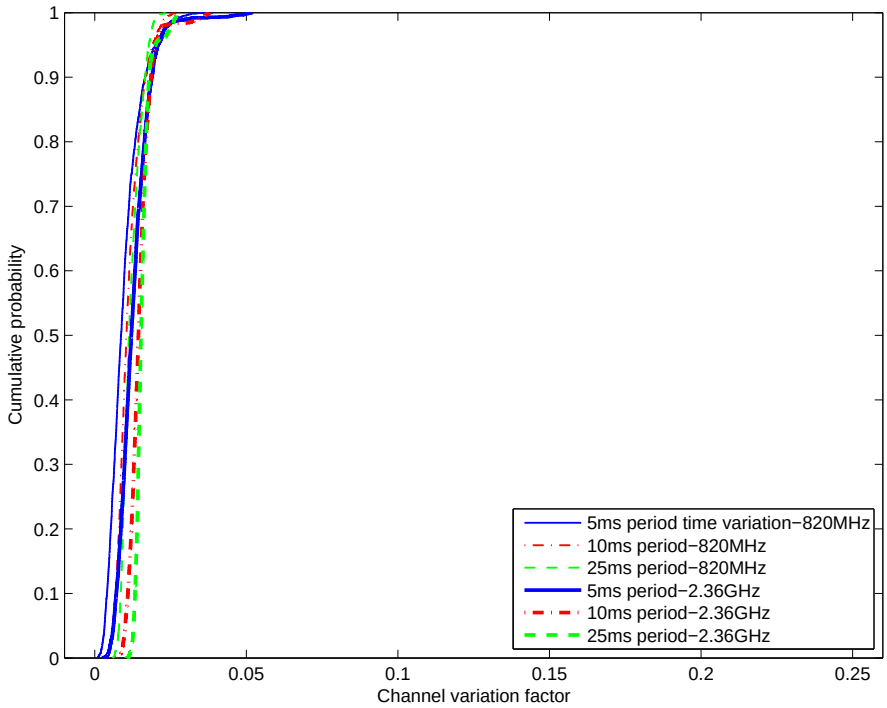

Figure 335: CDF of channel variation factor at 820 MHz and 2.36 GHz: chest to off-body; Standing; 2 m separation; 270° orientation

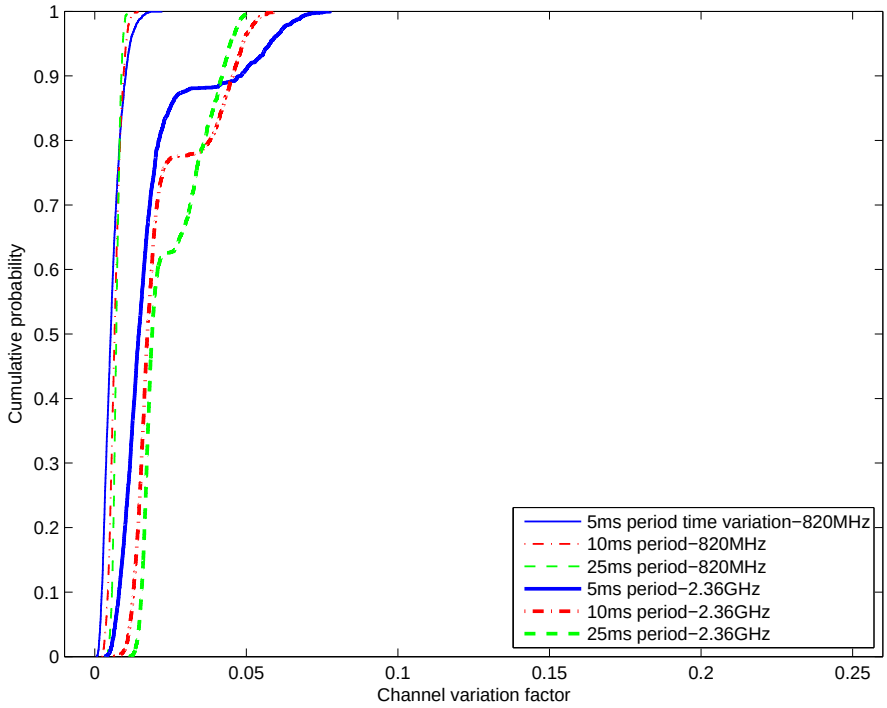

Figure 336: CDF of channel variation factor at 820 MHz and 2.36 GHz: chest to off-body; Standing; 2 m separation; 90° orientation

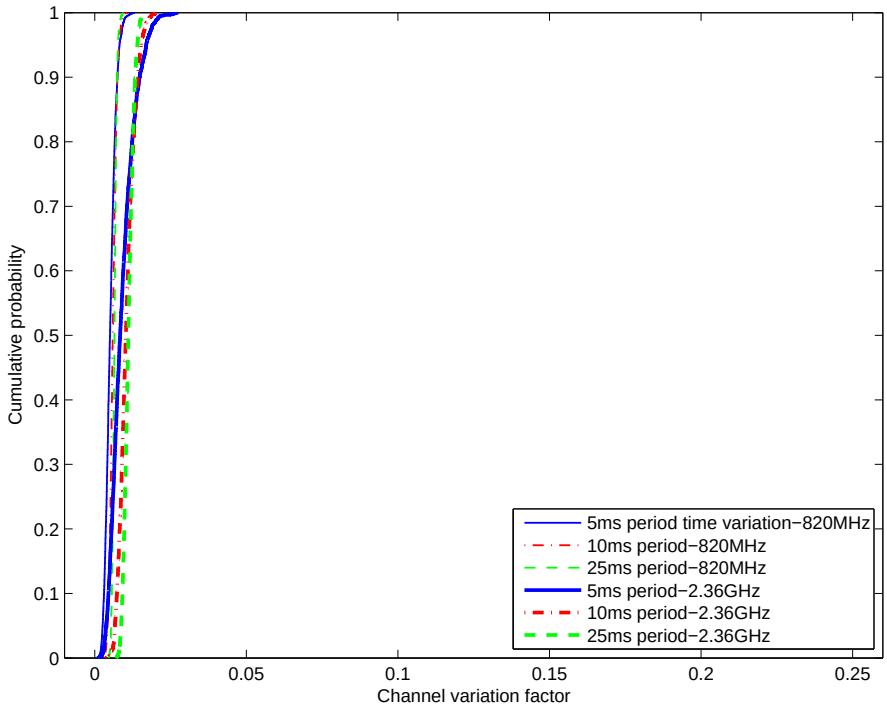

Figure 337: CDF of channel variation factor at 820 MHz and 2.36 GHz: chest to off-body; Standing; 3 m separation; 0° orientation

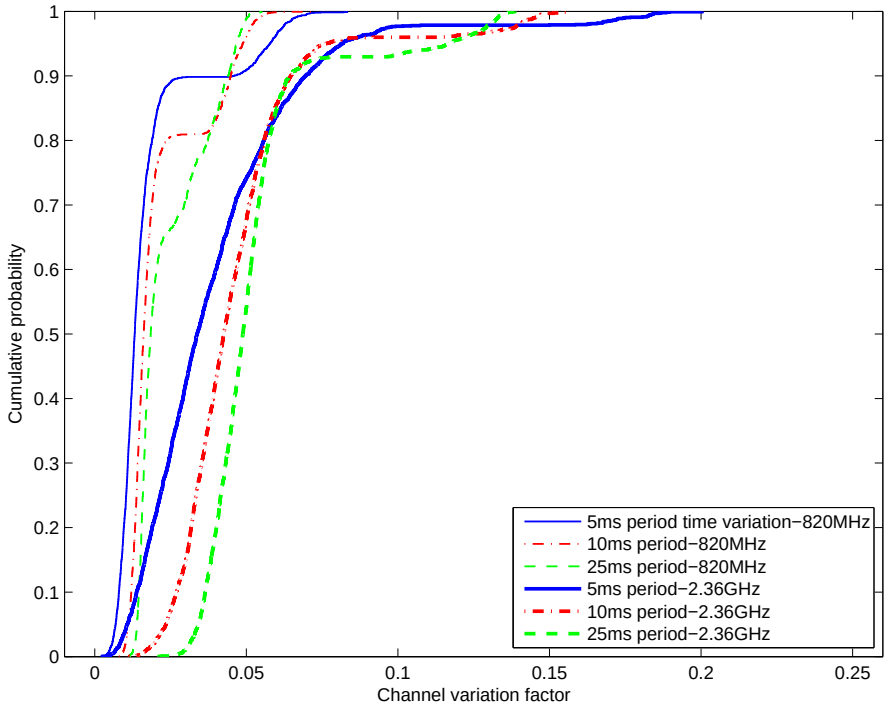

Figure 338: CDF of channel variation factor at 820 MHz and 2.36 GHz: chest to off-body; Standing; 3 m separation; 180° orientation

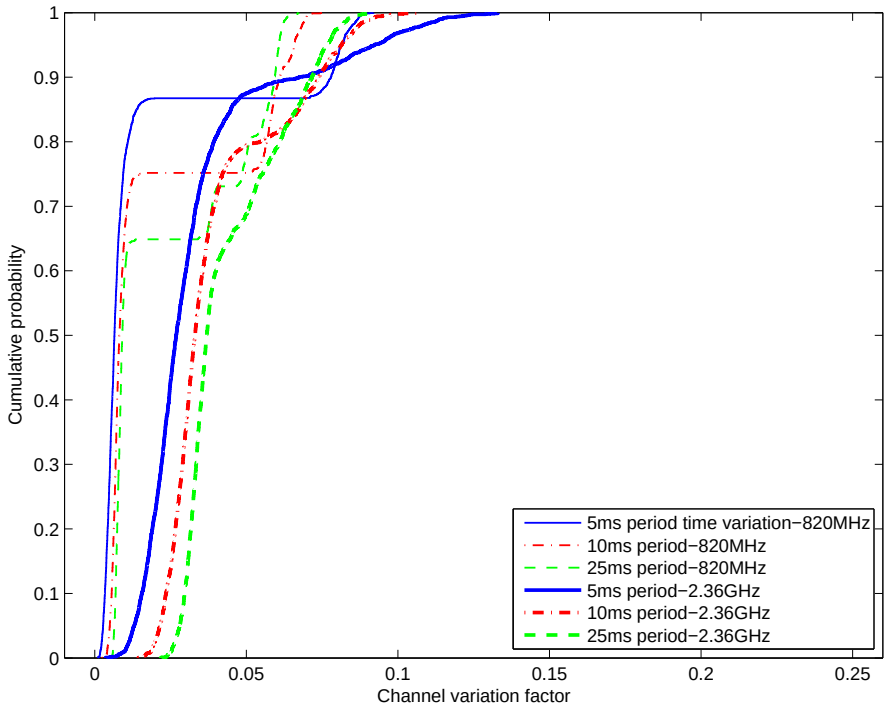

Figure 339: CDF of channel variation factor at 820 MHz and 2.36 GHz: chest to off-body; Standing; 3 m separation; 270° orientation

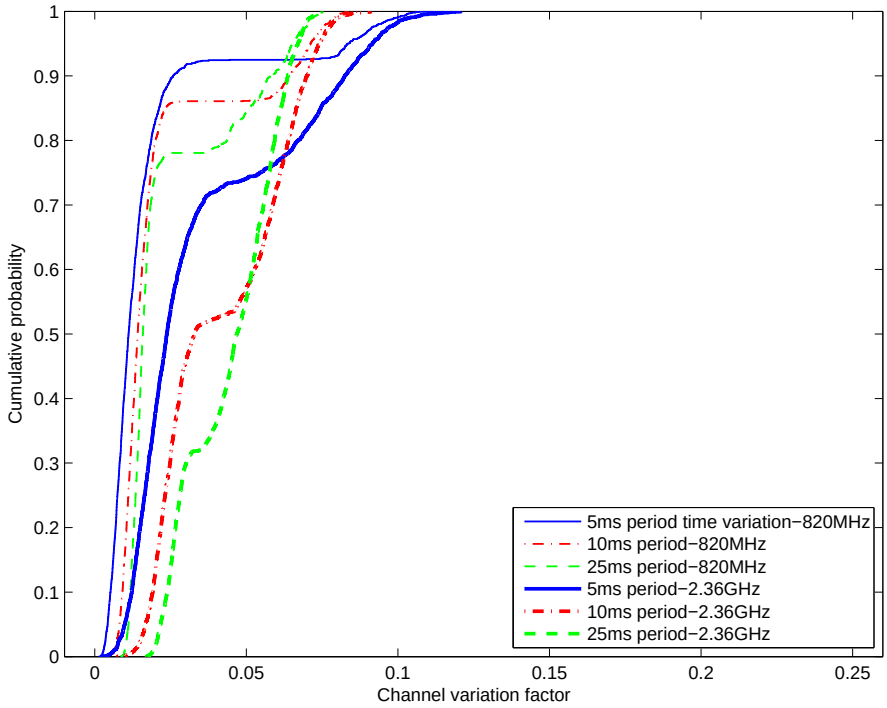

Figure 340: CDF of channel variation factor at 820 MHz and 2.36 GHz: chest to off-body; Standing; 3 m separation; 90° orientation

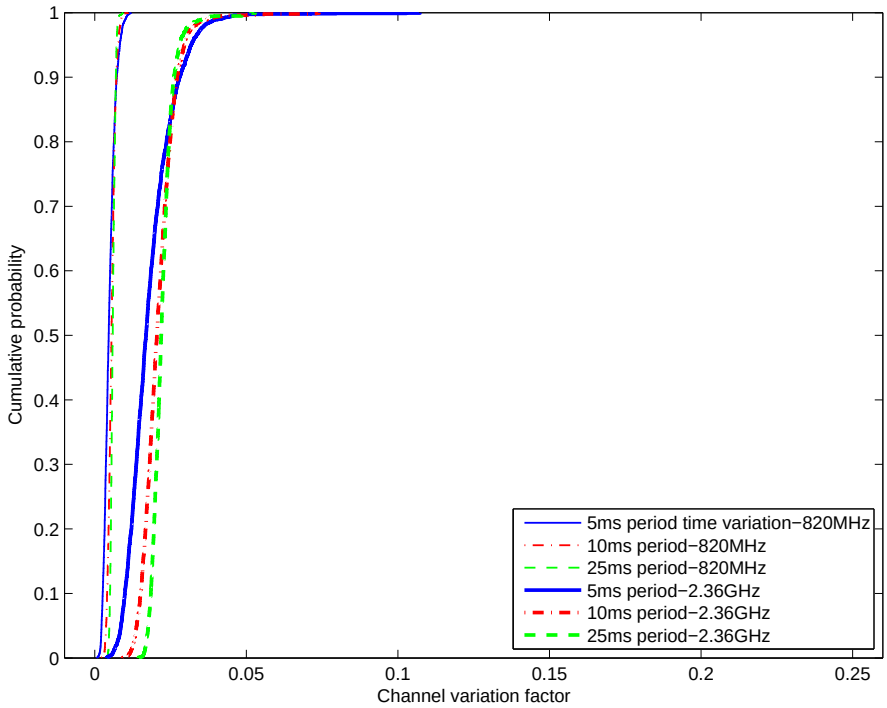

Figure 341: CDF of channel variation factor at 820 MHz and 2.36 GHz: chest to off-body; Standing; 4 m separation; 0° orientation

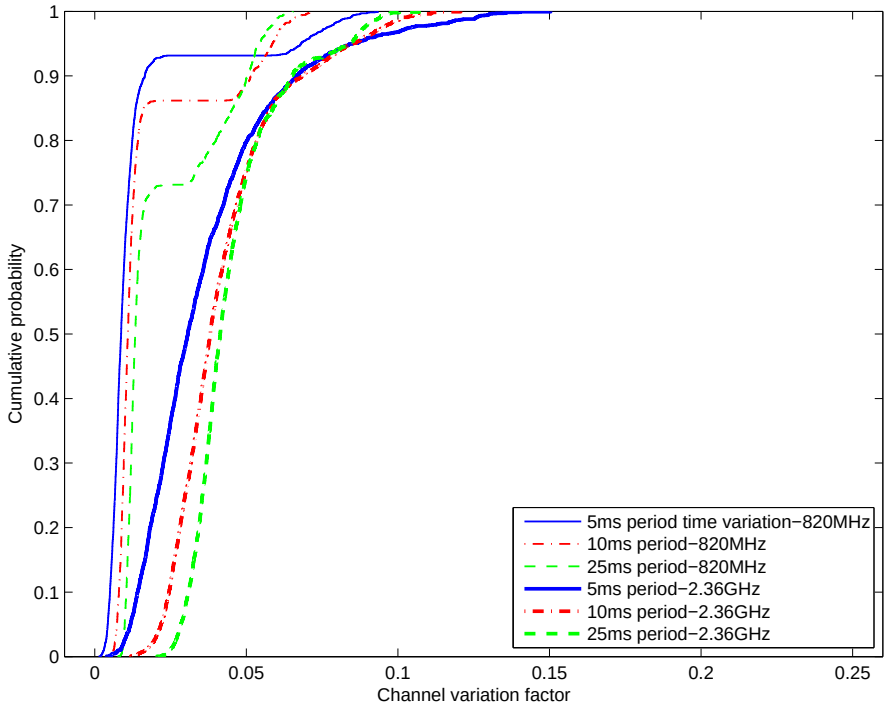

Figure 342: CDF of channel variation factor at 820 MHz and 2.36 GHz: chest to off-body; Standing; 4 m separation; 180° orientation

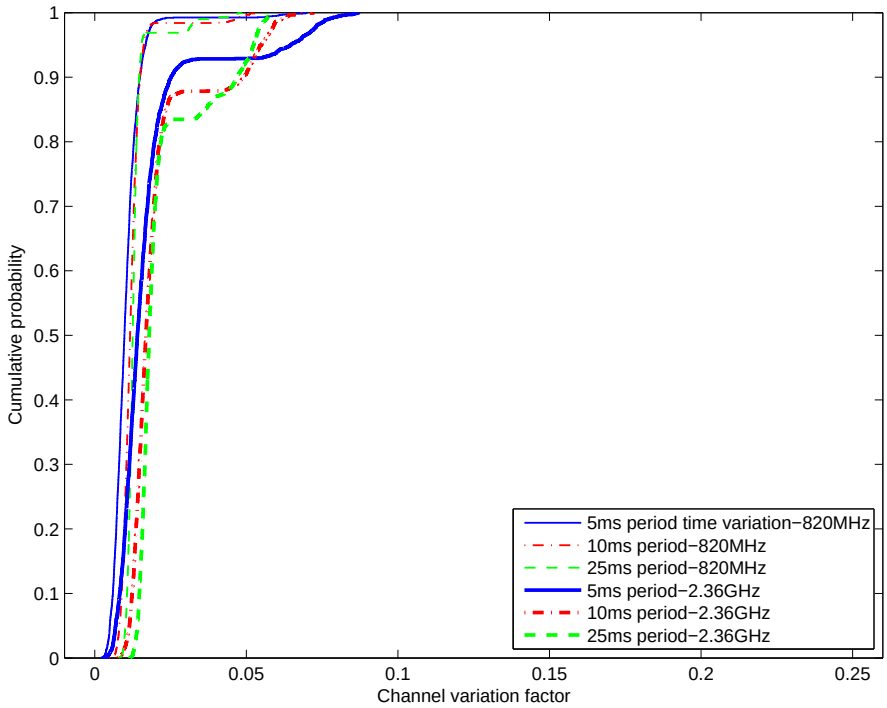

Figure 343: CDF of channel variation factor at 820 MHz and 2.36 GHz: chest to off-body; Standing; 4 m separation; 270° orientation

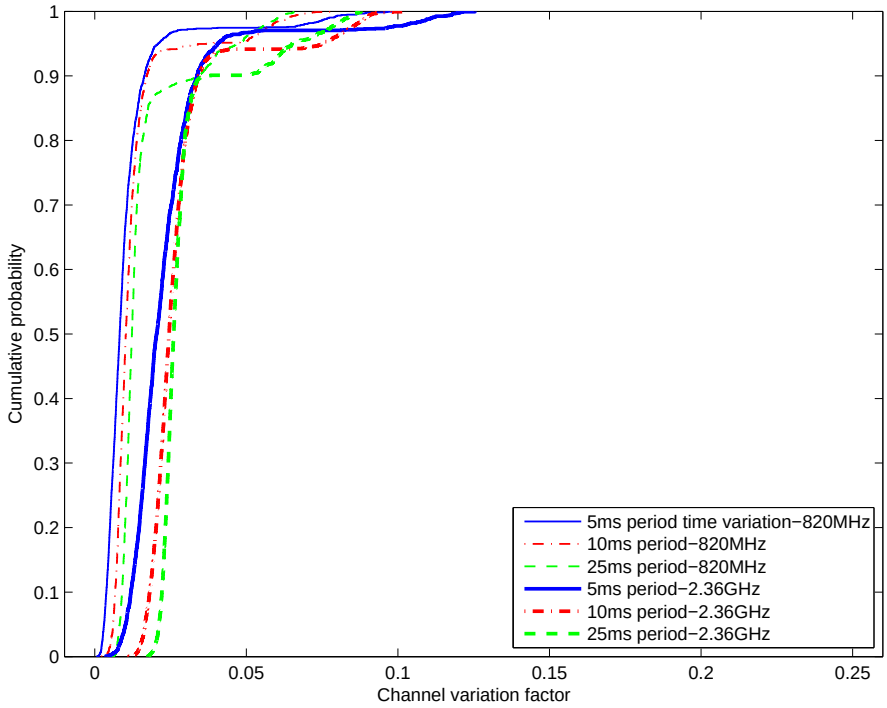

Figure 344: CDF of channel variation factor at 820 MHz and 2.36 GHz: chest to off-body; Standing; 4 m separation; 90° orientation

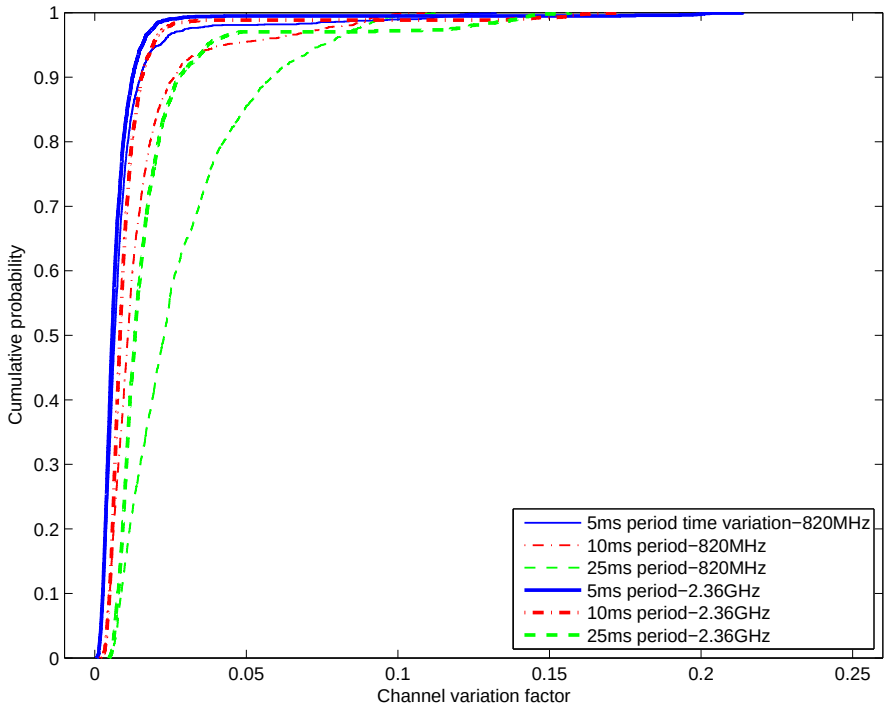

Figure 345: CDF of channel variation factor at 820 MHz and 2.36 GHz: chest to off-body; Walking; 1 m separation; 0° orientation

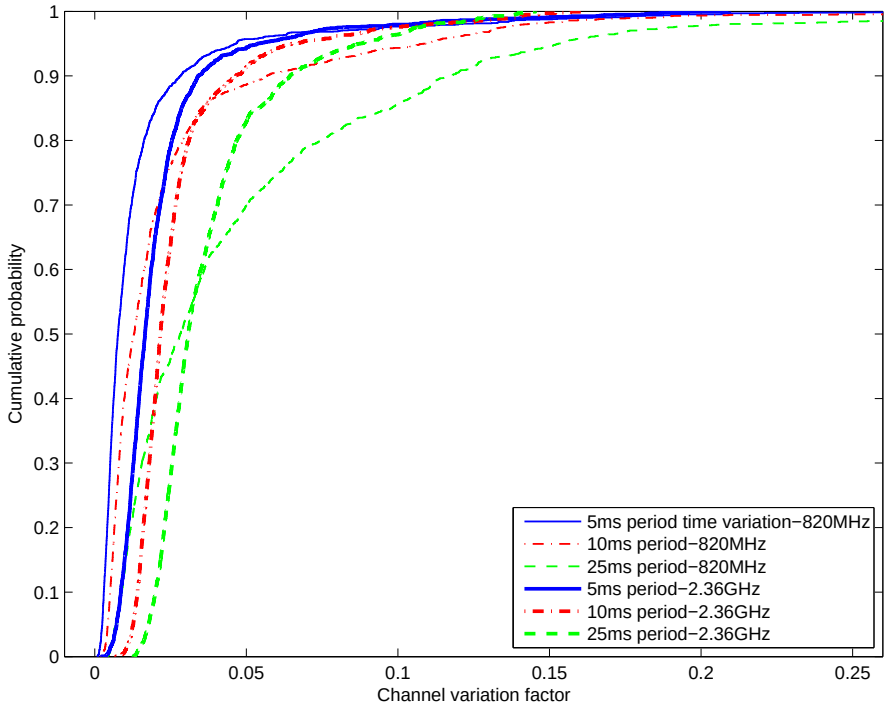

Figure 346: CDF of channel variation factor at 820 MHz and 2.36 GHz: chest to off-body; Walking; 1 m separation; 180° orientation

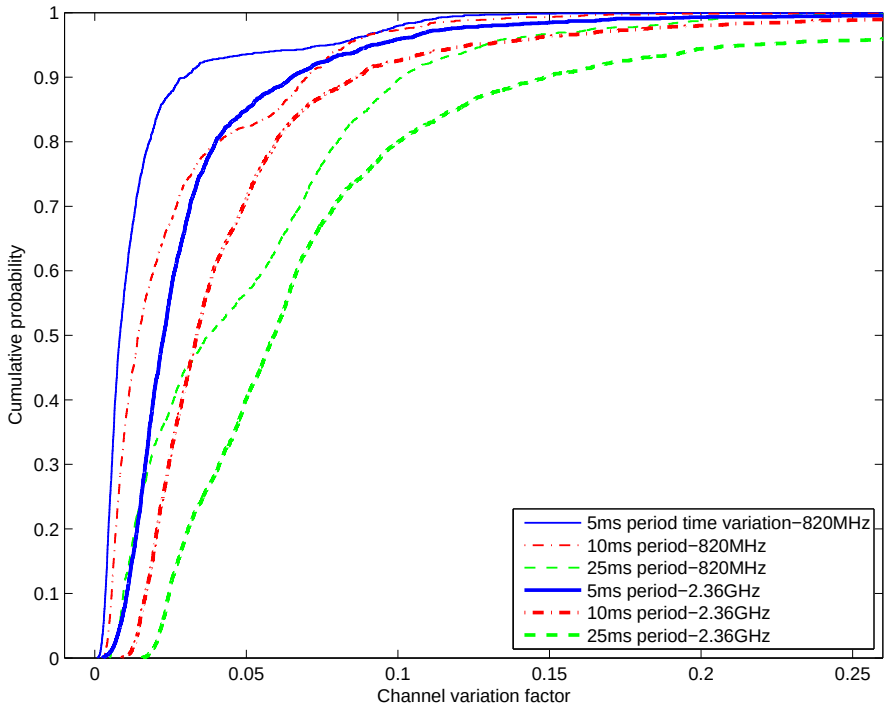

Figure 347: CDF of channel variation factor at 820 MHz and 2.36 GHz: chest to off-body; Walking; 1 m separation; 270° orientation

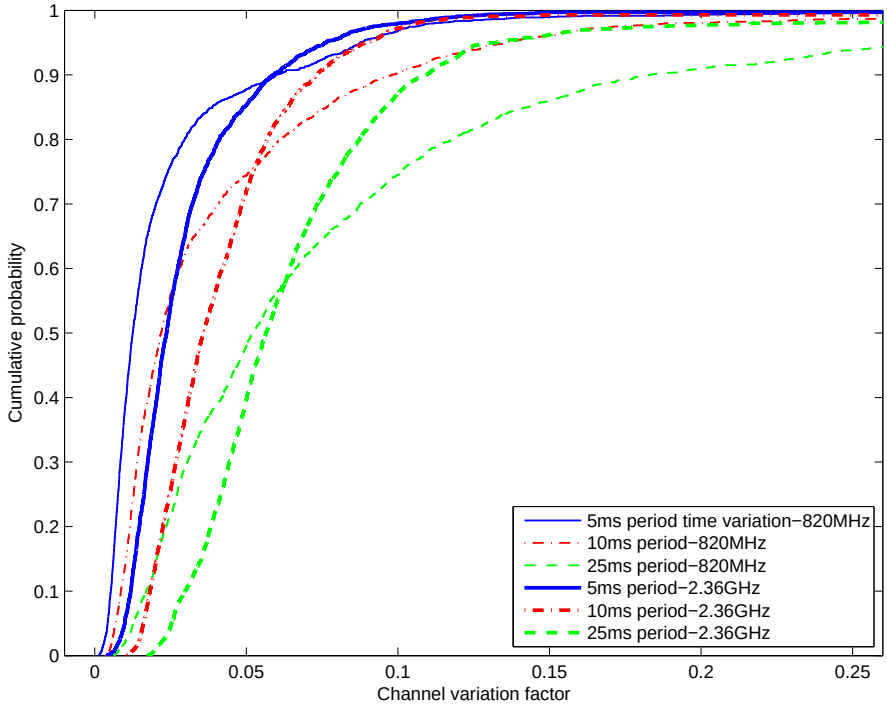

Figure 348: CDF of channel variation factor at 820 MHz and 2.36 GHz: chest to off-body; Walking; 1 m separation; 90° orientation

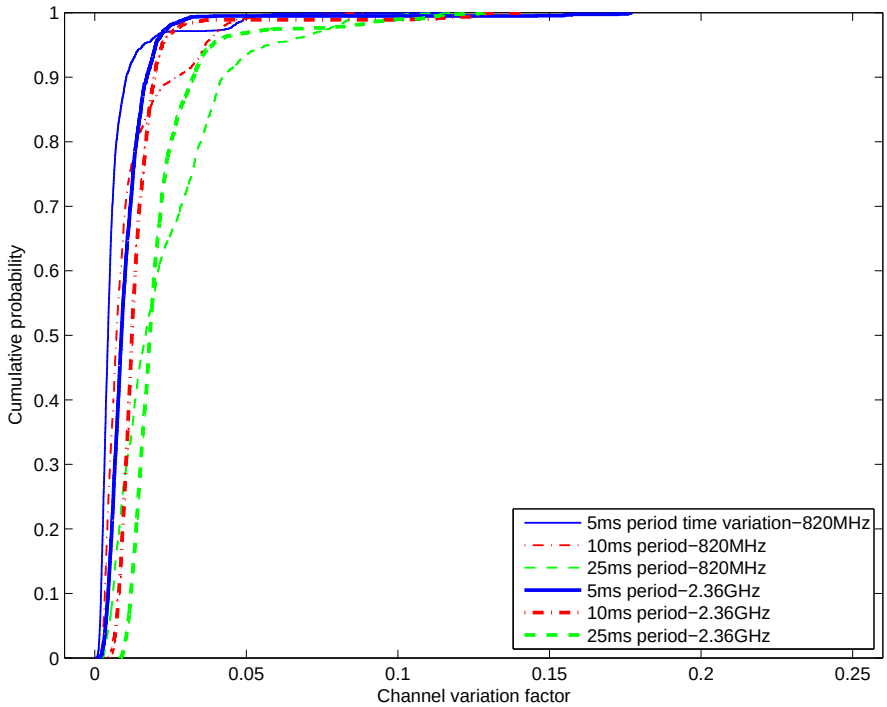

Figure 349: CDF of channel variation factor at 820 MHz and 2.36 GHz: chest to off-body; Walking; 2 m separation; 0° orientation

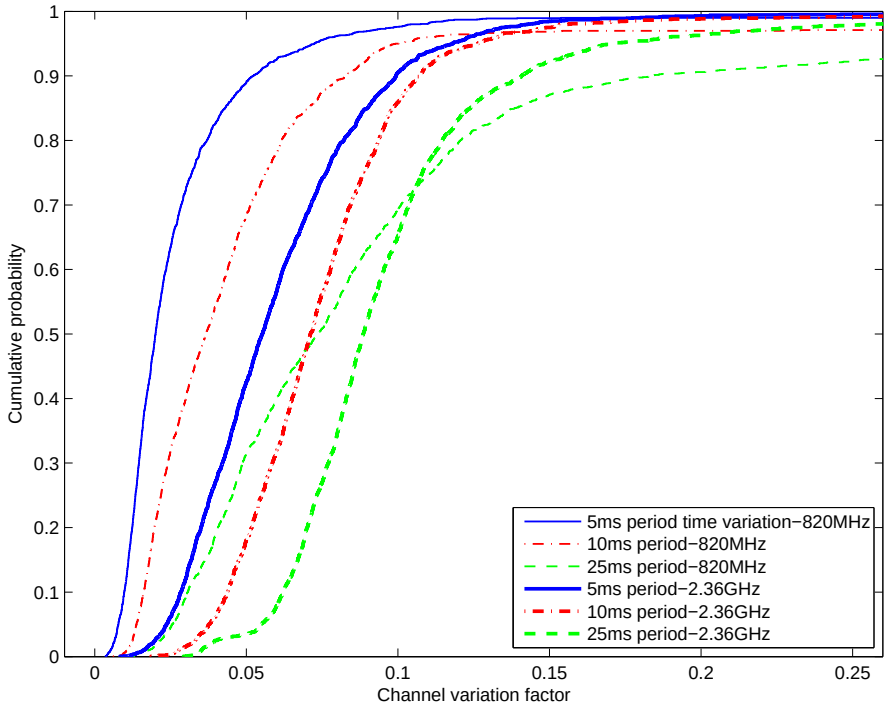

Figure 350: CDF of channel variation factor at 820 MHz and 2.36 GHz: chest to off-body; Walking; 2 m separation; 180° orientation

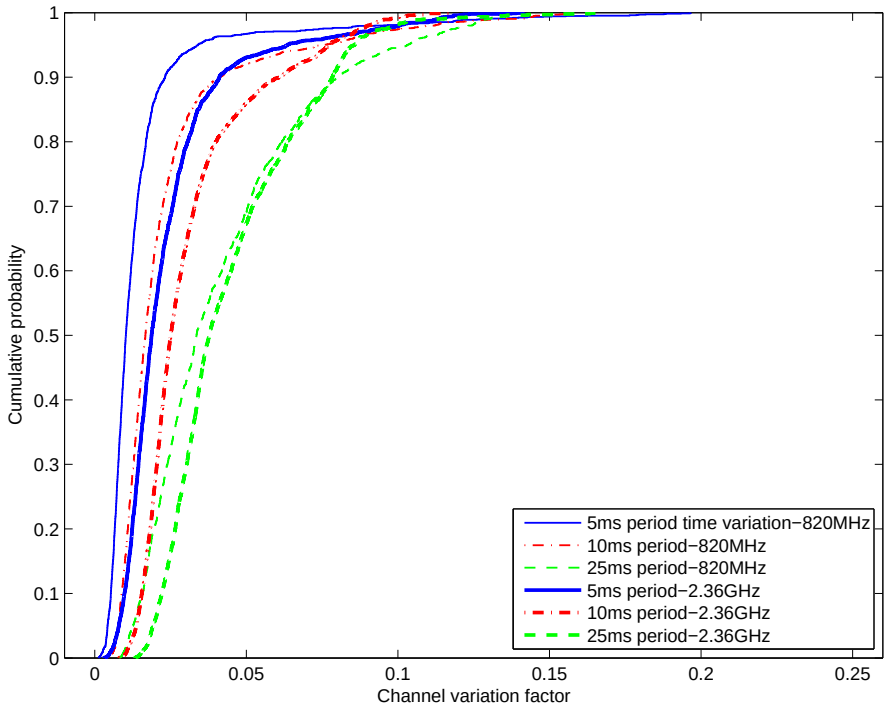

Figure 351: CDF of channel variation factor at 820 MHz and 2.36 GHz: chest to off-body; Walking; 2 m separation; 270° orientation

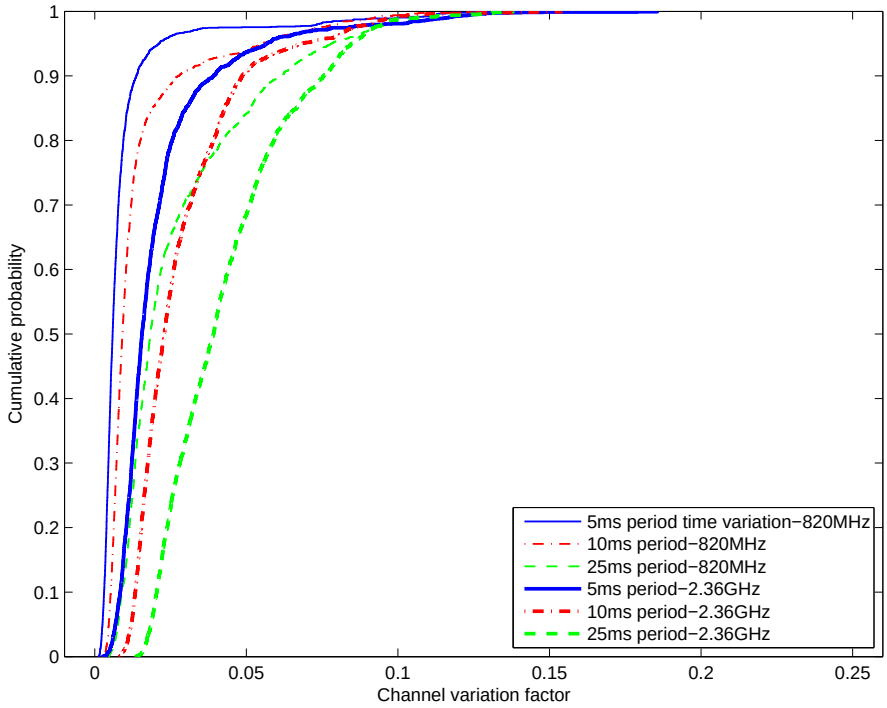

Figure 352: CDF of channel variation factor at 820 MHz and 2.36 GHz: chest to off-body; Walking; 2 m separation; 90° orientation

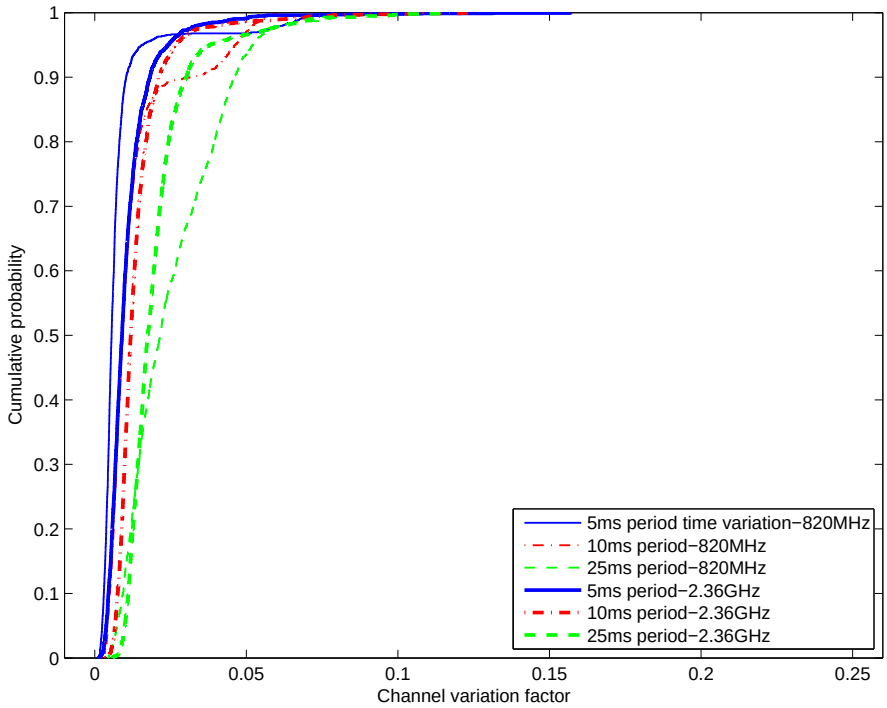

Figure 353: CDF of channel variation factor at 820 MHz and 2.36 GHz: chest to off-body; Walking; 3 m separation; 0° orientation

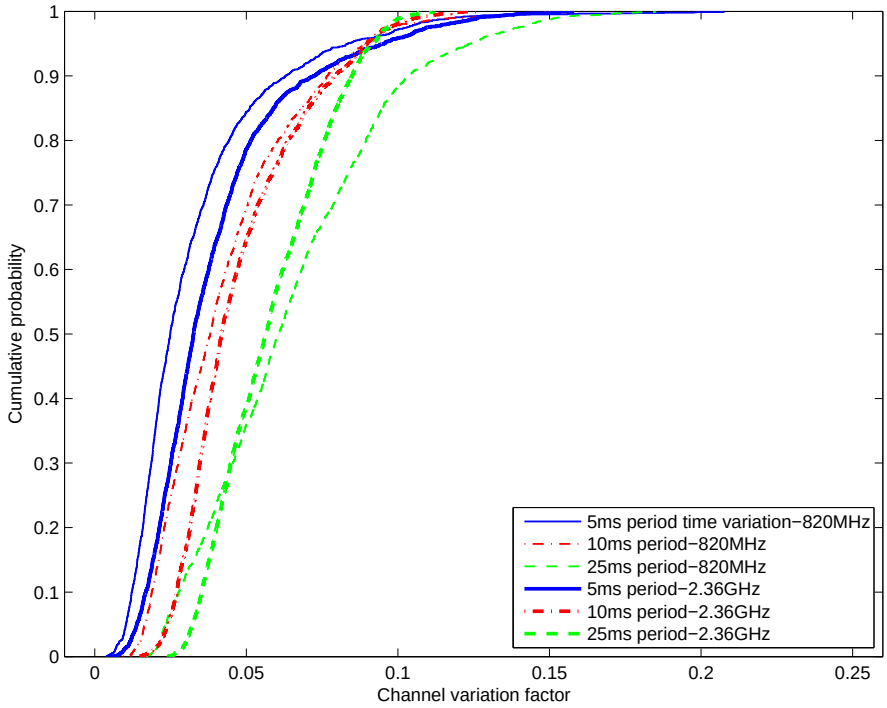

Figure 354: CDF of channel variation factor at 820 MHz and 2.36 GHz: chest to off-body; Walking; 3 m separation; 180° orientation

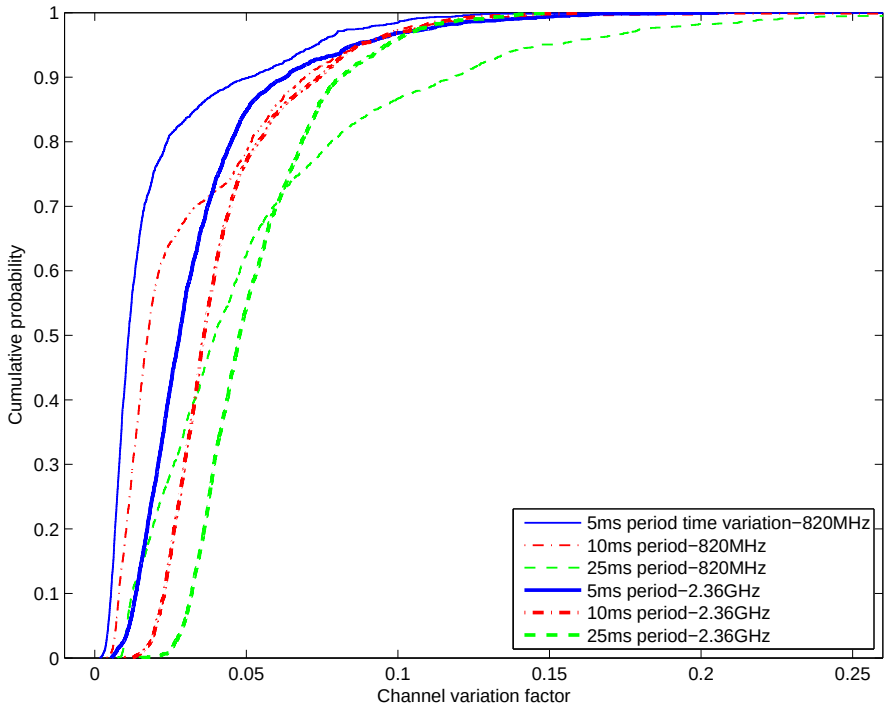

Figure 355: CDF of channel variation factor at 820 MHz and 2.36 GHz: chest to off-body; Walking; 3 m separation; 270° orientation

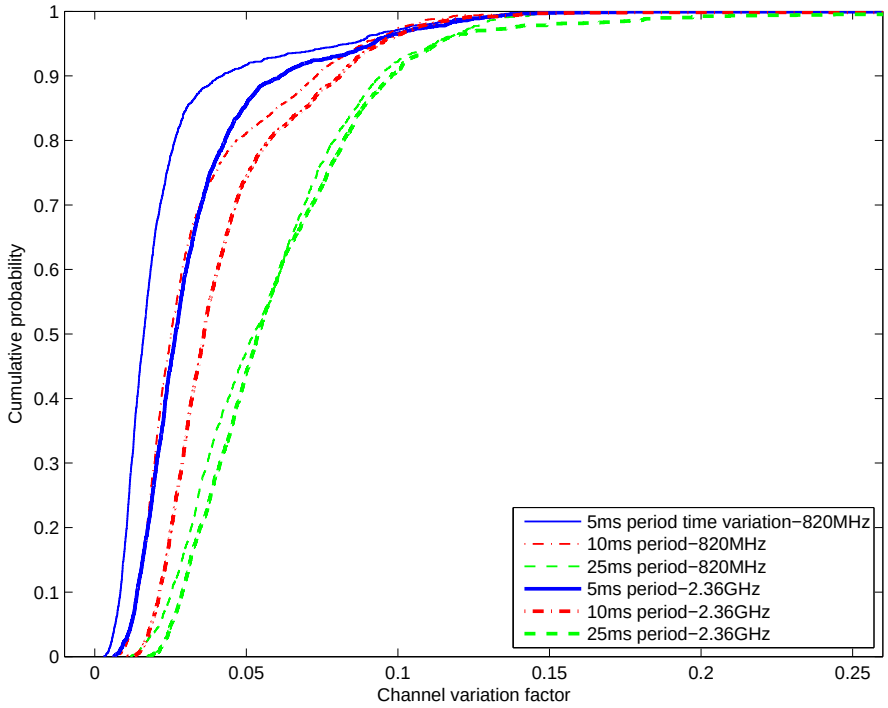

Figure 356: CDF of channel variation factor at 820 MHz and 2.36 GHz: chest to off-body; Walking; 3 m separation; 90° orientation

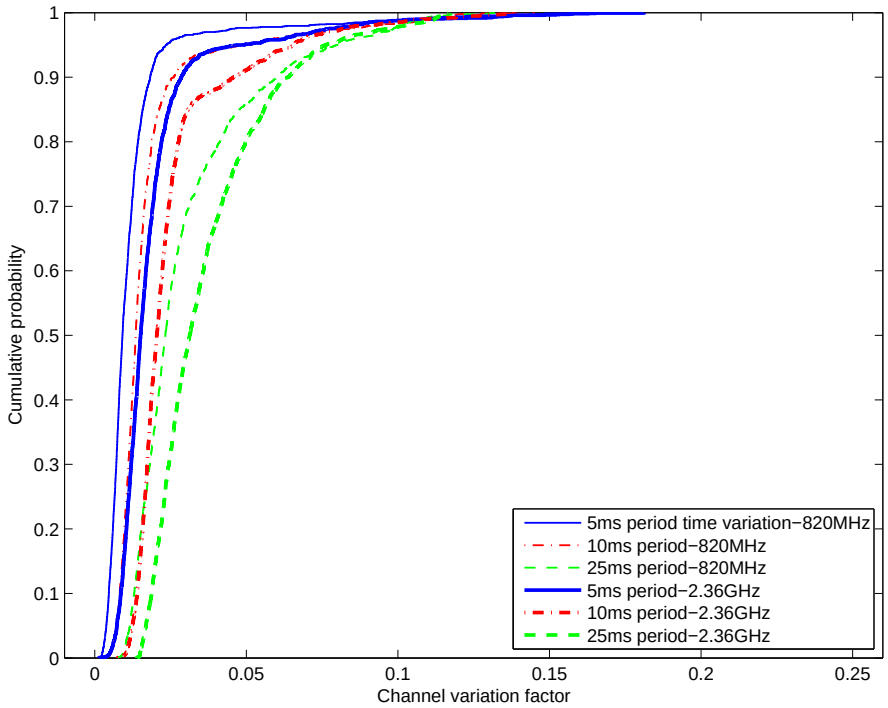

Figure 357: CDF of channel variation factor at 820 MHz and 2.36 GHz: chest to off-body; Walking; 4 m separation; 0° orientation

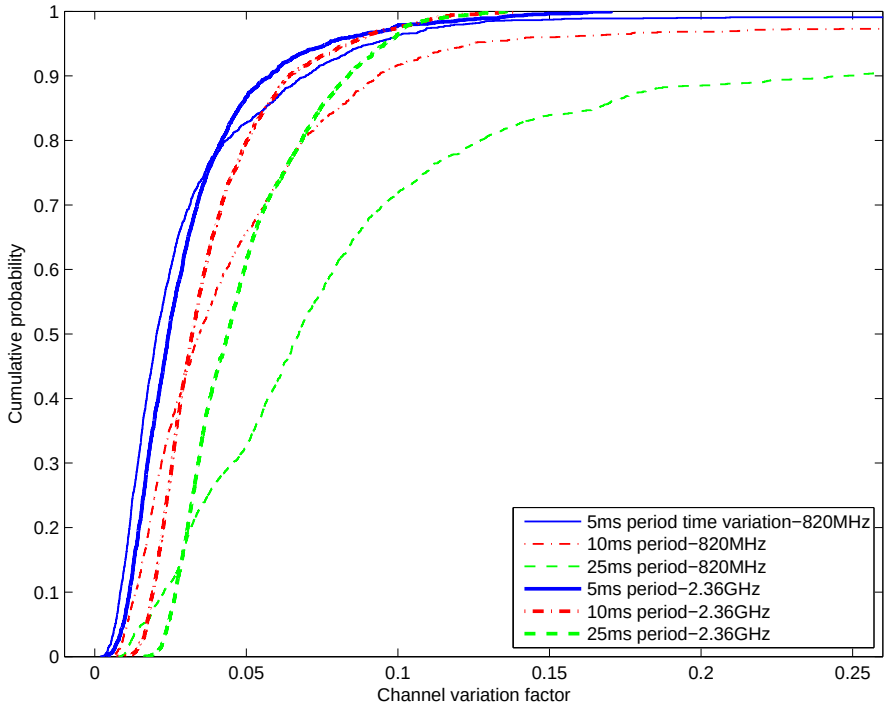

Figure 358: CDF of channel variation factor at 820 MHz and 2.36 GHz: chest to off-body; Walking; 4 m separation; 180° orientation

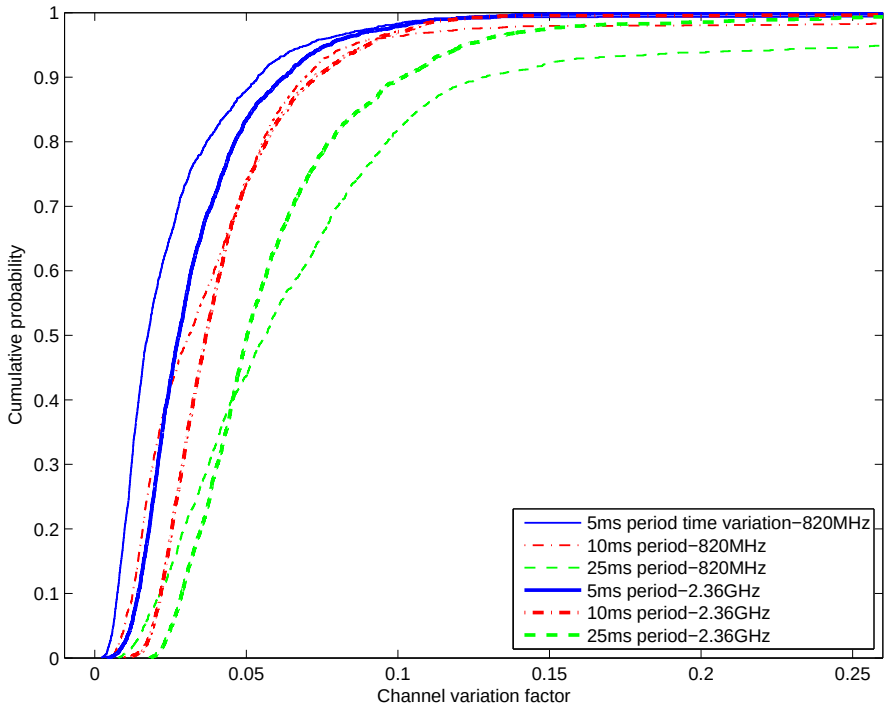

Figure 359: CDF of channel variation factor at 820 MHz and 2.36 GHz: chest to off-body; Walking; 4 m separation; 270° orientation

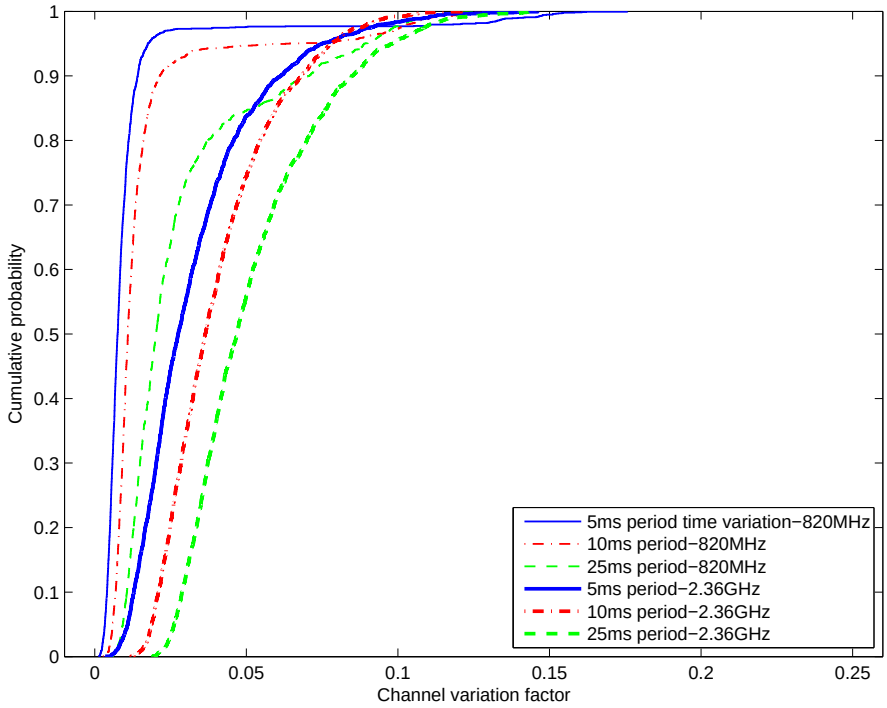

Figure 360: CDF of channel variation factor at 820 MHz and 2.36 GHz: chest to off-body; Walking; 4 m separation; 90° orientation

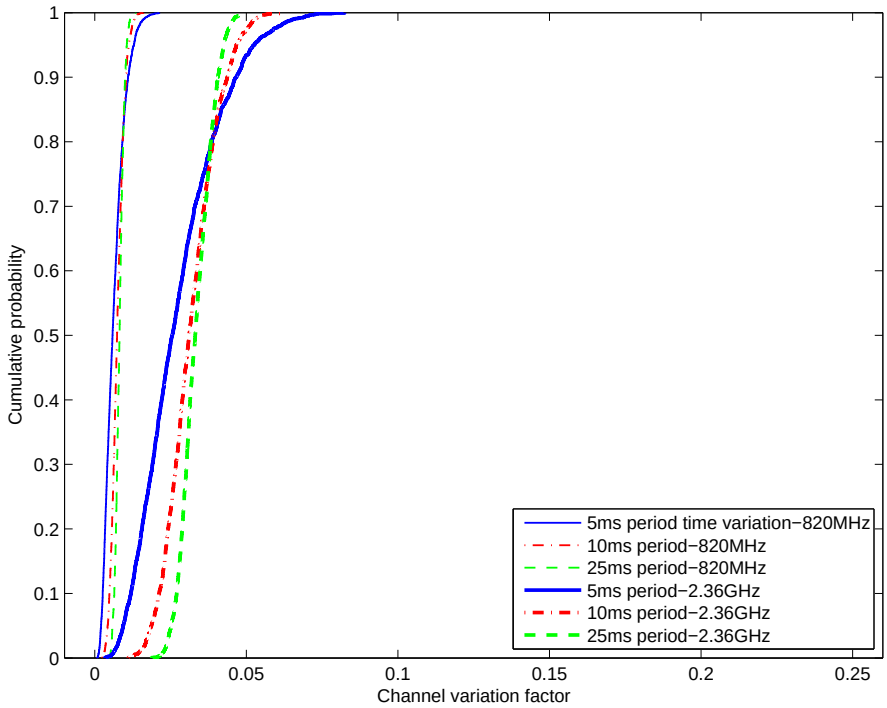

Figure 361: CDF of channel variation factor at 820 MHz and 2.36 GHz: right wrist to off-body; Standing; 1 m separation; 0° orientation

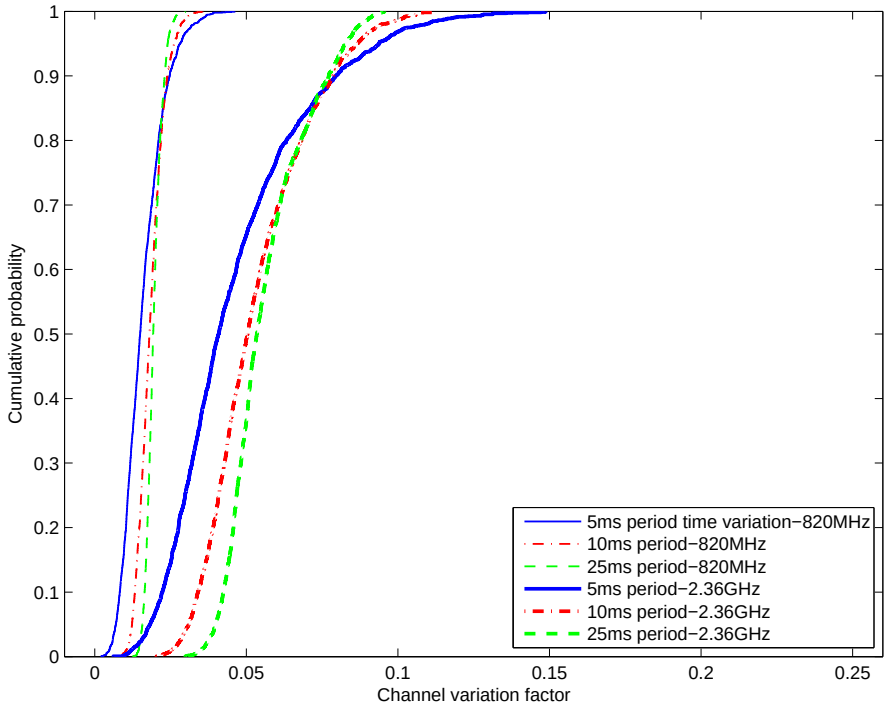

Figure 362: CDF of channel variation factor at 820 MHz and 2.36 GHz: right wrist to off-body; Standing; 1 m separation; 180° orientation

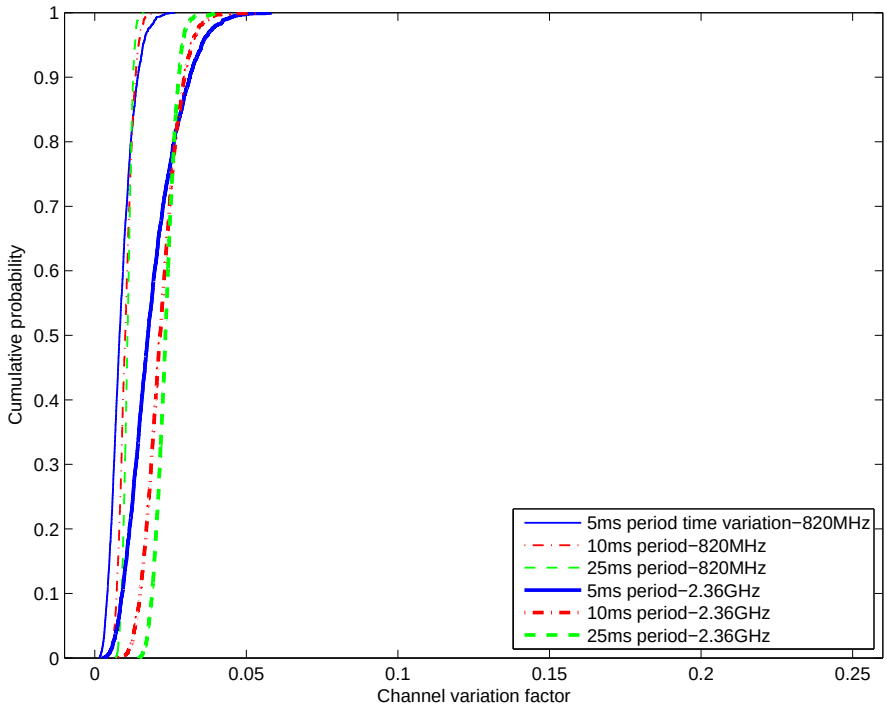

Figure 363: CDF of channel variation factor at 820 MHz and 2.36 GHz: right wrist to off-body; Standing; 1 m separation; 270° orientation

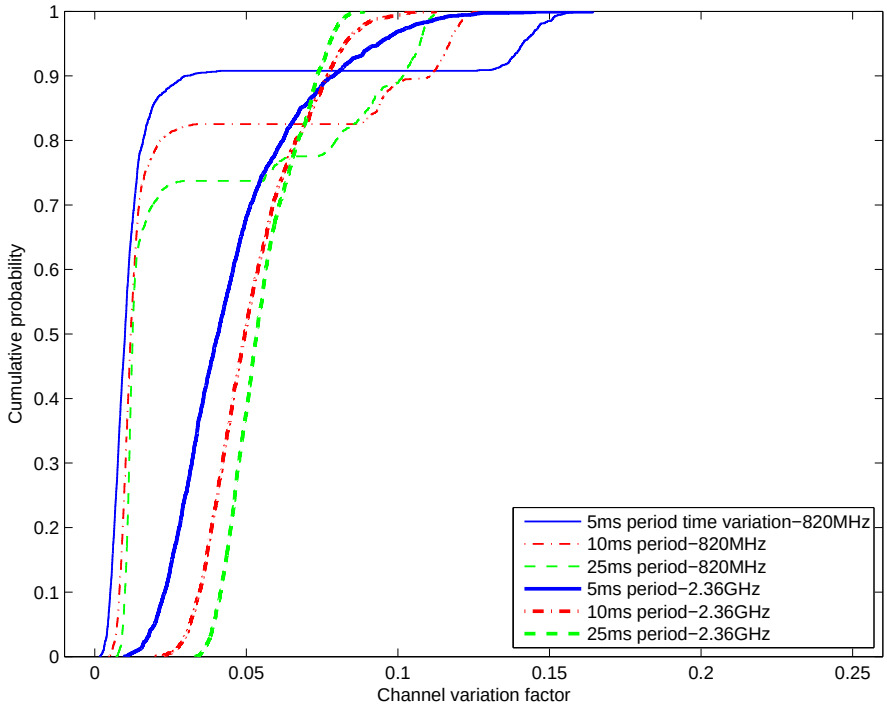

Figure 364: CDF of channel variation factor at 820 MHz and 2.36 GHz: right wrist to off-body; Standing; 1 m separation; 90° orientation

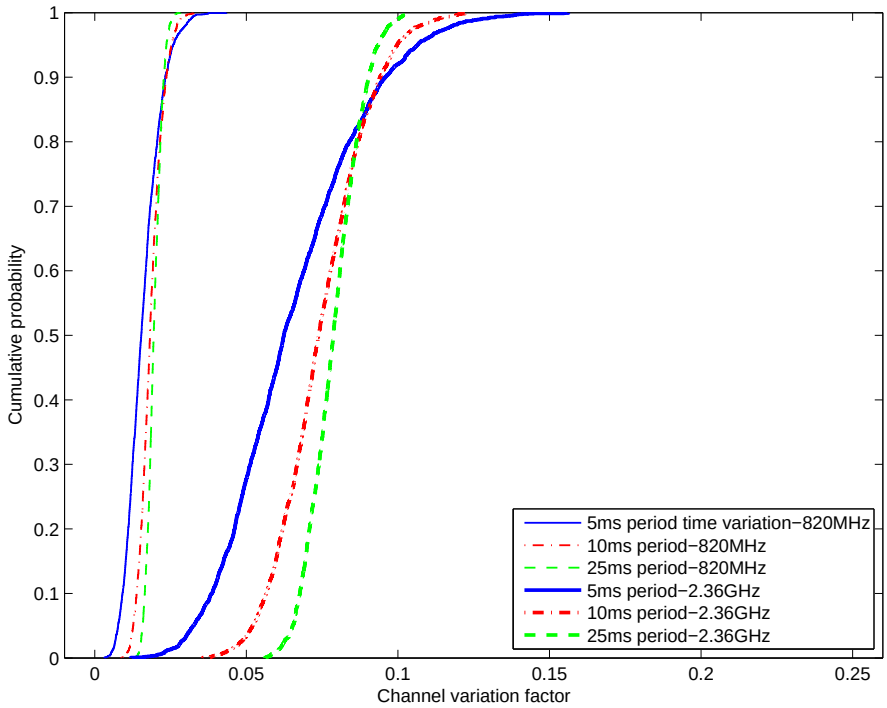

Figure 365: CDF of channel variation factor at 820 MHz and 2.36 GHz: right wrist to off-body; Standing; 2 m separation; 0° orientation

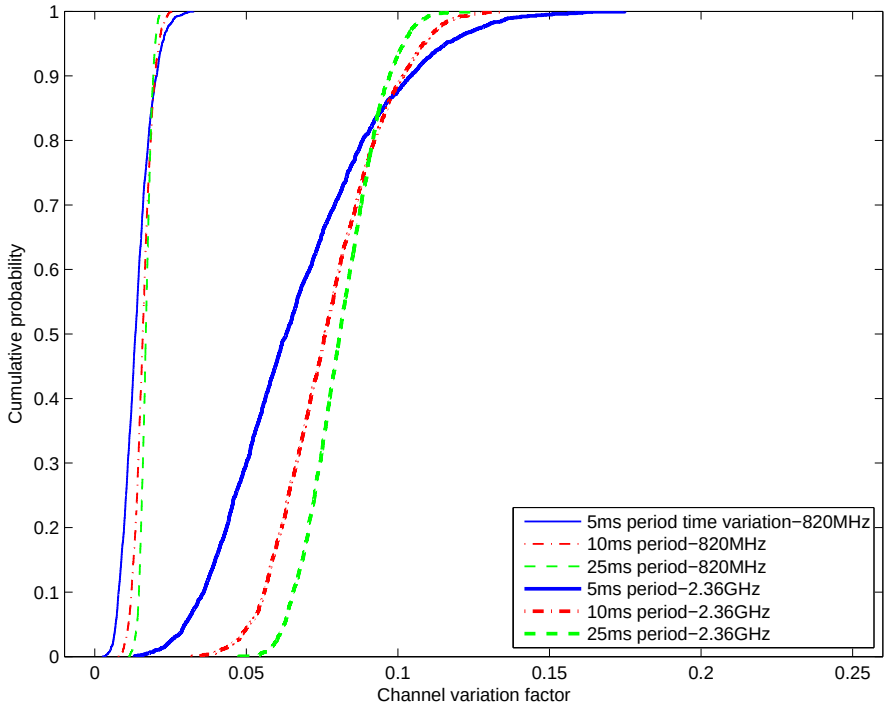

Figure 366: CDF of channel variation factor at 820 MHz and 2.36 GHz: right wrist to off-body; Standing; 2 m separation; 180° orientation

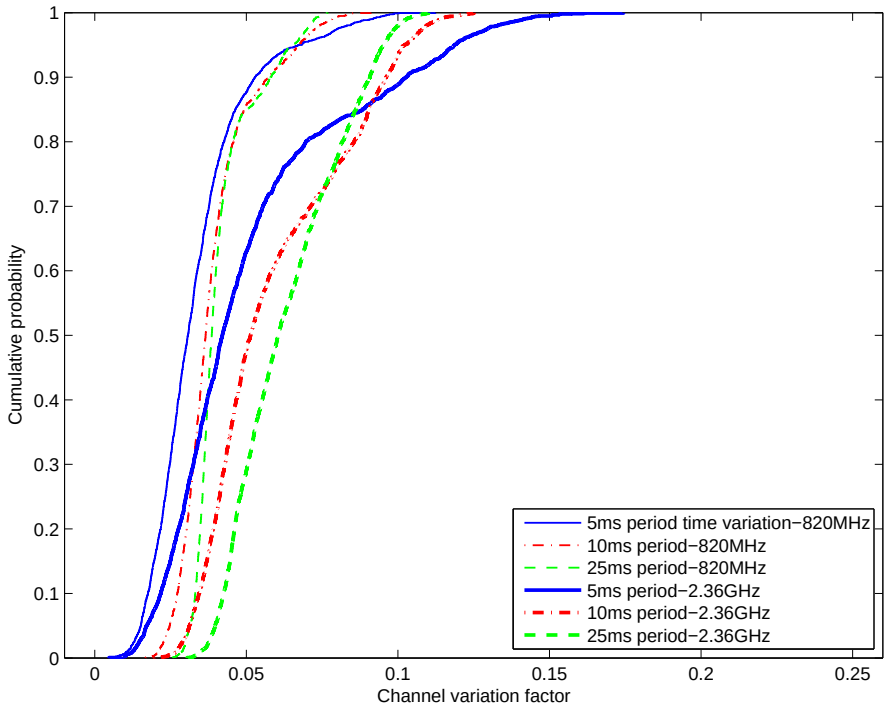

Figure 367: CDF of channel variation factor at 820 MHz and 2.36 GHz: right wrist to off-body; Standing; 2 m separation; 270° orientation

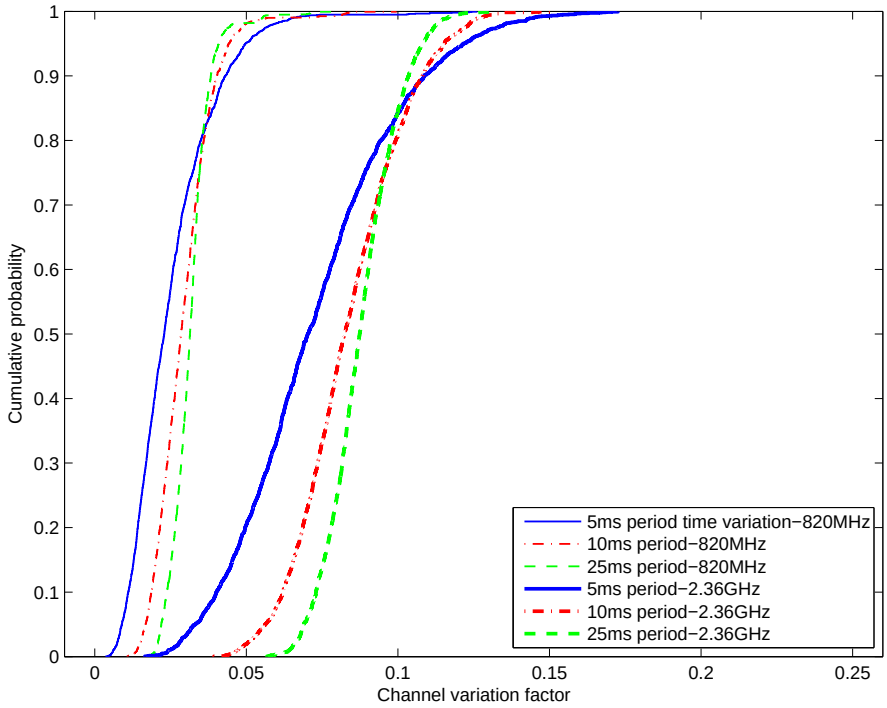

Figure 368: CDF of channel variation factor at 820 MHz and 2.36 GHz: right wrist to off-body; Standing; 2 m separation; 90° orientation

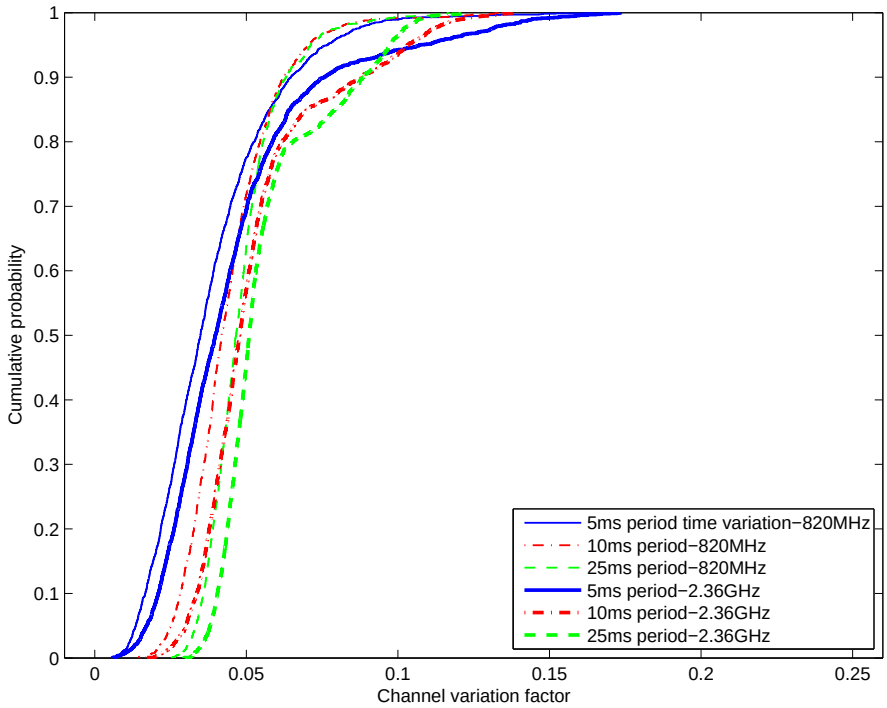

Figure 369: CDF of channel variation factor at 820 MHz and 2.36 GHz: right wrist to off-body; Standing; 3 m separation; 0° orientation

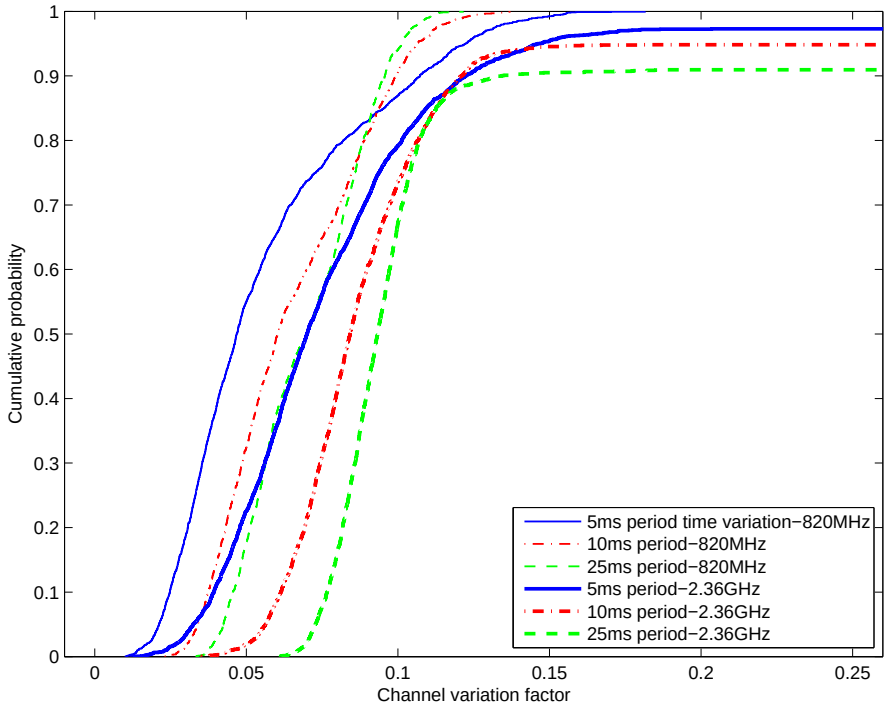

Figure 370: CDF of channel variation factor at 820 MHz and 2.36 GHz: right wrist to off-body; Standing; 3 m separation; 180° orientation

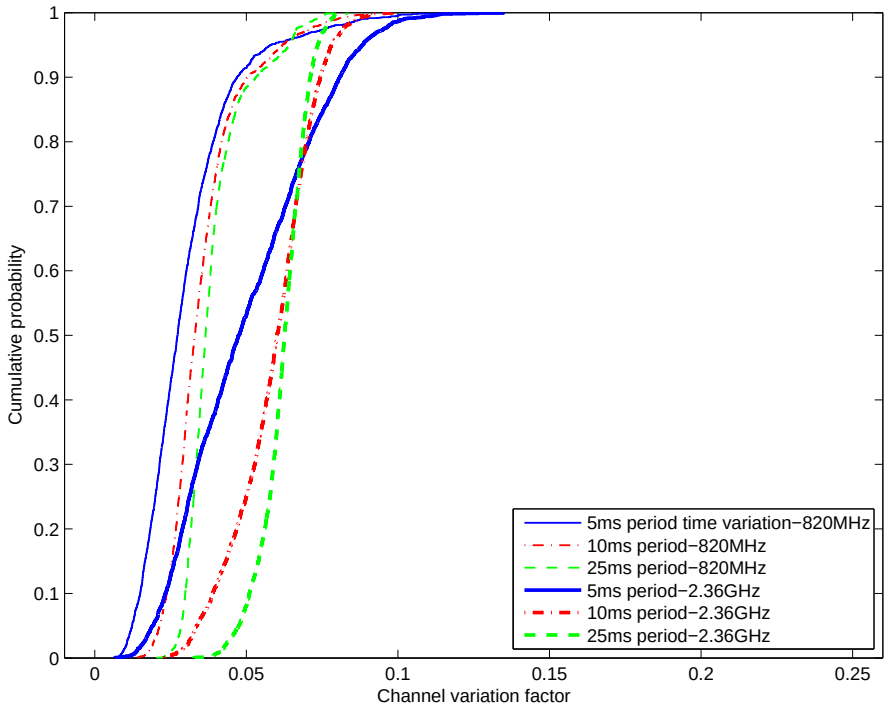

Figure 371: CDF of channel variation factor at 820 MHz and 2.36 GHz: right wrist to off-body; Standing; 3 m separation; 270° orientation

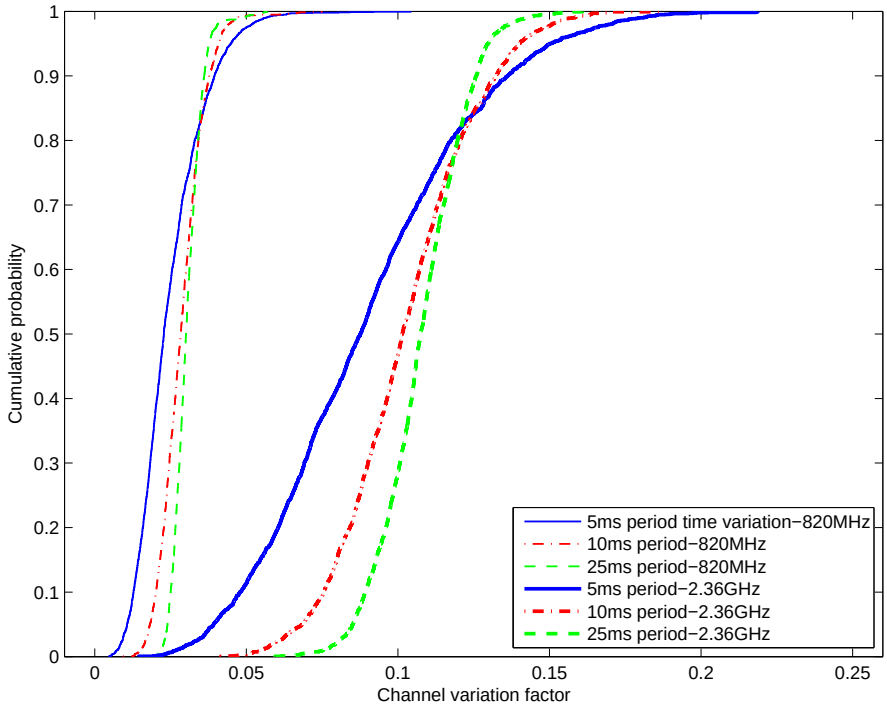

Figure 372: CDF of channel variation factor at 820 MHz and 2.36 GHz: right wrist to off-body; Standing; 3 m separation; 90° orientation

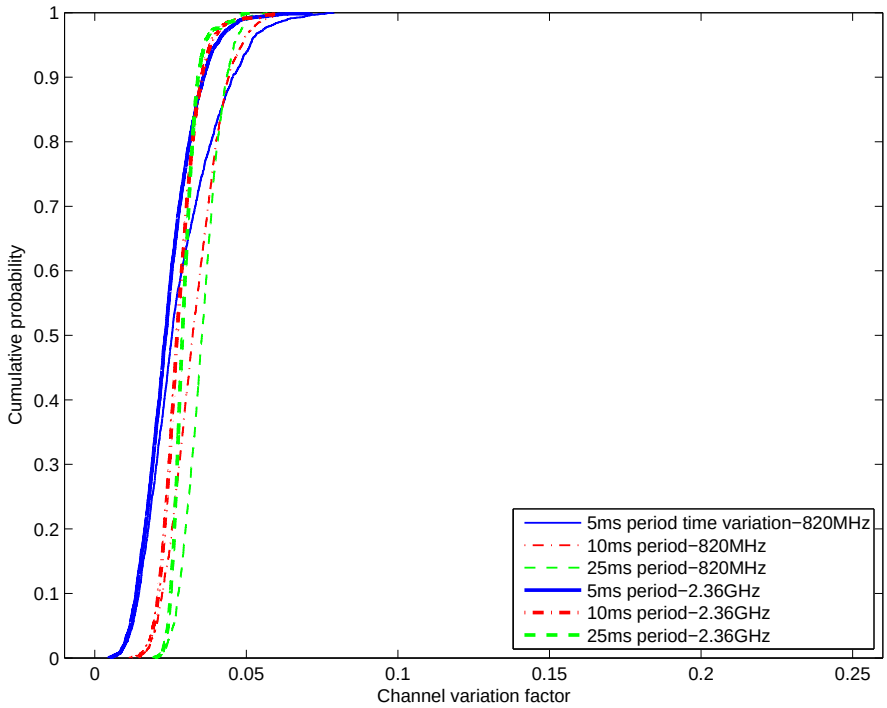

Figure 373: CDF of channel variation factor at 820 MHz and 2.36 GHz: right wrist to off-body; Standing; 4 m separation; 0° orientation

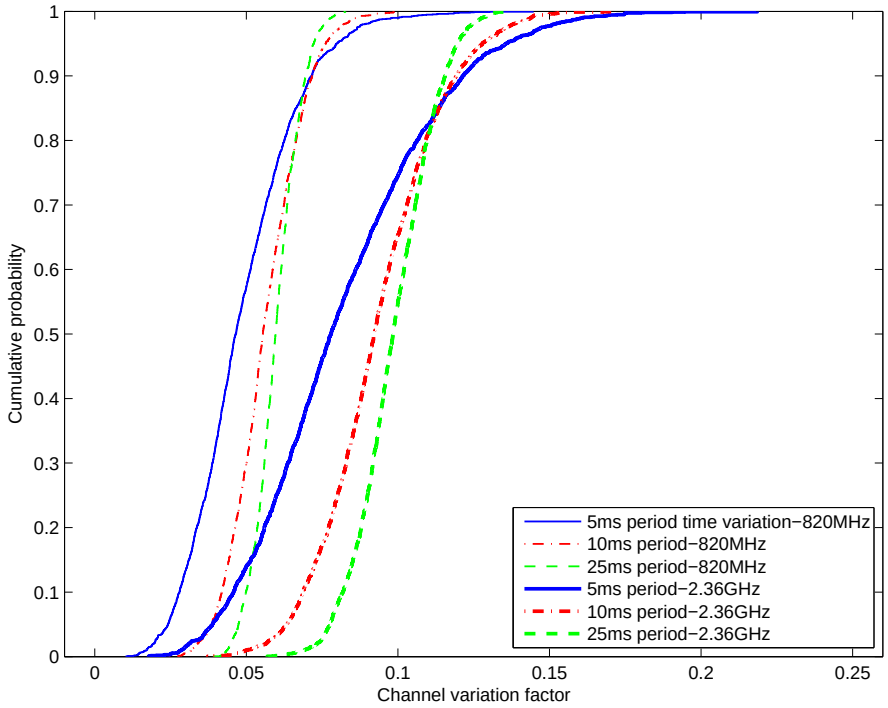

Figure 374: CDF of channel variation factor at 820 MHz and 2.36 GHz: right wrist to off-body; Standing; 4 m separation; 180° orientation

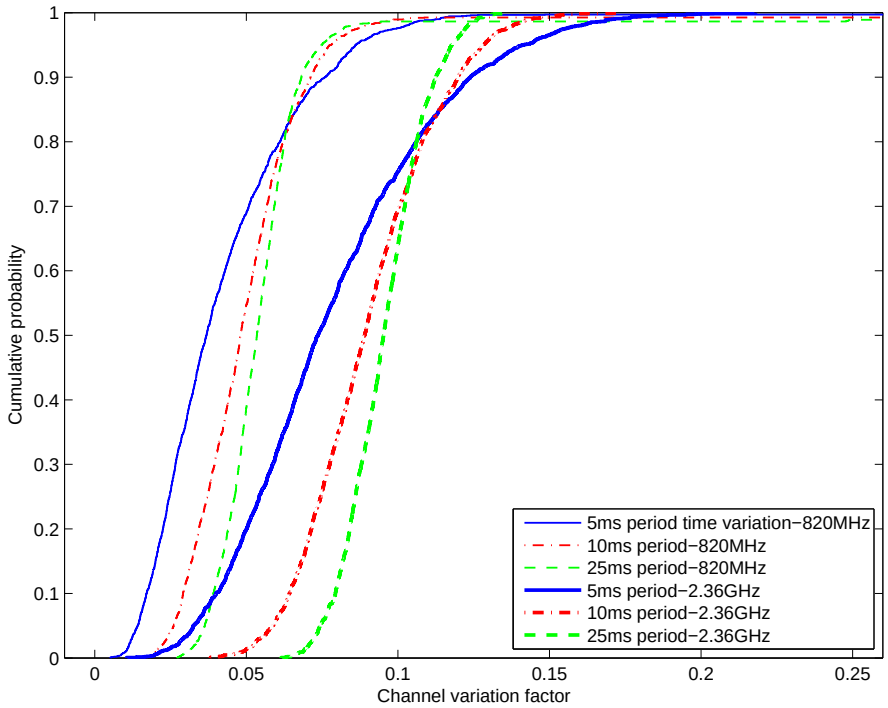

Figure 375: CDF of channel variation factor at 820 MHz and 2.36 GHz: right wrist to off-body; Standing; 4 m separation; 270° orientation

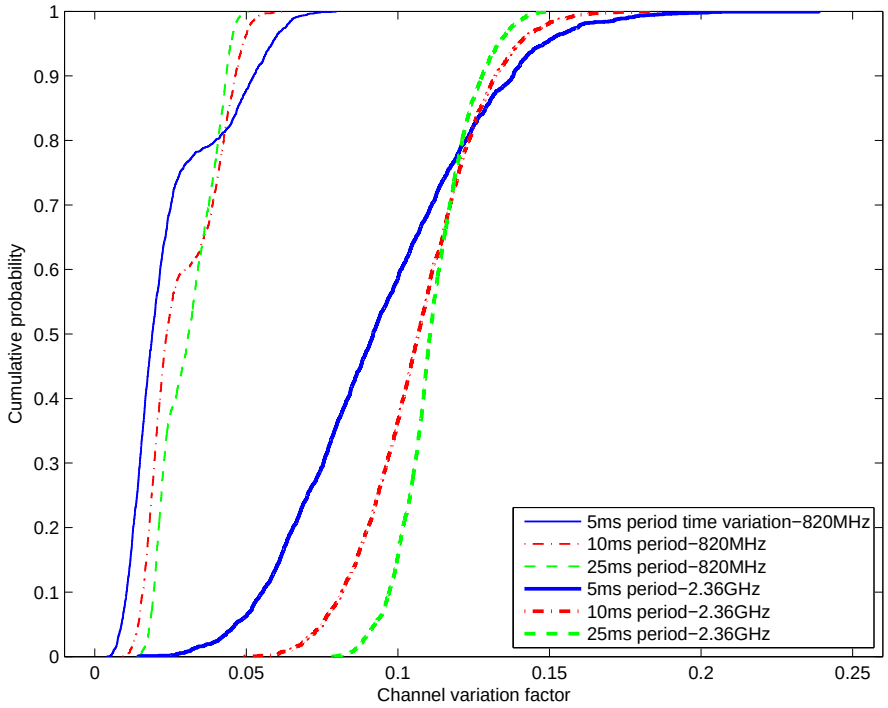

Figure 376: CDF of channel variation factor at 820 MHz and 2.36 GHz: right wrist to off-body; Standing; 4 m separation; 90° orientation

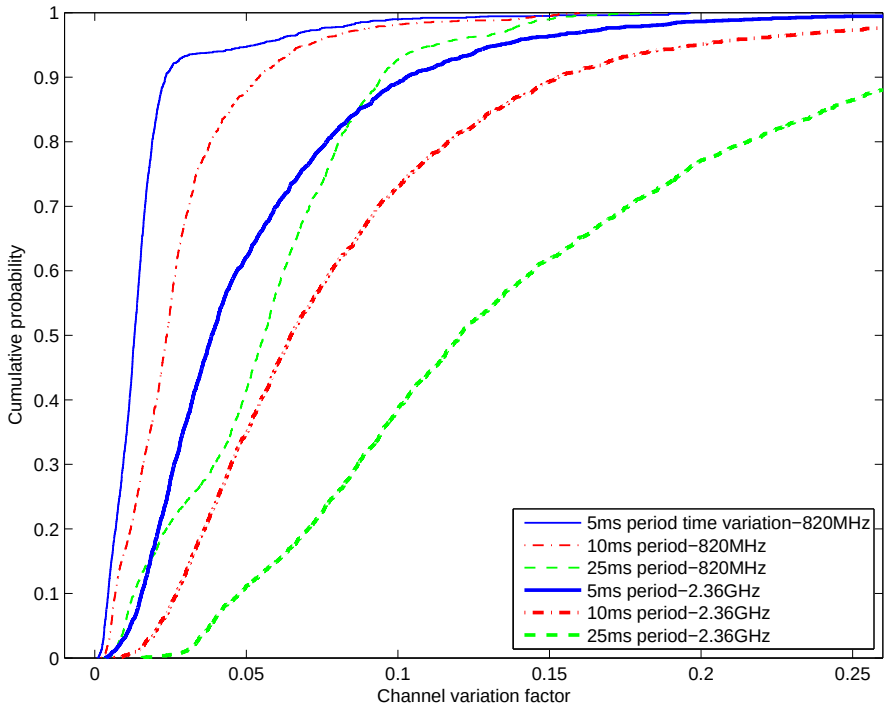

Figure 377: CDF of channel variation factor at 820 MHz and 2.36 GHz: right wrist to off-body; Walking; 1 m separation; 0° orientation

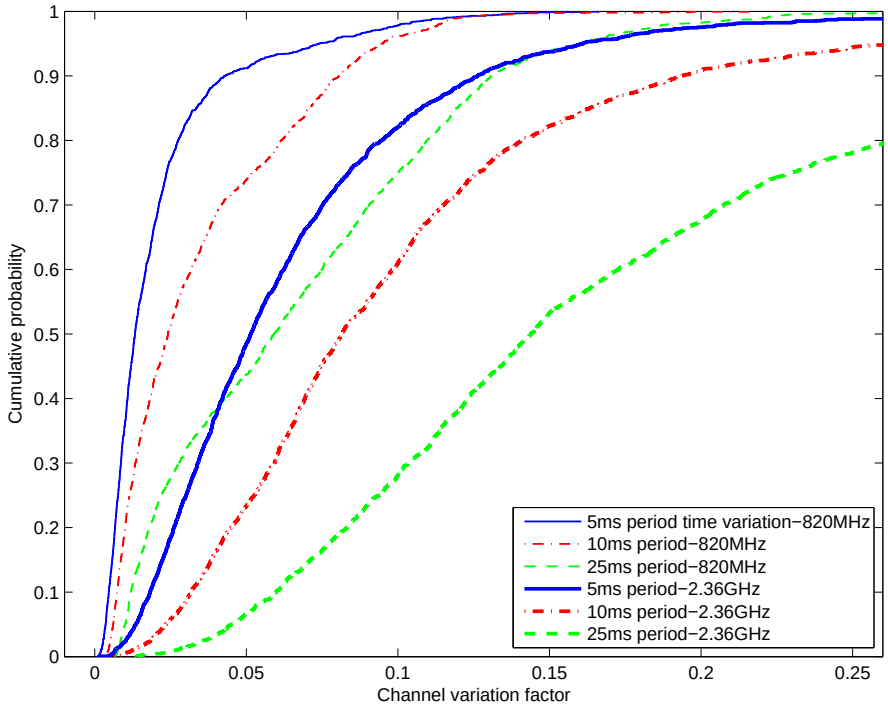

Figure 378: CDF of channel variation factor at 820 MHz and 2.36 GHz: right wrist to off-body; Walking; 1 m separation; 180° orientation

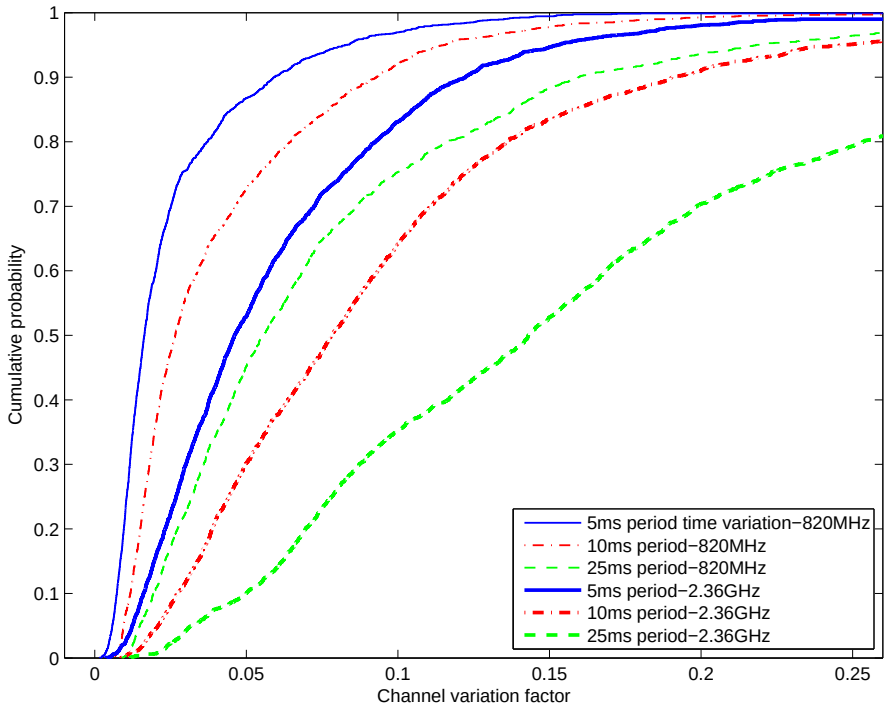

Figure 379: CDF of channel variation factor at 820 MHz and 2.36 GHz: right wrist to off-body; Walking; 1 m separation; 270° orientation

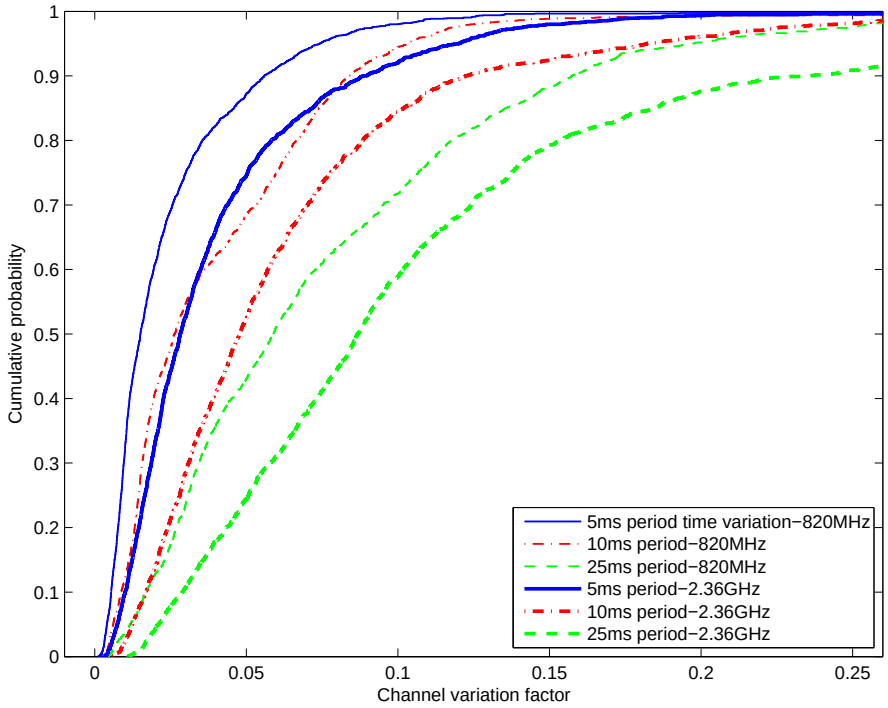

Figure 380: CDF of channel variation factor at 820 MHz and 2.36 GHz: right wrist to off-body; Walking; 1 m separation; 90° orientation

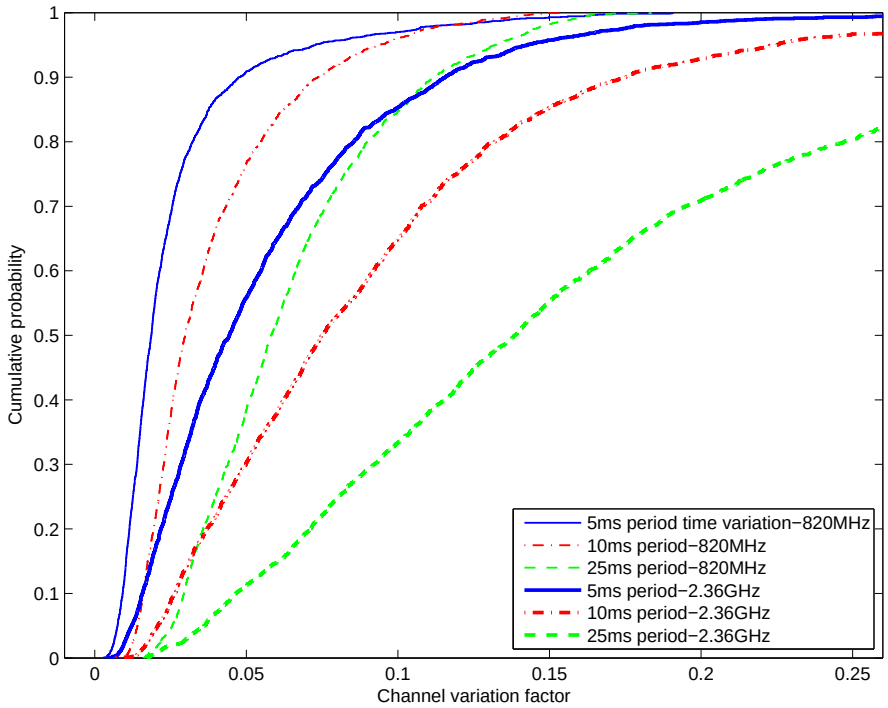

Figure 381: CDF of channel variation factor at 820 MHz and 2.36 GHz: right wrist to off-body; Walking; 2 m separation; 0° orientation

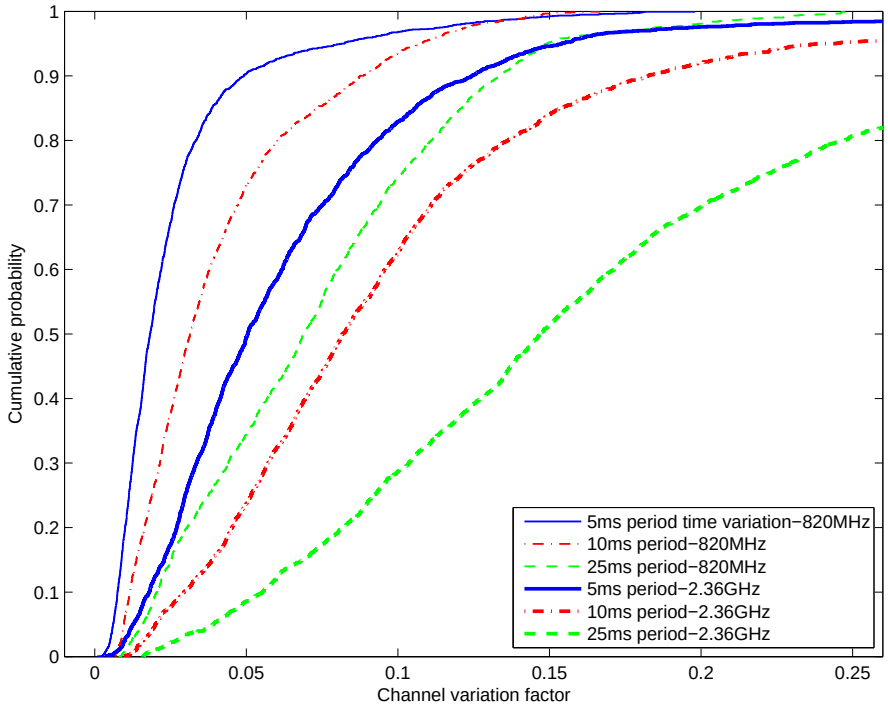

Figure 382: CDF of channel variation factor at 820 MHz and 2.36 GHz: right wrist to off-body; Walking; 2 m separation; 180° orientation

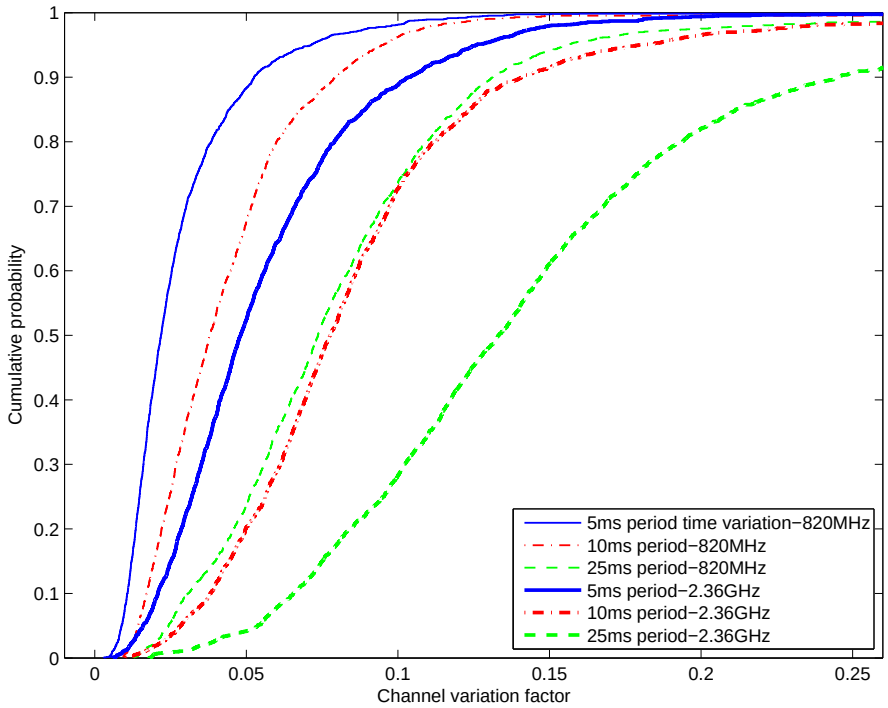

Figure 383: CDF of channel variation factor at 820 MHz and 2.36 GHz: right wrist to off-body; Walking; 2 m separation; 270° orientation

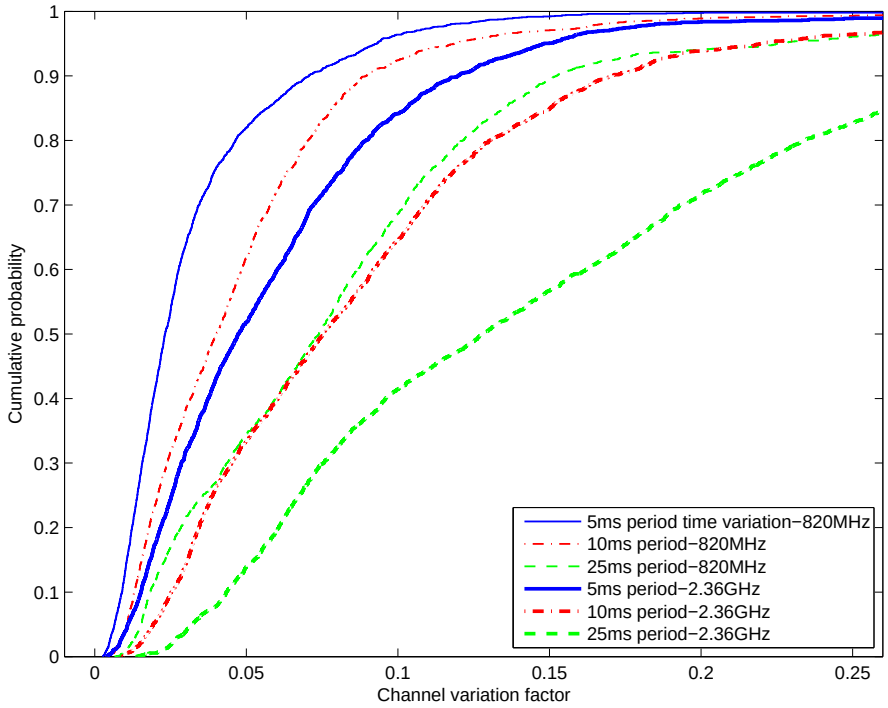

Figure 384: CDF of channel variation factor at 820 MHz and 2.36 GHz: right wrist to off-body; Walking; 2 m separation; 90° orientation

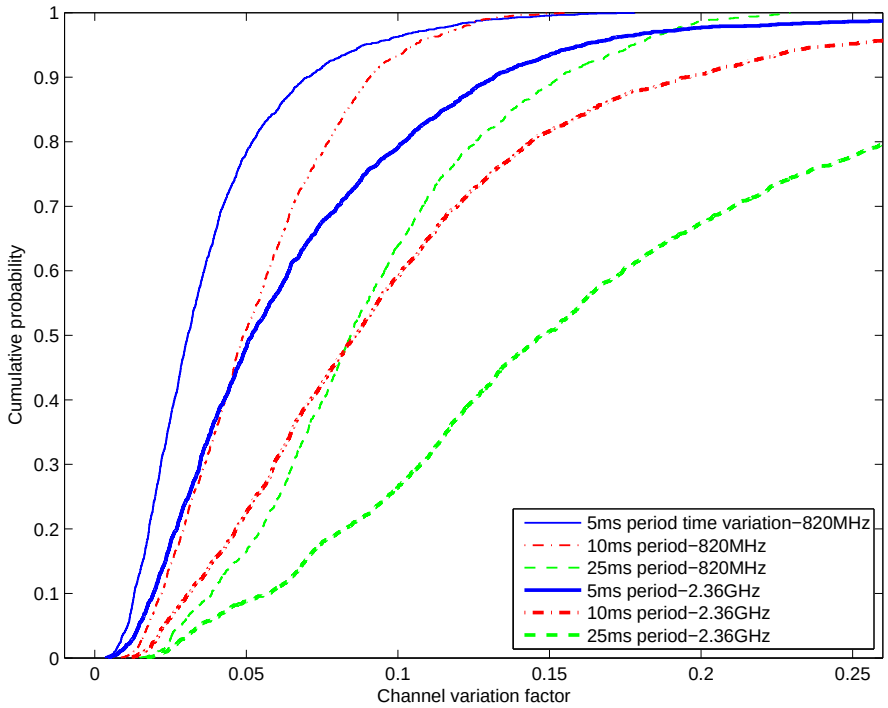

Figure 385: CDF of channel variation factor at 820 MHz and 2.36 GHz: right wrist to off-body; Walking; 3 m separation; 0° orientation

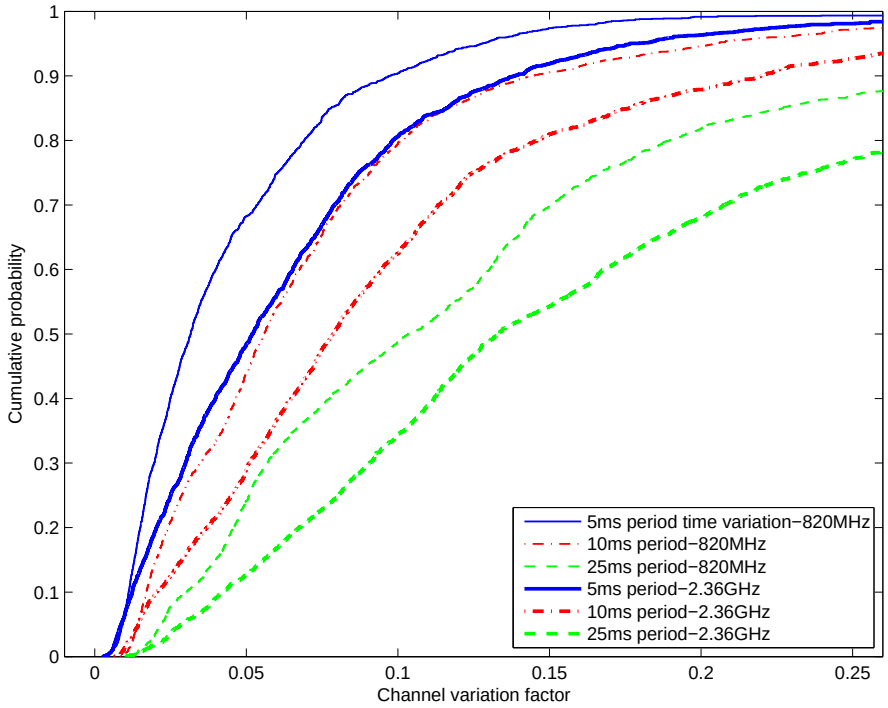

Figure 386: CDF of channel variation factor at 820 MHz and 2.36 GHz: right wrist to off-body; Walking; 3 m separation; 180° orientation

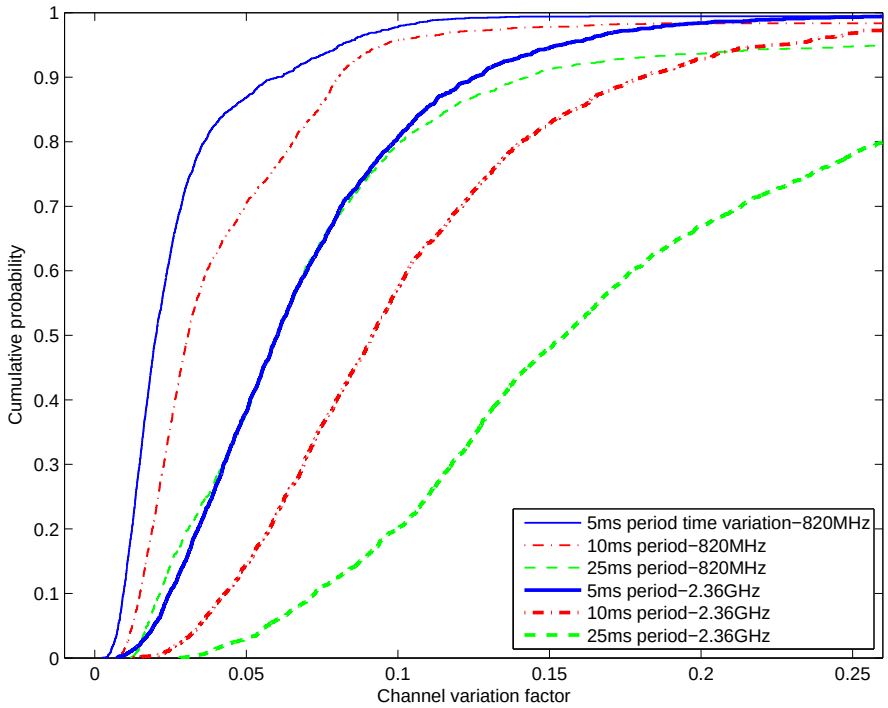

Figure 387: CDF of channel variation factor at 820 MHz and 2.36 GHz: right wrist to off-body; Walking; 3 m separation; 270° orientation

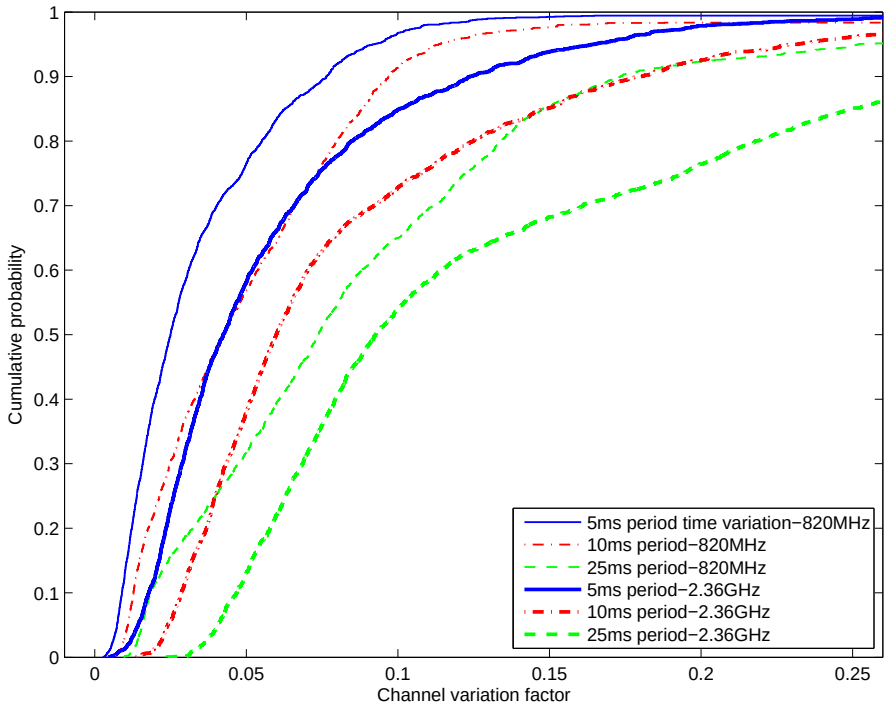

Figure 388: CDF of channel variation factor at 820 MHz and 2.36 GHz: right wrist to off-body; Walking; 3 m separation; 90° orientation

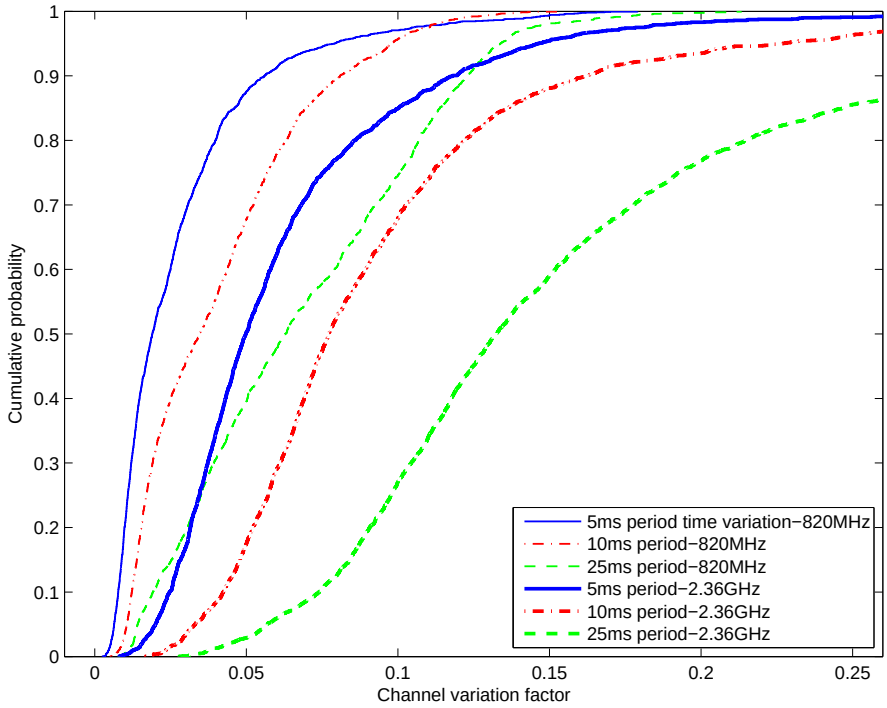

Figure 389: CDF of channel variation factor at 820 MHz and 2.36 GHz: right wrist to off-body; Walking; 4 m separation; 0° orientation

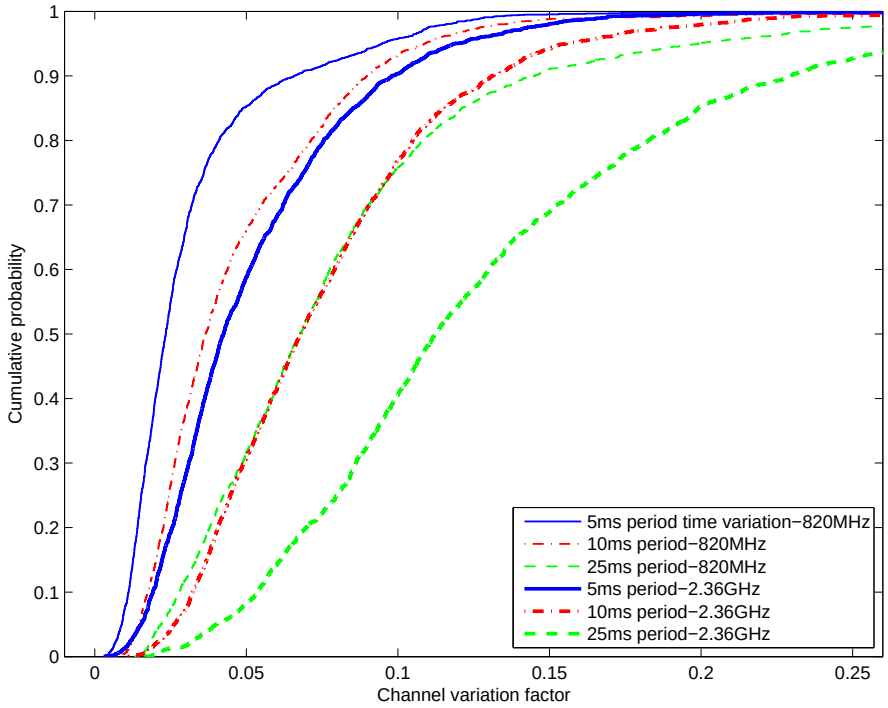

Figure 390: CDF of channel variation factor at 820 MHz and 2.36 GHz: right wrist to off-body; Walking; 4 m separation; 180° orientation

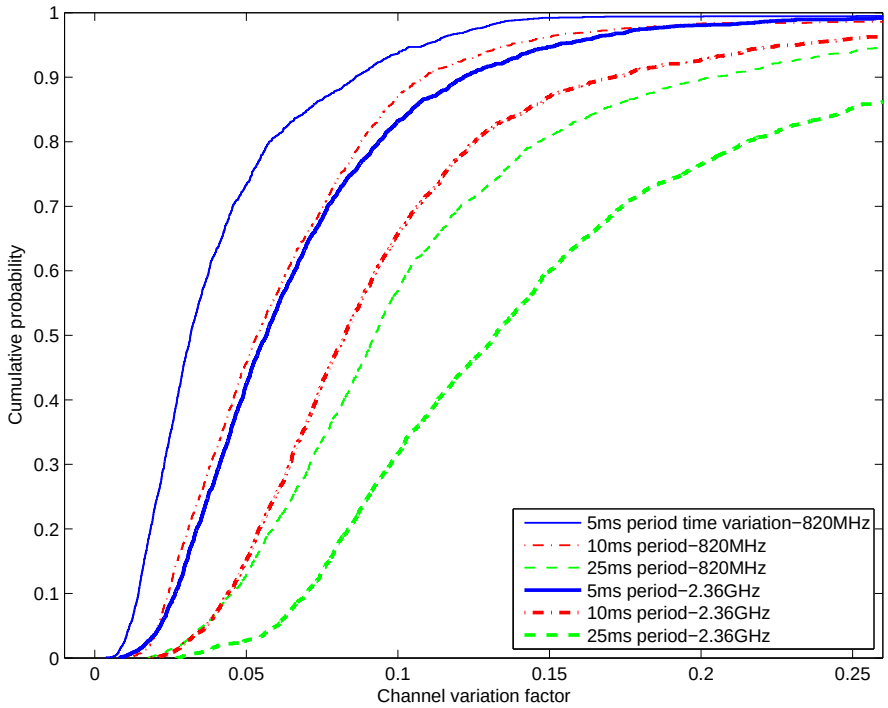

Figure 391: CDF of channel variation factor at 820 MHz and 2.36 GHz: right wrist to off-body; Walking; 4 m separation; 270° orientation

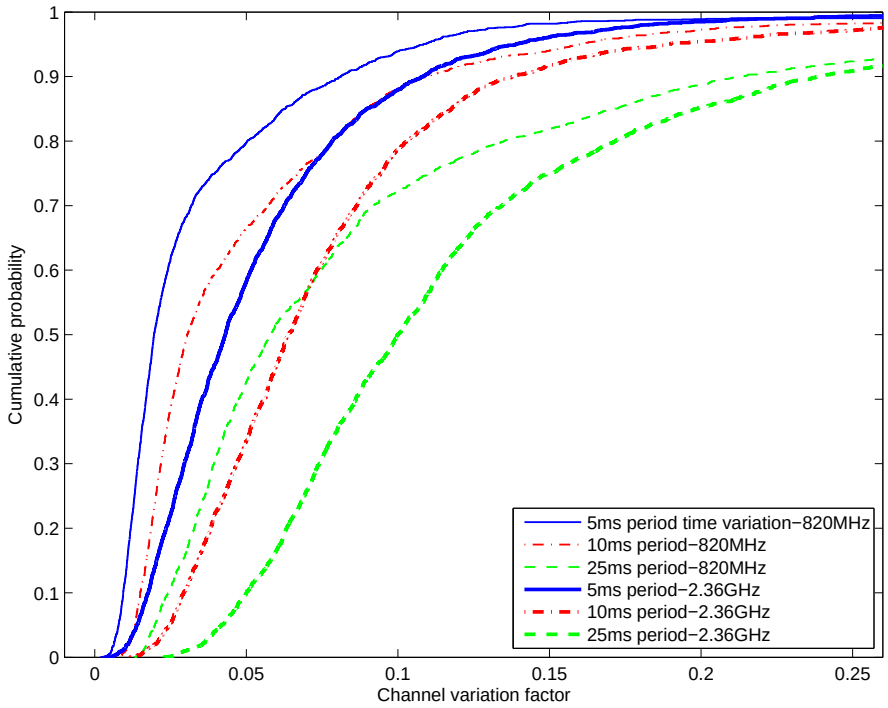

Figure 392: CDF of channel variation factor at 820 MHz and 2.36 GHz: right wrist to off-body; Walking; 4 m separation; 90° orientation